# QUANTUM TRANSPORT THEORY IN MAGNETIC FIELDS AND THE ELECTRON-HOLE-DROPLET MAGNETORESONANCE IN GERMANIUM

Richard T. Bridges

Ph.D. Thesis, University of Warwick, Department of Physics

Submitted June 1980

TABLE OF CONTENTS


| | Page No |
|---|---|
| Acknowledgements | |
| Declaration | |
| Abstract | |
| Table of Figures | |
| Chapter 1 : Introduction | 1 |
| Chapter 2 : Electron States in a Magnetic Field | |
| 2.1 Free Electron States | 6 |
| 2.2 Conduction Electrons in Germanium | 13 |
| Chapter 3 : Scattering Theory in a Magnetic Field | |
| 3.1 Introduction | 18 |
| 3.2 Exact Scattering Formalism | 23 |
| 3.3 Approximate Methods | 33 |
| 3.4 Cylindrical Square Well Potentials | 40 |
| Chapter 4 : Transport Theory in a Magnetic Field | |
| 4.1 Introduction | 49 |
| 4.2 The Derivation of Quantum Transport Equations | 54 |
| 4.3 The Boltzmann Transport Equation | 62 |
| 4.4 Relaxation Time Solutions of the Boltzmann Equation | 70 |
| 4.5 Time Dependent Relaxation in a Magnetic Field | 75 |
| 4.6 Approximate Inversions of the Relaxation Matrix | 80 |
| Chapter 5 : The Electron-Hole-Droplet Magnetoresonance in Germanium | |
| 5.1 Introduction | 86 |
| 5.2 Electron-Hole-Droplets in Germanium | 90 |
| 5.3 Discussion of the Transport Problem | 95 |

Page No

5.4 Calculation of the Longitudinal Magnetoconductivity 100

5.5 Comparison with Numerical Calculation and Experiment 122

5.6 Discussion and Conclusions 127

Chapter 6 : Summary 137

Appendix 1 : The Transformation Coefficient 142

Appendix 2 : The Wronskian Theorem 144

Appendix 3 : The Low Field Limit of the Relaxation Time 147

Appendix 4 : Matrix Theory 150

Appendix 5 : The Approximation of $J^{*}_{NM}$ 153

Appendix 6 : The Inversion of Matrices of Small Row Sum 155

Appendix 7 : Table of Constants and Parameter Values 157

Appendix 8 : Notation and Abbreviations 159

Bibliography 162

Acknowledgements

I would like to thank:

John Barker and George Rowlands of the University of Warwick, for their expert and tolerant supervision;
Professor Paul Butcher and the Physics Department of the University of Warwick, for providing all the necessary facilities and an atmosphere conducive to study;
The Science Research Council, for awarding a grant;
Lawrence Eaves of Nottingham University for making available his experimental data on the EHD magnetoresonance, and for valuable advice;
Margaret Peters and the Computing Department of the Queen Elizabeth Hospital, Birmingham, for the free use of their computing facilities; also the Computing Departments of the Universities of Warwick and Manchester;
Amanda Sharp for her expert and longsuffering typing of this thesis;
Ken Hayden for his companionship and encouragement through periods of frustration, disillusionment, idleness and occasional success.

Declaration

The relaxation matrix theory of §4.4, together with the numerical calculation of §5.5 has been published in J. Phys. C : Solid State Phys., Vol 10, 1977, pp 4523-38 (jointly with J R Barker). The time dependent theory of relaxation in §4.5 has been published in J. Phys. C : Solid State Phys., Vol 11, 1978, pp L887-91. These papers are bound in at the back of the thesis. To the best of my knowledge none of the other material here presented as original has been published elsewhere.

Abstract

This thesis develops a general procedure for the calculation of longitudinal magnetoconductivities in the high field quantum regime, assuming a transport equation of Boltzmann form. Earlier work has been extended, both in the treatment of the scattering problem, and in the generality of the solution to the Boltzmann equation.

Potential scattering in a magnetic field is treated via a quasi one-dimensional Schrödinger equation, giving a simple physical picture of the scattering process. The $\delta$ function scatterer is briefly mentioned, while scattering by a cylindrical square well is treated in detail. Green's Function methods for the solution of the scattering equations are developed, and general features of the theory, in particular resonant bound states, are noted.

Transport theory is developed from the Kubo formula by resolvent methods, to derive the Boltzmann equation with transition rates given either by the Born approximation or the t-matrix element. A general solution of the Boltzmann equation valid for elastic scattering is derived, involving multiple 'relaxation times' obtained by the inversion of a relaxation matrix. Time dependent relaxation is also treated and shown to involve multiple decay constants related to, but not identical with, the above 'relaxation times'. Regimes in which simple or approximate inversions of the relaxation matrix apply are investigated, in particular the quantum limit and isotropic scattering.

The above theory is applied to an analysis of the electron-hole-droplet (EHD) magnetoresonance of germanium. The practicability of the relaxation matrix method is shown, and accurate analytical approximations to the solution obtained. The experimentally observed features are explained by the analysis, which shows how accurate estimates of the droplet radius may be obtained from the data. Further resonances are predicted which, if observed, will reinforce these estimates. Certain features of the analysis also suggest that the strength of EHD's as scattering potentials is less than has been previously assumed.

TABLE OF FIGURES


| | | Page No |
|---|---|---|
| 2.1 | Landau energy band scheme | 9 |
| 2.2 | Constant energy surfaces in germanium conduction band | 14 |
| 2.3 | Geometry of cyclotron orbit in germanium conduction band | 14 |
| 3.1 | Stationary scattering state in a magnetic field | 26 |
| 3.2 | Wave packet scattering in a magnetic field | 26 |
| 3.3 | Diagonal potential integrals $I^m_{NN}(R)$ | 28 |
| 3.4 | Diagonal effective potentials for a spherical square well | 28 |
| 3.5 | Off-diagonal potential integrals $I^m_{NM}(R)$ | 29 |
| 3.6 | Off-diagonal coupling potentials for a spherical square well | 29 |
| 3.7 | Even stationary scattering state in a magnetic field | 40 |
| 3.8 | Resonant state in a magnetic field | 47 |
| 5.1 | Experimental magnetoresistance curve for germanium | 86 |
| 5.2 | Relaxation time spectrum in EHD scattering system | 87 |
| 5.3 | Band scheme and RR spectrum for EHD's in germanium | 91 |
| 5.4 | Schematic of several EHD experiments | 92 |
| 5.5 | Conduction band geometry in germanium | 95 |
| 5.6 | Inter-cyclotron-orbit scattering in an isotropic band | 103 |
| 5.7 | Inter-cyclotron-orbit scattering in germanium | 103 |
| 5.8 | Curves of maximum scattering contribution in the $k_x k_y$ plane | 104 |
| 5.9 | Scattering functions $F^*_{NM}(Q,Q_z)$ | 106 |
| 5.10 | Scattering integrals $J^*_{NM}(Q_z)$ | 107 |
| 5.11 | Relaxation time functions $Y_p(K)$ | 113 |
| 5.12 | Phonon relaxation times $T^{ph}$ in the low temperature limit | 114 |
| 5.13 | Steady part of the EHD magnetoconductivity | 114 |

Page No

5.14 Magnitude of the oscillatory magnetoconductivity 117

5.15 Approximation regions for phonon scattering 119

5.16 Calculated relaxation times in an isotropic band 122

5.17 Argyres relaxation times for EHD scattering 123

5.18 Relaxation times for phonon scattering 123

5.19 Relaxation times for combined EHD/phonon scattering 123

5.20 Calculated curves of $\partial\sigma/\partial B$ for EHD scattering 124

5.21 Fourier transforms of zonal contributions to $\partial\sigma/\partial B$ 124

5.22 Fourier transforms of experimental and calculated $\partial\sigma/\partial B$ curves 125

5.23 Comparison of t matrix elements with Born approximation 133

5.24 Possible form of effective EHD scattering potential 133

A3.1 Simple harmonic oscillator wave function for large N 147

# CHAPTER 1

## Introduction

The object of this thesis is to investigate and clarify certain problems encountered in the calculation of the transport properties of solids in high magnetic fields, in particular the longitudinal magnetoconductivity of semiconductors. The work has stemmed from an attempt to carry out an apparently straightforward longitudinal magnetoconductivity calculation for germanium, under conditions where Boltzmann transport could be assumed. It was found that the usual assumptions leading to a simple 'relaxation time' solution of the Boltzmann equation were not valid, and a more complex procedure had to be developed. Later consideration of the scattering potential involved led to a general study of quantum mechanical scattering in a magnetic field, an area which seems to have been hitherto neglected.

Quantum theory has always had a particularly important role in the description of magnetic effects, as the discreteness introduced into the quantisation scheme by a high magnetic field can give rise to clearly observable and classically inexplicable phenomena. Examples are the deHaas-van Alphen effect in the magnetic susceptibility, the corresponding Shubnikov-deHaas effect in magnetoresistance, and the more recent magnetophonon effect. Here, we shall restrict our attention to transport phenomena.

The formal theory of quantum transport is now well developed, having proceeded from the early heuristic quantum Boltzmann equation of Pauli (1928) to the later more rigorous work of van Hove (1955), Kohn and Luttinger (1957) and Kubo (1957). This and subsequent work has shown that in many situations quantum mechanical analogues of the classical Boltzmann

equation and electron distribution function are valid descriptions of the transport process. This is particularly true of longitudinal magnetoconductivity, and in almost all of the subsequent work we shall assume that Boltzmann transport is valid.

Even though a quantum Boltzmann equation exists, however, two major difficulties remain to be overcome before the conductivity may be evaluated. The first of these is to evaluate the transition rates between quantum states appearing in the equation. As will be shown, these are almost invariably calculated in the Born approximation, as a general formalism for treating scattering in a magnetic field seems to have been lacking until recently. The work of Ohtaka and Kondo (1977) on the Friedel oscillations and sum rule in a magnetic field has gone some way to filling this gap, and we shall attempt to extend their work to the dynamic problem of scattering.

The second difficulty is the form of the solution of the Boltzmann equation, in particular the nature of the perturbation to the electron distribution function caused by the applied electric field. In certain cases this perturbation can be described in terms of a single parameter, the relaxation time, so called because it is also the decay constant of an exponential relaxation back to equilibrium when the perturbing field is switched off. This solution is by no means always valid, however, and we have been forced to develop a description in terms of a finite small number of parameters. Closer investigation has shown that these are no longer true 'relaxation times' in the former sense, but we have also been able to find the true decay constants of the relaxation process. Our solution is restricted to elastic scattering, the inelastic problem being much more difficult.

With these tools available to us, it is possible to return to our original magnetoconductivity calculation. This is concerned with a resonant effect in the longitudinal magnetoresistance of germanium, observed by Eaves, Markiewicz and Furneaux (1976). In their experiment the scattering was almost exclusively by electron-hole droplets, created in large numbers by intense photo-excitation (see Pokrovsky, 1972). As the droplets were presumed to act as sharp edged scattering potentials of uniform size, a resonance of the droplet potential Fourier transform with the wave vectors of electrons at the top of Landau sub-zones in the magnetic quantisation scheme seemed possible. We have been able to verify that this is indeed so, and have investigated the conductivity curve in some detail using the methods previously developed.

The structure of the thesis is broadly as outlined above. After this introduction, Chapter 2 introduces the two magnetic quantisation schemes and sets of basis states which are used throughout the following work. §2.1 treats the states of free electrons, both in Landau gauge and axisymmetric gauge. Required transformation coefficients between the two systems are also obtained. §2.2 deals with electron states in germanium in a magnetic field, bringing out in particular the important effect of the anisotropy of the conduction band valleys in that material.

Chapter 3 deals with scattering theory in magnetic fields. An introductory section in §3.1 is followed by §3.2, which sets up the formalism involved in solving the scattering problem. A particular separation of the basic Schrödinger equation leads to a physically appealing quasi-one-dimensional description of the scattering process, in terms of a countably infinite set of coupled one-dimensional differential equations. §3.3 details methods of approximate solution of these equations, mainly in terms of Green's function theory. Several special cases, including the possible

existence of resonant bound states, are considered. Finally §3.4 treats scattering by a cylindrical square well potential, a relatively simple case which makes it possible to demonstrate some general features of the theory.

Chapter 4 is concerned with transport theory. After another introductory section, §4.2 sketches the development of quantum transport equations, starting from the Kubo formula and using resolvent methods. §4.3 deals with the Boltzmann approximation to the prece ding theory, and also takes the resolvent theory to the next stage of approximation, leading to a Boltzmann equation with t-matrix transition rates. §4.4 is devoted to the solution of the Boltzmann equation for elastic scattering, in terms of a relaxation matrix and multiple 'relaxation times'. Time dependent relaxation (via elastic scattering processes) is investigated in §4.5, and the status of the new 'relaxation times' in relation to the true decay constants of the relaxation process is made clear. The concluding §4.6 discusses different regimes in which simple or approximate solutions of the relaxation matrix equations are applicable, in particular, the quantum limit and isotropic scattering.

Chapter 5 presents in detail the calculation of the electron-hole droplet magnetoresonance in germanium. Again after the introduction, §5.2 reviews the experimental and theoretical work on electron-hole droplets in germanium, while §5.3 discusses other aspects of this particular transport calculation and settles on parameter values and approximations to be used. The actual calculation is described in §5.4, in which several mathematical approximations and simplifications are employed before arriving at curves of conductivity against magnetic field. The anisotropy of the germanium conduction band valleys is seen to have a quantitatively significant effect

on the results obtained. §5.5 briefly describes a purely numerical calculation of the same magnetoresonance and compares the results both with the experimental work and with the more analytical calculation previously described. The results are discussed in greater detail in §5.6, and some features are noted which suggest that droplet scattering potentials are weaker than previously assumed. Some recommendations as to the direction of future experimental and theoretical work on the magnetoresonance are made. The thesis as a whole is summarised in Chapter 6, which also indicates more general possibilities for future work in this area.

# CHAPTER 2

## Electron States in a Magnetic Field

### 2.1 Free electron states

This chapter will give a brief resume of the quantum theory of electrons in a uniform magnetic field, and will note properties of the states which will be of use later.

The classical Hamiltonian of a particle of charge q in a magnetic field described by a vector potential $\underline{A}$ is (see, e.g., Goldstein (1950)).

$$H = (\underline{\Pi} - q\underline{A})^2/2m_e + q\phi \qquad (2.1.1)$$

where the canonical momentum $\underline{\Pi}$ conjugate to the position vector $\underline{r}$ is

$$\underline{\Pi} = m_e\dot{\underline{r}} + q\underline{A} \qquad (2.1.2)$$

and $\phi$ is the electrostatic potential. When $\phi$ is zero (no electric field), $q = -e$ for an electron, and $\underline{A}$ is chosen such that $\nabla.\underline{A} = 0$ (Coulomb gauge), the Schrödinger equation in the co-ordinate representation is obtained by replacing the canonical momentum $\underline{\Pi}$ by $-i\hbar\nabla$ in the classical Hamiltonian, so that we have

$$(-(\hbar^2/2m_e)\nabla^2 - (ie\hbar/m_e)\underline{A}.\nabla + (e^2/2m_e)\underline{A}^2)\Psi = \varepsilon\Psi \qquad (2.1.3)$$

as the equation for stationary states with energy $\varepsilon$.

In classical theory the motion is invariant under 'changes of gauge' in which $\underline{A}$ is altered by the addition of an irrotational vector field, and it is interesting to see the corresponding effect in quantum mechanics. If $\Psi_1$ is a wave function satisfying the Schrödinger equation in the gauge $\underline{A} = \underline{A}_1$, and $\Psi_2$ is such a wave function in the gauge $\underline{A} = A_2$, then $\Psi_2$ may

be obtained from $\Psi_1$ by the transformation

$$\Psi_2(\underline{r}) = e^{(ie/\hbar)f_{12}(r)}\Psi_1(\underline{r}) \tag{2.1.4}$$

where $f_{12}(\underline{r})$ is any scalar field satisfying

$$\nabla f_{12} = \underline{A}_1 - \underline{A}_2 \tag{2.1.5}$$

Since $\underline{A}_1 - \underline{A}_2$ is irrotational we are assured that such a function exists, and since $\nabla.\underline{A} = 0$ it must satisfy Laplace's equation: $\nabla^2 f_{12} = 0$. Since f will be real we have $|\Psi_1{}^2| = |\Psi_2|^2$ everywhere, so that all observable quantities are unchanged by the gauge transformation, as we require. We note, however, that if other quantum members apart from $\varepsilon$ are needed to specify the states in the two gauges, the transformed state will not in general be an eigenstate for those other numbers.

Henceforward we assume a magnetic field in the z direction so that in cartesians

$$\underline{B} = (0,0,B) \tag{2.1.6}$$

In the Landau gauge

$$\underline{A} = (0,Bx,0) \tag{2.1.7}$$

the Schrödinger equation becomes

$$-(\hbar^2/2m_e)\nabla^2\Psi^0 - (ie\hbar/m_e)B\partial\Psi^o/\partial y + (e^2/2m_e)B^2x^2\Psi^o = \varepsilon\Psi^o \tag{2.1.8}$$

We now introduce the cyclotron frequency

$$\omega_c = eB/m_e \tag{2.1.9}$$

and the Landau length

$$\ell = (\hbar/eB)^{\frac{1}{2}} \tag{2.1.10}$$

whence, writing the wave function $\Psi^o = \phi(x)e^{ik_y y}e^{ik_z z}$, we have

$$-(\hbar^2/2m_e)\partial^2\phi/\partial x^2 + \tfrac{1}{2}m_e\omega_c{}^2(x+\ell^2k_y)^2\phi = (\varepsilon-\hbar^2k_z{}^2/2m_e)\phi \tag{2.1.11}$$

where the cyclotron orbit centre is given by $x = \ell^2 ky$. This equation is immediately recognisable as that for a simple harmonic oscillator of natural frequency $\omega_c$ centred on $x = -\ell^2k_y$, for which we know the energy eigenvalues and eigenfunctions. There are thus three quantum numbers: the Landau band number N, and the y and z wave numbers $k_y$ and $k_z$ respectively. N takes integral values from 0 to $\infty$, while in a box of side L $k_z$ takes the values $\pm 2\pi n/L$, where n is any positive integer, and $k_y$ takes the same values restricted by $|\ell^2k_y| < L/2$. The energy is given by

$$\varepsilon = (N+\tfrac{1}{2})\hbar\omega_c + \hbar^2k_z{}^2/2m_e \tag{2.1.12}$$

so that there are $L^2/4\pi\ell^2$ different states with the same values of $\varepsilon$, N and $k_z$. The corresponding normalised wave function is

$$\Psi^o{}_{Nk_yk_z} = L^{-1}\phi_N(x+\ell^2k_y)e^{ik_y y}e^{ik_z z} \tag{2.1.13}$$

where the oscillator wave function $\phi_N(x)$ is

$$\phi_N(x) = (2^N N!\ell\sqrt{\pi})^{-\frac{1}{2}}e^{-x^2/2\ell^2}H_N(x/\ell) \tag{2.1.14}$$

and $H_N(x)$ is the unnormalised Hermite polynomial of order N defined by

$$H_N(x) = (-1)^N e^{x^2}d^N/dx^N(e^{-x^2}) \tag{2.1.15}$$

The $\phi_N$ defined in this way obey the orthonormality condition

$$\int_{-\infty}^{\infty}\phi_N(x)\phi_M(x)dx = \delta_{NM} \qquad (2.1.16)$$

We see, therefore, that the motion in the z direction is identical to that of a free particle in one dimension, but that in the x-y plane is quantised, corresponding in some sense to the classical bounded motion in cyclotron orbits. This picture was first obtained by Landau (1930). We may interpret the x-y part of the above wave function as representing an ensemble of cyclotron orbits of energy $(N+\frac{1}{2})\hbar\omega_c$ with their centres uniformly distributed along the line $x = -\ell^2 k_y$ (Johnson and Lippmann, 1949). With $k_z$ fixed, we can check that there are the same number of energy eigenstates between $\varepsilon$ and $\varepsilon + \hbar\omega_c$ as for a free particle in two dimensions, but now they all have the same energy instead of being distributed over the interval. With the $k_z$ dependence included, the density of states has singularities at each multiple of $\hbar\omega_c$, and is

$$\rho(\varepsilon) = 2\Omega(\sqrt{2m_e}/4\pi^2\ell^2\hbar)\sum_{N=0}^{\infty}(\varepsilon-(N+\tfrac{1}{2})\hbar\omega_c)^{-\frac{1}{2}}\theta(\varepsilon-(N+\tfrac{1}{2})\hbar\omega_c) \qquad (2.1.17)$$

where $\theta$ is a Heaviside function and the factor 2 accounts for spin degeneracy. The resulting energy-momentum diagram, together with the density of states, is plotted in Fig. 2.1, which shows the familiar Landau band structure. From here on we shall conventionally call the region $(N+\frac{1}{2})\hbar\omega_c<\varepsilon<(N+\frac{3}{2})\hbar\omega_c$ 'Landau sub-zone N', or simply 'zone N'.

In §3 on scattering theory we shall be concerned with an axisymmetric problem in which the z component of angular momentum is a natural quantum number. Here the natural gauge is also axisymmetric; in cylindrical polars we have

$$\underline{A} = (0, B\rho/2, 0) \qquad (2.1.18)$$

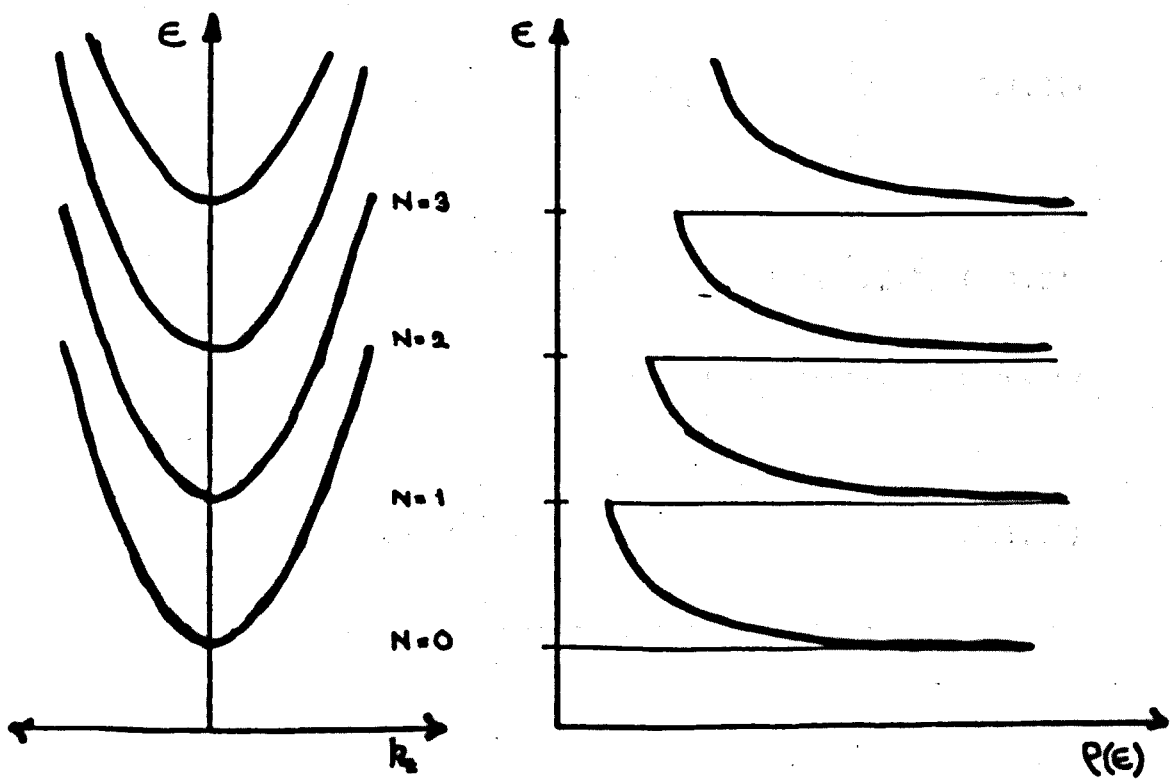


Fig 2.1 : Landau energy/momentum band scheme and energy density of states for free electrons in a magnetic field

corresponding to (-By/2,Bx/2,0) in cartesians. We shall not go through the derivation of the eigenstates here, but merely present the results (cf Kubo, Miyake and Hashitsume, 1965). The quantum numbers are now N and $k_z$ exactly as before, and the z component of angular momentum m. This takes integral values from -N to + ∞. The energy is also as before, given by (2.1.12), but the wave function is now

$$\Psi^{o}_{Nmk_z} = (2\pi L)^{-\frac{1}{2}}\phi^{m}_{N}(\rho)e^{-im\phi}e^{ik_z z} \tag{2.1.19}$$

where the radial wave function $\phi^m_N$ satisfies the equation

$$\underline{\mathbb{D}}^{m}\{\rho\}\phi = (N+\tfrac{1}{2})\hbar\omega_c\phi \tag{2.1.20}$$

where the differential operator $\mathbb{D}^m\{\rho\}$ is

$$\mathbb{D}^{m}\{\rho\} = -(\hbar^2/2m_e)\{\rho^{-1}d/d\rho\{\rho d/d\rho\}-m^2\rho^{-2}\}-\tfrac{1}{2}m\hbar\omega_c + m_e\omega_c{}^2\rho^2/8 \tag{2.1.21}$$

The solution to this equation is

$$\phi^{m}_{N}(\rho) = \ell^{-1}(n!/(n+|m|)!)^{\frac{1}{2}}e^{-\rho^2/4\ell^2}(\rho^2/2\ell^2)^{|m|/2}L_n^{|m|}(\rho^2/2\ell^2) \tag{2.1.22}$$

where $n = N + \frac{1}{2}(m-|m|)$ and $L_N^{|m|}(r)$ is the unnormalised associated Laguerre polynomial

$$L^{M}_{N}(r) = (N!)^{-1}e^{r}r^{-M}d^{N}/dr^{N}(e^{-r}r^{N+M}) \tag{2.1.23}$$

The $\phi^m_N$ defined in this way obey the orthonormality condition

$$\int_{\infty}^{\infty}\rho\phi^{m}_{N}(\rho)\phi^{m}_{N}(\rho)d\rho = \delta_{NM} \tag{2.1.24}$$

In this picture the bounded motion in the x-y plane is much more explicit, as the radial parts of the wave functions go to zero at infinity. In fact each state corresponds to an ensemble of cyclotron

orbits of energy $(N+\frac{1}{2})\hbar\omega_c$, with their centres uniformly distributed on the circle

$$\rho = \ell(2m+1)^{\frac{1}{2}} \quad \text{(Johnson and Lippmann, 1949)}$$

The two sets of states do not transform into each other under (2.1.4), and so we must calculate the transformation coefficients between the two representations. We shall also require the matrix elements of plane waves between the Landau states, and it is convenient to work out these first. The quantity we need is thus $\langle N,k_y,k_z|e^{i\underline{q}\cdot\underline{r}}|N',k_y',k_z'\rangle$. Assuming that the components of $\underline{q}$ take only values $2\pi n/L$ like $k_y$ and $k_z$, the integrations are straightforward apart from the use of the result

$$\int_{-\infty}^{\infty} du e^{-u^2} H_N(u+a) H_{N'}(u+b) = 2^{N'}\sqrt{\pi}N!b^{N'-N}L_N^{N'-N}(-2ab) \qquad (2.1.25)$$

for $N'>N$. We eventually have

$$\langle N,k_y,k_z|e^{i\underline{q}\cdot\underline{r}}|N',k_y',k_z'\rangle = \delta_{k_y,k_y'+q_y}\delta_{k_z,k_z'+q_z}G_{NN'}(q_x,q_y,k_x,k_y) \qquad (2.1.26)$$

where for $N'>N$

$$G_{NN'}(q_x,q_y,k_x,k_y) = (N!/N'!)^{\frac{1}{2}}(\ell(iq_x-q_y)/\sqrt{2})^{N'-N}L_N^{N'-N}(\ell^2q_\perp^2/2) \times$$

$$\times e^{-\ell^2q_\perp^2/4}e^{-i\ell^2q_x(k_y+k_y')/2} \qquad (2.1.27)$$

in which we introduce the magnitude of the component of $\underline{q}$ in the x-y plane, $q_\perp = (q_x^2+q_y^2)^{\frac{1}{2}}$. The squared matrix element is thus

$$|\langle N,k_y,k_z,|e^{i\underline{q}\cdot\underline{r}}|N',k_y',k_z'\rangle|^2 = \delta_{k_y,k_y'+q_y}\delta_{k_z,k_z'+q_z}F_{NN'}(\ell^2q_\perp^2/2) \qquad (2.1.28)$$

where for $N' \geq N$

$$F_{NN'}(u) = (N!/N'!)\, u^{N'-N} e^{-u} |L_N^{N'-N}(u)|^2 \qquad (2.1.29)$$

The $\delta$'s appearing in the above formulae are Kronecker symbols, and for $N'<N$ we merely interchange N and N' on the right hand side.

Finally, we require the transformation coefficients between the different types of state. In fact we shall want to transform symmetric states defined relative to the origin X, Y, Z (Corresponding to the gauge $(-B(y-Y)/2, B(x-X)/2, 0)$ in cartesians) to states in the Landau gauge. Thus state $\Psi_1$ is given by (2.1.19) with $\rho$ replaced by $\rho_{XY} = ((x-X)^2+(y-Y)^2)^{\frac{1}{2}}$ and z replaced by z-Z; this state will be written $|N',m,k'_z\rangle_{cyl:X,Y,Z}$. In the Landau gauge this state will transform to

$$|N',m,k'_z\rangle^{X,Y,Z}_{Landau} = e^{(ieB/2\hbar)(-xy+xY-Xy)} . |N',m,k'_z\rangle_{cyl:X,Y,Z} \qquad (2.1.30)$$

With the state now in the same gauge, we can find its matrix element with the Landau state $|N,k_y,k_z\rangle$. The details of this are tedious and are given in Appendix 1; here we merely quote the result (cf Kubo et al., 1965).

$$\langle N,k_y,k_z|N',m,k_{z'}\rangle^{X,Y,Z}_{Landau} = \delta_{NN'}\delta_{k_z k_{z'}} e^{-i(Yk_y+Zk_z+XY/2\ell^2)} \times$$

$$\times (-1)^m (2\pi\ell^2/L)^{\frac{1}{2}} \phi_{N+m}(X+\ell^2 k_y) \qquad (2.1.31)$$

## 2.2 Conduction electrons in germanium

In principle the derivation of the energy states in a crystal subject to a uniform magnetic field is an even more complex problem than that of calculation of band structure in zero field. Fortunately, however, an extremely simple approximation enables us to go over from the band structure in zero field with very little difficulty. Guided by the observation that the Hamiltonian for a free electron in a magnetic field is obtained by replacing its momentum $\underline{P}$ by $\underline{\Pi}-q\underline{A}$ in the energy, we postulate that the same is true when the energy is given by a band structure calculation, and the momentum $\underline{P}$ is the crystal momentum $\hbar\underline{k}$. Thus if the energy-momentum relationship in the crystal in zero field is

$$\varepsilon = E_o(\hbar\underline{k}) \tag{2.2.1}$$

we postulate that the 'classical' Hamiltonian in a magnetic field is

$$H = E_o(\underline{\Pi}+e\underline{A}) \tag{2.2.2}$$

and that the Schrödinger equation is

$$E_o(-i\hbar\nabla+e\underline{A})\Psi^* = \varepsilon\Psi^* \tag{2.2.3}$$

This is known as the effective mass approximation (Peierls, 1933; Luttinger, 1951) and it can be shown that it is equivalent to neglecting transitions between bands caused by the magnetic field. Harper (1955) has shown that it is a good approximation in a band which is not overlapped by other bands, as is the case in the germanium conduction band. We shall use it without question from here on.

The lowest part of the conduction band of germanium consists of four prolate spheroidal valleys with their longitudinal axes in the {111}

directions in $\underline{k}$ space (Dresselhaus, Kip and Kittel, 1955), as shown in Fig. 2.2. In §5 we shall be interested in an experimental situation in which the magnetic field is along a {100} direction; hence we shall choose a co-ordinate system in which this corresponds to the $k_z$ axis. Assuming for the moment that the valley is centred on the origin of $\underline{k}$ space, the zero field energy-momentum relation is then

$$E_o(\hbar\underline{k}) = \hbar^2 k_x^2/2m_t + \hbar^2(k_y\cos\Theta - k_z\sin\Theta)^2/2m_t + \hbar^2(k_y\sin\Theta + k_z\cos\Theta)^2 2m_\ell \qquad (2.2.4)$$

where $m_t$ and $m_\ell$ are respectively the transverse and longitudinal effective masses in the valley. The y axis has been chosen so that the longitudinal axis of the ellipsoid lies in the y-z plane, and $\Theta$ is the angle between this axis and the z axis. The geometry of this arrangement, and a typical semi-classical cyclotron orbit in $\underline{k}$ space, are shown in Fig. 2.3.

Replacing $\hbar\underline{k}$ by $-i\hbar\nabla + e\underline{A}$, where $\underline{A}$ is the Landau gauge (2.1.7), we write the wave function as $\Psi^* = \phi^*(x)e^{ik_y y}e^{ik_z z}$, and obtain the Schrödinger equation

$$-\hbar^2/2m_t\, d^2\phi^*/dx^2 + ((\hbar k_y + eBx)\cos\Theta - \hbar k_z\sin\Theta)^2\phi^*/2m_t +$$

$$+ ((\hbar k_y + eBx)\sin\Theta + \hbar k_z\cos\Theta)^2\phi^*/2m_\ell = \varepsilon\phi^* \qquad (2.2.5)$$

Grouping the terms in x to form a perfect square, this may be put in the canonical form

$$-\hbar^2/2m_t d^2\phi^*/dx^2 + \tfrac{1}{2}m_t\omega_c^2(x+X^*)^2\phi^* = (\varepsilon-\varepsilon_z^*)\phi^* \qquad (2.2.6)$$

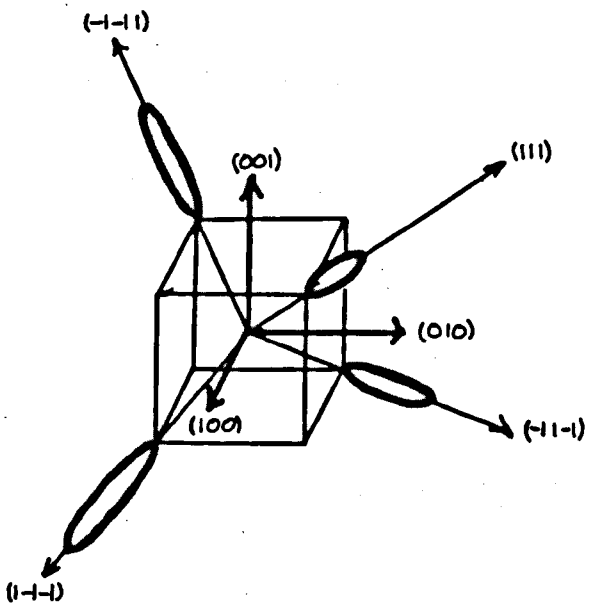


Fig. 2.2 : Geometry of the conduction band valleys of germanium

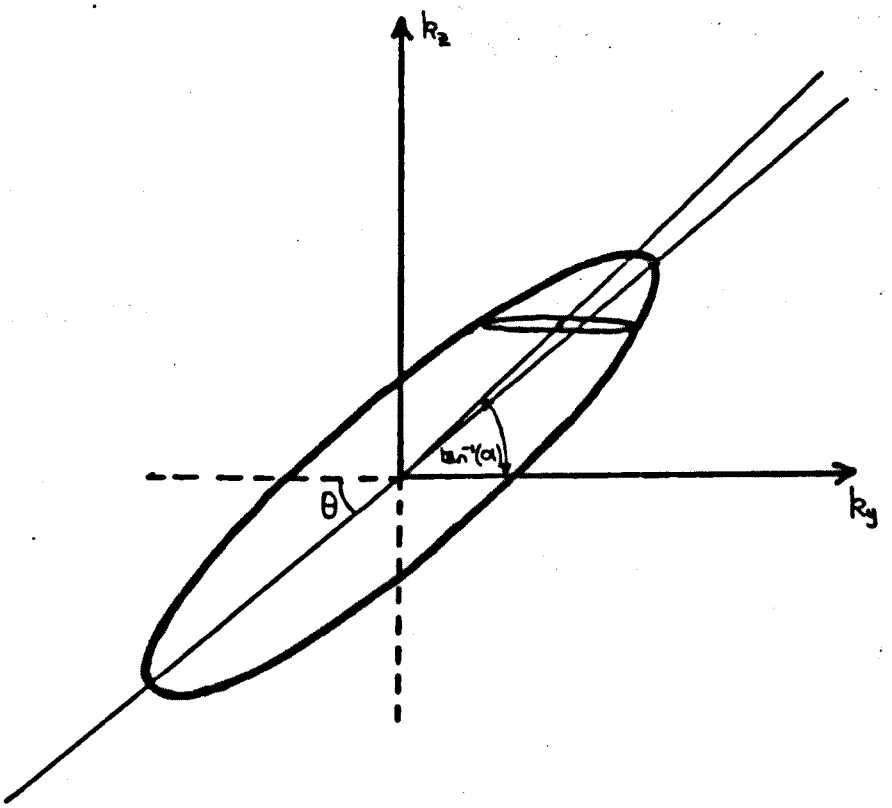


Fig. 2.3 : Geometry of the co-ordinate system for a single valley, B//z//100. A typical semi-classical cyclotron orbit is shown

where the new cyclotron frequency $\omega_c^*$ is given by

$$\omega_c^{*2} = e^2B^2(\cos^2\Theta/m_t+\sin^2\Theta/m_\ell)/m_t \tag{2.2.7}$$

and energy of motion in the z direction, $\varepsilon_z^*$, is

$$\varepsilon_z^* = \tfrac{1}{2}\hbar^2k_z^2(m_t\sin^2\Theta+m_\ell\cos^2\Theta)^{-1} \tag{2.2.8}$$

We may therefore define an effective kinetic mass $m_z$ by

$$m_z = m_t\sin^2\Theta + m_\ell\cos^2\Theta \tag{2.2.9}$$

and an effective cyclotron mass by

$$m_c = m_t^{\frac{1}{2}}(\cos^2\Theta/m_t+\sin^2\Theta/m_\ell)^{-\frac{1}{2}} = m_t(m_\ell/m_z)^{\frac{1}{2}} \tag{2.2.10}$$

in terms of which $\omega_c^* = eB/m_c$ and $\varepsilon_z^* = \hbar^2k_z^2/2m_z$. The energies are then given by

$$\varepsilon = (N+\tfrac{1}{2})\hbar\omega_c^* + \hbar^2k_z^2/2m_z \tag{2.2.11}$$

as before. To simplify the expression for the wave function we introduce the new length

$$\ell^* = (\hbar/eB)^{\frac{1}{2}}(m_c/m_t)^{\frac{1}{2}} = \ell(m_c/m_t)^{\frac{1}{2}} \tag{2.2.12}$$

The wave function $\phi^*$ is then given by $\phi_N^*(x+X^*)$ where

$$\phi_N^*(x) = (2^NN!\ell^*\sqrt{\pi})^{-\frac{1}{2}}e^{-x^2/2\ell^{*2}}H_N(x/\ell^*) \tag{2.2.13}$$

and the motion is centred on $-X^*$ given by

$$X^* = \ell^2k_y - \alpha\ell^2k_z \tag{2.2.14}$$

where $\alpha$ is

$$\alpha = (m_\ell - m_t)/(m_t \tan\Theta + m_\ell \cot\Theta) = (m_\ell - m_t)\sin 2\Theta / 2m_z \qquad (2.2.15)$$

The quantity $\alpha$ is a useful measure of the effect of the anisotropy of the valley and its tilt relative to the field, since $\alpha$ is zero if $m_\ell = m_t$ or if $\Theta = 0$ or $\pi/2$.

The appearance of the $k_z$ term in $X^*$ slightly complicates the evaluation of the squared matrix element (2.1.26) between the new states, but we eventually obtain

$$|\langle N k_y k_z | e^{i\underline{q}\cdot\underline{r}} | N' k_y', k_z' \rangle|^{*2} = \delta_{k_y, k_y'+q_y} \delta_{k_z, k_z'+q_z} F_{NN'}(\ell^{*2} q_\perp^{*2}/2) \qquad (2.2.16)$$

where the function $F$ is as defined previously in (2.1.27) and $q_\perp^*$ is given by

$$q_\perp^{*2} = q_x^2 + (\ell/\ell^*)^4 (q_y - \alpha q_z^2) \qquad (2.2.17)$$

which reduces to $q_\perp^2$ in the isotropic case discussed previously. The above analysis is an adaptation of that by Miller and Omar (1961), also for germanium. Slater (1967) discusses the most general possible ellipsoidal valley with three different principal effective masses, which was treated first by Shockley (1953). To construct an equivalent to the state (2.1.19) in the axisymmetric gauge (2.1.18) would be considerably more complicated in this case, and we do not attempt to do so here.

Another factor we have so far neglected is that the ellipsoids do not have their origins at (0,0,0) ; they are in fact the L-points $\underline{k}_L$ given by the intersection of the {111} axes with the Brillouin zone edge. The correct energy-momentum relation is therefore

$$\varepsilon = E_o(\hbar\underline{k} - \hbar\underline{k}_L) \tag{2.2.18}$$

where $E_o$ is the same function as that defined in (2.2.4). This change presents no difficulty, as we see that it can be interpreted as a change of gauge from $\underline{A}$ to $\underline{A} - (\hbar/e)\underline{k}_L$. Using the transformation (2.1.4) the correct wave function is therefore

$$\psi^{Ge}_{Nk_yk_z} = e^{i\underline{k}_L.\underline{r}}\psi^{*}_{Nk_yk_z} \tag{2.2.19}$$

So long as we are not interested in transitions between different valleys this extra factor plays no part in the calculation of matrix elements.

It remains to calculate the various parameters derived above for the case of germanium, when $m_\ell \sim 1.5\ m_e$ and $m_t = 0.082\ m_e$ (Dresselhaus *et al.*, 1955; Levinger and Frankl, 1961), and the angle $\theta$ between a {100} and a {111} axis is $\cos^{-1}(1/\sqrt{3}) = 54.7^o$. Then

$$m_z = 0.581\ m_e \qquad m_c = 0.135\ m_e \tag{2.2.20}$$

$$\alpha = 1.22 = \tan 50.7^o \qquad \ell^* = 1.28\,\ell$$

# CHAPTER 3

## Scattering Theory in a Magnetic Field

### 3.1 Introduction

In this chapter we shall discuss the quantum mechanical theory of potential scattering in the presence of a uniform magnetic field. When the scattering potentials are axisymmetric about the magnetic field direction it will be shown that the Schrödinger equation is separable into an infinite set of coupled second order ordinary differential equations for quantities which behave like wave functions in a one-dimensional scattering problem. The transition rates from one free state to another brought about by the scattering process are readily obtainable from the solution to these equations. We shall then go on to consider approximate methods of solution of the differential equations, which will be illustrated by an application to scattering by potential wells which are cylindrical in shape.

When classifying the energy eigenstates of any system a natural distinction exists between those of negative energy (bound states) and those of positive energy (free states). The theory of perturbations to these states thus falls also into two distinct parts; the perturbation of the free states being described by the theory of scattering. As one would expect, such an important aspect of the application of quantum mechanics to real systems and experimentally observable quantities has been studied in great detail. The early work on scattering by atoms and molecules emphasised the more intuitively understandable co-ordinate representation of the scattering process in which different angular momentum components of the incoming wave function are phase shifted by differing amounts in the scattering. A complete survey of this aspect of scattering theory has been made by Mott and Massey (1949). A cornerstone of the early work, and much of that since, is the Born approximation in which the transition

rates due to the scattering are found by taking matrix elements of the potential between the free states. The expression for the transition rate $\omega_{fi}$ from initial state i to final state f caused by the potential V is known as the Fermi Golden Rule (Fermi 1950)

$$\omega_{fi} = 2\pi/\hbar\delta(\varepsilon_f-\varepsilon_i)|\langle f|V|i\rangle|^2 \qquad (3.1.1)$$

The advent of high energy nuclear physics necessitated a more general, rigorous, and abstract approach to scattering theory, which was gradually developed by Schwinger (1947), Kohn (1948), Lippmann and Schwinger (1950) and Gell-Mann and Goldberger (1953). The scattering from initial to final states was now described by the scattering operator, or S matrix which contained all observable information on the scattering. Lippmann and Schwinger (1950) derived a variational principle for a scattering state wave function $\Psi^+$ obeying steady boundary conditions on the flux of in-going and out-going particles at infinity, and also gave expressions for the exact transition rates between asymptotically free states. These were expressed as matrix elements of the potential between the state $\Psi_i^+$ and the final free state f, but to symmetrise the expression a new operator, the transition matrix $t^+$, was introduced to act on the free, unperturbed states such that

$$\langle f|V|\Psi_i^+\rangle = \langle f|t^+|i\rangle \qquad (3.1.2)$$

where the exact expression for the transition rate in elastic scattering becomes

$$\omega_{fi} = 2\pi/\hbar\delta(\varepsilon_f-\varepsilon_i)|\langle f|t^+|i\rangle|^2 \qquad (3.1.3)$$

Gell-Mann and Goldberger (1953) showed that the time-dependent picture of scattering could be cast into this more abstract time independent form. Extensive treatises on these methods are to be found in the books by Roman (1965) and Rodberg and Thaler (1967).

Since it was primarily concerned with nuclear scattering, the above work made little mention of the effect a uniform magnetic field has on the scattering process, although the different nature of the asymptotic free states makes this an interesting problem. For a long time much of the theoretical work which necessitated a calculation of transition rates in a magnetic field went no further than the Born approximation; examples in transport theory are the papers of Adams and Holstein (1959), Argyres (1959), Efros (1965), Dubinskaya (1969) and Eaves, Markiewicz and Furneaux (1977).

Early attempts at approximate solutions to the Schrödinger equation in a magnetic field made use of the adiabatic approximation of Schiff and Snyder (1939), in which the motion within a single Landau band was described by a one-dimensional Schrödinger equation with a potential averaged over the radial part of the wave function, and inter Landau band transitions were forbidden. Though discussed with reference to scattering by Kubo, Miyake and Hashitsume (1965), the major application was to the study of bound states in the problem of magnetic freezeout by Yafet, Keyes and Adams (1956), followed by many authors of whom just a few are Mansfield (1970), Miyake (1973) and Jog and Wallace (1978). Fenton and Haering (1967) used the same approximation in the discussion of the Mott transition in a magnetic field, while Elliott and Loudon (1959) and Altarelli and Lipari (1974) have applied it to the study of exciton states in a magnetic field.

One case in which the exact scattering problem may be solved exactly (or at least subject to approximations of a milder nature) is that of scattering from a potential which is very small in comparison with the magnetic Landau length $\ell$. Kahn (1960), Skobov (1960) and Bychkov (1961) approached this problem via an approximation to the Green's function in the magnetic field which was further discussed by Kubo et al (1965). A feature of this study was that a divergence appeared in the exact treatment of scattering by a $\delta$ function, and the approximation is necessary to cut off the number of Landau levels involved.

The logical next step is the formulation and solution of the exact equations describing scattering from general potentials in a magnetic field. Until recently we believed that no such work existed, but after the theory described in this chapter was essentially complete our attention was drawn to the excellent paper of Ohtaka and Kondo (1977). This treats the problem of the Friedel oscillations and sum rule in a magnetic field, and proceeds by methods very similar to ours. The theory is treated in the abstract notation of the S and t matrices, and formally obtains expressions for the change in the density of states introduced by impurities in terms of the phase shifts of eigenvectors of the S matrix. The actual overlap with the content of this chapter is quite small, but we have naturally benefitted from an appreciation of their penetrating theoretical analysis of the problem.

In §3.2 we write the Schrödinger equation in separated form as an infinite set of coupled differential equations, and discuss the physical interpretation of the formalism. We also discuss the results which may be expected for a certain class of potentials, and briefly treat scattering by a $\delta$ function potential in the light of our methods. Section §3.3 deals

with approximate methods of solution of the infinite set of equations, which are very similar to the Born series of zero magnetic field theory. The problems of strong scattering within Landau bands, strong scattering between Landau bands, resonant and bound states are discussed. Finally §3.4 discusses the relatively simple problem of scattering by a cylindrical potential to illustrate some features of the theory.

## 3.2 Exact Scattering Formalism

We shall now formally solve the problem of the elastic scattering of an electron in the presence of a uniform magnetic field, for the case when the scattering is described by a potential which is axially symmetric about the magnetic field direction. The Schrödinger equation is

$$(\underline{p}-e\underline{A})^2/2m_e\Psi(\underline{r}) - \varepsilon\Psi(\underline{r}) = -V(\underline{r})\Psi(\underline{r}) \qquad (3.2.1)$$

The axial symmetry of the scatterer about the magnetic field axis leads to conservation of angular momentum about that axis, so it is appropriate to work in the axially symmetric gauge $\underline{A} = \underline{A}(\rho)$ in a cylindrical polar co-ordinate scheme centred on the symmetry axis of the scatterer. The angular momentum m about the field axis is then a good quantum number for the free basis states (2.1.19), and is also conserved throughout the collision. The solution of the scattering problem will thus consist asymptotically of an incoming free state and several outgoing free states, all with the same value of m, but with N and $k_z$ changed by the collision. Hence we may separate out the dependence of the wave function on the axial co-ordinate $\phi$, so that the Schrödinger equation (3.2.1) reduces to

$$\{D^m\{\rho\}\psi^m(\rho,z) - \hbar^2/2m_e\partial^2/\partial z^2\psi^m(\rho,z) - \varepsilon\psi^m(\rho,z)\}e^{-im\phi} = -V(\rho,z)\psi^m(\rho,z)e^{-im\phi} \qquad (3.2.2)$$

where $D^m\{\rho\}$ is the differential operator in $\rho$ defined in (2.1.21). Guided by the knowledge that far away from the potential $\Psi$ must consist of free Landau states, we write $\psi^m$ in the separated form

$$\psi^m(\rho,z) = \sum_{N=0}^{\infty} \phi_N^m(r) f_N^m(z) \qquad (3.2.3)$$

where $r = \rho^2/2\ell^2$ and the $\phi_N^m$ are the associated Laguerre functions previously derived in connection with the free Landau states (2.1.22). These functions form a complete set on $\{o,\infty\}$ and satisfy eqn. (2.1.20). With the wave function written in this form the Schrödinger equation further reduces to

$$\sum_{N=0}^{\infty} \{(N+\tfrac{1}{2})\hbar\omega_c f_N^m(z) - \hbar^2/2m_e f_N^{m''}(z) - \varepsilon f_N^m(z)\}\phi_N^m(r) = \sum_{N=0}^{\infty} -V(\rho,z)\phi_N^m(r) f_N^m(z) \tag{3.2.4}$$

We can now use the orthonormality property (2.1.24) of the $\phi_N^m$ to extract a differential equation for $f_N^m$, by multiplying (3.2.4) by $2\pi\rho$ and integrating from o to $\infty$ in $\rho$:

$$-\hbar^2/2m_e f_N^{m''}(z) - (\varepsilon-(N+\tfrac{1}{2})\hbar\omega_c) f_N^m(z) = \sum_{M=0}^{\infty} -V_{NM}^m(z) f_M^m(z) \tag{3.2.5}$$

$$V_{NM}^m(z) = \int_o^{\infty} 2\pi\rho d\rho \phi_N^m(r) V(\rho,z) \phi_M^m(r) \tag{3.2.6}$$

Were it not for the off-diagonal coupling terms $V_{NM}^m$, (3.2.5) would be a simple one dimensional Schrödinger equation describing motion in the z direction confined to a single Landau band. The coupling terms give rise to inter-Landau band transitions and also resonances with virtual bound states, as will be shown below.

Eqn (3.2.5) is incomplete without a discussion of the boundary conditions imposed on it to produce the desired scattering behaviour. If the potential falls off rapidly enough as $|z|\to\infty$, the asymptotic behaviour of the $f_N^m$ will be that of free wave functions

$$f_N^m(z) \underset{|z|=\infty}{\to} e^{\pm ik_N z} \qquad k_N = (2m_e/\hbar^2)^{\frac{1}{2}}(\varepsilon-(N+\tfrac{1}{2})\hbar\omega_c)^{\frac{1}{2}} \qquad \varepsilon>(N+\tfrac{1}{2})\hbar\omega_c \tag{3.2.7a}$$

$$f_N^m(z) \underset{|z|=\infty}{\to} e^{\pm k_N z} \qquad k_N = (2m_e/\hbar^2)^{\frac{1}{2}}((N+\tfrac{1}{2})\hbar\omega_c-\varepsilon)^{\frac{1}{2}} \qquad \varepsilon<(N+\tfrac{1}{2})\hbar\omega_c \tag{3.2.7b}$$

For convenience we shall henceforward follow Ohtaka and Kondo (1977) and say that we have an open channel (OC) when the wave function is asymptotically wavelike as in (3.2.7a), and that the channel is closed (CC) when the wave function is asympototically exponential as in (3.2.7b). Then the general scattering problem will take place at an energy $\varepsilon$ such that the first few channels are open, up to a maximum value P, and all the rest are closed.

If we want to calculate the scattering out of the free state $|N,m,+k_N\rangle$ (where N is an OC), we have to take boundary conditions on $\Psi$ such that as $z\to-\infty\Psi$ consists of the incoming free state $|N,m,+k_N\rangle$ and several outgoing free states $|M,m,-k_M\rangle$ (where M are OC's), and as $z\to+\infty\,\psi$ consists of outgoing free states $|M,m,+k_M\rangle$. The appropriate boundary conditions on the $f^m_M$ to achieve this are tabulated below.

$$
\begin{aligned}
f^m_{NN} \to\ & z=-\infty \ : \ L^{-\frac{1}{2}}R^m_{NN}e^{-ik_Nz} + L^{-\frac{1}{2}}e^{+ik_Nz} \\
& z=+\infty \ : \ L^{-\frac{1}{2}}T^m_{NN}e^{+ik_Nz} \\
f^m_{MN} \to\ & z=-\infty \ : \ L^{-\frac{1}{2}}R^m_{MN}e^{-ik_Mz} \qquad (M\ OC, \neq N) \\
& z=+\infty \ : \ L^{-\frac{1}{2}}T^m_{MN}e^{+ik_Mz} \\
f^m_{MN} \to\ & z=-\infty \ : \ L^{-\frac{1}{2}}R^m_{MN}e^{k_Mz} \qquad (M\ CC) \\
& z=+\infty \ : \ L^{-\frac{1}{2}}T^m_{MN}e^{-k_Mz}
\end{aligned}
\qquad (3.2.8)
$$

The solutions in the OCs consist only of outgoing travelling waves apart from channel N, which has its incoming wave normalised in a box of length L. The solutions in the CCs decay exponentially to zero as $|z|\to\infty$. The f's have acquired an extra index to show which is the incoming state.

The situation is illustrated schematically in Fig. 3.1.

Taking eqn. (3.2.3) for $\psi^m$, we see that asymptotically the full wave function has been decomposed into free Landau states as desired

$$\Psi^+_{Nm+k_N}(\underline{r}) \rightarrow \begin{array}{ll} z=-\infty : & \sum_{OC} R^m_{MN}\Psi^o_{Mm-k_M}(\underline{r}) + \Psi^o_{Nm+k_N}(\underline{r}) \\ z=+\infty : & \sum_{OC} T^m_{MN}\Psi^o_{Mm+k_M}(\underline{r}) \end{array} \qquad (3.2.9)$$

The wave function $\Psi$ has been given a + superscript to indicate that it is the outgoing solution which would be obtained by using the causal Green's function for the scattering problem (see Roman 1965). Essentially, this means that if we formed a wave packet from $\Psi^+$ states it would have the desired behaviour of approaching the scatterer as a single wave packet from $z=-\infty$, $t=-\infty$, and being scattered into several outgoing wave packets as $t\rightarrow+\infty$(Gell-Mann and Goldberger, 1953). This is illustrated in Fig. 3.2.

We may now obtain the elements of the scattering operator or t matrix introduced by Lippmann and Schwinger (1950), in terms of which the exact transition rate from one state to another is expressed. The expression for the t-matrix element is

$$\langle M,m,\pm k_M|t^+|N,m,+k_N\rangle = \int \underline{d^3r}\,\Psi^{o*}_{Mm\pm k_M}(\underline{r})V(\underline{r})\Psi^+_{Nm+k_N}(r) \qquad (3.2.10)$$

The integrations in $\rho$ and $\phi$ are simply performed to give

$$\langle M,m,\pm k_M|t^+|N,m,+k_N\rangle = L^{-\frac{1}{2}}\int_{-\infty}^{\infty} dz e^{\mp ik_M z}\{\sum_{N'=0}^{\infty} V^m_{MN'}(z) f^m_{N'N}(z)\} \qquad (3.2.11)$$

By refering to the Schrödinger equation (3.2.5) the quantity in brackets may be re-expressed as a differential operator acting on $f^m_{MN}(z)$,

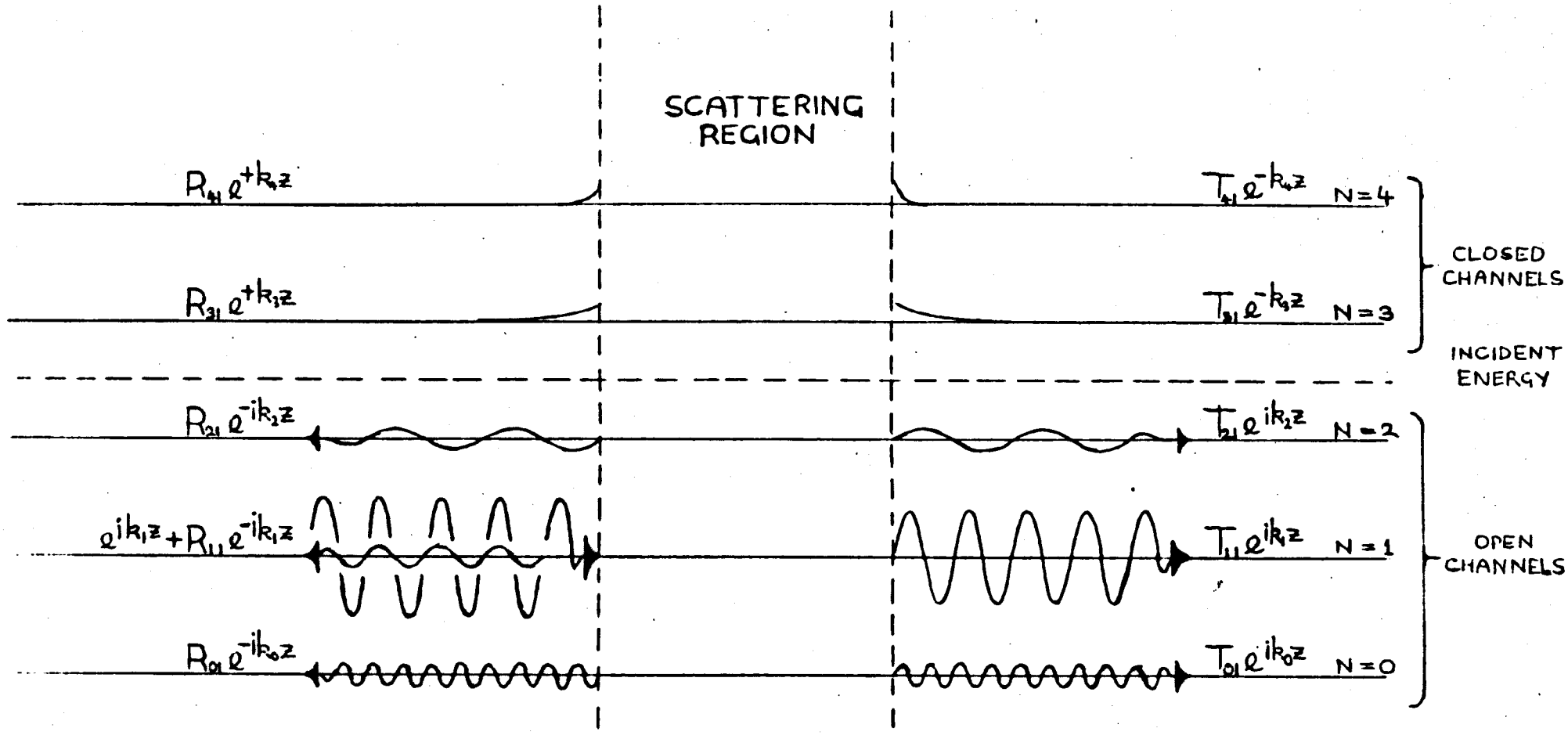


Fig. 3.1: Schematic of the longitudinal dependence of a stationary scattering state in a magnetic field. A wave of unit intensity is incident in the N = 1 channel

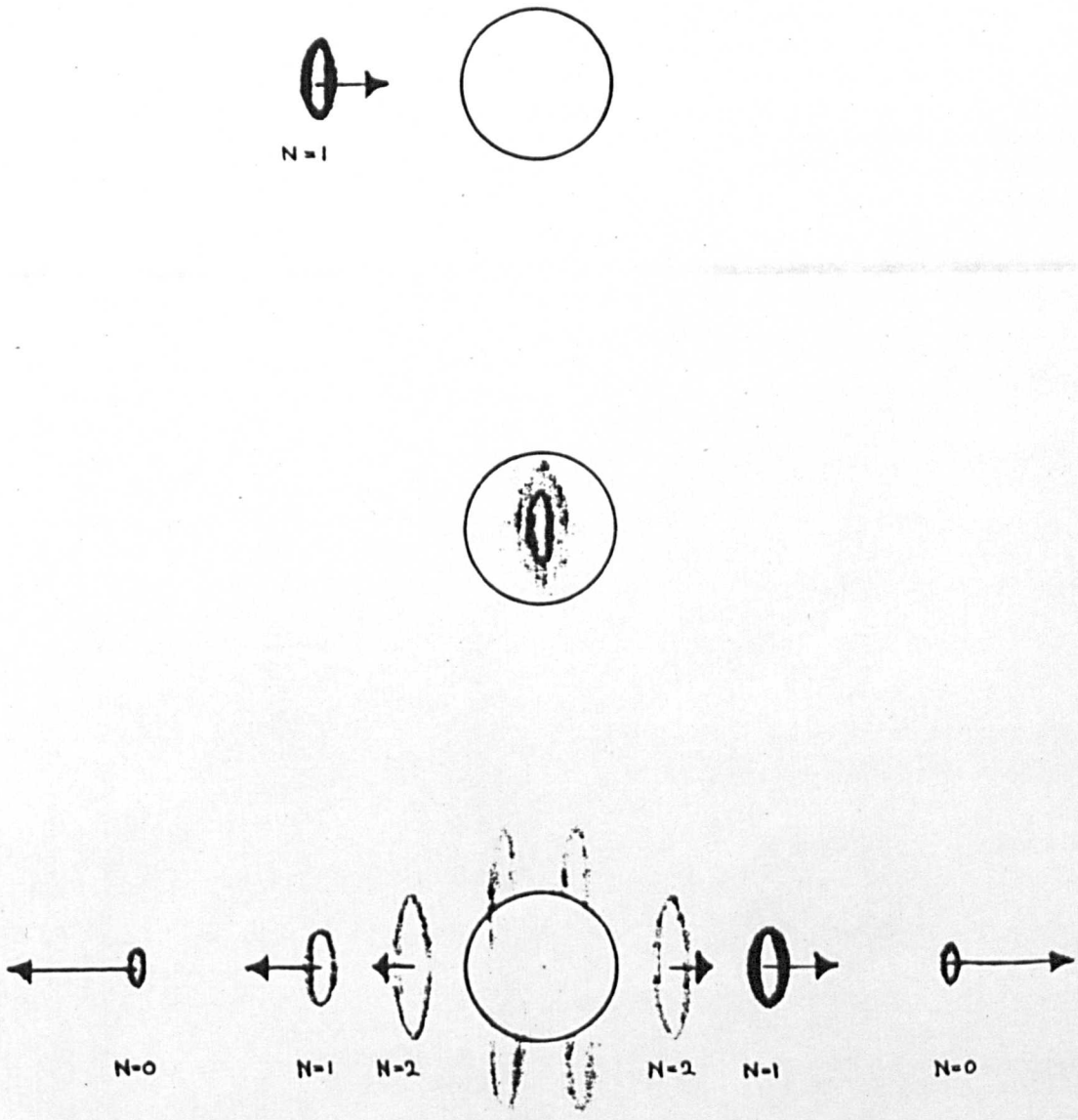


Fig. 3.2 : Schematic of the scattering of an axially symmetric wave packet in the N = 1 channel

after which we may use Green's theorem in one dimension to convert the integral to an evaluation of surface terms at $z=\pm\infty$. From these we obtain

$$\langle M,m,-k_M|t^+|N,m,+k_N\rangle = (i\hbar^2 k_M/m_e L)R^m_{MN} \qquad \text{(all OCs)}$$

$$\langle M,m,+k_M|t^+|N,m,+k_N\rangle = (i\hbar^2 k_M/m_e L)T^m_{MN} \qquad \text{(OCs, } M\neq N\text{)} \qquad (3.2.12)$$

$$\langle N,m,+k_N|t^+|N,m,+k_N\rangle = (i\hbar^2 k_N/m_e L)(T^m_{NN}-1)$$

At this point it is appropriate to discuss the form and physical interpretation of the separated Schrödinger eqn. (3.2.5). If the off-diagonal coupling terms are ignored we have the adiabatic approximation of Schiff and Snyder (1939), where the potential seen by an electron is taken to be an average of the full potential over the radial part of the wave function:

$$V^m_{NN}(z) = \int_0^\infty 2\pi\rho d\rho |\phi^m_N(r)|^2 V(\rho,z) \qquad (3.2.13)$$

The simplest case occurrs when the potential $V(\underline{r})$ is of finite range and flat bottomed, so that for each z V is some constant $V_o$ for $\rho<R(z)$ and zero for $\rho>R(z)$, whence

$$V^m_{NN}(z) = V_o\int_o^{R(z)} 2\pi\rho|\phi^m_N(r)|^2 d\rho \triangleq V_o I^m_{NN}(R(z)) \qquad (3.2.14)$$

Clearly $I^m_{NN}(R)$ so defined is zero for small R and unity for large R, changing most rapidly where $\rho|\phi^m_N(r)|^2$ is largest. Taking N=0 as an example, the maximum of $\rho|\phi^m_o(r)|^2$ occurrs at $\rho=\ell(2m+1)^{\frac{1}{2}}$, so that for values of z such that $R(z)<<\ell(2m+1)^{\frac{1}{2}}$ we have $V^m_{oo}(z)\sim 0$, and when $R(z)>>\ell(2m+1)^{\frac{1}{2}}$ $V^m_{oo}(z)\sim V_o$. Thus for a potential whose maximum radius is $R_{max}$ it will be possible to

ignore collisions with m much greater than $R_{max}^2/2\ell^2$ as far as 0-0 scattering is concerned, because of the smallness of $V_{oo}^m$. For N>0 $\rho|\phi_N^m(r)|^2$ has more than one turning point, and for large N an analytic formula for the positions of the peaks is not available. However, we can say that, for fixed N, the region of maximum contribution will be around $\rho = \ell m^{\frac{1}{2}}$, and for fixed m a region around $\rho = \ell N^{\frac{1}{2}}$ is important. This is illustrated in Fig. 3.3 where $I_{NN}^m(R)$ is plotted for low values of m and N. The net effect is that for finite ranged, flat bottomed potentials only a finite number of N and m values are significant in the diagonal elements of V.

The form of $V_{NN}^m$ as a function of z depends crucially on the shape of the potential. The simplest case of all is a cylindrical potential with its axis along the field direction, for which all the elements of V are constant along the length of the potential, and zero outside its range. This model will be investigated in §3.4. For the spherical square well, in which we shall be interested later, $V_{NN}^m$ does not have such a simple form. However, if the radius a of the sphere is much larger than the Landau length $\ell$,then for small N and m $V_{NN}^m(z)$ will be approximately a square well of depth $V_o$ and length 2a. This is shown in Fig. 3.4 where $V_{NN}^m(z)$ is plotted for the first few N values.

It is less easy to make general statements about potentials which extend to infinity. In this case $V_{NN}^m$ is given by

$$V_{NN}^m(z) = \int_0^\infty 2\pi\rho|\phi_N^m(r)|^2 V(\rho,z)\,d\rho \qquad (3.2.15)$$

For the region where $|z|$ is much larger than the radius at which $\rho|\phi_N^m(r)|^2$ is maximum, we may approximate $V(\rho,z)$ by $V(o,z)$, so that asymptotically $V_{NN}^m(z) \sim V(o,z)$. Thus, for example, the elements of V for an

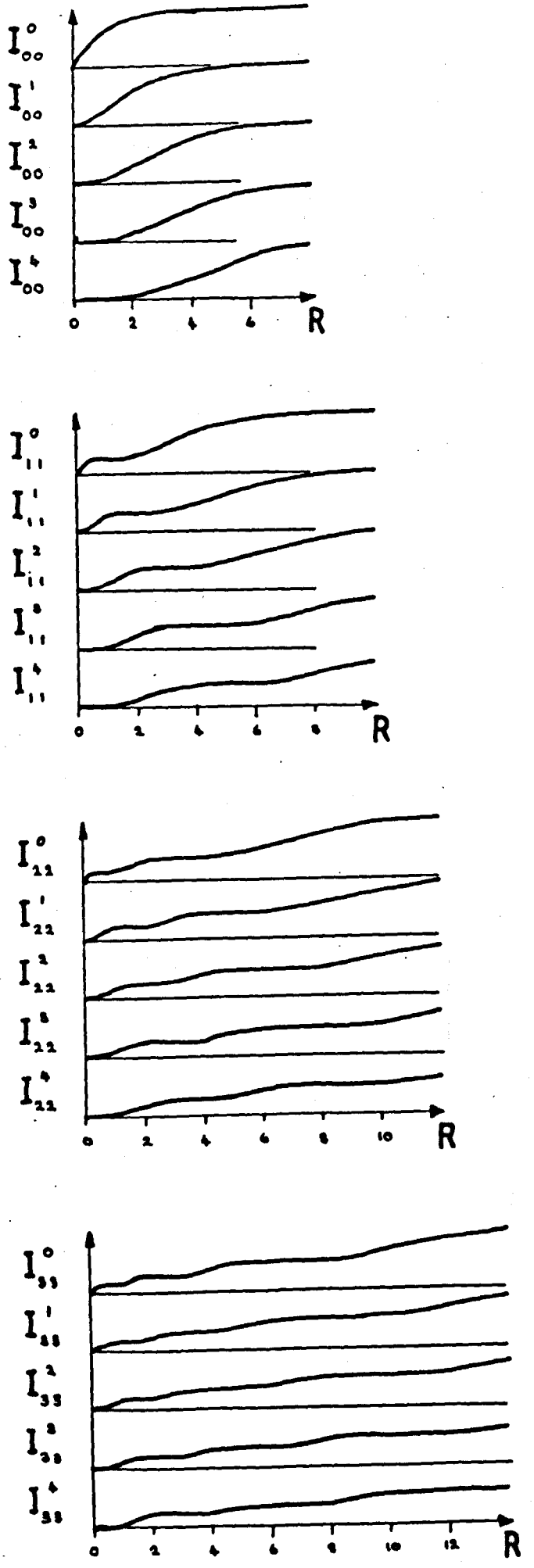


Fig. 3.3 The diagonal potential integrals $I^m_{NN}(R)$

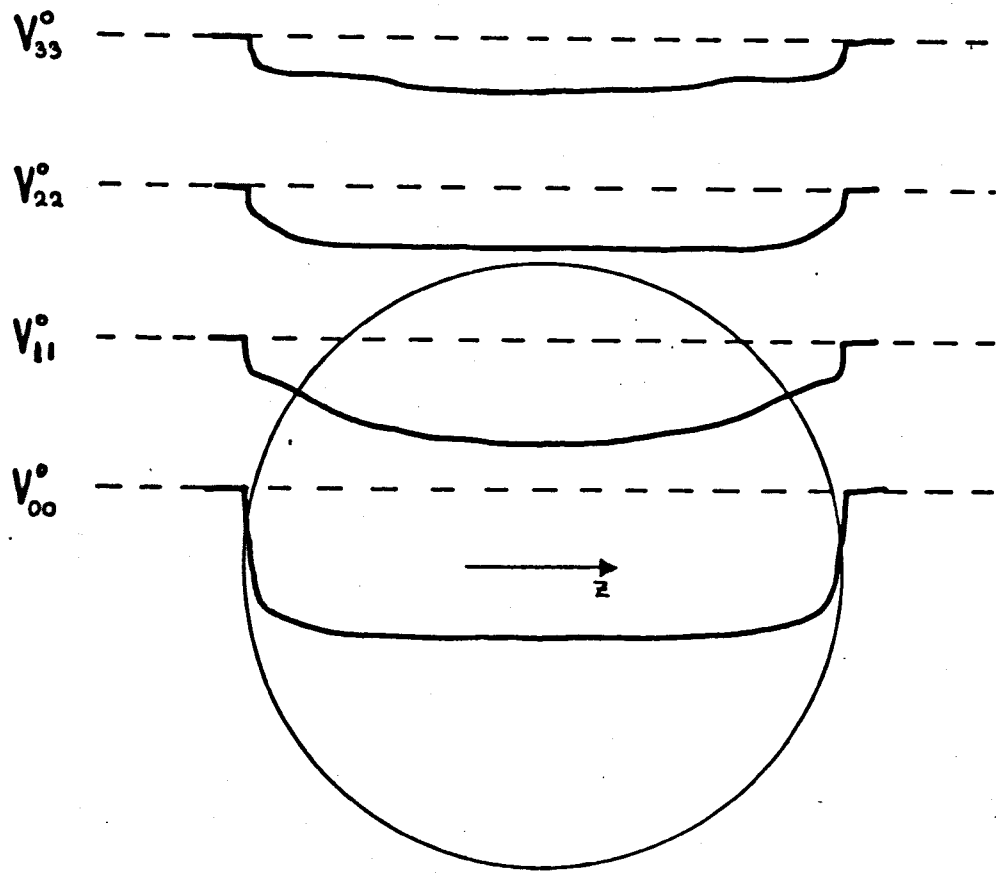


Fig. 3.4 : The diagonal effective scattering potentials $V^{\circ}_{NN}(z)$ for a spherical square well of radius : Landau length ratio a/l = 4

unscreened coulomb potential will fall off as $1/|z|$. In this case the asymptotic form of the function $f_N^m(z)$ is not $e^{\pm ik_N z}$, as before, but $e^{\pm i(k_N z+\alpha \log z)}$, as may be shown by using the WKB approximation. There is also a difficulty in deciding how many m and N values are needed, since although the magnitude of $V_{NN}^m(z)$ still decreases as m and N increase, the range of z over which it is still a significant proportion of its maximum value is increased. This is directly analagous to the situation when the magnetic field is zero, for which the scattering cross section is known to be infinite (see, e.g., Mott and Massey, 1969). A discussion of the potential matrix elements and resulting wavefunctions in the adiabatic approximation is given by Elliott and Loudon (1969).

We can deduce the behaviour of the off-diagonal elements of V in a similar manner. For a flat bottomed potential we now have

$$V_{NM}^m(z) = V_o \int_o^{R(z)} 2\pi\rho \, \phi_N^m(r)\phi_M^m(r) d\rho \triangleq V_o I_{NM}^m(R(z)) \qquad (3.2.16)$$

Now $I_{NM}^m(R)$ will tend to zero for large as well as small R, because of the orthogonality (2.1.24) of the radial wave functions. Between these two asymptotic regions it will be maximum at a point determined by m, N and M, and may be negative in some regions. In Fig. 3.5 we plot some of these functions for certain low values of m, N and M.

Returning to the example of a spherical square well, if $a >> \ell$ and m is small the only places where the coupling $I_{01}^m(z)$ is significant are around $|z|=a$, it being very small both outside and inside these points. If m is increased to $O(a^2)$, corresponding to grazing incidence on the sphere, the coupling is significant over the whole range $|z|<a$. This is illustrated in Fig. 3.6 where $V_{NM}^m(z)$ is plotted for a spherical square well. Thus it appears that the inter-channel scattering is dominated by m values corresponding in some sense to grazing incidence, while the intra channel

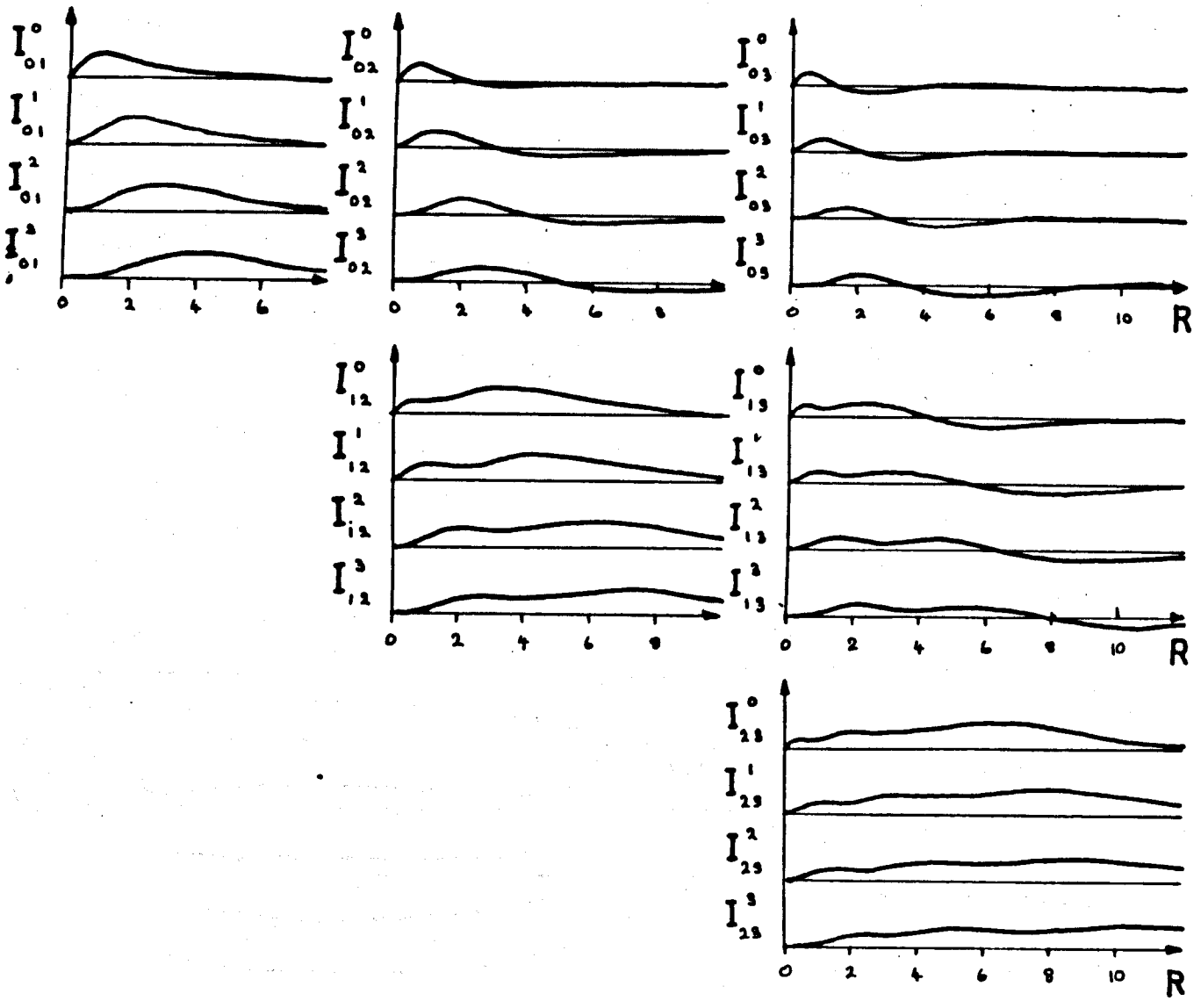


Fig. 3.5 The off-diagonal potential integrals $I^m_{NM}(R)$

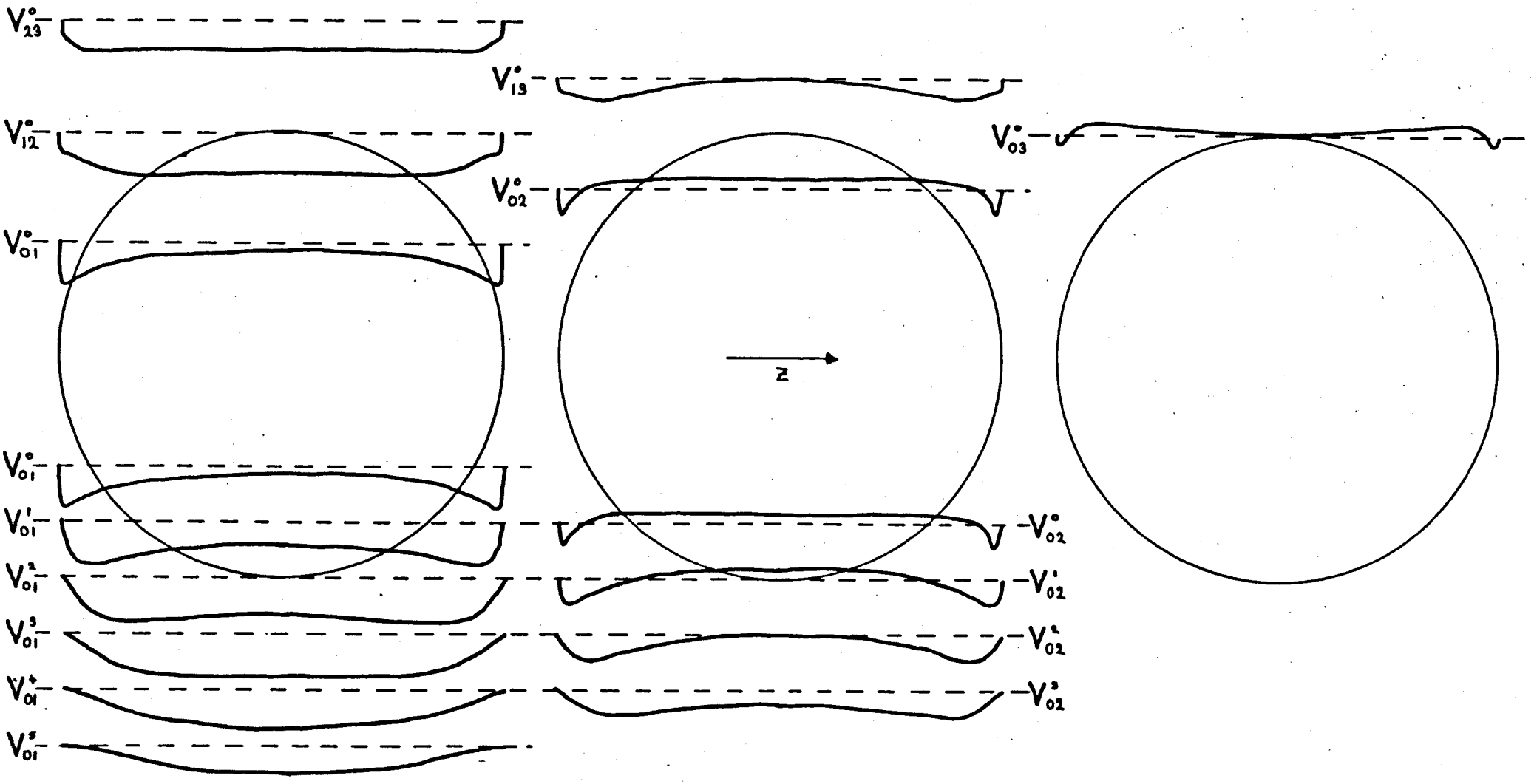


Fig. 3.6 The off-diagonal coupling potentials $V^{m}_{NM}(z)$ for a spherical square well, $a/\ell = 4$

scattering is strongest for lesser values of m.

An interesting phenomenon is the occurrence of resonances below the bottom of Landau bands with N>0. In many cases $V^m_{NN}(z)$ will be a potential well which, if considered as a potential for a one-dimensional problem, would have one or more bound states. When we consider the full set of coupled equations (3.2.5) there will no longer be a true bound state at these positive energies, but if the couplings $V^m_{NM}(z)$ to the open channels M are all small a resonant effect due to a 'nearly bound' state will occurr. This will be discussed further in §3.3 and §3.4 below.

We now return briefly to the more general properties of the Schrödinger equation (3.2.5). The analogy with the one-dimensional Schrödinger equation is so strong that it is a relatively simple task to generalise some important results in that theory to apply here. Firstly we have the property of conservation of particles

$$k_N = \sum_{OC} k_M (|R_{MN}|^2 + |T_{MN}|^2) \qquad (3.2.17)$$

in which the incoming particle flux in channel N equals the outgoing flux summed over all the open channels. Secondly, time reversal symmetry applies

$$\langle M,m,k_M|t^+|N,m,k_N\rangle = \langle N,m,-k_N|t^+|M,m,-k_M\rangle \qquad (3.2.18)$$

and finally, if $V(\rho,z) = V(\rho,-z)$ we also have inversion symmetry

$$\langle M,m,k_M|t^+|N,m,k_N\rangle = \langle M,m,-k_M|t^+|N,m,-k_N\rangle \qquad (3.2.19)$$

An elegant proof of these results is given in Appendix 2, in which we generalise the methods given by Messiah (1964) in order to develop a Wronskian theorem for sets of coupled equations such as (3.2.5).

Finally, we shall briefly discuss the exact scattering problem when $V(\underline{r})$ is a negative three dimensional $\delta$ function potential:

$$V(\underline{r}) = -V_o\delta^3(\underline{r}) = \lim_{a\to o} - V_o(2\pi a^2)^{-1}e^{-\rho^2/2a^2}\delta(z) \qquad (3.2.20)$$

The $\delta$ integral for the potential matrix elements may be performed to give

$$V^m_{MN}(z) = -V_o\phi^m_M(0)\phi^m_N(0)\delta(z) = -\ell^{-2}V_o\delta_{mo}\delta(z) \qquad (3.2.21)$$

so that scattering only takes place for states with zero angular momentum. The Schrödinger equation is

$$-(\hbar^2/2m_e)f^{o\,\prime\prime}_N - (\varepsilon-(N+\tfrac{1}{2})\hbar\omega_c)f^o_N = \ell^{-2}V_o\sum_{M=0}^{\infty} f^o_M\delta(z) \qquad (3.2.22)$$

The asymptotic equations (3.2.8) now give the exact form for the f's in the two regions $z<o$ and $z>o$. At $z=o$ $f^o_N(z)$ is continuous, and the matching condition on the derivatives is given by integrating (3.2.22) through a small region containing $z=o$.

$$-(\hbar^2/2m_e)\{f^{o\,\prime}_N\}^{o+}_{o-} = \ell^{-2}V_o\sum_{M=0}^{\infty} f^o_M(0) \qquad (3.2.23)$$

We then find that all the t-matrix elements of (3.2.12) are equal to a single constant t, given by the implicit equation

$$t = -(V_o/L\ell^2)\{1 - (m_eL/\hbar^2)t(i\sum_{oc}k_M^{-1} + \sum_{cc}k_M^{-1})\} \qquad (3.2.24)$$

which is easily solved to give:

$$t = -(V_o/L\,\ell^2)\{1 + (m_eV_o/\hbar^2\ell^2)(i\sum_{oc}k_M^{-1} + \sum_{cc}k_M^{-1})\}^{-1} \qquad (3.2.25)$$

This is very similar to the expressions obtained by Kahn (1960), Bychkov (1961), and more recently by Gerhardts and Hajdu (1971). Also as

in their results, it suffers from a divergence of the $\sum_{cc} k_M^{-1}$ term in the denominator. The conclusion must be that the exact scattering is zero for a true 3-D δfunction potential. If the potential is of a finite size $a \ll \ell$ , however, the integral for $V_{MN}$ is no longer of such a simple form, and we must rather write $V^m_{MN}(z) = -\ell^{-2} V^m_{MN} \delta(z)$. For low values of M, N and m the wave functions $\phi^m_M(r)$ are smooth in comparison to the potential, and $V^m_{MN}(z)$ is given by (3.2.19) as before. For very large values of M, N or m, however, the potential is smoother than the wave function and the quantities $V^m_{MN}$ become small. The solution of the Schrödinger equation (3.3.20) is then no longer obtainable in analytic form, but may be approximated as follows. For m=0 we suppose that for M, N larger than some cut-off value $N_o$ (determined by $\ell/a$, and much greater than P, the highest OC) the $V^o_{MN}$ may be neglected, whereas for N, $M \leq N_o$ the t-matrix elements are all equal. This leads to

$$t \sim -(V_o/L\ell^2)\{1 + (m_e V_o/\hbar^2 \ell^2)(i \sum_{oc} k_M^{-1} + \sum_{cc<N_o} k_M^{-1})\}^{-1} \qquad (3.2.26)$$

Where there is now no divergence. This is similar to the aforementioned results, but differs in that we have cut off the summation at $M=N_o$ rather than M=P, giving an additional real part in the denominator of t.

## 3.3 Approximate Methods

The infinite set of coupled differential equations (3.2.5) is in practice impossible to solve analytically, and we must therefore develop approximation schemes which make the problem tractable. Our aim will be to derive expressions for the t-matrix elements which approximate closely the exact formula (3.2.10).

The simplest, and hence most useful, approximation for the t-matrix element is to replace the exact solution $\Psi^+$ by the corresponding free wave function $\Psi^o$ in the integral of (3.2.10). This is the familiar Born Approximation, which has been exhaustively discussed elsewhere (cf Mott and Massey, 1950), and which is almost invariably used in transport problems of the type we shall be discussing (see, e.g., Argyres (1959), Eaves et al (1977). This procedure gives for the t-matrix element

$$\langle M,m,\pm k_M|t|N,m,+k_N\rangle_{BA} = \int d^3\underline{r}\,\Psi^{o*}_{Mm\pm k_M} V(\underline{r})\Psi^o_{Nm+k_N} \qquad (3.3.1)$$

The accuracy of the above expression depends on our being able to neglect the scattered part of the wave function $\Psi^+$ in comparison with the unperturbed part $\Psi^o$. Hence an estimate of the size of the scattered part of the wave function is necessary to determine the validity of the Born Approximation; such an estimate will be generated by the Green's function analysis which follows.

We seek Green's functions for the solution of the scattering Schrödinger equation

$$-\hbar^2/2m_e f^{m\prime\prime}_N(z) - (\varepsilon-(N+\tfrac{1}{2})\hbar\omega_c) f^m_N(z) = -\sum_{M=0}^{\infty} V^m_{NM}(z) f^m_M(z) \qquad (3.3.2)$$

If we regard the left hand side of this equation as the homogeneous part, then the appropriate Green's function for scattering boundary conditions is easily obtained by solving

$$-(\hbar^2/2m_e)\partial^2/\partial z^2 G_N^{mo+}(\varepsilon;z,z') - (\varepsilon-(N+\tfrac{1}{2})\hbar\omega_c) G_N^{mo+}(\varepsilon;z,z') = \delta(z-z') \tag{3.3.3}$$

with the boundary condition:

$$G_N^{mo+}(\varepsilon;z,z') \underset{|z|\to\infty}{\alpha} e^{ik_N|z|} \qquad \text{(Open channel)} \tag{3.3.4a}$$

$$e^{-k_N|z|} \qquad \text{(Closed channel)} \tag{3.3.4b}$$

The appropriate solutions are

$$G_N^{mo+}(\varepsilon;Z,Z') = im_e/\hbar^2 k_N e^{ik_N|z-z'|} \qquad \text{(Open channel)} \tag{3.3.5a}$$

$$m_e/\hbar^2 k_N\, e^{-k_N|z-z'|} \qquad \text{(Closed channel)} \tag{3.3.5b}$$

that is; a purely outgoing wave for an open channel, and an exponentially decaying solution for a closed channel. We can now use the right hand side of (3.3.2) as an inhomogenous part to derive the following integral equation for the $f_N^m(z)$:

$$f_N^{m+}(Z) = f_N^{m(o)}(z) - \int_{\infty}^{\infty} dz' G_N^{mo+}(\varepsilon;z,z') \sum_{M=0}^{\infty} V_{NM}^m(z') f_M^{m+}(z) \tag{3.3.6}$$

where $f_N^{mo}$ is a solution of the homogeneous part of the equation. If the scattering potential is in some sense a small perturbation to the set of equations, we can use (3.3.6) as a basis for iteration. Thus if we wish to solve the problem of scattering from the state $|Nm+k_N\rangle$ to some other open channel, the zeroth order approximation will be an unperturbed travelling wave $f_{NN}^{m(o)} = e^{ik_N z}$ in the N channel only. Iterating once, we

obtain the first order approximation

$$f^{m(1)}_{NN} = e^{ik_N z} - \int_{-\infty}^{\infty} dz' G^{mo+}_N(\varepsilon;z,z') V^m_{NN}(z') e^{ik_N z'}$$

$$f^{m(1)}_{MN} = -\int_{-\infty}^{\infty} dz' G^{mo+}_M(\varepsilon;z,z') V^m_{MN}(z') e^{ik_N z'} \qquad (3.3.7)$$

When z is large $V_{MN}(z')$ is significantly different from zero only for $z'<z$, and hence (3.3.5a) may be used to derive the asymptotic expression

$$f^{m(1)}_{MN} \underset{z\to\infty}{=} -im_e/\hbar k_M \int_{\infty}^{\infty} e^{-ik_M z'} V^m_{MN}(z') e^{ik_N z'} dz' \; e^{ik_M z} \qquad (3.3.8)$$

This asymptotic expression for the wave function yields the first order approximation to the t-matrix element on using (3.2.12):

$$\langle Mmk_M | t | Nmk_N \rangle^{(1)} = \int \underline{d^3 r} \Psi^{o*}_{Mmk_M} V(\underline{r}) \Psi^{o}_{Nmk_N} \quad M\neq N \qquad (3.3.9)$$

Thus we have formally derived the Born Approximation of (3.3.1) as the first order term in a perturbation scheme based on the Green's function for free propagation in the magnetic field. Inside the potential we may use (3.3.7) to show that the first order correction to the wave function is of order $V^m_{NN}\,(\varepsilon-(N+\tfrac{1}{2})\hbar\omega_c)^{-1}$ in channel N and $V^m_{MN}/(N-M)\hbar\omega_c$ in the other channels. As far as propagation within a channel is concerned the Born Approximation therefore works well for high energies or shallow, short-ranged potentials. For inter-channel scattering the coupling must be small or the inter-channel energy large.

Continued iteration of (3.3.6) leads to the Born series for $f^+$:

$$f^{m+}_{MN}(z) = f^{m(1)}_{MN}(z) + f^{m(2)}_{MN}(z) + f^{m(3)}_{MN}(z) + \qquad (M\neq N) \qquad (3.3.10)$$

where

$$f_{MN}^{m(2)}(z) = (-1)^2 \int_{-\infty}^{\infty} dz'' dz' G_M^{mo+}(z,z') \sum_{M'=0}^{\infty} V_{MM'}^m(z') G_{M'}^{mo+}(z',z'') V_{M'N}^m(z'') e^{ik_N z}$$

(3.3.11)

If the energy is high enough or the potential shallow enough that the Born series converges, it will generally be acceptable to use the simple Born Approximation in describing the scattering. One may, however, foresee circumstances in which the Born series converges slowly if at all. We will distinguish two cases worthy of special attention, the first being when the difficulty is caused by a sub-set of terms of the form $\{V_{MM}+V_{MM}^2+V_{MM}^3+ \ldots\}$ (strong intra-channel scattering), and the second being when a sub-set of terms of the form $\{V_{MN}^2+V_{MN}^4+V_{MN}^6+ \ldots\}$ causes trouble (strong inter-channel scattering).

When strong intra-channel scattering is present convergence may be improved by treating propagation within each channel exactly with respect to the diagonal part of the potential. The new Green's function for this exact propagation is obtained by solving

$$-\hbar^2/2m_e \partial^2/\partial z^2 G_N^{m+}(\varepsilon;z,z') - [\varepsilon-(N+\tfrac{1}{2})\hbar\omega_c - V_{NN}^m(z)] G_N^{m+}(\varepsilon;z,z') = \delta(z-z')$$

(3.3.12)

subject to the same outgoing wave boundary conditions (3.3.4) as before. The free propagator $G^o$ may be used to derive an integral equation for the full propagator $G$:

$$G_N^{m+}(\varepsilon;z,z') = G_N^{mo+}(\varepsilon;z,z') - \int_{-\infty}^{\infty} G_N^{mo+}(\varepsilon;z,z'') V_{NN}^m(z'') G_N^{m+}(\varepsilon;z'',z) dz''$$

(3.3.13)

This equation may be formally iterated to derive the usual Born expansion for $G$:

$$G^{+} = G^{o+} - G^{o+}V_{NN}G^{o+} + G^{o+}V_{NN}G^{o+}V_{NN}G^{o+} \ldots \qquad (3.3.14)$$

showing that the use of $G^{+}$ amounts to a resummation of the slowly convergent terms in the previous Born series.

It is also necessary to obtain an improved zero'th order approximation to the wave function $f_{NN}$ by again taking $V_{NN}$ into account exactly and solving

$$-\hbar^2/2m_e f_{NN}^{m(o)''}(z) - \left[\varepsilon-(N+\tfrac{1}{2})\hbar\omega_c - V_{NN}^{m}(z)\right]f_{NN}^{m(o)}(z) = 0 \qquad (3.3.15)$$

subject, naturally, to appropriate scattering boundary conditions. The Born series for $f_{MN}^{+}$ is of the same form (3.3.10) as before, but now

$$f_{MN}^{m(1)}(z) = -\int_{-\infty}^{\infty} G_M^{m+}(\varepsilon;z,z')V_{MN}^{m}(z')f_{NN}^{m(o)}(z')dz' \qquad (M\neq N) \qquad (3.3.16)$$

$$f_{MN}^{m(2)}(z) = (-1)^2\int_{-\infty}^{\infty}\int G_M^{m+}(\varepsilon;z,z'')\sum_{N'\neq M,N} V_{MN'}^{m}(z'')G_{N'}^{m+}(\varepsilon;z'',z')V_{N'N}^{m}(z')f_{N}^{m(o)}(z')dz'dz'' \qquad (3.3.17)$$

The convergence of the resummed Born series now depends only on the inter-channel matrix elements of $V$, which may be small in situations of interest. The price to be paid for this improved convergence is the introduction of the functions $G^{+}$ and $f^{(o)}$ for which analytical expressions may no longer be obtainable. The WKB approximation is not adequate to provide approximate expressions for $G^{+}$ and $f^{(o)}$, as it ignores backscattering by the potential. The Bremmer series (Bremmer, ), however, of which the WKB approximation is the first term, does take the backscattering into account and should give appropriate approximations for $G^{+}$ and $f^{(o)}$, while

if necessary powerful methods of numerical integration are available for differential equations such as (3.3.12) and (3.3.15). We shall not pursue these difficulties further here.

A further problem which may arise in a closed channel is that of divergence of the exact propagator $G^+$ at certain energies due to the presence of a bound state of the diagonal element of the potential. This divergence may only be removed by coupling to channels which are open at the same energy. Thus in calculating the effect of a closed channel on the scattering between the open channels at or near a bound state energy for the closed channel, it is necessary to solve simultaneously the Schrödinger equations (3.3.2) for these three channels, though coupling terms to other channels may be ignored to lowest order. This situation is investigated in the next section for a simple cylindrical potential.

Finally, we mention the case where strong inter-channel scattering is present, so that the interaction between some channels must be taken into account exactly; such may be the case for two channels near grazing incidence, for example. The Green's function now becomes off diagonal in the channel number, so that instead of (3.3.6) we have the integral equation

$$f_N^{m+}(z) = f_N^{m(o)}(z) - \int_{\infty}^{\infty} dz' \sum_{N'} G_{NN'}^{m+}(\varepsilon;z,z') \sum_{M} V_{N'M}^{m}(z') f_M^{m+}(z') \qquad (3.3.18)$$

If only channels $N_1$ and $N_2$ are strongly coupled the off diagonal elements of the matrix $G_{NN'}$ are zero apart from $G_{N_1N_2}$ and $G_{N_2N_1}$, and the diagonal elements apart from $N_1$ and $N_2$ are just the same as the $G_N$ previously

derived from (3.3.12). Within the $N_1, N_2$ submatrix we have

$$-\hbar^2/2m_e \partial^2/\partial z^2 G^{m+}_{NN}(\varepsilon;z,z') - (\varepsilon-(N+\tfrac{1}{2})\hbar\omega_c - V^m_{NN}(z)) G^{m+}_{NN}(\varepsilon;z,z') +$$

$$+ V^m_{NN'} G^{m+}_{N'N}(\varepsilon;z,z') = \delta(z-z') \qquad (3.3.19)$$

$$-\hbar^2/2m_e \partial^2/\partial z^2 G^{m+}_{N'N}(\varepsilon;z,z') - (\varepsilon-(N'+\tfrac{1}{2})\hbar\omega_c - V^m_{N'N'}(z)) G^{m+}_{N'N}(\varepsilon;z,z') +$$

$$+ V^m_{N'N} G^{m+}_{NN}(\varepsilon;z,z') = 0$$

where $(N,N') = (N_1,N_2)$ or $(N_2,N_1)$. If necessary simultaneous solution must also be used for the zero'th order solution $f^{m(o)}_N$. Iteration of (3.3.18) then leads to a Born series which includes the interaction between channels $N_1$ and $N_2$ exactly. The extension to a larger number of strongly coupled channels is obvious, but unwieldy.

## 3.4 Cylindrical Square Well Potentials

We now illustrate some features of the preceding theory by considering the case where the potential is flat bottomed, of depth V, and is cylindrical in shape with the axis of the cylinder lying along the direction of the magnetic field. For a cylinder of length $2\ell$ we have:

$$V^m_{MN}(z) = V^m_{MN} \quad (|z|\leq\ell) \text{ and } V^m_{MN}(z) = 0 \quad (|z|>\ell) \tag{3.4.1}$$

where the constants $V^m_{MN}$ depend on the radius a of the cylinder and the magnetic field strength. The Schrödinger equation (3.2.5) becomes:

$$-\hbar^2/2m_e f^{m\prime\prime}_N(z) - (\varepsilon-(N+\tfrac{1}{2})\hbar\omega_c - V^m_{NN}) f^m_N(z) = \sum_{M\neq N} -V^m_{NM} f^m_M(z), \quad |z|\leq\ell \tag{3.4.2}$$

$$-\hbar^2/2m_e f^{m\prime\prime}_N(z) - (\varepsilon-(N+\tfrac{1}{2})\hbar\omega_c) f^m_N(z) = 0 \quad , \quad |z|>\ell$$

Clearly the asymptotic behaviour (3.2.8) is exact for the whole region $|z|>\ell$, and it remains to find the $f^m_N$ inside the potential. The Green's function methods of §3.3 are readily applicable here, as simple analytical expressions are obtainable for $G^+$ and $f^{(o)}$ by standard methods such as are illustrated by Schiff (1968). However, a more elegant approach is possible due to the constancy of the coefficients in the Schrödinger equation.

We look for a solution in $|z|\leq\ell$ of the form:

$$f^m_N(z) = A_{N\,\sin}^{\cos}(Kz) \tag{3.4.3}$$

for some constant K, where choice of cos or sin gives an even or odd solution respectively. The form of the even solution is illustrated schematically in Fig. 3.7.

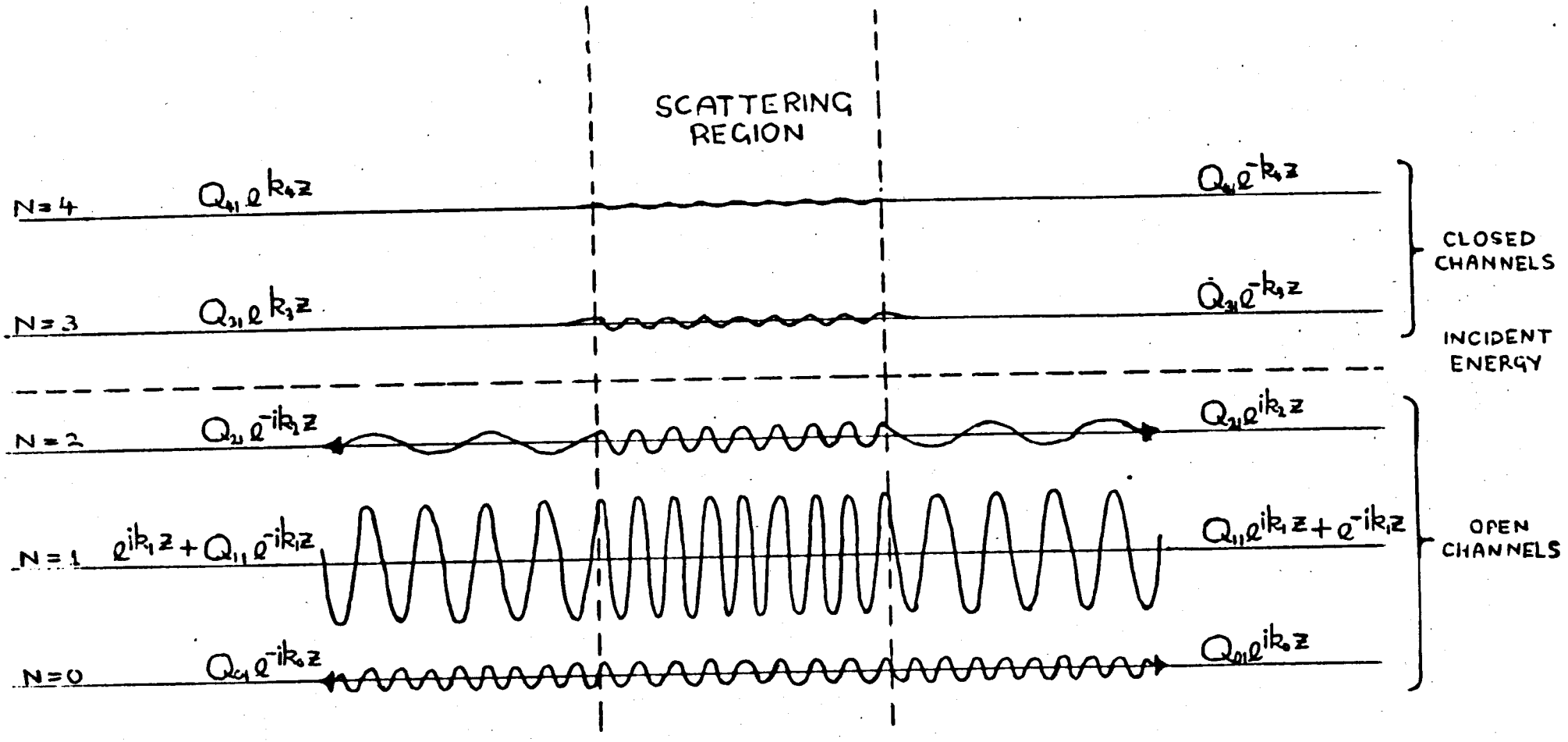


Fig. 3.7 Schematic longitudinal dependence of an even stationary scattering state, incident waves in the N = 1 channel

Substitution into (3.4.2) yields:

$$\{-\hbar^2K^2/2m_e - (\varepsilon-(N+\tfrac{1}{2})\hbar\omega_c-V^m_{NN})\}A_N + \sum_{M\neq N} V^m_{NM}A_M = 0 \qquad (3.4.4)$$

or

$$\{K^2\}\{A\} = K^2\{A\} \qquad (3.4.5)$$

where the matrix $\{K^2\}$ has the elements:

$$\{K^2\}_{NN} \equiv K^2_{NN} = 2m_e/\hbar^2((N+\tfrac{1}{2})\hbar\omega_c+V^m_{NN}-\varepsilon) \qquad (3.4.6)$$

$$\{K^2\}_{NM} \equiv K^2_{NM} = 2m_e/\hbar^2V^m_{NM} \qquad (3.4.6)$$

We have thus transformed the problem into one of finding the eigenvalues $K^2$ and the eigenvectors $\{A\}$ of the infinite matrix $\{K^2\}$. Since $\{K^2\}$ is real and symmetric, its eigenvectors will also be real. We assume without proof that there is a largest eigenvalue $K^2_o$ so that the eigenvalues may be labelled in decreasing order as $K^2_o$, $K^2_1$, $K^2_2$, . . . . and the corresponding eigenvectors as $\{A^o\}$, $\{A^1\}$, $\{A^2\}$, . . . . with $A^N_N$ chosen to be 1. The notation is convenient, for, if $\{K^2\}$ is diagonal, $K^2_N = K^2_{NN}$ and $A^N_M = \delta_{NM}$. (We also take this as our justification for the assertion that the eigenvalues may be ordered in the above manner, even when $\{K^2\}$ is non-diagonal).

We now solve for even and odd wave functions on $(0,\infty)$, assuming that channels 0 to P are open at the given energy, and that the incoming wave is in channel N. We expand the wave function in terms of the eigenvectors, so that

$$f^m_{MN}(z) = L^{-\frac{1}{2}}\sum_{L=0}^{\infty}(A^L_M \cos K_L z)\alpha^{L(E)}_N \qquad |z|\leq \ell \tag{3.4.7}$$

$$f^m_{MN}(z) = L^{-\frac{1}{2}}\{Q^{(E)}_{MN} e^{ik_M|z|} + \delta_{NM} e^{-ik_N|z|}\} \quad |z|>\ell$$

Here $\alpha^{L(E)}_N$ is the amount of the L'th eigenvector which is excited; hence the L sum is over eigenvalues rather than channel numbers. Also $K_L = (K_L^2)^{\frac{1}{2}}$ and $k_M = (2m_e/\hbar^2)^{\frac{1}{2}}(\varepsilon-(N+\frac{1}{2})\hbar\omega_c)^{\frac{1}{2}}$, with the convention that $K_L$ and $k_M$ always have positive real or imaginary parts. (Note that this is so that we may treat closed and open channels alike, whereas in §3.2 we treated them separately, as in (3.2.7)). The superscript E indicates that the even cos function has been chosen; for the odd function sin is used.

The function f and its first derivative must be continuous across $z = \ell$, whence we obtain the matching conditions:

$$\delta_{NM} e^{-ik_N\ell} + Q^{(E)}_{MN} e^{ik_M\ell} = \sum_{L=0}^{\infty} A^L_M \cos K_L \ell . \alpha^{L(E)}_N \tag{3.4.8}$$

$$ik_M(-\delta_{NM} e^{-ik_N\ell} + Q^{(E)}_{MN} e^{ik_M\ell}) = -\sum_{L=0}^{\infty} A^L_M \sin K_L \ell . K_L \alpha^{L(E)}_N$$

Eliminating the Q's, we obtain a matrix equation for the $\alpha$'s:

$$\sum_{L=0}^{\infty} A^L_M(\cos K_L\ell - i(K_L/k_M)\sin K_L\ell)\alpha^{L(E)}_N = \delta_{NM} 2e^{-ik_N\ell} \tag{3.4.9}$$

This may be re-expressed as

$$\{\alpha^{(E)}_N\} = \sum_L \{A^{(E)}\}^{-1}_{ML}\{\delta_{LN} 2e^{-ik_N\ell}\} \tag{3.4.10}$$

Here the matrix $\{A^{(E)}\}$ is defined by $\{A^{(E)}\}_{ML} = A^L_M(\cos K_L\ell - i(K_L/k_M)\sin K_L\ell)$, $\{\alpha^{(E)}_N\}$ is the column vector of eigenvector coefficients for scattering from the N channel and $\{\delta_{LN} e^{-ik_N\ell}\}$ is a column vector which is non-zero

only in its N'th row. Using the Cramer formula for $\{A^{(E)}\}^{-1}$ we obtain:

$$\alpha_N^{L(\varepsilon)} = (-1)^{L+N} 2e^{-ik_N \ell} ||A^E_{(N,L)}||/||A^E|| \tag{3.4.11}$$

where $\{A^E_{(N,L)}\}$ is the matrix obtained by deleting the N'th row and the L'th column from $\{A^E\}$. Therefore, from (3.4.8), the Q's are given by:

$$Q_{MN}^{(E)} = \tfrac{1}{2} \sum_{L=0}^{\infty} A_M^L (\cos K_L \ell + i(K_L/k_M)\sin K_L \ell)(-1^{L+N}||A^E_{(N,L)}||e^{-i(k_M+k_N)\ell}.2/||A^E|| \tag{3.4.12}$$

or:

$$Q_{MN}^{(E)} = e^{-i(k_M+k_N)\ell}||B^E_{(N,M)}||/||A^E|| \tag{3.4.13}$$

where $\{B^E_{(N,M)}\}$ is the matrix obtained by replacing the N'th row of $\{A^E\}$ with $(A_M^L(\cos K_L \ell + i(K_L/k_M)\sin K_L \ell))$.

Similarly, the odd solutions are given by

$$Q_{MN}^{(o)} = e^{-i(k_M+k_N)\ell}||B^o_{(N,M)}||/||A^o|| \tag{3.4.14}$$

where the matrix $\{A^o\}$ has elements $\{A^o\}_{ML} = A_M^L(\sin K_L \ell + i(K_L/k_M)\cos K_L \ell)$ and $\{B^o_{(N,M)}\}$ is the matrix obtained by replacing the N'th row of $\{A^o\}$ with $A_M^L(\sin K_L - i(K_L/k_M)\cos K_L \ell)$.

From the form of the wave function in $|z|>\ell$ (3.4.7), we see that the required asymptotic conditions (3.2.8) are obtained by subtracting the even and odd wave functions, and hence

$$T_{MN} = \tfrac{1}{2}(Q_{MN}^{(E)} - Q_{MN}^{(o)})$$

or: (3.4.15)

$$R_{MN} = \tfrac{1}{2}(Q_{MN}^{(E)} + Q_{MN}^{(o)})$$

We have therefore arrived at a formal solution to the exact scattering problem for this potential. Difficulties still remain, however, as all the matrices $\{A\}$, $\{B\}$ and $\{K^2\}$ are infinite, and the eigenvalues of $\{K^2\}$ still have to be found.

Let us begin by evaluating the solution when $\{K^2\}$ is diagonal, corresponding to completely decoupled channels. Then $\{A\}$ is also diagonal, and hence $||B_{(N,M)}|| = 0$ from the definition of $\{B\}$, unless $N = M$. It follows readily that $||A||$ and $||B||$ then only differ in one factor, so that

$$Q^{(\varepsilon)}_{MN} = \delta_{MN} e^{-2ik_N \ell} \frac{(\cos K_{NN}\ell + i(K_{NN}/k_N)\sin K_{NN}\ell)}{(\cos K_{NN}\ell - i(K_{NN}/k_N)\sin K_{NN}\ell)}$$

and (3.4.16)

$$Q^{(o)}_{MN} = \delta_{MN} e^{-2ik_N \ell} \frac{(\sin K_{NN}\ell - i(K_{NN}/k_N)\cos K_{NN}\ell)}{(\sin K_{NN}\ell + i(K_{NN}/k_N)\cos K_{NN}\ell)}$$

whence $T$ and $R$ are readily obtained. This result may, of course, be obtained by much simpler methods in this special case.

Next we consider the case when the off-diagonal inter-channel coupling terms in $\{K^2\}$ are small, so that its eigenvalues are perturbed only a little from $K^2_{NN}$. We therefore write $K^2_N = K^2_{NN} + \delta_N$ and solve the equation $||\{K^2\} - K^2\{1\}|| = 0$ to first order in small quantities, ignoring all terms of the form $(K^2_{NM}/(K^2_{NN}-K^2_{MM}))^2$ and higher order. To this order of approximation:

$$\delta_N = 0 \qquad A^N_M = K^2_{NM}/(K^2_{NN}-K^2_{MM}) = V^m_{NM}/((N-M)\hbar\omega_c + V_{NN} - V_{MM}) \qquad (3.4.17)$$

Thus the first order theory is valid if the coupling potentials are small compared with the cyclotron energy.

Substituting into eqns (3.4.14 and 15) we find that the intra channel scattering terms $Q_{NN}$ are unchanged to first order, as we would expect from the form of the Green's function expansion (3.3.16). The inter-channel scattering terms $Q_{MN}$ are now first order, and may be evaluated by picking out the first order terms in $||B_{(N,M)}||$. The expression for the even term is

$$Q_{MN}^{(E)} = ie^{-i(k_M+k_N)\ell} K_{MN}^2/2k_M \times$$

$$\times \frac{\{(K_{MM}+k_{NN})^{-1}\sin(K_{MM}+K_{NN})\ell + (K_{MM}-K_{NN})^{-1}\sin(K_{MM}-K_{NN})\ell\}}{(\cos K_{NN} - i(K_{NN}/k_N)\sin K_{NN}\ell)(\cos K_{MM}\ell - i(K_{MM}/k_M)\sin K_{MM}\ell)} \qquad (3.4.18)$$

These terms may also be obtained by evaluating the first order term (3.3.16) of the Green's function expansion.

We now investigate the effect of resonances, which have only been briefly mentioned before. A resonance occurrs at values of the energy $\varepsilon$ such that, if there were no coupling between channels, a bound state would be possible in one of the closed channels R. The condition for an even bound state under such circumstances is (see Schiff 1968)

$$(\cos K_{RR}\ell - i(K_{RR}/k_R)\sin K_{RR}\ell) = 0 \qquad (3.4.19)$$

(Bearing in mind that $k_R$ is positive imaginary). We see from (3.4.16) that this is precisely the condition for $Q_{RR}^{(E)}$ to diverge to zeroth order, as its denominator becomes zero. Since this factor appears also in $\{A^{(E)}\}$, $||A^{(E)}|| = 0$ to zeroth order at this energy, and hence in the neighbourhood of the resonance $||A^{(E)}||$ and $||B^{(E)}||$ must be evaluated to second order in small terms, as the first order terms of $||A^{(E)}||$ are identically zero, and those of $||B^{(E)}||$ vanish at the resonance. The expressions obtained for

$Q_{MN}^{(\varepsilon)}$ and $Q_{NN}^{(\varepsilon)}$ are complex, but the denominator is fairly simple, and is

$$(\cos K_{RR}\ell - i(K_{RR}/k_R)\sin K_{RR}\ell) +$$

$$+ \sum_{\substack{L=0 \\ L\neq R}}^{\infty} \frac{K_{RR}^4}{K_{RR}^2 - K_{LL}^2} \cdot \frac{(\cos K_{LL}\ell - i(k_{LL}/k_R)\sin K_{LL}\ell)(\cos K_{RR}\ell - i(K_{RR}/k_L)\sin K_{RR}\ell)}{(\cos K_{LL}\ell - i(K_{LL}/k_L)\sin K_{LL}\ell)} \qquad (3.4.20)$$

At the resonance the lowest order terms in numerator and denominator vanish, so that the $Q_{MN}$ suddenly become of zeroth order in the coupling potential, giving rise to a large peak in the inter-channel scattering. The width of this peak is most easily estimated by finding the imaginary part of the energy of the decaying stationary state which gives rise to the resonance; this we shall now do.

We suppose that for the decoupled channel a resonance occurrs at energy $\varepsilon_R$. We shall therefore seek a stationary state for the complete coupled system of equations (3.4.5) at energy $\varepsilon_R + \Delta - i\Gamma$ where $\Delta$ and $\Gamma$ are small and real. The quantity $\Delta$ gives a slight 'level shift' of the resonance energy due to the coupling, while if $\Gamma$ is positive the time dependence of the state has factor $e^{-\Gamma t/\hbar}$, showing a decay with time. The wave numbers k and K are therefore slightly perturbed, giving

$$k_M \sim \pm(ik_M^R + (m_e/\hbar^2 k_M^R)\Gamma) \qquad \text{OC}$$

$$k_M \sim \pm(k_M^R + i(m_e/\hbar^2 k_M^R)\Gamma) \qquad \text{CC} \qquad (3.4.21)$$

where $k_M^R = (2m_e/\hbar^2)^{\frac{1}{2}}|\varepsilon_R + \Delta - (M+\frac{1}{2})\hbar\omega_c|^{\frac{1}{2}}$ is real and positive, and with similar expressions for the K's. The boundary conditions on the solution (3.4.7) must be modified by the removal of the incoming wave in the N channel, which is not required for the quasi-bound state. The asymptotic behaviour of the

wave function is therefore

$$f_M(z) = L^{-\frac{1}{2}} Q_M^{(\varepsilon)} e^{ik_M^R z} . e^{+(\Gamma m_e/\hbar^2 k_M^R)z} \qquad \text{OC}$$

$$f_M(z) = L^{-\frac{1}{2}} Q_M^{(\varepsilon)} e^{-k_M^R z} . e^{-i(\Gamma m_e/\hbar^2 k_M^R)z} \qquad \text{CC} \tag{3.4.22}$$

We have thus shown explicitly that the decay of the state takes place via a small incoming flux of probability in the closed channels escaping in the outgoing waves of the open channels. The increase in amplitude as $|z|$ increases in the OC's reflects the past time when the whole wave function was larger; when coupled with the time dependence we have in an open channel

$$f_M(z,t) = L^{-\frac{1}{2}} Q_M^{(\varepsilon)} e^{i(k_M^R z - \varepsilon_R t/\hbar)} . e^{(z-vt)\Gamma m_e/\hbar^2 k_M^R} \tag{3.4.23}$$

showing that the amplitude of the wave function at a point travelling with the velocity $v = \hbar k_M^R/m_e$ of the wave remains constant. The form of the even resonant bound state is illustrated schematically in Fig. 3.8.

When this form for the wave function is inserted into the matching conditions (3.4.8) we obtain the equation $\{A^{(\varepsilon)}\}(\alpha) = 0$ for the coefficients of the eigenvectors of $\{K^2\}$ in the bound state. For non-trivial solutions we must therefore have $||A^{(\varepsilon)}|| = 0$. To zeroth order in the coupling potential this is satisfied, as we are perturbing about the energy $\varepsilon_R$ for which the resonance condition (3.4.19) is satisfied. By demanding that $||A^{(\varepsilon)}|| = 0$ also to first order in the coupling potentials we may obtain expressions for $\Delta$ and $\Gamma$. After some manipulation we obtain the imaginary part of the energy

$$\Gamma = \frac{\hbar^2 K_{RR}^2 k_R^2}{m_e(k_R + \ell k_R^2 + \ell K_{RR}^2)} \cdot \sum_{M=0}^{P} \frac{K_{RM}^4}{(K_{RR}^2 - K_{MM}^2)^2} \frac{(\cos K_{MM}\ell - (K_{MM}/k_R)\sin K_{MM}\ell)^2}{(\cos^2 K_{MM}\ell + (K_{MM}^2/k_M^2)\sin^2 K_{MM}\ell)\, k_M} \tag{3.4.24}$$

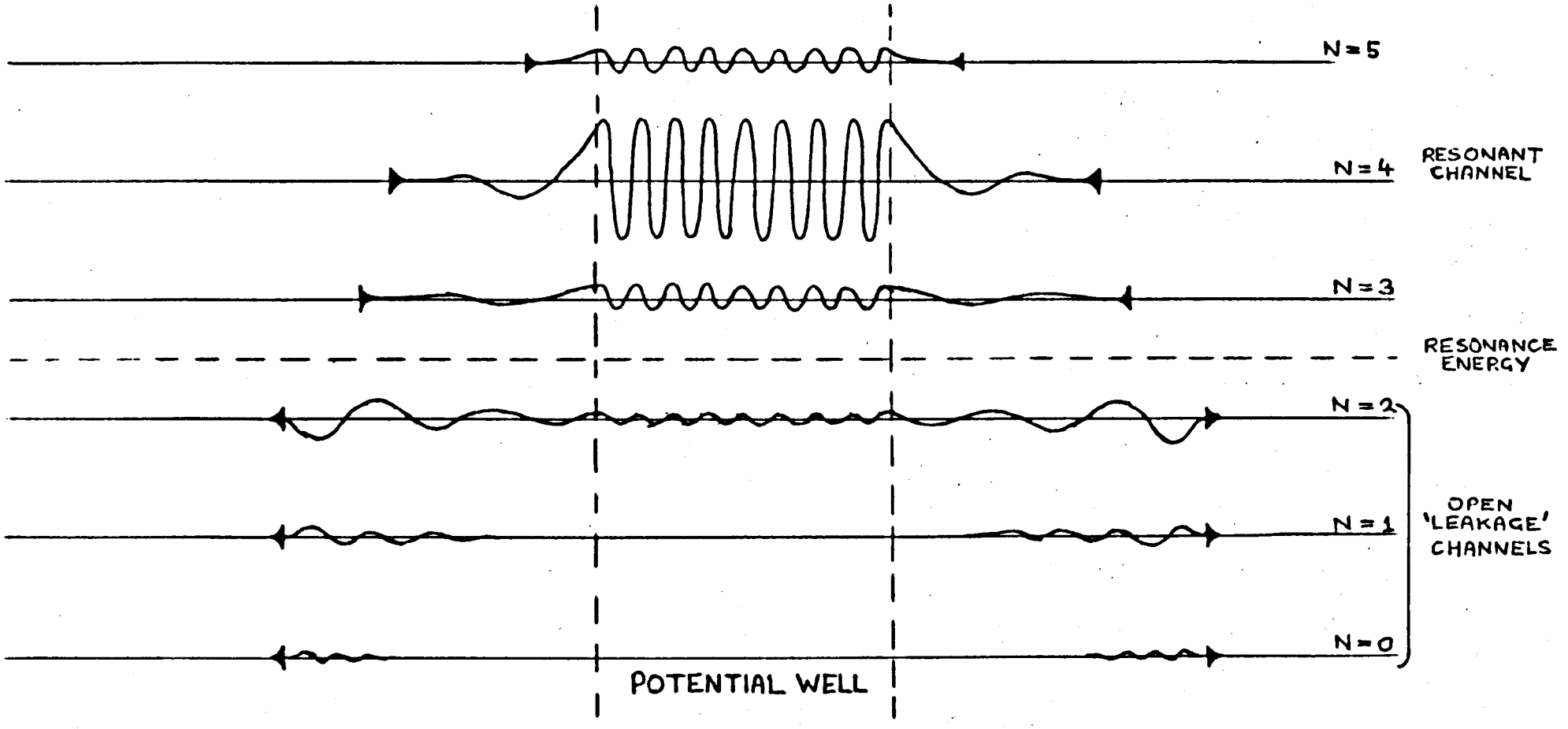


Fig. 3.8 Schematic longitudinal dependence of a resonant or nearly-bound state in channel 4. Fluxes of probability are incoming in the closed channels and outgoing in the open channels

where $k_R$ now stands for a real quantity. It is important to note two special features of the above expression. Firstly, it is positive definite, so that the quasi-bound state does decay with time as we have assumed. Secondly, the decay rate is governed only by the couplings to the open channels, as we would expect in a first order theory. This expression for $\Gamma$ may now be used as a measure of the width of the resonant peak in the scattering rates.

Finally, we must briefly mention the situation when two or more channels are so strongly coupled that the zeroth order approximation $K_N^2 \sim K_{NN}^2$ is not good enough. In this case the correct zeroth order approximation is to use the eigenvalues and eigenvectors of the sub-matrices of $\{K^2\}$ containing only the strongly coupled channels. There will then be extra terms present in the evaluation of $Q_{NM}$ if either of the channels is strongly coupled, due to the presence of zeroth order off-diagonal terms in the determinants. Needless to say, the expressions obtained will be very complex, and we shall not attempt to derive them here.

# CHAPTER 4

## Transport Theory in a Magnetic Field

### 4.1 Introduction

In this chapter we shall concern ourselves with the quantum mechanical theory of transport processes, and in particular that part of the theory from which expressions for the longitudinal magnetoconductivity of a semiconductor may be obtained. Having derived a Boltzmann-like transport equation for a distribution function, we shall investigate the circumstances in which a separate 'relaxation time' exists for the carriers in each Landau sub-band of the energy-level spectrum. Such a solution is useful when the scattering mechanisms are elastic, and the magnetic field of such a strength that only a small number of sub-bands, but more than one, are occupied. We shall show that the transport equation then reduces to a finite matrix equation for the 'relaxation times', one for each sub-band occupied at the given energy. The 'relaxation matrix' appearing in this equation is found to have a structure which enables us to make certain general statements about the expression for the conductivity, and about the process of relaxation back to equilibrium on removing the field.

Historically, the observation of Shubnikov and de Haas (1930) of oscillations in the magnetoresistance of bismuth crystals, inversely periodic in the field strength, was one of the earliest for which an explanation in terms of classical transport was not feasible. Peierls (1933) gave an explanation in terms of the semi-discrete nature of the energy spectrum produced by quantisation of the cyclotron orbit motion of the electrons, previously described by Landau (1930). Interest in quantum

magnetic effects was further stimulated by the observation of a non-zero transverse magnetoresistance in certain materials, which contradicted classical theory. In a very early calculation Titeica (1935) interpreted the transverse transport as a hopping of the cyclotron-orbit centres, though a divergence was obtained. This problem was overcome by Davydov and Pomeranchuk (1940), but a rigorous quantum mechanical theory of transport processes, whether in magnetic fields or not, was still lacking. All work was still based on a quantum transport equation due to Pauli (1928), derived heuristically by analogy with the classical Boltzmann equation. A clear exposition of the 'semi-classical' approach to transport is by Butcher (1973).

One of the earliest satisfactory derivations of a quantum mechanical equivalent to the Boltzmann equation was given by Van Hove (1955). He used a property called diagonal singularity to decouple the equation for the diagonal elements of the density matrix (which is in some ways analagous to the classical distribution function; see Fano (1957)) from the off-diagonal parts, leaving a transport equation for an object interpretable as a carrier distribution function. A similar analysis for scattering by randomly distributed static impurities was given by Kohn and Luttinger (1957), and later refined by the inclusion of more exact scattering rates (1958). Subsequently Chester and Thellung (1959) used methods similar to Van Hove's to derive a transport equation when scattering was by lattice vibrations.

Meanwhile Kubo (1957) adopted a different approach, deriving an exact expression for transport coefficients from a theory of linear response to an applied field. The final expression, a Laplace transform of a current autocorrelation function, still included all many-body effects exactly, and

approximate methods of analysis had to be found. Greenwood (1958), Edwards (1958) and Langer (1960) introduced Green's function and diagram methods from field theory, and succeeded in making a link with the transport equation theories. A more sophisticated picture in terms of re-normalised transport equations for quasi-particles gradually emerged; progress was reviewed by Chester (1963), who showed the formal equivalence of the two approaches. Further work relating the Kubo formula - Green's function approach to the Kohn-Luttinger transport equations was carried out by Moore (1967) and Scott and Moore (1972), working to higher order in impurity density and scattering amplitude.

Returning to magneto-transport calculations, an early study of longitudinal magnetoresistance was made by Argyres and Adams (1956). Here the transport equation was taken over from classical theory and scattering was by acoustic phonons in the extreme quantum limit (EQL) where only one Landau sub-band is occupied. Subsequently Argyres (1958) derived the transport equation by methods related to those of Van Hove, and was able to extend his analysis to allow for the occupation of several Landau sub-bands, due to special features of the acoustic phonon scattering which allowed a relaxation time solution. The transverse magnetoresistance effect was analysed by Adams and Holstein (1959), Argyres and Roth (1959) and Argyres (1959), using transport equation methods in the EQL with scattering by various mechanisms including acoustic phonons and ionised impurities. The work of Argyres was later extended to a more general form (1960, 1963) while Kahn (1960) and Bychkov (1961) refined the treatment of scattering by very small impurities.

In parallel to the transport equation work, the 'Kubo formula' approach was used in the theory of the transverse magnetoconductivity by Kubo,

Hashitsume and Hasegawa (1959). This method was also applied by Gurevich and Firsov (1961), to scattering by acoustic and optic phonons. An elegant diagrammatic analysis of Kubo formulae for magnetotransport coefficients was made by Lodder and Van Zuylen (1970). Here some of the difficulties of Green's function calculations were by-passed by working instead with super-resolvents; further progress was made by Lodder (1974), who obtained a re-normalised transport equation. The same methods were used to analyse the magnetophonon effect by Barker (1973a), who also derived a high-electric-field Boltzmann transport equation (1976).

Several reviews of these developments exist, of which we cite Kahn and Frederikse (1959), Dresden (1961), Adams and Keyes (1962), Roth and Argyres (1966) and Landwehr (1967) as presentations of the transport equation approach. The 'Kubo formula' methods are extensively covered in the review of Kubo, Miyake and Hashitsume (1965). Relaxation time methods (in the absence of a magnetic field) are reviewed by Conwell (1967).

Application of quantum magneto-transport theory has been very wide, and we shall merely note a few papers on the longitudinal effect which are of particular interest to us. Gurevich and Firsov (1965) and Efros (1965) treated systems in which the scattering mechanisms (optic phonons and ionised impurities respectively) precluded the use of the simple relaxation time of Argyres. Instead, a solution was proposed in which a separate 'relaxation time' was associated with each Landau sub-band. The resulting matrix equation was only solved in the simplest circumstances, however. Dubinskaya (1969) extended the work on ionised impurity scattering and solved the matrix equations in a more general magnetoconductivity calculation. The necessity of the multiple 'relaxation time' solution was again noted by Rohlfing and Pokrovsky (1974), but use of the simple single

'Argyres relaxation time' continued, even when not valid (see, e.g., Wallace and Gupta 1972, Serre and Leroux-Hugon 1974, Eaves, Markiewicz and Furneaux 1976, 1977). The multiple relaxation time/relaxation matrix theory was set out in its most explicit form by Barker and Bridges (1977), who used it to analyse magnetoconductivity in Ge in the presence of scattering by electron-hole-drops (See §5).

In §4.2 we summarise the derivation of transport equations from the Kubo formula, following closely the methods of Lodder and Van Zuylen (1970) and Barker (1973a), and expanding the averaged super-resolvent in terms of a self-energy super-operator. This expansion is evaluated to lowest order in §4.3, obtaining a Boltzmann transport equation with Born approximation transition rates. We then expand the self-energy to higher order in an attempt to derive the transport equation of Luttinger and Kohn (1958), in which exact transition rates appear; we find, however, that the approximation does not follow consistently from the super-resolvent approach. In §4.4 we analyse the Boltzmann equation when elastic scattering only is present, and obtain the aforementioned 'multiple relaxation time' solution by inverting a 'relaxation matrix'. The process of time-dependent relaxation back to equilibrium is treated in §4.5, the positive definiteness of the decay constants (and hence also the magnetoconductivity) being shown. Finally §4.6 discusses certain situations in which an approximate inversion of the relaxation matrix is possible immediately.

## 4.2 The Derivation of Quantum Transport Equations

In a large system in which many microscopic quantum states correspond to the same macroscopic thermodynamic state, macroscopic quantities such as total current must be expressed as averages over an ensemble of identical systems. Such an ensemble and its evolution are described by a density matrix $\rho(t)$ (Fano 1957) and its equation of motion, the Liouville equation:

$$i\hbar\partial\rho/\partial t = \{\mathcal{H},\rho\} \tag{4.2.1}$$

where $\mathcal{H}$ is the Hamiltonian operator for the complete system. Macroscopic quantities are obtained by taking the trace of the relevant operator with the density matrix, so that for the current:

$$\langle \underline{J}(t)\rangle = Tr(\underline{J}\rho(t)) \tag{4.2.2}$$

Kubo (1957) has shown how first order perturbation theory, applied to the Liouville equation when a small electric field is present, may be used to obtain the Linear response of the density matrix to the field, and hence the conductivity expressed in the well known formula

$$\sigma_{\mu\nu} = \Omega^{-1} \lim_{S\to 0+} \int_0^\infty dt \int_0^\beta d\gamma e^{-st/\hbar} Tr\{J_\mu(t)\rho_0(\mathcal{H})J_\nu(-i\gamma)\}_{T.L.} \tag{4.2.3}$$

Here $\rho_0(\mathcal{H})$ is the equilibrium density matrix for the grand canonical ensemble, given in terms of the partition function $Z$, the chemical potential $\mu$, and the number operator $\mathcal{N}$ for the electrons by:

$$\rho_0(\mathcal{H}) = Z^{-1} e^{-(\mathcal{H}+\mu\mathcal{N})/kT} \tag{4.2.4}$$

The letters T.L. indicate that the thermodynamic limit $\Omega,N\to\infty$, $N/\Omega$ fixed, is taken <u>before</u> the limit $S\to 0+$. If the limits are not taken in this order one

is effectively considering a completely isolated, finite system for which the Poincaré (1890) recurrence theorem applies and for which, therefore, the D.C. conductivity is infinite (Bocchieri and Loinger 1957).

It is of some convenience, in dealing with operators such as $J_\mu(t)$ in the Heisenberg representation, to introduce the Liouville super operator for $\mathcal{H}$ used in this context by Lodder and Van Zuylen (1970), and defined by

$$\hat{\mathcal{H}} A \equiv \{\mathcal{H}, A\} \tag{4.2.5}$$

In any representation $\hat{\mathcal{H}}$ is a fourth rank object which is a linear operator on the set of quantum mechanical operators; thus

$$\{\hat{\mathcal{H}} A\}_{ij} = \sum_{k,\ell} \mathcal{H}_{ijk\ell} A_{k\ell} \tag{4.2.6}$$

For super operators of the commutator generating type the elements are of the form

$$\hat{\mathcal{H}}_{ijk\ell} = \mathcal{H}_{ik}\delta_{j\ell} - \mathcal{H}_{\ell j}\delta_{ik} \tag{4.2.7}$$

With this compact notation the Heisenberg representation for $J_\mu$ becomes

$$J_\mu(t) \equiv e^{i\mathcal{H}t/\hbar} J_\mu e^{-i\mathcal{H}t/\hbar} \equiv J_\mu e^{-i\hat{\mathcal{H}}t/\hbar} \tag{4.2.8}$$

So that we have

$$\sigma_{\mu\nu} = \Omega^{-1} \lim_{s\to 0+} \int_0^\infty dt \int_0^\beta d\gamma \, \mathrm{Tr}\{J_\mu e^{-i(\hat{\mathcal{H}} - is)t/\hbar} \rho_0(\mathcal{H}) J_\nu(-i\gamma)\}_{T.L} \tag{4.2.9}$$

It is now possible to perform the t integration, and also to eliminate the $\gamma$ integration by the method of Lodder and Van Zuylen (1970), to obtain

$$\sigma_{\mu\nu} = \Omega^{-1} \underset{s\to o+}{Lt}\ \underset{k\to o}{Lt} - i\hbar\partial/\partial k_\nu Tr\{J_\mu \hat{R} \rho_o (\mathcal{H}-\underline{J}.\underline{k})\} \qquad (4.2.10)$$

where the resolvent super operator defined by

$$\hat{R} = (\hat{\mathcal{H}}-is)^{-1} \qquad (4.2.11)$$

has been introduced.

At this stage the expression for $\sigma$ is still exact. However, $\mathcal{H}$ and $J$ are many-body operators for the complete interacting system of electrons and crystal lattice, which is infinite in the T.L. From this point on approximations have to be made in order to obtain a formula which is capable of being evaluated.

Firstly, we eliminate the many body nature of the trace operation by neglecting electron-electron interactions, both direct (as in the electrostatic forces) and mediated by the lattice or scatterers (as in Cooper pair formation). In this approximation the density matrix factorises into separate parts for the electrons and the scattering system (Lodder and Van Zuylen, 1970). The trace over the electron system may be reduced to a single-electron trace by using the commutation relations for the set of fermion operators for the electrons, and hence

$$\sigma_{\mu\nu} = \Omega^{-1} \underset{s\to o+}{Lt}\ \underset{k\to o}{Lt} -i\hbar\partial/\partial k_\nu \langle tr\{J_\mu \hat{R} f^o (H_e+U-\underline{J}.\underline{k})\}\rangle_{s,T.L.} \qquad (4.2.12)$$

Here $f^o$ is the Fermi-Dirac function given by $f^o(\varepsilon) = (e^{(\varepsilon-\mu)/kt}+1)^{-1}$, $H_e$ and $U$ are respectively the second quantised Hamiltonian for a single electron in the crystal lattice (and static magnetic field), and the potential of interaction with the scattering mechanisms. The bracket

$\langle\rangle_{s,T.L.}$ denotes the trace, or average, over all configurations of the scattering system in the thermodynamic limit. If the anticommutation of the electron operators is ignored we obtain (4.2.12) with the modification that $f^o(\varepsilon) = e^{-\varepsilon/kT}$, the Maxwell distribution; we shall use this as an approximation when the electron system is non-degenerate.

The scattering interaction $\hat{U}$ appears in the distribution function $f^o$ for the equilibrium state, in the super resolvent $\hat{R} = (\hat{H}_e+\hat{H}_s+\hat{U}-is)^{-1}$, and also possibly in the current operator $\underline{J}$. The averaging over the scatterer configuration should take all these dependencies into account simultaneously in any expansion of (4.2.12) in powers of the interaction. For example, Barker (1976) has shown that the terms in $\hat{U}$ from $f^o$, the 'initial state correlations', play an important part in the description of conduction in systems where the electrons are localised. In evaluating the transverse magnetoconductivity (Kubo et al 1965, Barker 1973) the transverse current operators are in fact directly proportional to $\hat{U}$. However, we shall restrict our attention to the evaluation of the longitudinal magnetoconductivity in a non-localised system, in which case Barker (1973) has shown that initial state correlations may be neglected. In a basis which simultaneously diagonalises $J_z$ and $H_e$ we have

$$\sigma_{zz} = \Omega^{-1} \lim_{s\to o+} i\hbar\langle tr\{J_z\hat{R}J_z f^{o'}(H_e)\}\rangle_{s,T.L.} \qquad (4.2.13)$$

This may be interpreted as saying that the perturbation to the one electron distribution function produced by the field is given by the diagonal part of $i\hbar\langle\hat{R}J_z f^{o'}(H_e)\rangle_{s,T.L.}$ We must now derive a transport equation for this perturbed distribution function by expanding the resolvent $\hat{R}$.

A return to Green's function formalism is possible here by obtaining $\hat{R}$ as a convolution integral, due to Barker

$$(\hat{H}-is)^{-1}A = (2\pi i)^{-1}\int dz'(H-z')^{-1}A(H-z'+is)^{-1} \qquad (4.2.14)$$

{This is proved by Fourier transorming the relation $e^{-ist}e^{\hat{H}t}A = e^{-ist}e^{-Ht}Ae^{Ht}$}. Luttinger and Kohn (1958) then write the Green's functions $(H-z')^{-1}$ in terms of the t matrix for the complete scattering system, and expand in terms of t matrices for clusters of scattering centres. If only terms due to scattering off single centres are retained in this expansion, on averaging a Boltzmann equation for the perturbed distribution function $f'$ per unit electric field is obtained:

$$-e\partial f^{o}(\varepsilon_\lambda)/\partial k_z = \sum_{\lambda'} 2\pi N_s \delta(\varepsilon_\lambda-\varepsilon_{\lambda'})|t(\varepsilon_\lambda)_{\lambda\lambda'}|^2(f'_{\lambda'}-f'_\lambda) \qquad (4.2.15)$$

We do not adopt this approach here, however, but instead follow Lodder and Van Zuylen (1970) in assuming that the averaged super resolvent may be expressed in terms of a self energy super operator $\hat{\Sigma}$:

$$\langle(\hat{H}_e+\hat{H}_s+\hat{U}-is)^{-1}\rangle_{s,T.L.} = (\hat{H}_e+\hat{H}_s-\hat{\Sigma}-is)^{-1} \qquad (4.2.16)$$

An expression for $\hat{\Sigma}$ is obtained by expanding the LHS of (4.2.16) as a power series in $\hat{U}$, taking the T.L. and performing the scatterer average, after which a resummation may be carried out to give an expansion for $\hat{\Sigma}$ in powers of the scatterer density. In our investigations we shall consider only a low density of scatterers, and hence we shall retain only the single scattering centre terms in the expansion of $\hat{\Sigma}$.

The required terms of the single-centre series are

$$\hat{\Sigma}_{ss} = N_s\langle -\hat{U}_i + \hat{U}_i\langle\hat{R}\rangle\hat{U}_i - \hat{U}_i\langle\hat{R}\rangle\hat{U}_i\langle\hat{R}\rangle\hat{U}_i + \ldots\rangle_{s,T.L.} \qquad (4.2.17)$$

where $\hat{U}_i = \hat{U}(\underline{r}-\underline{R}_i)$ and the average is over the scatterer location $\underline{R}_i$, assumed uniform over the volume of the crystal. $N_s$ is the total number of scatterers in the crystal; as the averaging brings in an $\Omega^{-1}$ term, $\hat{\Sigma}_{ss}$ is proportional to the scatterer density. It is important to notice that the averaged resolvent $\langle\hat{R}\rangle$ appears in the expansion of $\hat{\Sigma}_{ss}$; hence the pair of equations (4.2.16 and 17) are implicit for $\langle\hat{R}\rangle$ and $\hat{\Sigma}_{ss}$. Lodder and Van Zuylen have also given an expansion for $\hat{\Sigma}$ when more than one scattering mechanism is present; in the low density approximation, however, $\hat{\Sigma}_{ss}$ is just the sum of the single site series for each mechanism individually. Interference terms are of a higher order.

To recap, we now have

$$\sigma = \Omega^{-1} tr\{J_z \rho'\} \qquad (4.2.18)$$

where the perturbation to the density matrix, $\rho'$ is given by

$$\rho' = \underset{s\to 0+}{Lt}\, i\hbar\langle\hat{R}\rangle J_z f^{o'}(H_e) = \underset{s\to 0+}{Lt}\, i\hbar(\hat{H}_e+\hat{H}_s-\hat{\Sigma}_{ss}-is)^{-1} J_z f^{o'}(H_e) \qquad (4.2.19)$$

Barker (1973) has shown how to convert this equation to a more familiar form. Expanding,

$$(\hat{H}_e+\hat{H}_s-\hat{\Sigma}_{ss}-is)^{-1} = (\hat{H}_e+\hat{H}_s-is)^{-1} + (\hat{H}_e+\hat{H}_s-is)^{-1}\hat{\Sigma}_{ss}(\hat{H}_e+\hat{H}_s-\hat{\Sigma}_{ss}-is)^{-1} \qquad (4.2.20)$$

which may substituted into (4.2.19) to obtain

$$\rho' = \underset{s\to 0+}{Lt}\{i\hbar(\hat{H}_e+\hat{H}_s-is)^{-1} J_z f^{o'}(H_e) + (\hat{H}_e+\hat{H}_s-is)^{-1}\hat{\Sigma}_{ss}\rho'\} \qquad (4.2.21)$$

We recall that, in a representation diagonalising $\hat{H}_e$ and $\hat{H}_s$, the elements of $\hat{\mathcal{H}}$ will be

$$\hat{\mathcal{H}}_{\lambda\mu\nu\phi} = H_{\lambda\nu}\delta_{\mu\phi} - H_{\phi\mu}\delta_{\lambda\nu} = (\varepsilon_\lambda - \varepsilon_\mu)\delta_{\lambda\nu}\delta_{\mu\phi} \qquad (4.2.22)$$

Thus $\hat{\mathcal{H}}$ is 'diagonal' in the super operator sense, and hence the elements of its inverse are readily found:

$$(\hat{\mathcal{H}} - is)^{-1}_{\lambda\mu\nu\phi} = (\varepsilon_\lambda - \varepsilon_\mu - is)^{-1}\delta_{\lambda\nu}\delta_{\mu\phi} \qquad (4.2.23)$$

We see from (4.2.18) that, since $J_z$ has also been diagonalised, only the diagonal elements of $\rho'$ are required. From (4.2.21 and 23) these are

$$\rho'_{\lambda\lambda} = \underset{s\to 0+}{Lt}\; s^{-1}\{-\hbar J_{z\lambda} f^{o'}(\varepsilon_\lambda) + i(\hat{\Sigma}_{ss}\rho')_{\lambda\lambda}\} \qquad (4.2.24)$$

It is clear that the only way of preventing a divergence in $\rho'$ as the limit is taken is for a cancellation of the terms inside the bracket to take place. This is not unexpected, as the DC response of a system without scattering is infinite. It is only relaxed to a finite value by the collision processes manifested in the $\hat{\Sigma}_{ss}\rho'$ term. We must therefore have

$$\hbar J_{z\lambda} f^{o'}(\varepsilon_\lambda) - i(\hat{\Sigma}_{ss}\rho')_{\lambda\lambda} = 0 \qquad (4.2.26)$$

This equation is already beginning to approach the classic Boltzmann form, as a split has been made into a driving term dependent on the equilibrium distribution function only, and a collision term involving the scattering potentials and the perturbation to the distribution function.

In general the second term in this equation contains contributions from the off-diagonal terms of $\rho'$ as well as the diagonal ones which we are taking to define the distribution function. However, Barker (1973), has

shown via an expansion in diagonal and off-diagonal parts that the off-diagonal terms may be neglected in a low-density expression. (If the system were isotropic this approximation would be exact, as one can then show that $\hat{\Sigma}_{\lambda\lambda\mu\nu} = \hat{\Sigma}_{\lambda\lambda\mu\mu}\delta_{\mu\nu}$. In a magnetic field, however, this simplifying feature is not present). Equation (4.2.25) then involves only the diagonal part of $\rho'$, which will henceforward be called the perturbed electron distribution function $f^1$:

$$\pi J_{z\lambda} f^{o'}(\epsilon_\lambda) - i\sum_{\lambda'} \hat{\Sigma}_{\lambda\lambda\lambda'\lambda'} f^1_{\lambda'} = 0 \qquad (4.2.26)$$

In terms of $f^1$ the conductivity is obtained from (4.2.18) as

$$\sigma_{zz} = \Omega^{-1}\sum_{\lambda} J_{z\lambda} f^1_\lambda . \qquad (4.2.27)$$

It will be the work of the next section to obtain suitable approximate expressions for the self-energy $\hat{\Sigma}_{ss}$ so that (4.2.26) may be solved for the distribution function and hence the conductivity evaluated. It will become apparent that, in a suitable approximation, the collision operator $\hat{\Sigma}$ produces the familiar scattering in and scattering out terms of the Boltzmann equation.

## 4.3 The Boltzmann Transport Equation

The low density, single scattering centre approximation for $\hat{\Sigma}$ is

$$\hat{\Sigma}_{ss} = N_s\langle -\hat{U}_i + \hat{U}_i\langle\hat{R}\rangle\hat{U}_i - \hat{U}_i\langle R\rangle\hat{U}_i\langle\hat{R}\rangle\hat{U}_i + \ldots\rangle_{S,T.L.} \tag{4.3.1}$$

$$\langle\hat{R}\rangle = (\hat{H}_e+\hat{H}_s-\hat{\Sigma}_{ss}-is)^{-1} \tag{4.3.2}$$

We would expect that the above approximation scheme is formally equivalent to the self consistent t-matrix approximation (STMA) of conventional Green's function theory (Gerhardts & Hajdu, 1971, Scott and Moore, 1972), though it has not yet been found possible to demonstrate this equivalence. For the purposes of our later calculation it will prove to be sufficient to neglect all forms of collision broadening and derive the conventional Boltzmann transport equation, firstly with transition rates given by the Born approximation, and secondly with exact rates given by t-matrix elements.

Lodder and Van Zuylen (1970) and Barker (1973) have shown that when U represents the electron-phonon interaction, the lowest order approximation to $\hat{\Sigma}$ is given by

$$\hat{\Sigma}^{(2)} = N_s\langle\hat{U}\hat{R}_o\hat{U}\rangle \equiv N_s\langle\hat{U}(\hat{H}_e+\hat{H}_s-is)^{-1}\hat{U}\rangle \tag{4.3.3}$$

since the first term vanishes (there must be a change in phonon number). By replacing $\langle\hat{R}\rangle$ by $\hat{R}_o$ we have explicitly discarded all collision broadening terms. The scatterer Hamiltonian $H_s$ is now $\sum_{\underline{q}} N_{\underline{q}}\hbar\omega_{\underline{q}}$, and the scatterer average replaces $N_{\underline{q}}$, the occupation number operator for phonons with wave vector $\underline{q}$, by its average $\bar{N}_{\underline{q}} = (e^{\hbar\omega_{\underline{q}}/kT}-1)^{-1}$ given by the Bose-Einstein distribution. After some manipulation we arrive at

$$\sum_{\lambda'}\hat{\Sigma}^{(2)}_{\lambda\lambda\lambda'\lambda'}f^1_{\lambda'} = -i\hbar\sum_{\lambda'}\{p_{\lambda'\lambda}f^1_{\lambda'} - p_{\lambda\lambda'}f^1_{\lambda}\} \tag{4.3.4}$$

where the transition rates $p_{\lambda\lambda'}$ from state $\lambda$ to state $\lambda'$ are given by

$$p_{\lambda\lambda'} = \sum_{\underline{q}} 2\pi/\hbar |C(q)|^2 \{(\bar{N}_{\underline{q}}+1)\delta(\varepsilon_{\lambda'}-\varepsilon_{\lambda}+\hbar\omega_{\underline{q}}) + \underset{\text{CREATION}}{}$$

$$+ \underset{\text{ANNIHILATION}}{\bar{N}_{\underline{q}}\delta(\varepsilon_{\lambda'}-\varepsilon_{\lambda}-\hbar\omega_{\underline{q}})}\} |\langle\lambda| e^{i\underline{q}\cdot\underline{r}} |\lambda'\rangle|^2 \qquad (4.3.5)$$

When substituted into (4.2.27) we obtain

$$J_{z\lambda} f^{o'}(\varepsilon_{\lambda}) = \sum_{\lambda'} \{p_{\lambda'\lambda} f^1_{\lambda'} - p_{\lambda\lambda'} f^1_{\lambda}\} \qquad (4.3.6)$$

which is identical in form to the Boltzmann equation of classical transport theory. The flux of particles driven into a given state by the electric field is equated to the flux out due to point collisions, in this case with phonons.

We shall now illustrate how the gain-loss structure of (4.3.4) arises by a more detailed derivation of $\hat{\Sigma}^{(2)}$ when the scattering is by randomly distributed impurity potentials. In this case $N_s\langle\hat{U}_i\rangle$ is not identically zero, but its diagonal $(\lambda\lambda,\lambda'\lambda')$ elements are, and so we need only evaluate

$$\hat{\Sigma}^{(2)} = N_s\langle\hat{U}\hat{R}_o\hat{U}\rangle_s = (N_s/\Omega)\iiint d^3\underline{R}\,\hat{U}(\underline{r}-\underline{R})(\hat{H}_e+\hat{H}_s-is)^{-1}\hat{U}(\underline{r}-\underline{R}) \qquad (4.3.7)$$

As the effect of the electron scatterer interaction on the scatterers is being neglected, $H_s$ is a constant and hence $\hat{H}_s$ contributes zero in the resolvent. The $(\lambda\lambda,\lambda'\lambda')$ element of the integrand is therefore

$$\sum_{\mu\nu} (U_{\lambda\mu}\delta_{\lambda\nu} - U_{\nu\lambda}\delta_{\lambda\mu})(\varepsilon_{\mu}-\varepsilon_{\nu}-is)^{-1}(U_{\mu\lambda'}\delta_{\nu\lambda'} - U_{\lambda'\nu}\delta_{\mu\lambda'})$$

$$= \sum_{\mu}\frac{U_{\lambda\mu}U_{\mu\lambda'}\delta_{\lambda\lambda'}}{\varepsilon_{\mu}-\varepsilon_{\lambda}-is} + \sum_{\nu}\frac{U_{\nu\lambda}U_{\lambda'\nu}\delta_{\lambda\lambda'}}{\varepsilon_{\lambda}-\varepsilon_{\nu}-is} - \frac{U_{\lambda\lambda'}U_{\lambda'\lambda}}{\varepsilon_{\lambda'}-\varepsilon_{\lambda}-is} - \frac{U_{\lambda\lambda'}U_{\lambda'\lambda}}{\varepsilon_{\lambda}-\varepsilon_{\lambda'}-is}$$

$$= \delta_{\lambda\lambda'}\sum_{\mu}|U_{\lambda\mu}|^2\{\frac{1}{\varepsilon_\lambda-\varepsilon_\mu-is} - \frac{1}{\varepsilon_\lambda-\varepsilon_\mu+is}\} - |U_{\lambda\lambda'}|^2\{\frac{1}{\varepsilon_\lambda-\varepsilon_{\lambda'}-is} - \frac{1}{\varepsilon_\lambda-\varepsilon_{\lambda'}+is}\}$$

Using the result $\underset{s\to 0+}{Lt}\{\frac{1}{x-is} - \frac{1}{x+is}\} = 2\pi i\delta(x)$ we obtain

$$\underset{s\to 0+}{Lt}\ \hat{\Sigma}^{(2)}_{\lambda\lambda'\lambda'} = (N_s/\Omega)\iiint \underline{d^3R}\,2\pi i\{\delta_{\lambda\lambda'}\sum_{\mu}|U_{\lambda\mu}|^2\delta(\varepsilon_\lambda-\varepsilon_\mu) - |U_{\lambda\lambda'}|^2\delta(\varepsilon_\lambda-\varepsilon_{\lambda'})\} \tag{4.3.8}$$

and hence the expected gain-loss structure

$$\sum_{\lambda}\hat{\Sigma}^{(2)}_{\lambda\lambda'\lambda'}f^1_{\lambda'} = -i\hbar\sum_{\lambda'}\{p_{\lambda'\lambda}f^1_{\lambda'} - p_{\lambda\lambda'}f^1_{\lambda}\} \tag{4.3.9}$$

where the transition rates $p_{\lambda\lambda'}$ are given by

$$p_{\lambda\lambda'} = (2\pi/\hbar)N_s\langle|U_{\lambda\lambda'}|^2\rangle\delta(\varepsilon_\lambda-\varepsilon_{\lambda'}) = p_{\lambda'\lambda} \tag{4.3.10}$$

In other words, the transition rate from state $\lambda$ to state $\lambda'$ is an average over the rate given by the Fermi Golden Rule, or Born Approximation. At this point we note that, if more than one scattering mechanism is present, the transition rates $p_{\lambda\lambda'}$ in the low-density approximation are simply sums over the transition rates for the separate processes.

Before proceeding to a solution of the Boltzmann equation (4.3.6) we shall give some consideration to the case when the scattering potentials are strong, so that the lowest order approximation (4.3.3) for $\hat{\Sigma}$ is no longer a good one. In this case we really need the STMA of Scott and Moore (1972), but we shall not proceed to this degree of sophistication here. More naïvely, one might expect a better approximation to be obtainable by replacing the Fermi Golden Rule of (4.3.10) by the exact transition rate given by the t-matrix element. Luttinger and Kohn (1958) have obtained this result via

Green's function theory; we now demonstrate the equivalent result in the resolvent expansion.

By analogy with Green's function theory, we take

$$\hat{T} \equiv -\hat{U} + \hat{U}\hat{R}_o\hat{U} - \hat{U}\hat{R}_o\hat{U}\hat{R}_o\hat{U} + \ldots = -\hat{U} - \hat{U}\hat{R}_o\hat{T} \tag{4.3.11}$$

as our next approximation to $\hat{\Sigma}$. Only the diagonal $(_{\lambda\lambda'}{}_{\lambda'}{}_{\lambda})$ elements of $\hat{T}$ are required; in a representation

$$\begin{aligned}
\hat{T}_{\lambda\mu\lambda'\lambda'} &= -\hat{U}_{\lambda\mu\lambda'\lambda'} - \sum_{\nu\phi} \hat{U}_{\lambda\mu\nu\phi}(\varepsilon_\nu - \varepsilon_\phi - is)^{-1}\hat{T}_{\nu\phi\lambda'\lambda'} \\
&= -U_{\lambda\lambda'}\delta_{\mu\lambda'} + U_{\lambda'\mu}\delta_{\lambda\lambda'} + \\
&+ \sum_\nu U_{\lambda\nu}(\varepsilon_\mu - \varepsilon_\nu + is)^{-1}\hat{T}_{\nu\mu\lambda'\lambda'} + \sum_\phi \hat{T}_{\lambda\phi\lambda'\lambda'}(\varepsilon_\lambda - \varepsilon_\phi - is)^{-1}U_{\phi\mu} \\
&= -U_{\lambda\lambda'}\delta_{\mu\lambda'} + U_{\lambda'\mu}\delta_{\lambda\lambda'} + \\
&+ \sum_\nu U_{\lambda\nu}G^{o+}_{\nu\nu}(\varepsilon_\mu)\hat{T}_{\nu\mu\lambda'\lambda'} + \sum_\phi \hat{T}_{\lambda\phi\lambda'\lambda'}G^{o-}_{\phi\phi}(\varepsilon_\lambda)U_{\phi\mu}
\end{aligned} \tag{4.3.12}$$

We have here introduced the free Green's functions $G^{o\pm}(\varepsilon) = (\varepsilon - H_e \pm is)^{-1}$. The above implicit equation for the $(\lambda\mu,\lambda'\lambda')$ elements of $\hat{T}$ is strongly suggestive of the ordinary operator equation for the t-matrix:

$$t^{\pm}(\varepsilon)_{\lambda\mu} = U_{\lambda\mu} + \sum_\nu U_{\lambda\nu}G^{o\pm}_{\nu\nu}(\varepsilon)t^{\pm}(\varepsilon)_{\nu\mu} = U_{\lambda\mu} + \sum_\nu t^{\pm}(\varepsilon)_{\lambda\nu}G^{o\pm}_{\nu\nu}(\varepsilon)U_{\nu\mu} \tag{4.3.13}$$

In fact, the above suggests a basis for the iterative solution of (4.3.12). We write

$$\hat{T}_{\lambda\mu\lambda'\lambda'} = -t^{+}(\varepsilon_\mu)_{\lambda\lambda'}\delta_{\mu\lambda'} + t^{-}(\varepsilon_\lambda)_{\lambda'\mu}\delta_{\lambda\lambda'} + x_{\lambda\mu\lambda'\lambda'} \tag{4.3.14}$$

which, when substituted into (4.3.12) gives

$$-t^{+}(\varepsilon_{\mu})_{\lambda\lambda',\delta_{\mu\lambda'}} \qquad -(U_{\lambda\lambda'} + \sum_{\nu} U_{\lambda\nu} G^{o+}_{\nu\nu}(\varepsilon_{\mu}) t^{+}(\varepsilon_{\mu})_{\nu\lambda'})\delta_{\mu\lambda'}$$

$$+t^{-}(\varepsilon_{\lambda})_{\lambda'\mu}\delta_{\lambda\lambda'} \;=\; +(U_{\lambda'\mu} + \sum_{\phi} t^{-}(\varepsilon_{\lambda})_{\lambda'\phi} G^{o-}_{\phi\phi}(\varepsilon_{\lambda}) U_{\phi\mu})\delta_{\lambda\lambda'} \qquad (4.3.15)$$

.....

$$+x_{\lambda\mu\lambda'\lambda'} \qquad +U_{\lambda\lambda'} G^{o+}_{\lambda'\lambda'}(\varepsilon_{\mu}) t^{-}(\varepsilon_{\lambda'})_{\lambda'\mu} - t^{+}(\varepsilon_{\lambda'})_{\lambda\lambda} G^{o-}_{\lambda'\lambda'}(\varepsilon_{\lambda}) U_{\lambda'\mu}$$

$$+\sum_{\nu} U_{\lambda\nu} G^{o+}_{\nu\nu}(\varepsilon_{\mu}) x_{\nu\mu\lambda'\lambda'} + \sum_{\phi} x_{\lambda\phi\lambda'\lambda'} G^{o-}_{\phi\phi}(\varepsilon_{\lambda}) U_{\phi\mu}$$

Equality is satisfied above and below the dotted line separately, so that the lower part is an implicit equation for x. This iteration may be continued indefinitely, at each stage proceeding to the next order by replacing U in the implicit equation by $t^{+}$ or $t^{-}$. The expansion eventually obtained begins as

$$\hat{T}_{\lambda\mu\lambda'\lambda'} = t^{-}(\varepsilon_{\lambda})_{\lambda'\mu}\delta_{\lambda\lambda'} - t^{+}(\varepsilon_{\mu})_{\lambda\lambda'}\delta_{\mu\lambda'}$$

$$+t^{+}(\varepsilon_{\mu})_{\lambda\lambda'} G^{o+}_{\lambda'\lambda'}(\varepsilon_{\mu}) t^{-}(\varepsilon_{\lambda'})_{\lambda'\mu} - t^{+}(\varepsilon_{\lambda'})_{\lambda\lambda} G^{o-}_{\lambda'\lambda'}(\varepsilon_{\lambda}) t^{-}(\varepsilon_{\lambda})_{\lambda'\mu}$$

$$+\sum_{\phi} t^{+}(\varepsilon_{\phi})_{\lambda\lambda'} G^{o+}_{\lambda'\lambda}(\varepsilon_{\phi}) t^{-}(\varepsilon_{\lambda'})_{\lambda'\phi} G^{o-}_{\phi\phi}(\varepsilon_{\lambda}) t^{-}(\varepsilon_{\lambda})_{\phi\mu} - \ldots . \qquad (4.3.16)$$

We have thus expressed $\hat{T}$ as a series in t-matrix rather than potential matrix elements. We now approximate $\hat{T}$ by taking only the first two sets of terms in this series, which we shall call $\hat{T}^{(2)}$. The expression required for the transport equation (4.2.27) is thus

$$\sum_{\lambda'} \hat{T}^{(2)}_{\lambda\lambda\lambda'\lambda'} f^{1}_{\lambda'} = \{t^{-}(\varepsilon_{\lambda})_{\lambda\lambda} - t^{+}(\varepsilon_{\lambda})_{\lambda\lambda}\}\, f^{1}_{\lambda} +$$

$$+ \sum_{\lambda} f^{1}_{\lambda'} \{ \frac{t^{+}(\varepsilon_{\lambda})_{\lambda\lambda'} t^{-}(\varepsilon_{\lambda'})_{\lambda'\lambda}}{\varepsilon_{\lambda} - \varepsilon_{\lambda'} + is} - \frac{t^{+}(\varepsilon_{\lambda'})_{\lambda\lambda'} t^{-}(\varepsilon_{\lambda})_{\lambda'\lambda}}{\varepsilon_{\lambda} - \varepsilon_{\lambda'} - is} \} \qquad (4.3.17)$$

We can now use the Optical Theorem (see, e.g., Rodberg and Thaler (1967), which states that

$$t^-(\varepsilon) - t^+(\varepsilon) = 2\pi i t^-(\varepsilon)\delta(\varepsilon - H_e)t^+(\varepsilon) \tag{4.3.18}$$

and hence that

$$\{t^-(\varepsilon_\lambda) - t^+(\varepsilon_\lambda)\}_{\lambda\lambda} = 2\pi i \sum_{\lambda'} t^-(\varepsilon_\lambda)_{\lambda\lambda'} t^+(\varepsilon_\lambda)_{\lambda'\lambda} \delta(\varepsilon_\lambda - \varepsilon_{\lambda'}) =$$

$$= 2\pi i \sum_{\lambda'} |t^+(\varepsilon_\lambda)_{\lambda\lambda'}|^2 \delta(\varepsilon_\lambda - \varepsilon_{\lambda'}) \tag{4.3.19}$$

The second term of (4.3.17) may be rearranged as

$$\frac{(\varepsilon_\lambda - \varepsilon_{\lambda'})}{((\varepsilon_\lambda - \varepsilon_{\lambda'})^2 + s^2)} \{t^+(\varepsilon_\lambda)_{\lambda\lambda'} t^-(\varepsilon_{\lambda'})_{\lambda'\lambda} - t^+(\varepsilon_{\lambda'})_{\lambda\lambda'} t^-(\varepsilon_\lambda)_{\lambda'\lambda}\} -$$

$$- \frac{is}{((\varepsilon_\lambda - \varepsilon_{\lambda'})^2 + s^2)} \{t^+(\varepsilon_\lambda)_{\lambda\lambda'} t^-(\varepsilon_{\lambda'})_{\lambda'\lambda} + t^+(\varepsilon_{\lambda'})_{\lambda\lambda'} t^-(\varepsilon_\lambda)_{\lambda'\lambda}\}$$

$$= \mathcal{P}\int_\Gamma \frac{\{t^+(\varepsilon_\lambda)_{\lambda\lambda'} t^-(\varepsilon_{\lambda'})_{\lambda'\lambda} - t^+(\varepsilon_{\lambda'})_{\lambda\lambda'} t^-(\varepsilon_\lambda)_{\lambda'\lambda}\}}{\varepsilon_\lambda - \varepsilon_{\lambda'}} - 2\pi i \delta(\varepsilon_\lambda - \varepsilon_{\lambda'}) |t^+(\varepsilon_\lambda)_{\lambda\lambda'}|^2 \tag{4.3.20}$$

as the limit $s \to 0+$ is taken.

At the moment we are unable to interpret the significance of the principal part term in (4.3.20), although it is possible that it represents a re-normalisation of the current operators, as found in the STMA by Scott and Moore (1972). For the present we shall assume that it may be ignored, whence we have, on averaging over $\underline{R}$:

$$\sum_{\lambda'} \hat{T}^{(2)}_{\lambda\lambda\lambda'\lambda'} f^1_{\lambda'} = -i\hbar \sum_{\lambda'} \{p^T_{\lambda'\lambda} \quad f^1_{\lambda'} - p^T_{\lambda\lambda'} f^1_{\lambda'}\} \tag{4.3.21}$$

where the transition rates are now given by

$$p^{T}_{\lambda\lambda'} = (2\pi/\hbar)N_s\langle|t^{+}(\varepsilon_\lambda)_{\lambda\lambda'}|^2\rangle\delta(\varepsilon_\lambda-\varepsilon_{\lambda'}) \qquad (4.3.22)$$

as required.

The approach via super-resolvent theory has made it clear, however, that this is not such a natural approximation as at first appears. Even though we have replaced the implicit equation (4.3.1) by the explicit (4.3.11), and have neglected all terms of order higher than two in the t-matrix, we still have to ignore the principal part integral of (4.3.20) in order to obtain the required structure. A more detailed analysis of the resolvent t-matrix expansion is clearly necessary, but we shall not attempt it here.

It remains to perform the scatterer average over $\underline{R}$ for the matrix elements in (4.3.10 and 22). In the Born approximation it is advantageous to express U as a Fourier series:

$$U(\underline{r}-\underline{R}) = \sum_{\underline{q}}\Omega^{-1}U(\underline{q})e^{i\underline{q}.(\underline{r}-\underline{R})} \qquad (4.3.23)$$

$$U(\underline{q}) = \iiint d^3\underline{r}'U(\underline{r}')e^{-i\underline{q}.\underline{r}'}$$

where the summation in $\underline{q}$ is over a set of points uniformly distributed with density $\Omega/8\pi^3$ in $\underline{q}$ space. When $U(\underline{r})$ is spherically symmetric $U(\underline{q}) = U(|\underline{q}|)$, while for axial symmetry $U(\underline{q}) = U(q_\perp, q_z)$. The average of the matrix element over $\underline{R}$ is

$$\langle|U_{\lambda\lambda'}|^2\rangle = \Omega^{-1}\iiint d^3\underline{R}\sum_{\underline{q}}\sum_{\underline{q}'}\Omega^{-2}U(\underline{q})U(\underline{q}')\langle\lambda|e^{i\underline{q}.\underline{r}}|\lambda'\rangle\langle\lambda'|e^{i\underline{q}'.\underline{r}}|\lambda\rangle e^{i(\underline{q}'-\underline{q}).\underline{R}}$$

$$=\Omega^{-2}\sum_{\underline{q}}|U(\underline{q})|^2|\langle\lambda|e^{i\underline{q}.\underline{r}}|\lambda_1\rangle|^2 \qquad (4.3.24)$$

since the $\underline{R}$ integration produces a Kronecker $\delta$ in $(\underline{q}'-\underline{q})$. One of the $\Omega$'s in the above expression cancels with the density factor in the $\underline{q}$ summation, and the other combines with the $N_s$ in (4.3.10) to produce a scattering rate proportional to the density of scatterers.

To average the t-matrix elements in (4.3.22) we must transform to the $(N,m,k_z)$ representation centred on $\underline{R}$, as the methods of §3 produce the matrix elements in this representation. The averaging then amounts to an average over the transformation coefficients. Using the expression (2.1.31) for these, we have (see Kubo et al, 1965)

$$\langle Nk_y k_z|t^+|N';k_y+q_y,k_z+q_z\rangle = \sum_m e^{iq_y Y} e^{iq_z z} 2\pi\ell^2/L \quad \times$$

$$\times\ \phi_{N+m}(X+\ell^2 k_y)\phi_{N'+m}(X+\ell^2 k_y+\ell^2 q_y)\ \langle Nmk_z(\underline{R})|t^+|N'mk_z+q_z(\underline{R})\rangle \qquad (4.3.25)$$

whence, on averaging over $\underline{R}$,

$$\langle|t_{\lambda\lambda'}|^2\rangle =$$

$$= 4\pi^2\ell^4\Omega^{-1}\int_{-\infty}^{\infty}\Big|\sum_m \phi_{N+m}(X')\phi_{N'+m}(X'+\ell^2(k_{y'}-k_y))\langle Nmk_z|t^+|N'mk_{z'}\rangle\Big|^2 dX' \qquad (4.3.26)$$

The transition rate is again proportional to the density of scatterers.

Referring to (2.1.28) for $|\langle\lambda|e^{i\underline{q}\cdot\underline{r}}|\lambda'\rangle|^2$ we see that both of these transition rates depend on the quantum number $k_y$ only through the difference $k_{y'}-k_y$ in the quantum numbers between the states. This fundamental feature arises from the translational invariance of the scattering system, and is of vital importance to the solution of the Boltzmann equation derived in the next section.

## 4.4 Relaxation Time Solutions of the Boltzmann Equation

We now have to solve the Boltzmann equation

$$J_{z\lambda} f^{o\prime}(\varepsilon_\lambda) = \sum_{\lambda'} \{p_{\lambda'\lambda} f^1_{\lambda'} - p_{\lambda\lambda'} f^1_\lambda\} \tag{4.4.1}$$

for the perturbed distribution function $f^1_\lambda$. The exact dependence of the transition rates $p_{\lambda'\lambda}$ on the particular potential involved is not important to the type of solution we shall discuss, but two features are vital. Firstly, we shall require the scattering to be elastic, so that the summation over $\lambda'$ includes only states with the same energy as $\lambda$ (In the case of phonon scattering this means that we must be able to ignore $\hbar\omega_{\underline{q}}$ in comparison with other characteristic energies of the system). Henceforth, therefore, we shall assume that $p_{\lambda\lambda'}$ may be written

$$p_{\lambda\lambda'} = \omega_{\lambda\lambda'} \delta(\varepsilon_\lambda - \varepsilon_{\lambda'}) \tag{4.4.2}$$

Secondly, as we have already noted, $\omega_{\lambda\lambda'}$ depends on the quantum numbers $k_y$ and $k_{y'}$ in the Landau gauge only through their difference $k_{y'} - k_y$. This is a rather weaker symmetry than for the case of spherically symmetric scatterers in zero magnetic field, when $\omega_{\underline{k}\underline{k}'}$ is a function of $|\underline{k}-\underline{k}'|$ only. In this latter case it is usual (see, e.g, Conwell, 1967) to postulate a solution for (4.4.1) of the form

$$f^1_{\underline{k}} = -J_{z\underline{k}} f^{o\prime}(\varepsilon_{\underline{k}}) \tau(\varepsilon_{\underline{k}}) \tag{4.4.3}$$

where $\tau$ is assumed to depend on $\varepsilon_{\underline{k}}$ alone. On substituting back into (4.4.1), remembering that the scattering is elastic, we obtain

$$\begin{aligned} \tau^{-1}(\varepsilon_{\underline{k}}) &= \sum_{\underline{k}'} \omega_{\underline{k}\underline{k}'} (1 - k'_z / k_z) \delta(\varepsilon_{\underline{k}} - \varepsilon_{\underline{k}'}) \\ &= \sum_{\underline{k}'} \omega(|\underline{k}-\underline{k}'|)(1 - k'_z/k_z) \delta(\varepsilon_{\underline{k}} - \varepsilon_{\underline{k}'}) \end{aligned} \tag{4.4.4}$$

If the band of states is spherically symmetric the surface ($\varepsilon_{\underline{k}'} = \varepsilon_{\underline{k}}$) is a sphere of radius $|\underline{k}|$, and hence only the projection of $\underline{k}'$ on $\underline{k}$ contributes to the summation in the $k_{z'}/k_z$ term. This projection is $\cos\theta.\underline{k}$ where $\theta$ is the angle between $\underline{k}$ and $\underline{k}'$; hence

$$\tau^{-1}(\varepsilon_{\underline{k}}) = \sum_{\underline{k}'} \omega(|\underline{k}-\underline{k}'|)(1-\cos\theta)\delta(|\underline{k}|-|\underline{k}'|)\ |\partial k/\partial\varepsilon \qquad (4.4.5)$$

The essential feature of the above expression for $\tau$ is that it is independent of the state $\underline{k}$ which appears in the summation, and hence dependent only on the energy $\varepsilon_{\underline{k}}$. Thus the assumption that $\tau$ is a function of energy alone is self consistent, and the solution (4.4.3) is valid in this case. The quantity $\tau$ has the dimension of time, and if the electric field were suddenly removed the perturbed distribution function would relax back to zero exponentially in time with time constant $\tau$; hence $\tau$ is coventionally called the relaxation time. Further, the expression for $\tau$ is clearly positive definite, so that the current flows in the same direction as the applied field (See Conwell, 1967 and Butcher, 1974, for reviews of relaxation time methods).

Analagously, in a magnetic field we might postulate that

$$f_\lambda^1 = -J_{z\lambda} f^{o'}(\varepsilon_\lambda)\tau(\varepsilon_\lambda)$$
$$\tau^{-1} = \sum_{\lambda'} \omega_{\lambda\lambda'}(1-k_{z'}/k_z)\delta(\varepsilon_\lambda-\varepsilon_{\lambda'}) \qquad (4.4.6)$$

We shall call this the 'Argyres formula', as it is introduced explicitly in his 1958 paper. Argyres in fact applied this formula only to cases when only one Landau band was occupied or when the scattering was 'isotropic' in that $\omega_{\lambda\lambda'}$ was a constant (Argyres 1958, 1960). In more general cases we find that the above expression for $\tau$ depends, not solely on the energy

$\varepsilon_\lambda$, but also on the Landau band number N of the state $\lambda$. Hence the postulate that $\tau$ given by (4.4.6) is a function of energy alone is not self-consistent for general elastic scattering mechanisms, and this form of solution is not possible in such cases.

We therefore generalise (4.4.6) and postulate (following Gurevich and Firsov, 1965)

$$f^1_{Nk_yk_z} = -J_z f^{o'}(\varepsilon_\lambda)\tau_N(\varepsilon_\lambda) \qquad (4.4.7)$$

in which each Landau sub-band is assigned a separate relaxation time. Substituting into the Boltzmann equation, remembering again that the summation is only over states of the same energy, we have

$$J_z f^{o'}(\varepsilon_\lambda) = \sum_{\lambda'} \omega_{\lambda\lambda'}\{J_z f^{o'}(\varepsilon_\lambda)\tau_N(\varepsilon_\lambda) - J_{z'} f^{o'}(\varepsilon_{\lambda'})\tau_{N'}(\varepsilon_{\lambda'})\}\delta(\varepsilon_\lambda - \varepsilon_{\lambda'})$$

$$\text{or} \qquad 1 = \sum_{\lambda'} \omega_{\lambda\lambda'}\{\tau_N(\varepsilon_\lambda) - \tau_{N'}(\varepsilon_\lambda)k_{z'}/k_z\}\delta(\varepsilon_\lambda - \varepsilon_{\lambda'}) \qquad (4.4.8)$$

The restriction $\varepsilon_{\lambda'} = \varepsilon_\lambda$ in (4.4.8) means that only a finite number of sub-bands contribute to the sum, since any state $\lambda'$ which contributes must have $(N'+\frac{1}{2})\hbar\omega_c < \varepsilon_\lambda$. Similarly, for a given sub-band only two values of $k_{z'}$ are allowed, determined by

$$k_{z'} = \pm(2m_z\hbar^2)^{\frac{1}{2}}(\varepsilon_\lambda - (N'+\tfrac{1}{2})\hbar\omega_c)^{\frac{1}{2}} \equiv \pm k_{N'}. \qquad \text{Thus (4.4.8) becomes}$$

$$1 = 2\sum_{N'=0}^{P}\sum_{k_{z'},k_{y'}}\sum \omega_{\lambda\lambda'}\{\tau_N(\varepsilon_\lambda) - \tau_{N'}(\varepsilon_\lambda)k'_z/k_z\}\left|\partial k_{z'}/\partial\varepsilon\right| L/2\pi \times$$

$$\times \quad \delta(|k_{z'}| - (2m_z/\hbar^2)^{\frac{1}{2}}(\varepsilon_\lambda - (N'+\tfrac{1}{2})\hbar\omega_c)^{\frac{1}{2}}) \qquad (4.4.9)$$

where the factor 2 accounts for spin degeneracy, and $L/2\pi$ is the density of points in the $k'_z$ sum. We see that this can be written in matrix form as

$$\{1\} = \{R^{OUT}(\varepsilon) - R^{IN}(\varepsilon)\}\{\tau(\varepsilon)\} = \{R(\varepsilon)\}\{\tau(\varepsilon)\} \tag{4.4.10}$$

where $\{1\}$ and $\{\tau\}$ are column vectors, and the P+1 x P+1 matrices $\{R^{OUT}\}$ and $\{R^{IN}\}$ derive from the scattering out and scattering in terms, given by

$$R^{OUT}_{NN'}(\varepsilon) = \delta_{NN'}\sum_{M=0}^{P}(m_z L/\hbar^2\pi)\{\sum_{k_{y'}}\omega_{\lambda;Mk_{y'},+k_M'}/k_M + \sum_{k_{y'}}\omega_{\lambda;Mk_{y'},-k_M'}/k_M\} \tag{4.4.11}$$

$$R^{IN}_{NN'}(\varepsilon) = (m_z L/\hbar^2\pi)\{\sum_{k_{y'}}\omega_{\lambda;N'k_{y'},+k_N'}/k_N - \sum_{k_{y'}}\omega_{\lambda;N'k_{y'},-k_N'}/k_N\} \tag{4.4.12}$$

Since the transition rates $\omega_{\lambda\lambda'}$ depend on the $k_y$ and $k_{y'}$ quantum numbers only through their difference, the $k_y$ dependence in the above summation vanishes, and we may write

$$(m_z L/\hbar^2\pi)\sum_{k_{y'}}\omega_{Nk_yk_N;N'k_{y'},\pm k_N'} = W_{NN'}(k_N,\pm k_N') \tag{4.4.13}$$

Using the detailed balance relation $\omega_{\lambda\lambda'} = \omega_{\lambda'\lambda}$ and time reversal symmetry we may show that $W_{NN'}(k_N,k_N') = W_{NN'}(-k_N,-k_N')$. Hence any possible dependence of $R^{OUT}$ and $R^{IN}$ on the sign of $k_N$ may be eliminated, and $R^{OUT}$ and $R^{IN}$ may be written

$$R^{OUT}_{NN'}(\varepsilon) = \delta_{NN'}\sum_{M=0}^{P}k_M^{-1}(W_{NM}(k_N,k_M)+W_{NM}(k_N,-k_M)) \tag{4.4.14}$$

$$R^{IN}_{NN'}(\varepsilon) = k_N^{-1}((W_{NN'}(k_N,k_N')-W_{NN'}(k_N,-k_N')) \tag{4.4.15}$$

The essential feature here is that, since $k_N$ and $k_{N'}$ depend only on N,N' and $\varepsilon$, the elements of $R^{OUT}$ and $R^{IN}$ also depend only on N,N' and $\varepsilon$. Thus the form for $f^1$ postulated in (4.4.7) in which $\tau$ depends only on N and $\varepsilon$ is consistent with the solution for $\tau$ obtained from (4.4.10), and is therefore a valid solution of the Boltzmann equation.

The matrix $\{R(\varepsilon)\}$ will henceforth be called the relaxation matrix at energy $\varepsilon$. Its order, and hence the number of separate relaxation times $\tau_N$, is the number $P(\varepsilon)+1$ of Landau sub-bands which include states of energy $\varepsilon$, and is given by $(\varepsilon/\hbar\omega_c)-\frac{1}{2}\leqslant P<(\varepsilon/\hbar\omega_c)+\frac{1}{2}$. Hence the order of $\{R\}$ and the number of relaxation times increase by one as each new Landau sub-zone is entered. (Note that the highest band number involved is P).

Finally, we may now work out the expression for the longitudinal magnetoconductivity derived from the perturbed distribution function $f^1$ of (4.4.7). From (4.2.28) we have

$$\sigma_{zz} = \Omega^{-1}\sum_{\lambda} J_{z\lambda} f^1_{\lambda} \qquad (4.4.16)$$

which therefore now becomes

$$\sigma_{zz} = 2\Omega^{-1}\sum_{Nk_yk_z} e^2 k_z^2 \hbar^2/m_z^2 (-f^{o'}(\varepsilon_{Nkz}))\tau_N(\varepsilon_{Nkz}) \qquad (4.4.17)$$

Combined with

$$\{\tau(\varepsilon)\} = \{R(\varepsilon)\}^{-1}\{1\} \qquad (4.4.18)$$

where $\{R\}$ is the relaxation matrix defined above, we have a formula for $\sigma_{zz}$ which is capable of direct evaluation.

## 4.5 Time Dependent Relaxation in a Magnetic Field

We must now discuss some important general properties of the relaxation time solutions of (4.4.18), and in particular of the expression (4.4.17) for $\sigma_{zz}$. Firstly, we must assure ourselves that the expression obtained for $\sigma_{zz}$ is positive definite, as otherwise we could have the current produced by the field flowing counter to the direction of the field! Intuitively, it appears that we have to prove that all the relaxation times $\tau_N(\varepsilon)$ must be positive definite, but, surprisingly, we will find that this cannot be guaranteed.

A closely related problem is that of the time dependent relaxation of a perturbed distribution back to equilibrium on removal of the perturbing force. We must investigate the nature and time-scale of the relaxation process, and verify that the perturbation does indeed decay away. In order to do this, we shall assume without proof that the equation describing the time development of f in the absence of any electric field is

$$\partial f_\lambda/\partial t = \sum_{\lambda'}\{p_{\lambda'\lambda} f_{\lambda'} - p_{\lambda\lambda'} f_\lambda\} \qquad (4.5.1)$$

corresponding to the steady state Boltzmann equation (4.4.1). We may expect this equation to be valid in a low density system for which the time constants of the relaxation of f are much longer than the collision duration (Kohn and Luttinger, 1957).

Using the same assumption of elastic scattering as in §4.4, we may postulate a solution of the form

$$f_{Nk_yk_z} = k_z f_N(\varepsilon_\lambda) e^{-\omega(\varepsilon_\lambda)t} \qquad (4.5.2)$$

which decays exponentially in time with time constant $\omega^{-1}$, and which depends only on the band number and the energy.

By a process identical to that used in §4.4 we obtain, on summing (4.5.1) over $k_y$ and $k_z$,

$$\omega f_N(\varepsilon) = \{R(\varepsilon)\} f_N(\varepsilon) \tag{4.5.3}$$

where $\{R(\varepsilon)\}$ is exactly the same relaxation matrix as in (4.4.10). This, however, is an eigenvalue equation, with its P+1 solutions $\omega^i$ determined by:

$$||R(\varepsilon) - \omega I|| = 0 \tag{4.5.4}$$

The structure of $\{R\}$ fortunately allows us to draw some general conclusions about its eigenvalues $\omega^i$. We first define the two matrices

$$W^{\pm}_{NN'} = W_{NN'}(k_N, \pm k_{N'}) \tag{4.5.5}$$

and note that, by the time reversal and detailed balance relations, $W^+$ and $W^-$ are positive definite and symmetric. Then from (4.4.14) and (4.4.15) we see that $\{R\}$ is of the form

$$\{R\} = \{D(k^{-1})\}\{S\} \tag{4.5.6}$$

where $\{D(k^{-1})\}$ is a diagonal, positive definite matrix defined by

$$D_{NN'}(k^{-1}) = \delta_{NN'} k_N^{-1} \tag{4.5.7}$$

and $\{S\}$ is the symmetric matrix given by

$$S_{NN'} = \delta_{NN'} \sum_{M=0}^{P} (W^+_{NM} + W^-_{NM}) k_N / k_M - (W^+_{NN'} - W^-_{NN'}) \tag{4.5.8}$$

For a matrix $\{R\}$ of this form it is easily shown (see Appendix 4) that the eigenvalues $\omega^i$ are all real, and that the eigenvectors $f^i$

corresponding to them may be made orthonormal in the sense

$$\sum_{N=0}^{P} f_N^i f_N^j k_N = \delta_{ij} \tag{4.5.9}$$

Further, all the $\omega^i$ are positive definite if and only if $\{S\}$ is positive definite. That $\{S\}$ is indeed positive definite is readily shown, for from (4.5.8)

$$\begin{aligned}\sum_{N,M} a_N S_{NM} a_M &= \sum_N a_N^2 \sum_M (W^+_{NM}+W^-_{NM}) k_N/k_M - \sum_{N,M} a_N a_M (W^+_{NM}-W^-_{NM}) \\ &= \sum_{N,M} \{W^+_{NM}\{(k_N/k_M)^{\frac{1}{2}} a_N - (k_M/k_N)^{\frac{1}{2}} a_M\}^2/2 \\ &\quad + W^-_{NM}\{(k_N/k_M)^{\frac{1}{2}} a_N + (k_M/k_N)^{\frac{1}{2}} a_M\}^2/2\}\end{aligned} \tag{4.5.10}$$

Since $W^+$ and $W^-$ are positive definite, the above expression is positive for an arbitrary non-zero vector a, as required.

We recall that the $\omega^i$ are the decay constants of the time dependent relaxation described by (4.5.2). Hence any perturbation to the distribution function of the form $f^1_{Nk_yk_z} = k_z x_N(\varepsilon_{Nk_z})$ will decay to zero as:

$$f^1_{Nk_yk_z}(t) = \sum_i k_z x^i f^i_N(\varepsilon_{Nk_z}) e^{-\omega^i(\varepsilon_{Nk_z})t} \tag{4.5.11}$$

where the coefficient $x^i$ of the eigenvector i in x is given by

$$x^i = \sum_N x_N f^i_N k_N \tag{4.5.12}$$

It is thus seen that the general form of relaxive decay of the electron distribution function in a magnetic field (via elastic scattering processes) is exponential in time. At a single energy, such as would be the case in a

highly degenerate material, the number of time constants involved is finite, but in general greater than one. Conditions necessary to observe such multiple decay constant effects in a time resolved experiment with pulsed electric fields would be $\hbar\omega_c >> kT$ and $P(\varepsilon_F) > 1$. The dominant scattering mechanisms would also have to be of a type such that the $\omega^i$ were well separated from each other.

We can now see that the true 'relaxation times' of the system are the set of values $(\omega^i)^{-1}$, rather than the $\tau_N$ previously defined. However, returning now to these, we may solve equation (4.4.18) by using the spectral resolution of $\{R\}$, namely (see Appendix 4)

$$\{R^{-1}\}_{NN'} = \sum_i (\omega^i)^{-1} f_N^i f_{N'}^i k_N \qquad (4.5.13)$$

The $\tau_N$ may now be easily found:

$$\tau_N \quad \{R^{-1}\}\{I\} = \sum_i (\omega^i)^{-1} f_N^i \sum_M f_M^i k_M \qquad (4.5.14)$$

It is interesting to note that, although the $\omega^i$ are all positive, there is nothing in the above expression to guarantee that $\tau_N$ will always be positive. We have already seen that this would have no unphysical effect in the time dependent relaxation; we must verify also that the conductivity remains positive.

Substituting into (4.4.17), and replacing the $k_z$ summation by an energy integral

$$\sigma_{zz} = ne^2/m \int_0^\infty d\varepsilon (-\rho^{o\,\prime}(\varepsilon)) \sum_i (\omega^i)^{-1} \left(\sum_{N=0}^{P} f_N^i k_N\right)^2 \qquad (4.5.15)$$

where the normalised equilibrium distribution function $\rho^o$ is defined so that

$$\int_o^\infty d\epsilon 2\Sigma_N \rho^o(\epsilon_{Nk_z}) = 1 \qquad (4.5.16)$$

and the number density of electrons is n. For a Maxwell-Boltzmann or Fermi Dirac distribution function $-\rho^{o\,\prime}(\epsilon)$ is positive, and hence the above expression for $\sigma_{zz}$ is positive definite as it should be.

## 4.6 Approximate Inversions of the Relaxation Matrix

We shall now discuss several regimes where the inversion of the relaxation matrix in (4.4.18) may be simplified or approximated. Firstly, we may now compare the exact solution of the Boltzmann equation with that given by the Argyres formula (4.4.6). The column vector of exact relaxation times is given by

$$\{\tau(\varepsilon)\} = \{R^{-1}(\varepsilon)\}\{I\} \tag{4.6.1}$$

whereas the Argyres formula may easily be shown to be equivalent to

$$\{\tau_A^{-1}(\varepsilon)\} = \{R(\varepsilon)\}\{I\} \tag{4.6.2}$$

Except under the special circumstances discussed below, these two equations for the relaxation times produce different results, and as previously mentioned the solution (4.4.6 ) is then not self consistent.

There are two special situations in which the solutions to (4.6.1) and (4.6.2) coincide, so that the matrix inversion in (4.6.1) may be avoided. Firstly, in the Quantum Limit, when the magnetic field is so high that only the lowest Landau sub-band is occupied, we have P=0 and hence $\{R\}$ is just a number. This simple case has been extensively studied (see, e.g., Argyres 1958, 1960, Bychkov, 1961), and presents no difficulty in the evaluation of the single relaxation time $\tau_o(\varepsilon)$ involved.

Secondly, for certain types of potential $\{R(\varepsilon)\}$ may be diagonal for all values of the energy, in which case (4.6.1) and (4.6.2) are identical. The off-diagonal part of $\{R\}$ is due to the scattering in terms, and from (4.4.15) the condition for these to vanish is

$$W_{NN'}(k_N,k_{N'}) = W_{NN'}(k_N,-k_{N'}) \tag{4.6.3}$$

This is satisfied for a scattering potential which is of such a small extent relative to the magnetic length that it may be considered to be a $\delta$ function, for in this case $U(q) = a^3U$ (where a is a characteristic length) and $\langle Nnk_N|t|N'mk_{N'}\rangle = \delta_{mo}t$ (see §3.2). It then follows from the expressions (4.3.24) and (4.3.26) that

$$W_{NN'}(k_N,\pm k_{N'}) = W = 4\pi n_s m_z \ell^4/\hbar^3 (a^3U/2\pi\ell^3)^2 \qquad (4.6.4)$$

$$\text{or} \qquad = 4\pi n_s m_z \ell^4 |t|^2/\hbar^3$$

depending on whether the Born approximation or the t matrix is used. The single relaxation time $\tau(\varepsilon)$ is then given by

$$\tau^{-1}(\varepsilon) = 2W \sum_{M=0}^{P} k_M^{-1}(\varepsilon) \qquad (4.6.5)$$

This solution is well known (see, e.g., Argyres 1958), and is important because it also describes scattering by acoustic phonons at high temperature. In this case the electron-phonon coupling coefficient $|C(q)|^2$ in (4.3.5) combines with $\bar{N}_q$ to produce a term independent of q, giving the same isotropic scattering behaviour.

Use of the Argyres formula when the scattering mechanisms are not isotropic can lead to serious errors in the evaluation of the conductivity. Using the notation of §4.5 in the solution of (4.6.2) we have

$$\tau_{AN}^{-1} = k_N^{-1} \sum_{M=0}^{P} \{W_{NM}^{-}(1+k_N/k_M) - W_{NM}^{+}(1-k_N/k_M)\} \qquad (4.6.6)$$

Away from the bottom of the band the q vector for a transition which changes the sign of the z momentum is much larger than that for one in which the sign is unaltered. For many potentials the Fourier transform falls off

fairly rapidly with q so that, away from the bottom of the band, $W^+$ is much larger than $W^-$. Given this situation, it is obvious that for some bands the inverse of the Argyres relaxation time given by (4.6.6) can go through zero and become negative. This will result in a non-integrable singularity in the formula (4.4.17) for $\sigma_{zz}$, and a region in which $\sigma(\varepsilon)$ is negative. We have demonstrated this effect for a specific potential in §5, thus emphasising the necessity of using the correct form (4.6.1) for the relaxation times.

Very near the bottom of each Landau sub-band it is always possible to simplify the matrix inversion in (4.6.1), and this was the regime in which such an equation was originally solved by Efros (1965). Near the bottom of sub band P $k_P \ll k_N$ for all other bands N<P, and the approximate solutions of (4.4.10) are

$$\tau_P^{-1} \sim k_P^{-1}(2W_{PP}^- - \sum_{N=0}^{P}(W_{PN}^- - W_{PN}^+)) \qquad (4.6.7)$$

$$\tau_N^{-1} \sim k_P^{-1}(W_{PN}^- + W_{PN}^+) \qquad N<P$$

Since for any finite ranged potential $W_{PN}^+ - W_{PN}^- \to 0$ as $k_P \to 0$, we have the simple solution

$$\tau_N \sim k_P / 2W_{PN}^- \qquad (4.6.8)$$

so that the relaxation times all drop to zero at the bottom of each Landau sub-band, as for isotropic scattering. In this limit there is no distinction between the Argyres formula and the matrix inversion.

When two scattering mechanisms X and Y are present the relaxation matrix becomes the sum of the two matrices $\{R^X\}$ and $\{R^Y\}$. If we suppose

that mechanism X is dominant, then $\{R^Y\}$ can be regarded as a small perturbation, in which case an approximate solution of (4.6.1) is

$$\{\tau\} = \{R^X\}^{-1}\{1\} - \{R^X\}^{-1}\{R^Y\}\{R^X\}^{-1}\{1\} \tag{4.6.9}$$

If the relaxation times $\tau_X$ have already been obtained,

$$\{\tau\} = \{\tau_X\} - \{R^X\}^{-1}\{R^Y\}\{\tau_X\} \tag{4.6.10}$$

and in the simplest case when X is an isotropic scattering mechanism

$$\{\tau\} = \tau_X\{1\} - \tau_X^2\{R^Y\}\{1\} \tag{4.6.11}$$

In this case the Argyres formula again agrees with the exact result.

Finally, we mention the zero magnetic field limit of the relaxation matrix solution. Isotropic scattering is easily dealt with ; from (4.6.5) we have

$$\tau^{-1}(\varepsilon) = 2W\sum_{M=0}^{P} k_M^{-1}(\varepsilon) = 2W(\hbar^2/2m_z)^{\frac{1}{2}}\sum_{M=0}^{P}(\varepsilon-(M+\tfrac{1}{2})\hbar\omega_c)^{\frac{1}{2}} \tag{4.6.12}$$

As the field becomes small and $\hbar\omega_c \to 0$ the summation over M can be converted to an integral

$$\tau^{-1}(\varepsilon) = 2W(\hbar^2/2m_z)\int_0^{\varepsilon/\hbar\omega_c}(\varepsilon-(M+\tfrac{1}{2})\hbar\omega_c)^{\frac{1}{2}}dM$$

$$= (4W/\omega_c\sqrt{2m_z})\sqrt{\varepsilon} \tag{4.6.13}$$

On substituting from (4.6.4) we obtain

$$\tau^{-1}(\varepsilon) = n_s(2m_z)^{\frac{3}{2}}|a^3U|^2/\pi\hbar^4 \tag{4.6.14}$$

in agreement with the usual result (see, e.g. Butcher 1974). The smoothing introduced by replacing the sum over M by an integral removes the characteristic singularities in $\tau^{-1}$ at the bottom of each Landau sub-band. As $\hbar\omega_c \to 0$, $N \to \infty$ such that $\varepsilon = (N+\frac{1}{2})\hbar\omega_c$ remains constant, the singular part of $\tau^{-1}$ becomes confined to a proportion $N^{-1}$ of the energy range. Thus the characteristic magnetic field structure of the relaxation time spectrum disappears as soon as $N^{-1}\hbar\omega_c = (\hbar\omega_c)^2/\varepsilon$ becomes of the same order as the collision broadening in the system.

For the general case when the matrix $\{R(\varepsilon)\}$ is non-diagonal, the low field limit is much more difficult to obtain. Equation (4.4.10) now becomes an integral equation:

$$1 = \tau(N;\varepsilon)\int_0^P R^{OUT}(N,N';\varepsilon)\,dN' - \int_0^P R^{IN}(N,N';\varepsilon)\tau(N';\varepsilon)\,dN' \qquad (4.6.15)$$

Obtaining the low field limit of the kernels $R^{OUT}$ and $R^{IN}$ is non trivial, and the details, for a spherically symmetric scatterer in the Born approximation, are relegated to Appendix 3. The main difference from the isotropic case considered above is that it is not now sufficient to obtain the low field limit of the energy density of states, as $\tau(N;\varepsilon)$ may vary for different values of N at the same energy. It is necessary to go further and obtain low field limits for the state wave functions in order to evaluate the kernels $R^{IN}$ and $R^{OUT}$. We essentially show that, in the low field limit, the infinite N summation over Landau states is identical, with suitable changes of variable, to a spherical integral over zero magnetic field plane wave states. Having evaluated the kernels, we find that a solution in which $\tau(N;\varepsilon)$ is independent of N is self consistent and

that

$$\tau^{-1}(N;\varepsilon) = \tau^{-1}(\varepsilon) = n_s/2\pi^2\hbar^2(m_z/2\varepsilon)^{\frac{1}{2}}\int\int d^2k' |V(\underline{k}'-\underline{k}|^2(1-\cos\theta) \quad (4.4.16)$$

where the integral is over the surface of a sphere of radius $(2m_z\varepsilon/\hbar^2)^{\frac{1}{2}}$. This again agrees with the usual result in the absence of a magnetic field.

# CHAPTER 5

## The Electron-Hole-Droplet Magnetoresonance in Germanium

### 5.1 Introduction

In this chapter we shall present a detailed account of a theoretical study of a resonant effect in the longitudinal magnetoresistance of germanium, which was discovered experimentally by Eaves, Markiewicz and Furneaux (1976). Their experiments were carried out on a sample of ultra-pure crystalline germanium at a temperature of $2^{o}K$ under conditions of strong photo-excitation by radiation from a mercury arc lamp. These conditions are known to favour the production of electron-hole droplets (EHDs); small spherical volumes of strongly interacting excitons in a condensed liquid-like phase in which individual particles are no longer distinguished (See §5.2). A large number of these EHDs was indeed produced in the samples of Eaves et al; as could be detected by the emission of a characteristic radiation due to recombination of electrons and holes.

On measuring the longitudinal magnetoresistance in a magnetic field parallel to a {100} axis, the curve of Fig. 5.1 was obtained. The marked oscillations of the curve were found to be closely periodic in $B^{\frac{1}{2}}$, as illustrated by the dashed lines in Fig. 5.1 which are spaced at regular intervals of $0.0124T^{\frac{1}{2}}$ in $B^{\frac{1}{2}}$.

It was postulated by Eaves et al that the oscillatory effect was caused by the presence of the EHDs, acting as scattering potentials for the conduction electrons in the form of spherical square wells. The Fourier transform of such a potential, which appears in the matrix elements

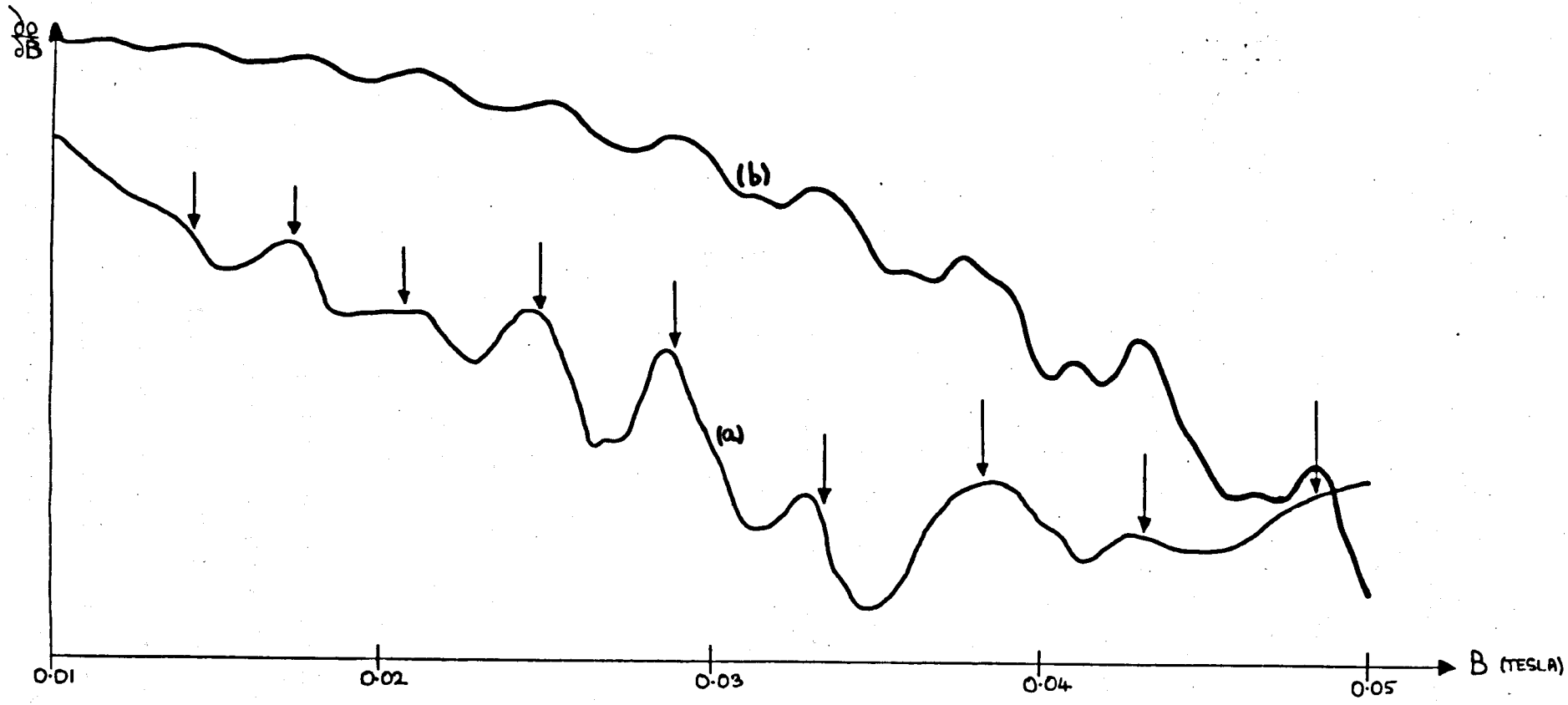


Fig. 5.1 Magnetoresistance curves for ultra pure germanium under strong photo-excitation at $2^{o}K$ (Eaves, Markiewicz and Furneaux 1976)

a) Experimental curve with peaks at regular intervals of $0.0124T^{\frac{1}{2}}$ in $B^{\frac{1}{2}}$.

b) Curve obtained from elementary theory of Eaves et al

for scattering (See §4.3), has an oscillatory structure with a period $\pi/a$ in wave-vector space, where a is the radius of the well. We must therefore expect any relaxation time (See §4.4) to be oscillatory. It also follows from the analysis of §4.4 that the relaxation times have an overall sawtooth structure, in which they drop to zero at the bottom of each new Landau zone, due to the infinite density of states for scattering, and rise to a maximum at the top of each zone (See Fig. 5.2). The major contribution to the longitudinal magnetoconductivity thus comes from energies just below the top of each Landau zone.

If we consider just the innermost Landau band in each zone, then the momentum transfer $q_o$ for scattering just below the top of the P=N zone is $q_o = 2k_N = 2\sqrt{2}/\ell = 2(2e/\hbar)^{\frac{1}{2}}B^{\frac{1}{2}}$. When this value of q is inserted in the scattering matrix elements, the periodic nature of the Fourier transform will give a higher or a lower value, depending on the precise value of $B^{\frac{1}{2}}$. Effectively, the relaxation time $\tau_o$ just below the top of a Landau zone will oscillate as $B^{\frac{1}{2}}$ varies, with period

$$\Delta B^{\frac{1}{2}} = (\pi/2a)(\hbar/2e)^{\frac{1}{2}} \qquad (5.1.1)$$

By our previous argument, we may expect this oscillation to be reflected in the overall magnetoconductivity, which should have a component with the same periodic behaviour in $B^{\frac{1}{2}}$.

It is thus seen that the periodicity of the magnetoresistance oscillations can be used as a measurement of the radius of the EHDs, by analysis of the period (5.1.1). Droplet radii have been measured by many different techniques, with a spread of values in the range 2-10 μm (See §5.2), and yet another method is not amiss. In practice, however, we first have to take account of the detailed band structure of germanium, in which the anisotropy of the conduction band valleys leads to separate

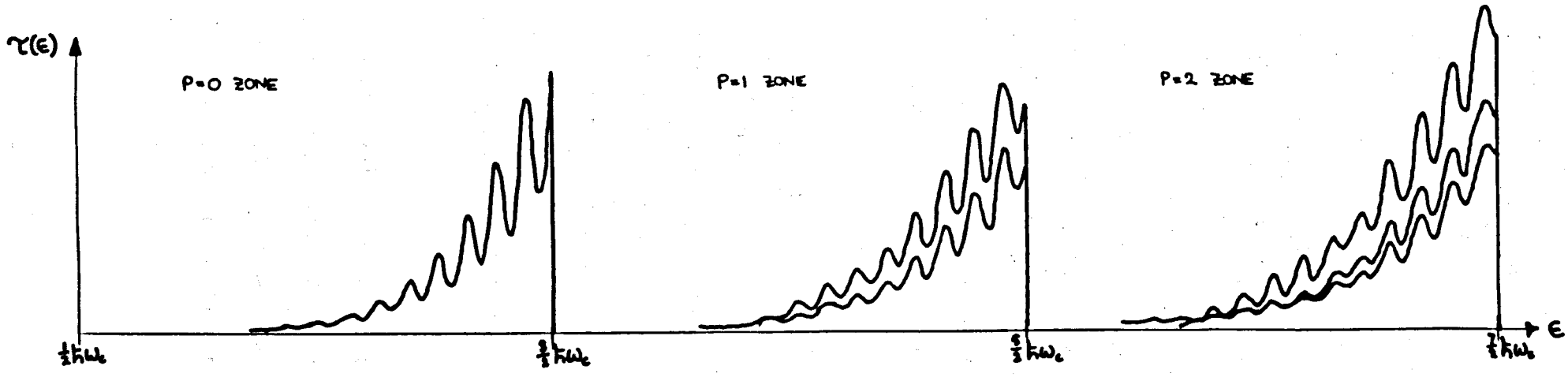


Fig. 5.2 Expected conduction band relaxation time spectrum in the EHD scattering system

values of the cyclotron mass $m_c$ and the kinetic mass $m_z$ (See §2). When this is taken into account the period of the oscillations becomes

$$B^{\frac{1}{2}} = (\pi/2a)(\hbar m_c/2e m_z)^{\frac{1}{2}} \qquad (5.1.2)$$

which leads to an estimate of 1.1 μm for the droplet radius (Eaves et al 1977).

A similar resonant effect in the magnetoresistance of InSb doped with NiSb was reported by Nicholas, Stradling and Eaves (1976), Nicholas and Stradling (1979). Here the NiSb was known to be present in the form of long rod-like cylindrical inclusions in the bulk material, and a similar interpretation in terms of a hard cylindrical potential gave a radius of ~1 μm.

The experimental curve of Eaves et al was also compared with a theoretical calculation (curve (b) in Fig. 5.1) based on evaluation of a single relaxation time by the 'Argyres fomula'. In the light of our analysis of §4.4 we do not believe this approach to be tenable in this problem, and indeed our work indicates that it may run into serious difficulties. Instead, we base our calculation on the relaxation matrix - multiple relaxation time theory developed in §4.4, as summarised by Barker and Bridges (1977).

In §5.2 we present the experimental evidence for the existence of EHDs, and, once established, their properties. Other aspects of the transport problem are discussed in §5.3, where we give the values we have used for all parameters, and our reasons for adopting them.

§5.4 presents the calculation in detail, and shows how various approximations allow simple analytic formulae to be derived for the conductivity. In §5.5 we present the results of an earlier numerical calculation of the magnetoconductivity and compare it with the theory of §5.4 and with the experimental work of Eaves et al. Finally in §5.6 we discuss problems raised by the calculation and comparison with experiment, and conclude that the effective EHD scattering potential cannot be as strong as has been assumed. We also indicate some areas which would repay more detailed investigation in the future.

## 5.2 Electron-Hole-Droplets in Germanium

It has long been known that a single electron-hole pair may exist in a crystalline solid in a state of close spatial association, forming a hydrogen-like 'molecule' bound together by the Coulomb attraction of the oppositely charged electron and hole at an energy lying slightly below the bottom of the conduction band. These elementary excitations are known as excitons, and an extensive review of their theory has been made by Knox (1963). McLean (1961) has reviewed their properties in germanium and silicon.

A characteristic indication of the presence of excitons in semiconductors is the emission of radiation as a sharp peak in the infra-red when the electron drops back into the valence band to annihilate the hole; the lifetime of the exciton against this process may, however, be as long as 8 μs in an indirect gap semiconductor such as germanium (Pokrovsky, Kaminsky and Svistunova 1970a).

With intense photo-excitation one can thus produce a high density of long-lived excitons of large radius (~0.018 μm in Ge, Rice, 1974), and there was at first some controversy as to the expected effects of an attractive interaction between them. Haynes (1966) interpreted a new peak in the recombination radiation (RR) spectrum of excitons in silicon to be due to the formation of an excitonic molecule or bi-exciton, while Asnin, Rogachev and Ryvkin (1968) interpreted a jumpwise increase in conductivity in germanium as a Mott transition to metallic conduction. Keldysh (1968) discussed the various possibilities and suggested that at low enough temperature the excitons might condense into a dense liquid-like state in which individual electron-hole pairs were no longer distinct; this came to be known as the electron-hole liquid (EHL).

These remarks stimulated an intense period of experimental investigation into the condensed state, mainly in Ge. The first report was by Pokrovsky and Svistunova (1969, 1970a and b) who detected a new peak in the RR at $4^{o}K$, 4.6 meV below the main free exciton peak at 714 meV, which disappeared on raising the temperature. From their data they were able to deduce a lifetime for e-h pairs in the liquid of $\tau \sim 20$ $\mu$s, a density of e-h pairs in the condensed phase of $n_c \sim 2 \times 10^{23} m^{-3}$ and work functions for electrons and holes against removal from the liquid of $\phi_e \sim 3.3$ meV and $\phi_h \sim 2.5$ meV respectively (See Fig. 5.3). It was soon recognised that the EHL existed in small droplets, and Bagaev, Galkina, Gogolin and Keldysh (1969) demonstrated the movement of these electron-hole droplets (EHD) towards regions of greater deformation of the crystal sample, interpreted as being due to a reduction of the binding energy of the droplet particles under stress, which was detected by a shift in the RR peak. Vavilov, Zayats and Murzin (1969) measured scattering by EHDs at a frequency in the far IR postulated to be that of the plasma oscillations of the EHL ($2 \times 10^{13} s^{-1}$) and deduced values of $n_c$ as $\sim 2 \times 10^{23} m^{-3}$, and the radius a of the droplet as $\sim$10-20 $\mu$m. Yet another method of detection of the EHDs in Ge was that of Asnin, Rogachev and Sablina (1970), who detected large current pulses in a p-n junction at $4.2^{o}K$, disappearing above $6^{o}K$, which were interpreted as being due to the annihilation of complete droplets. A similar experiment was later performed by Benoit a la Guillaume, Voos, Salvan, Laurant and Bonnot (1971). Ben oit a la Guillaume, Voos and Salvan (1971, 1972) also estimated the diffusion constant of EHDs as 0.015 $m^2 s^{-1}$ from a spatial resolution of the RR from the cloud of droplets, and estimated the formation time for a dropletcontaining$\sim 10^6$e-h pairs to be $\sim$0.5 $\mu$s, with a lifetime of 40 $\mu$s. The most conclusive evidence up to this point for the existence of EHL in

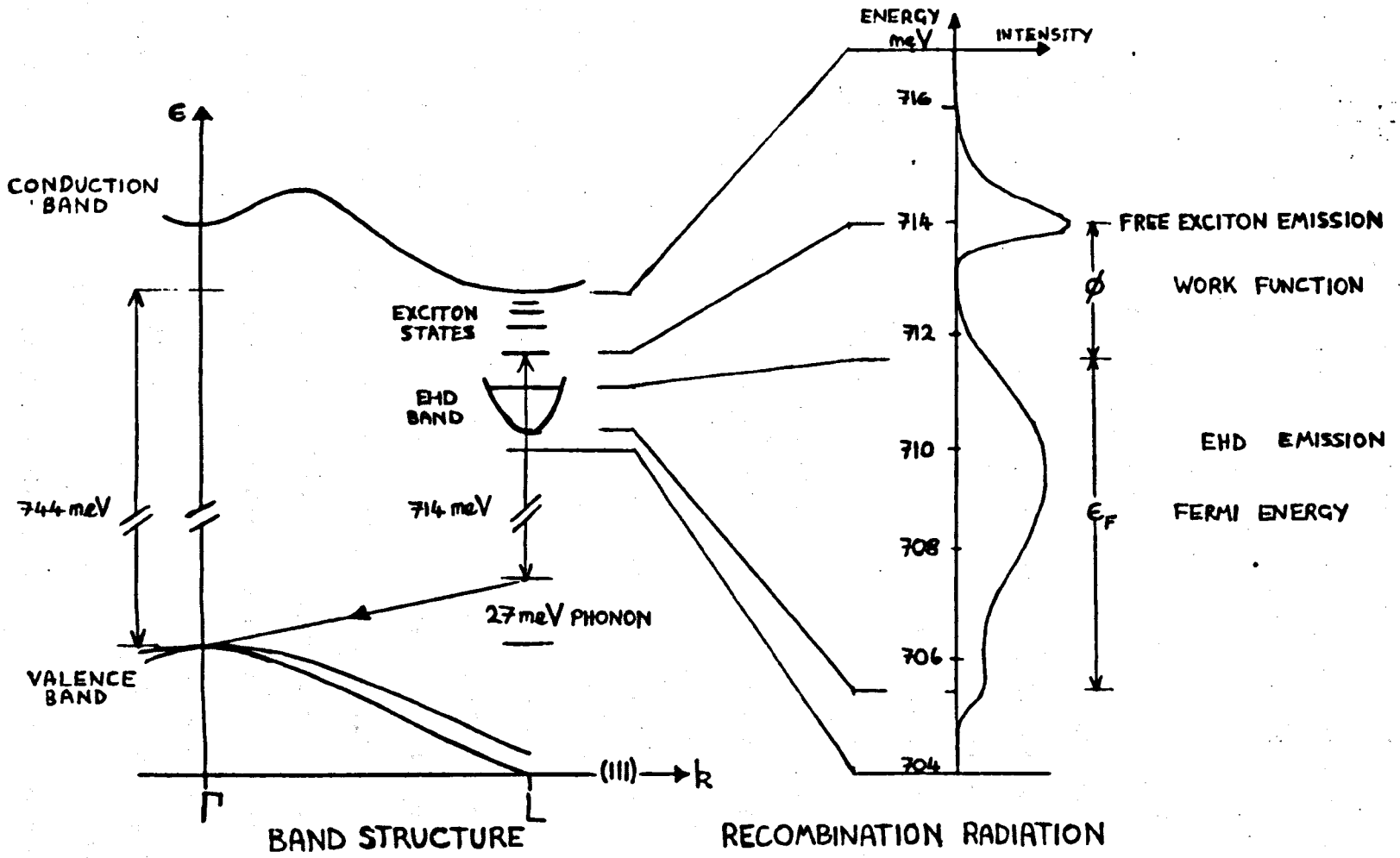


Fig. 5.3 Energy/momentum band scheme for germanium including exciton and EHD states, and showing also the resulting electron-hole recombination radiation spectrum.

in the form of small droplets was the observation by Pokrovsky and Svistunova (1971) of classical Rayleigh scattering of light by the droplet cloud. By altering the excitation power they were able to measure variations in the radius of the EHDs from 3.8 μm at an excitation rate of $1.8 \times 10^{24} m^{-3} s^{-1}$ to 8.8 μm at the higher excitation rate of $4.5 \times 10^{24} m^{-3} s^{-1}$. A schematic representation of some of these experiments appears in Fig. 5.4. A review of the experimental data thus far was made by Pokrovsky (1972).

At this point theoretical investigations of the e-h liquid phase began to appear in an attempt to predict the ground state energy and carrier concentration. Combescot and Nozieres (1972) carried out a calculation in the RPA for Ge and Si, arriving at a binding energy per e-h pair in Ge of 6.1 meV which, on consideration of the exciton binding energy of 3.6 meV, gave a work function of $\phi_{ex} = 2.5$ meV against removal of an exciton from the droplet. They also found very close agreement with the experimental value of $n_c = 2 \times 10^{23} m^{-3}$ for the carrier density. Brinkman, Rice, Anderson and Chui (1972) carried out a similar, though less accurate calculation. These results could soon be compared, with fair agreement, with the experimental data of Hensel, Phillips and Rice (1973 : Cyclotron resonance), Thomas, Phillips, Rice and Hensel (1973 : R R Lineshape) and Sibel'din, Bagaev, Tsvetkov and Penin (1973 : Light scattering). Of interest from the point of view of magnetic effects was the observation by Bagaev, Galkina, Penin, Stopachinsky and Churaeva (1972) of oscillations in the RR intensity with magnetic field, interpreted as a Shubnikov-deHaas type oscillation due to the changing Fermi level of the electrons in the droplet. The oscillations were periodic in $B^{-1}$ and consistent with a carrier density of $2 \times 10^{23} m^{-3}$. This followed earlier work by Alekseev, Bagaev, Galkina, Gogolin, Penin, Semenov and Stopachinsky (1970) which gave evidence for an increase of the binding energy of the EHL with magnetic

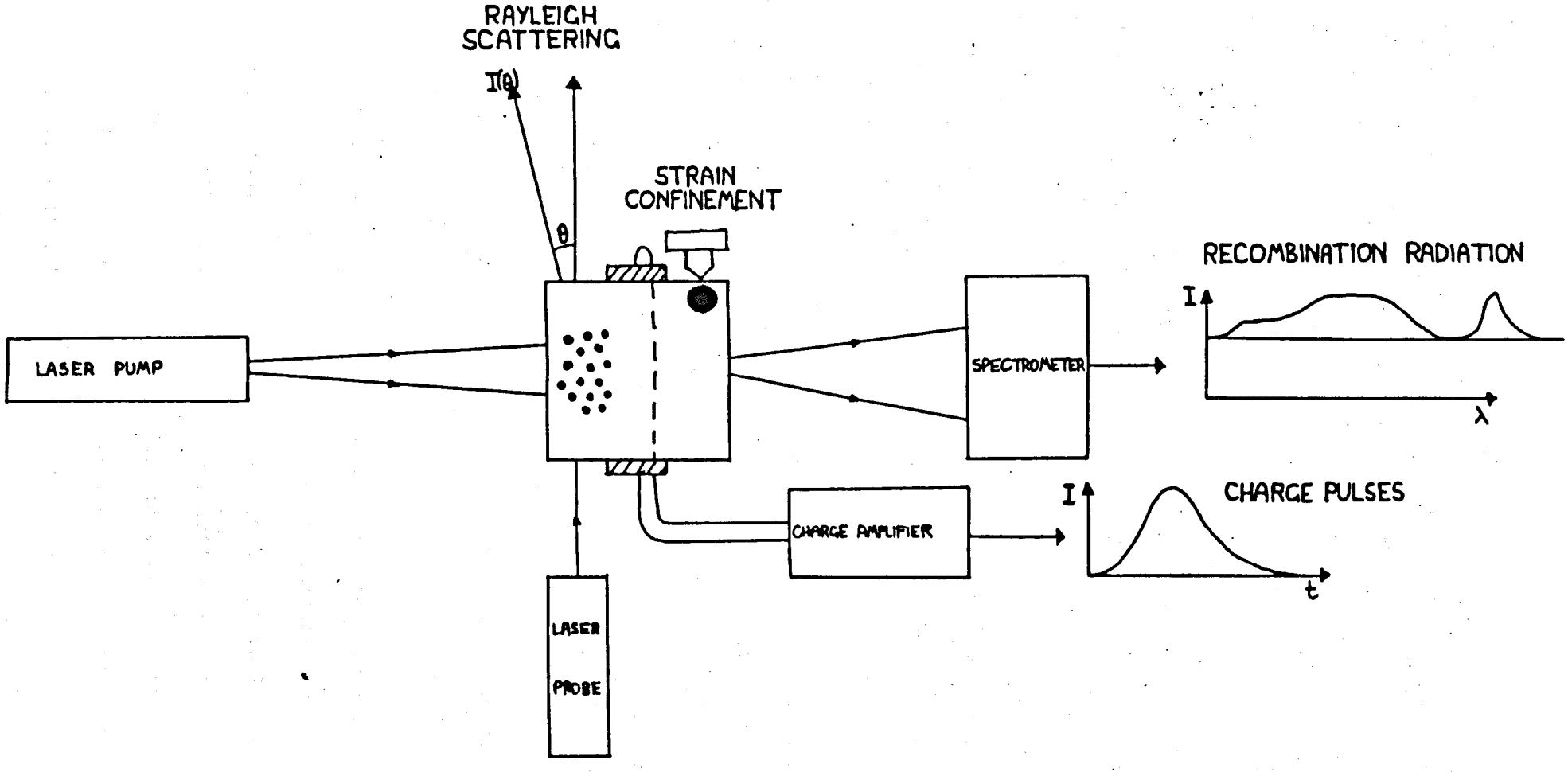


Fig. 5.4 Schematic representation of several experimental probes of the EHD parameters in germanium

fields up to 100 kG. A theoretical treatment by Büttner (1974) was in agreement with this finding. Estimates of droplet radius continued to get smaller (Voos, Shaklee and Worlock, 1974 : a ∿2 μm from light scattering; Prieur, Etienne, Sander, Benoit at la Guillaume and Voos, 1976 : a ∿2 μm from resonant absorption of ultrasound), though very large drops up to 1 mm across could be produced in potential wells caused by applied stress (Jeffries, Markiewicz and Wolfe, 1974 and 1976). Droplets were reported to carry electric charges of the order of -100e by Pokrovsky and Svistunova (1974), which was explained theoretically by Rice (1974a) in terms of the difference between the work functions for electrons and holes in the drop. Later experimental work by Nakamura (1977) gave the charge as ∿-400e.

At this point the volume of experimental and theoretical work on EHDs had become so large that we shall henceforth refer only to that which is of particular interest to us. For a wider coverage there are reviews by Voos (1974), Hensel, Phillips and Thomas (1977) (both experimental) and Rice (1974b, 1977) (both theoretical) as well as the sessions on EHDs in the proceedings of the 12th and 13th International Conferences on the Physics of Semiconductors at Stuttgart and Rome respectively, which deal with exciton condensation in many other materials besides Ge.

Grossman, Shaklee and Voos (1977) measured the dependence of droplet radius on temperature and excitation level by detection of current pulses in a p-n junction, and found variations from 2.9 μm to 10 μm, while Rose, Shore and Rice (1978) reported that their data on infrared absorption and scattering by EHDs were consistent with the very small (compared with previous estimates) radius of 1 μm. Work on the effect of magnetic fields continued, with Wolfe, Furneaux and Markiewicz (1976) observing flattening

of a large strain-confined EHD parallel to the applied magnetic field, which they interpreted as being due to the deflection of recombination currents inside the drop. Gavrilenko, Kononenko, Mandel'shtam, Murzin and Saunin (1977) observed a similar effect in cyclotron resonance experiments on small droplets, in which they were able to show that the effective masses and resonance behaviour of electrons actually inside the droplets were not greatly altered from normal values. Again the flattening was parallel to the field, so that the droplets became oblate spheroids with principle radius ratios of up to 1.7 at $\sim$2T, at which field the radius parallel to the field was estimated to be 1.1 μm. Finally, there was the measurement of an oscillatory effect in the magnetoresistance of a sample containing EHDs by Eaves, Markiewicz and Furneaux (1976, 1977) discussed already in §5.1. A similar experiment has been performed by Vitins, Aggarwal and Lax (1978), obtaining the same oscillatory effect, but of a different period corresponding to a smaller droplet size.

## 5.3 Discussion of the transport problem

We now discuss the problem of transport in the Ge electron-hole droplet system in greater detail, and introduce some of the approximations involved in the numerical calculation. For a lengthy review of previous experiments and theoretical calculations of transport properties in Ge we refer to the work of Paige (1963).

The crystalline Ge on which the experiments of Eaves et al (1976) were performed is such an extensively studied and well understood material that we may confidently use data appearing in the literature as sources for band structure and lattice scattering parameters. Germanium (See, e.g., Kittell 1971) is a group IV semiconductor with an indirect band gap of 0.74 eV at $2^{o}$K. The valence band consists of one heavy hole and two light hole valleys of masses $0.3m_e$ and $0.04m_e$ respectively. The bottom of the conduction band may be regarded as consisting of four ellipsoidal valleys, their long axes pointing in the {111}directions, and with longitudinal and transverseeffective masses of $1.59m_e$ and$0.082m_e$ respectively (Dresselhaus et al 1955, Levinger and Frankl, 1961). We expect the effective mass approximation (Luttinger and Kohn, 1955) to be valid in the magnetic field, as the bands are non overlapping (Harper, 1955).

A magnetic field in a {100} direction is equally inclined to each of these valleys (Fig. 5.5), and hence the cyclotron mass $m_c$ and the kinetic mass $m_z$ are the same for each. These have been derived already in §2.2; the values are $m_c = 0.135m_e$, $m_z = 0.581m_e$. The separation of the Landau bands in energy is $\hbar\omega_c$ or $\hbar eB/m_c$, which is approximately BmeV when B is measured in tesla. At $2^{o}$K a spread of 5kT above the bottom of the conduction band is equivalent to about 1meV, so the number of Landau bands occupied at a given field is of the order of 1/B. Thus at the field used

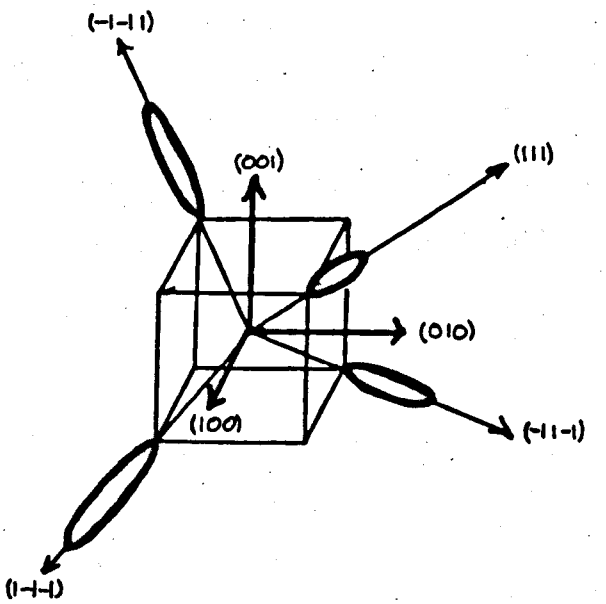


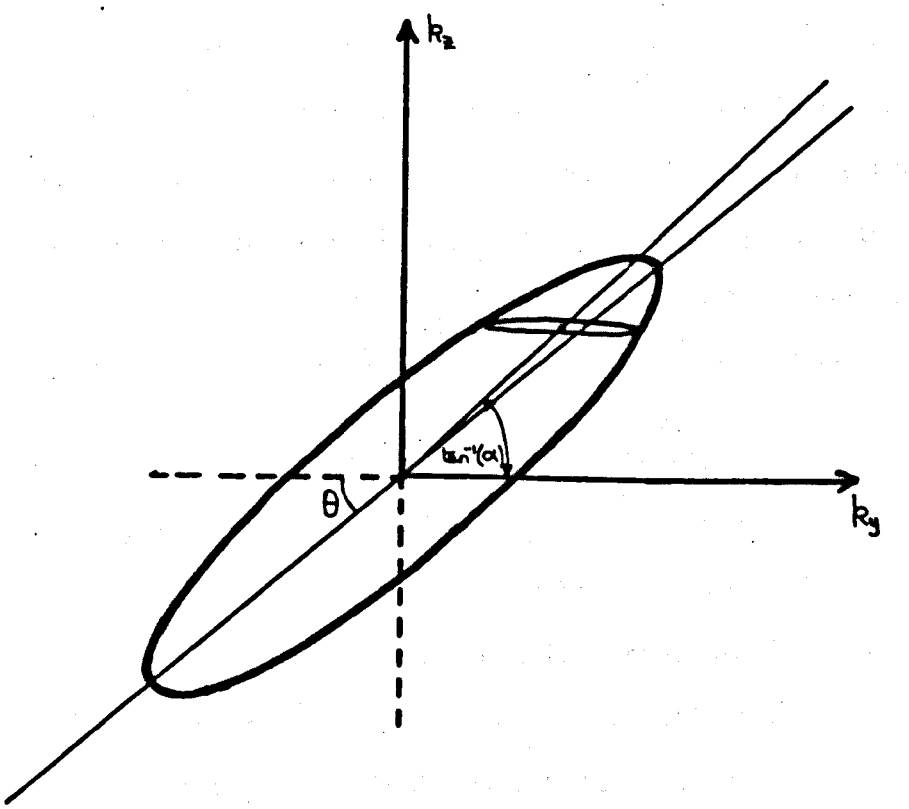


Fig. 5.5 Conduction band geometry in germanium

by Eaves et al (0.01 - 0.05T) over 20 Landau bands will be occupied, the quantum limit regime being for B greater than 1T. With so many bands occupied it is pertinent to consider whether the Landau band structure will in fact be resolved, or whether it will be broadened out by scattering processes. Eaves et al report $\omega_c\tau \sim 100$ from cyclotron resonance experiments on their material, which is consistent with a well resolved structure (Kubo et al, 1965). We shall return to this point when the EHD scattering has been calculated. A further indication of the scales involved is that the Landau length $\ell$ is $(\hbar/eB)^{\frac{1}{2}}$ which is roughly $0.025B^{-\frac{1}{2}}$ μm.

In the ultra pure Ge used by Eaves et al the doping level is extremely low ($N_A - N_D \sim 10^{17} m^{-3}$), and at $2^oK$ thermal activation is also very small, so that the conduction band valleys are populated exclusively as a result of photo excitation by the intense illumination. Eaves reports a density $n_e$ of $10^{20} m^{-3}$ for free carriers not bound into EHDs or excitons, which is far too high to arise from the other mechanisms. Since the relaxation time of these carriers is long, they may be expected to thermalise (Barker and Hearn, 1973), and so we assume a Maxwell-Boltzmann equilibrium carrier distribution function in the conduction band.

We shall choose to ignore any possible contribution to the conduction process made by the holes, following Eaves et al. As they point out, the complex nature of the Landau band scheme for holes would make a proper analysis difficult, and in any case the Fourier transform in B which we shall use would separate electron and hole contributions due to their different anisotropy ratios. A significant hole contribution seems likely, however, as their masses and number density are of the same order of magnitude as for the electrons. We shall return to this point in our concluding discussion.

We now consider the scattering mechanisms expected to be present in Ge of this purity at $2^{o}K$. Measurements of the mobility of electrons (Fukai, Kawamuta, Sekido and Imai, 1964) and holes (Ottaviani, Canali, Nava and Mayer, 1973) in such material show a $T^{-\frac{3}{2}}$ dependence characteristic of scattering dominated by acoustic phonons. Impurity scattering may therefore be safely ignored; the only other scatterers are the EHDs themselves.

We use the usual deformation potential approximation to describe the phonon scattering (Bardeen and Shockley, 1950; Herring and Vogt, 1956; Ziman, 1963), in which the electron-phonon interaction coupling constant is $D^2\hbar q^2/2\rho\Omega\omega_q$. Here D is the deformation potential, $\rho$ is the density, $\Omega$ is the material volume, and the acoustic phonon frequency $\omega_q$ is sq where s is the sound velocity, q is the phonon wave number. These parameters are readily available for Ge (Kirkpatrick, 1973) and are:
$D = 11.4eV$, $\rho = 5320\ kgm^{-3}$ and $s = 5490\ ms^{-1}$.

At high temperatures this interaction is effectively isotropic, as the above coupling coefficient combines with an occupancy factor $(2\bar{N}_q+1) = \coth(\hbar\omega_q/2kT) \tilde{\sim} 2kT/\hbar\omega_q$ to produce an interaction which is independent of q. This fact has been used, among others, by Argyres (1958, 1959) to obtain an analytic expression for the longitudinal magnetoconductivity outside the quantum limit regime. This approximation is not applicable here, however, for considering a typical phonon transition across the top of the first Landau sub-zone (for which $q = 2\ell^{-1}(2m_z/m_c)^{\frac{1}{2}}$) we find $\hbar\omega_q/kT$ is approximately $4.8\ B^{\frac{1}{2}}$. This is not sufficiently small, for the fields which are of interest to us, for the approximation $\coth(\hbar\omega_q/2kT) \tilde{\sim} 2kT/\hbar\omega_q$ to be tenable.

A measure of the degree to which the inelasticity of the phonon scattering is important is the value of the ratio $\omega_q/\omega_c$ for a phonon assisted

transition across the top of the first Landau sub zone. This is approximately $0.97B^{-\frac{1}{2}}$, so that the energy of the phonons involved in transitions across the Landau bands is comparable with the energy separation of the bands, apart from at the very highest fields. It therefore seems that any calculation which takes phonon scattering into account correctly must be inelastic, precluding the use of the relaxation matrix theory developed in §4. As our main interest is in the EHD scattering, however, we shall proceed with an elastic calculation of the phonon contribution until it appears that we may drop it altogether. The point will be discussed further in §5.6.

We now come to the scattering by the EHDs themselves. Eaves et al have taken these to be perfectly spherical in shape, with a well defined radius a of 1.1 μm deduced from their magnetoresistance data. There is reason to doubt that the shape is in fact perfectly spherical, as Wolfe et al (1976) and Gavrilenko et al (1977) have reported a flattening of EHDs parallel to the magnetic field. Distortion of the EHDs into oblate spheroids would not qualitatively change the nature of the resonance, however, and ease of calculation justifies an assumption that they are spherical.

The size and distribution of the droplet radii are more controversial, and various estimates in the range 1 - 10 μm exist (Voos 1974, Pokrovsky et al 1974, Prieur et al 1976). We shall assume that all droplets have the same radius for ease of calculation, and use the value 1.1 μm deduced by Eaves et al. They also report the number density $n^{EHD}$ of the droplets to be $10^{16} m^{-3}$, and we shall use this value.

Finally, we must consider the depth V of the potential the EHD presents to a scattering electron. Eaves et al have taken a figure of 4meV, derived from previous estimates of the work function against escape of an electron

from the droplet (see, e.g., Pokrovsky, 1972). These figures are not particularly accurate, however, so no great significance should be attached to this particular value. Indeed, the representation of this obviously complex scattering process by a simple square well potential needs careful consideration, and we shall discuss it in more detail later. For the moment we shall assume that the procedure is valid, and that the scattering matrix elements may be calculated in the Born approximation.

## 5.4 Calculation of the Longitudinal Magnetoconductivity

In this section we shall carry out the complete calculation of the longitudinal magnetoconductivity of ultra-pure germanium, where scattering is by acoustic phonons and electron-hole droplets. As this calculation is long and complex, we shall split it into several sub-sections. After an initial summary of the prece ding work we shall consider the evaluation of the averaged transition rates which appear in the relaxation matrix. A sub-section on approximation of these transition rates is followed by one dealing with the assembly and inversion of the relaxation matrix. The next sub-section deals with the calculation of the magnetoconductivity itself, for EHD scattering alone, while another discusses various approximations to the conductivity for pure phonon scattering. Finally there is a summary and discussion of the numerical approximations made in various parts of the calculation.

The longitudinal magnetoconductivity, from (4.4.17), is

$$\sigma_{zz}(B) = \Omega^{-1} 4.2.\sum_{Nk_yk_z} (e^2 k_z^2 \hbar^2/m_z^2)(-f^{o'}(\varepsilon_{Nk_z}))\tau_N(\varepsilon_{Nk_z}) \qquad (5.4.1)$$

The factor 2 is for spin, and the 4 for the number of conduction band valleys. The equilibrium distribution function $f^o(\varepsilon)$ is equal to $ne^{-\varepsilon/kT}$ where n is chosen so that the total number of excited carriers, $4.2.\sum_{Nk_yk_y} f^o(\varepsilon)$, is equal to $\Omega n_e$, where $n_e$ is the observed number density. After performing the integrations necessary to determine n and substituting in (5.4.1), we obtain

$$\sigma_{zz}(B) = \frac{n_e e^2}{m_z}\frac{\hbar}{kT}\left(\frac{2}{\pi m_z kT}\right)^{\frac{1}{2}} \sinh(\hbar\omega_c/2kT) \int_{\frac{1}{2}\hbar\omega_c}^{\infty} d\varepsilon e^{-\varepsilon/kT} \sum_{N=0}^{P(\varepsilon)} k_N \tau_N(\varepsilon) \qquad (5.4.2)$$

in the classical form '$n_e e^2\tau/m$'. $P(\varepsilon)+1$ is the number of Landau bands with

states of energy $\varepsilon$, and the P+1 relaxation times $\tau$ are determined by solving the matrix equation (4.4.10)

$$\{R(\varepsilon)\}\{\tau(\varepsilon)\} = \{1\} \tag{5.4.3}$$

The elements of the (P+1)x(P+1) square relaxation matrix $\{R\}$ are given by

$$R_{NN'}(\varepsilon) = \delta_{NN'} \sum_{M=0}^{P} k_M^{-1}(W_{NM}(k_N,k_M)+W_{NM}(k_N,-k_M)) -$$

$$- k_N^{-1}(W_{NN'}(k_N,k_{N'})-W_{NN'}(k_N,-k_{N'})) \tag{5.4.4}$$

where $W$ is given in terms of the transition rates $\omega$ between Landau states by

$$W_{NN'}(k_z,k_{z'}) = (m_z L/\hbar^2\pi) \sum_{k_y'} \omega_{Nk_yk_z;N'k_y'k_{z'}} \tag{5.4.5}$$

The $W_{NN'}$ are thus averaged transition rates, retaining only their dependence on Landau band number and longitudinal momentum change.

Transition Rates

The transition rates are derived from the transport theory of §4.3, and are the sum of the rates due to the two scattering mechanisms; the acoustic phonons and the electron-hole drops. Thus $\omega = \omega^{ph} + \omega^{EHD}$, and hence $W = W^{ph} + W^{EHD}$.

The transition rate $\omega^{ph}$ due to acoustic phonon scattering is derived from (4.3.5), assuming that the scattering is elastic:

$$\omega^{ph} = 2\pi\Omega/\hbar \sum_{\underline{q}} (2\bar{N}_{\underline{q}}+1)\,|C(\underline{q})|^2 |\langle Nk_yk_z|e^{i\underline{q}\cdot\underline{r}}|N'k_yk_z'\rangle|^2 \tag{5.4.6}$$

The coupling coefficient for the electron-phonon interaction is

$$|C(\underline{q})|^2 = D^2\hbar q/2\rho s \tag{5.4.7}$$

and the average number of phonons in mode $\underline{q}$ is $\bar{N}_{\underline{q}} = (e^{\hbar sq/kT} - 1)^{-1}$.

The transition rate $\omega^{EHD}$ due to EHD scattering is derived in the Born approximation from (4.3.9) to (4.3.24); it is

$$\omega^{EHD} = 2\pi\Omega/\hbar \sum_{\underline{q}} n^{EHD} |U(\underline{q})|^2 |\langle Nk_y k_z | e^{i\underline{q}\cdot\underline{r}} | N'k_y' k_z' \rangle|^2 \qquad (5.4.8)$$

Here $U(\underline{q})$ is the spatial Fourier transform of the EHD potential; since the square well is spherically symmetric, it depends only on $q = |\underline{q}|$, and an integration yields

$$U(q) = 4\pi V(\sin qa - qa\cos qa)/q^3 \qquad (5.4.9)$$

where the radius is $a$ and the well depth is $V$.

The matrix elements of plane waves $e^{i\underline{q}\cdot\underline{r}}$ between the Landau states are given in (2.2.16); they are

$$|\langle Nk_y k_z | e^{i\underline{q}\cdot\underline{r}} | N'k_y' k_z' \rangle|^2 = \delta(k_y', k_y + q_y)\delta(k_z', k_z + q_z) F_{NN'}(u^*) \qquad (5.4.10)$$

where $u^* = \ell^{*2} q_\perp^{*2}/2$, $\ell^* = \ell(m_c/m_t)^{\frac{1}{2}}$, and $q_\perp^{*2} = q_x^2 + (\ell/\ell^*)^4 (q_y - \alpha q_z)^2$ from (2.2.17), where $\alpha = (m_\ell - m_t)\sin 2\theta / m_z$. The function $F$ from (2.1.29) is

$$F_{NN'}(u) = (N!/N'!) u^{N'-N} e^{-u} |L_N^{N'-N}(u)|^2 \qquad (N' \geq N) \qquad (5.4.11)$$

The $\delta$ terms in (5.4.10) are Kroneckers, and hence the integral for $W$ is reduced to

$$W_{NN'}^{EHD}(k_z, k_z') = (2m_z/4\pi^2\hbar^3) \iint_{q_z = |k_z - k_z'|} dq_x dq_y n^{EHD} |U(q)|^2 F_{NN'}(u^*) \qquad (5.4.12)$$

with a very similar expression for $W^{ph}$.

The averaged transition rates are now expressed as integrals over the $q_x q_y$ momentum plane, within which the areas of maximum contribution to the integral are determined by two factors. The nature of the scattering mechanism manifests itself in the $|U(q)|^2$ term, while the overlap of the basis Landau wave functions is taken into account by $F_{NN'}(u^*)$. It is in this second term that any anisotropy in the underlying band structure becomes extremely important.

The effect of anisotropy is most easily seen by studying the semi-classical picture of scattering between electron orbits in $\underline{k}$ space, illustrated for the isotropic and anisotropic cases in Figs. 5.6 and 5.7. respectively. Here the only possible elastic transitions are those with $\underline{q}$ vectors linking points on electron orbits of the same energy. It may readily be seen that for transitions involving a large transfer of z-momentum (Figs. 5.6a, 5.7a) the magnitude of the $\underline{q}$ vector required is much greater in the anisotropic case because of the need for it to point roughly along the constant energy ellipsoid. In fact, the vectors required for a transition of given $q_z$ will be clustered around $q_x = o$, $q_y = \alpha q_z \tilde{\sim} q_z \tan\theta$ in the anisotropic case, whereas most will contribute around $q_x = q_y = 0$ in an isotropic band. This means that for a scattering mechanism whose effect falls off sharply with increasing q, scattering will be greatly reduced in materials with anisotropic band structure, as has been noted by Miller and Omar (1961) with regard to ionised impurity scattering in Ge.

Quantum mechanically the effect is simplest in 0-0 scattering where $F_{oo}(u^*) = e^{-u^*}$. The $u^*$ argument makes this function greatest around $q_x = 0$, $q_y = \alpha q_z$ and it is only in the isotropic case when $\alpha = 0$ that this maximum occurrs for the least possible value of q.

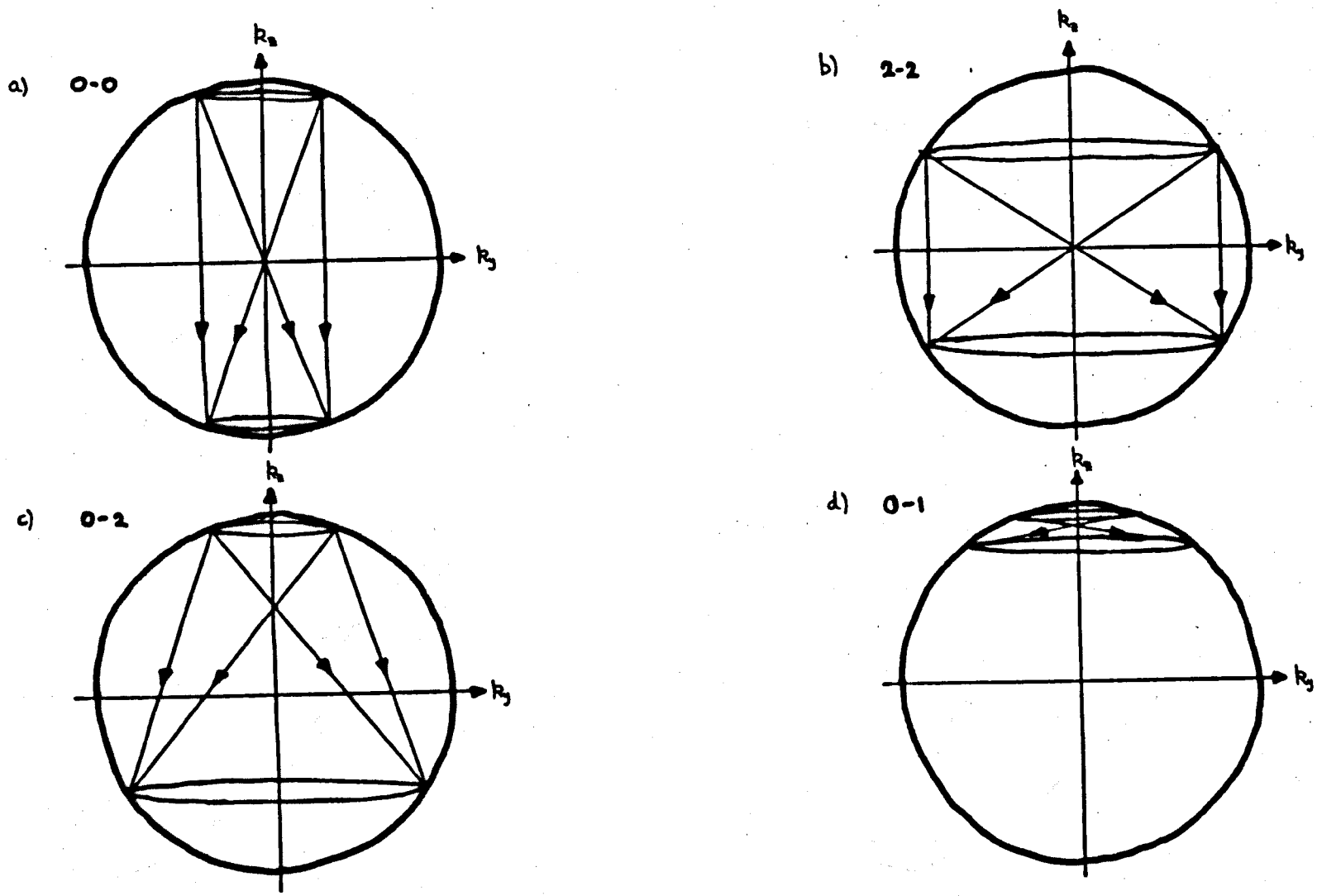


Fig. 5.6 Possible elastic scattering transitions at a single energy in an isotropic band; semi classical picture of scattering between cyclotron orbits

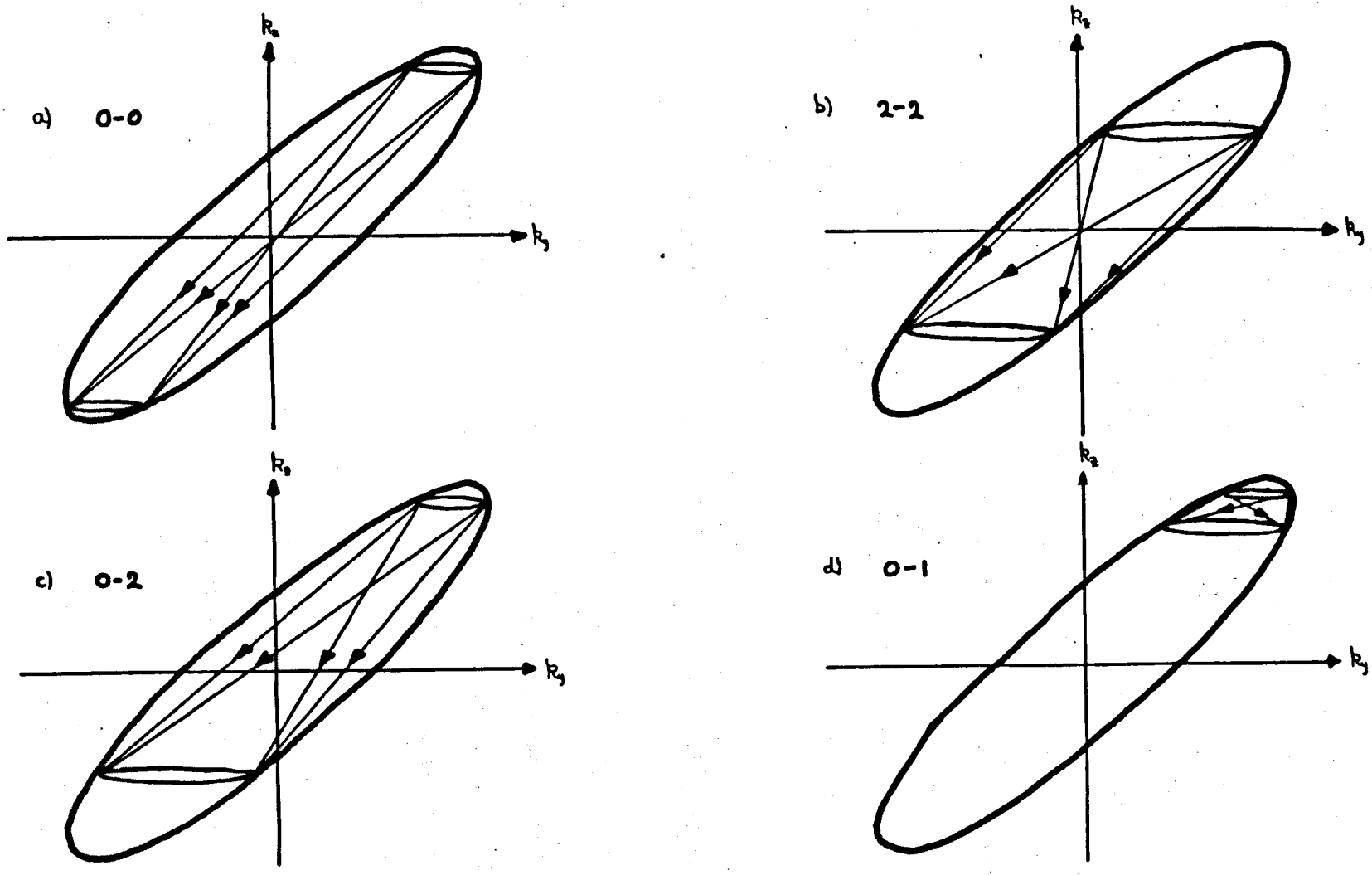


Fig. 5.7 Possible elastic scattering transitions at a single energy in the germanium conduction band

For transitions between higher Landau bands the semi-classical picture is illustrated in Figs. 5.6 and 5.7b, c, d and it may be seen that in certain cases (d) a shorter transition in $\underline{q}$ space is possible in the anisotropic band. The higher order $F_{NN'}$ are more complicated functions of $u^*$, having maxima at values $u^{*max}_{NN'}$, and hence giving maximum contributions to scattering on ellipses in the $q_x q_y$ plane, as shown in Fig. 5.8. In the isotropic case the maximum contribution would occur on circles centred on (0,0).

Since the scattering potential terms in the transition rate integrals are independent of direction in the $q_x q_y$ plane, it is advantageous to change to polar co-ordinates and perform the angular integration, thus reducing the effect of the overlap of Landau states to a single angular averaged function of $u = \ell^2(q_x^2+q_y^2)/2$:

$$F^*_{NN'}(u,Q_z) = (2\pi)^{-1}\int_0^{2\pi} d\phi F_{NN'}\{(\ell^*/\ell)^2\{u\cos^2\phi+(\ell/\ell^*)^4(\sqrt{u}\sin\phi-\alpha Q_z/\sqrt{2})^2\}\} \tag{5.4.13}$$

Here the dimensionless parameter $Q_z = \ell q_z$ has been introduced, and the argument of $F_{NN'}$ is just $u^*$ in the new co-ordinate system. In an isotropic band $\ell = \ell^*$ and $\alpha = 0$ (see §2), whence $F^*_{NN'}(u,Q_z)$ reduces simply to $F_{NN'}(u)$.

The transition rate integrals are now

$$W^{ph}_{NN'}(k_z,k_{z'}) = (m_z/\pi\hbar^3\ell^2)\int_0^\infty du(D^2\hbar q/2\rho s)\coth(\hbar sq/2kT)F^*_{NN'}(u,Q_z) \tag{5.4.14}$$

$$W^{EHD}_{NN'}(k_z,k_{z'}) = (2m_z/4\pi^2\hbar^3)\int_0^\infty du\{n^{EHD}|U(q)|^2\}F^*_{NN'}(u,Q_z) \tag{5.4.15}$$

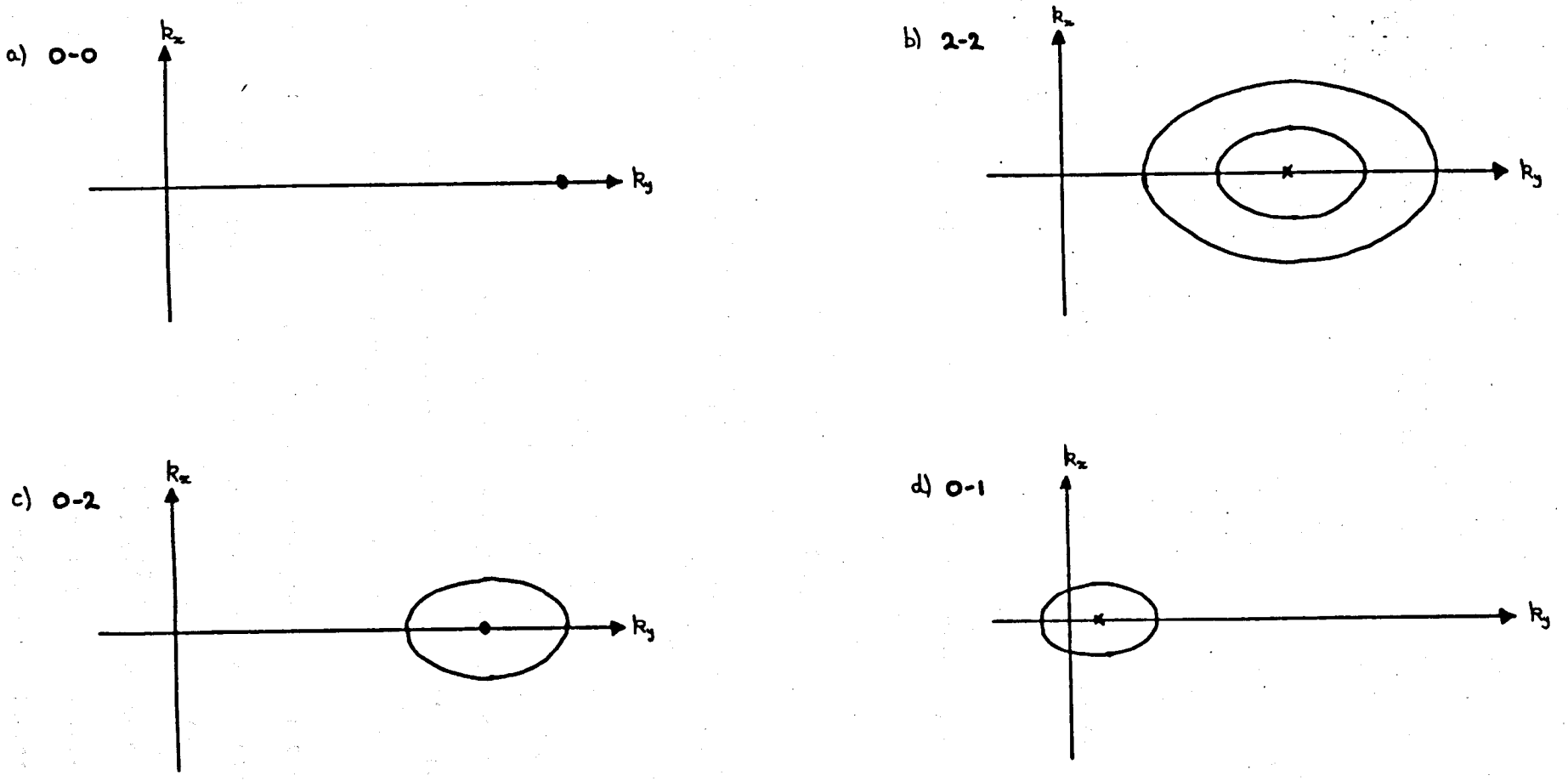


Fig. 5.8 Curves of maximum contribution to scattering between quantum states in the $k_x k_y$ plane of the germanium conduction band

where $Q_z = \ell|k_z - k_{z'}|$.

We may reduce the integrals to completely dimensionless variables by multiplying all momenta by $\ell$ so that $\underline{Q} = \ell\underline{q}$ and $\underline{K} = \ell\underline{k}$, and bringing in one parameter for the phonon energies:

$$C^{ph} = \hbar s/\ell kT \approx 0.75B^{\frac{1}{2}} \tag{5.4.16}$$

and one for the droplet radii:

$$R = a/\ell \approx 43B^{\frac{1}{2}} \tag{5.4.17}$$

Here we have shown how each varies numerically with magnetic field B, measured in tesla.

Changing the variable of integration to $|\underline{Q}| = Q$ given by $u = \frac{1}{2}(Q^2 - Q_z^2)$, the averaged transition rates become

$$W^{ph}_{NN'}(k_z,k_{z'}) = (m_z D^2/2\pi\hbar^2\ell s^3)\int_{Qz}^{\infty} dQQ^2 \coth(C^{ph}Q/2)F^*_{NN'}(u,Q_z) \tag{5.4.18}$$

$$W^{EHD}_{NN'}(k_z,k_{z'}) = (16\pi m_z V^2 n^{EHD}\ell^4/\hbar^3)\int_{Qz}^{\infty} dQQ^{-5}(\sin RQ - RQ\cos RQ)^2 F^*_{NN'}(u,Q_z) \tag{5.4.19}$$

where in each case the value of $Q_z$ is $|K_z - K_{z'}|$. We note that the integral in the latter expression is sharply cut off at the lower end $Q = Q_z$, and hence will oscillate in magnitude as this initial point corresponds to a peak or trough in the oscillatory component $(\sin RQ - RQ\cos RQ)^2$. It is this oscillation which gives rise to the magnetoresonance.

It is of interest to note that the constants in front of the two integrals above, which give the relative strengths of the two scattering processes, have the dimensionless ratio EHD : phonon of $32\pi^2(V/D)^2 n^{EHD}\ell^7\rho s/\hbar$. This is numerically approximately equal to $0.29B^{-7/2}$ when the magnetic field B is in Tesla, showing that phonon scattering becomes increasingly important at higher magnetic fields. This is because the larger $\underline{q}$ vectors

involved in interband transitions at higher fields favour phonon scattering, as the coupling increases with q rather than falling off sharply as it does for the EHDs. It therefore appears that phonon scattering will be negligible for fields around 0.01T, while there will still be a difference of two orders of magnitude at B = 0.025T. We may not, however, discount the possibility that the integrals themselves, though dimensionless, are very different in magnitude. In fact we shall find that this is the case, and that phonon scattering is more important than the above argument would indicate.

Evaluation of the Transition Rates

In evaluating the transition rate integrals it is necessary to bear constantly in mind the variation of $F^*$ and $F$ with $Q$ and $Q_z$. In Fig. 5.9 we plot some of these functions for low N,N' values, and it can be seen how the maxima of $F^*$ move outwards with increasing $Q_z$. Most important is the behaviour at values of $Q_z$ corresponding to transitions across the top of a Landau sub-zone, since these give the greatest contribution to the conductivity. In Ge the value $Q_o$ of $Q_z$ corresponding to a transition across the top of zone 0 is $Q_o = 2\sqrt{2m_z/m_c} \approx 5.94$.

The integral for $W^{EHD}$ commences with $RQ = RQ_z$. For all values of the field which we consider this will be much greater than 1 in the parts of the zone which contribute most to $\sigma$, and we henceforth neglect the sinRQ term in comparison with RQcosRQ. The remaining $\cos^2 RQ$ term may then be split, to express $W^{EHD}$ as a sum of an oscillating and a non-oscillating part:

$$W^{EHD}_{NN'} = (8\pi m_z V^2 n^{EHD} \ell^2 a^2/\hbar^3)\{J^*_{NN'}(Q_z) + J^{*osc}_{NN'}(Q_z)\} \qquad (5.4.20)$$

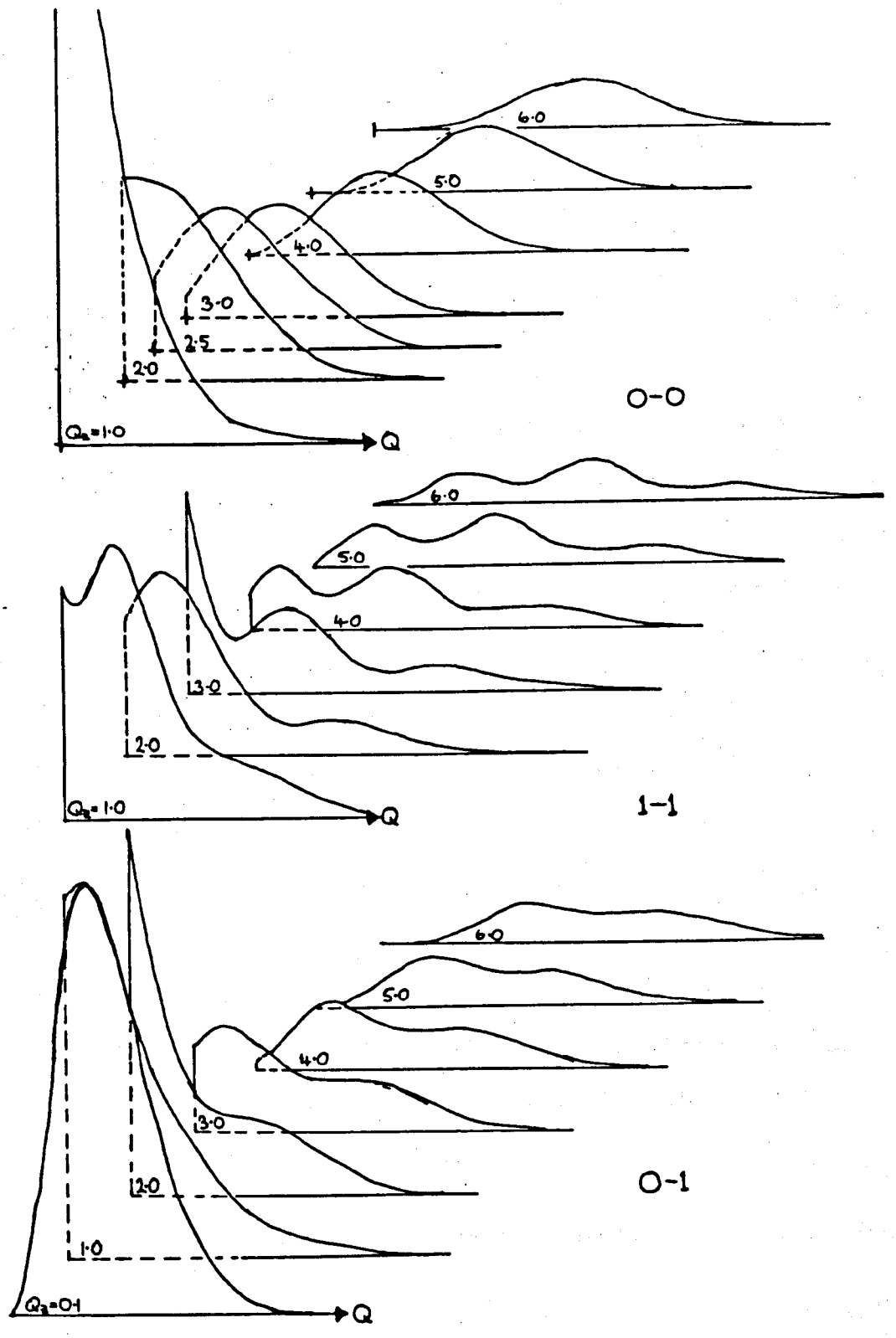


Fig. 5.9 The scattering functions $F^{*}_{NM}(Q,Q_z)$ for germanium

where

$$J^*_{NN'}(Q_z) = \int_{Q_z}^{\infty} dQ Q^{-3} F^*_{NN'}(u,Q_z) \tag{5.4.21}$$

and

$$J^{*osc}_{NN'}(Q_z) = \int_{Q_z}^{\infty} dQ Q^{-3} \cos 2RQ F^*_{NN'}(u,Q_z) \tag{5.4.22}$$

We have not been able to evaluate these integrals analytically. However, an approximation may be obtained for $J^*$ by returning to a $Q_x Q_y$ integration and expanding $Q^{-4}$ in a Taylor series about $Q_x = 0$, $Q_y = \alpha Q_z$. The details of this are tedious, and are in Appendix 5; the result is that

$$J^*_{NN'} \approx 0.162 Q_z^{-4} + 0.471\ (N+N'+1) Q_z^{-6} \tag{5.4.23}$$

in Ge, the first coefficient being $(1+\alpha^2)^{-2}$. In an isotropic band the corresponding integral is

$$J_{NN'} \approx Q_z^{-4} + 4(N+N'+1) Q_z^{-6} \tag{5.4.24}$$

showing the reduction of $J^*$ by a factor of about 6 purely due to the anisotropy of the Ge band. These approximations have been checked by numerical integration and are adequate for low N,N' in the first few Landau zones as illustrated in Fig. 5.10.

The phonon integral may be similarly approximated, the result being

$$W^{ph}_{NN'} \approx (m_z D^2/2\pi\hbar^3 \ell^3 \rho s)\, 1.58 Q_z \coth(0.79 c^{ph} Q_z) \tag{5.4.24}$$

in Ge and

$$(m_z D^2/2\pi\hbar^3 \ell^3 \rho s) Q_z \coth(0.5 c^{ph} Q_z) \tag{5.4.25}$$

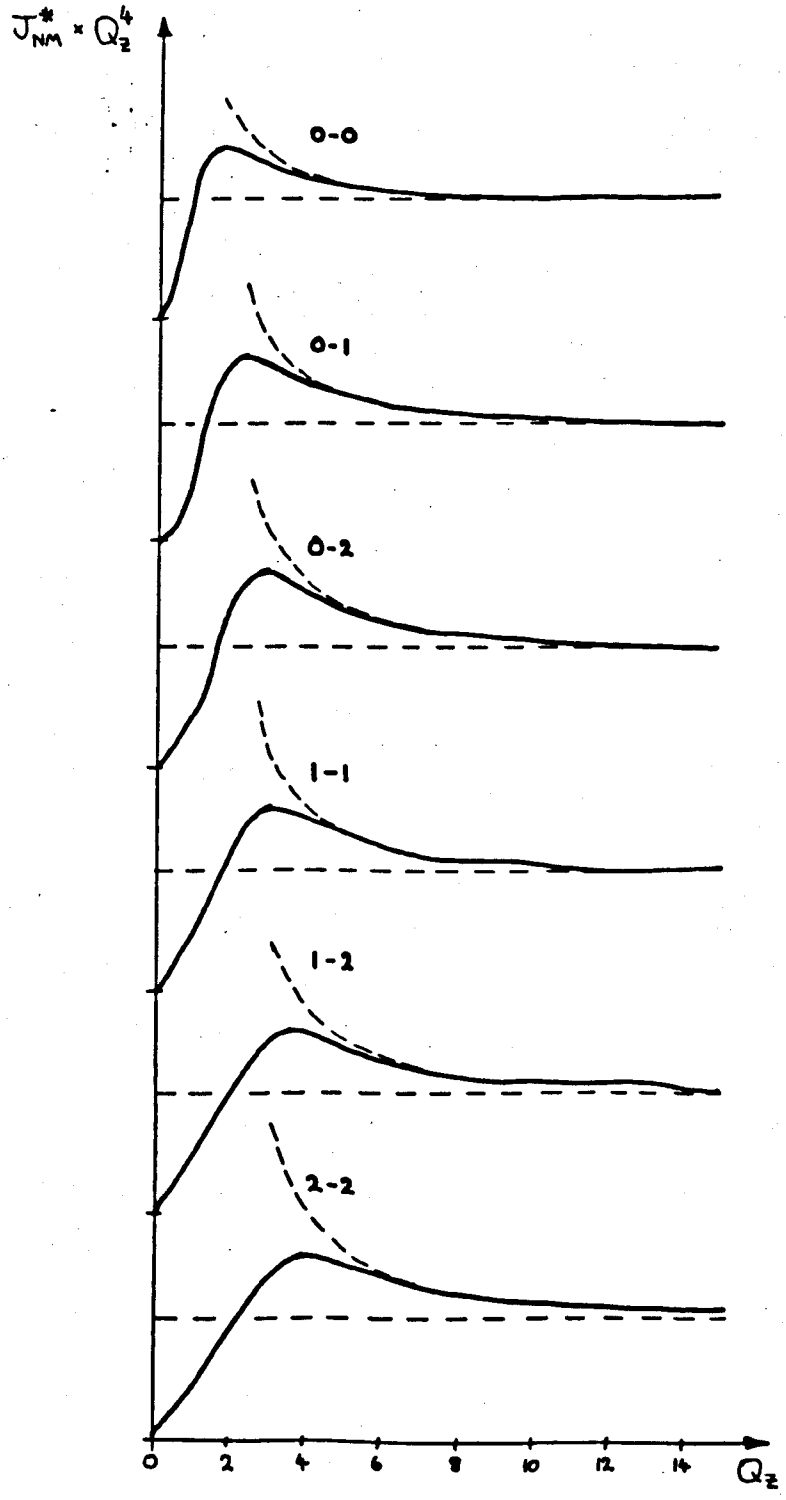


Fig. 5.10 The scattering integrals $J^*_{NM}(Q_z)$ for germanium. Dotted curves give the first two terms of the approximate expansion.

in an isotropic band. We note that, since the phonon scattering increases with q, its effect is increased by the anisotropy, though not by such a large factor.

We may now compare the strengths of the two scattering mechanisms directly. Ignoring for the moment the oscillating part of $W^{EHD}$, and taking only the first term in the approximation, we find

$$W^{EHD}/W^{ph} \approx 0.015B^{-7/2}Q_z^{-5}\tanh(0.79C^{ph}Q_z) \qquad (5.4.27)$$

Evaluated at the top of sub-zone 0 where $Q_z = Q_o = 5.94$, this ratio is $\approx 8$ for B = 0.01, and $\approx 0.0003$ for B = 0.25. In an isotropic band these figures are increased by a factor of $\approx 10$. This strongly decreasing dependence on B means that EHD scattering only dominates at low field values of 0.01-0.04T, and explains Eaves' observation of the disappearance of the EHD oscillations at higher fields. It also means that we must be careful in extrapolating results calculated at high fields (which are more tractable due to the lower band numbers involved) for comparison with experimental data taken at low fields. It is clear that the phonon scattering, though dominant at high fields, is of little relevance in this comparison, and we shall feel free to discard it when necessary.

We now return to the oscillating part of the EHD integral. Since R is large, and hence the oscillation is rapid, we may expect the major contribution to this integral to come from the surface term at $Q = Q_z$. Integrating once by parts and retaining only this surface term, we have

$$J_{NN'}^{*osc} \approx -Q_z^{-3}F_{NN'}^{*}(u(Q_z),Q_z)\sin 2RQ_z/2R = -Q_z^{-3}F_{NN'}(u_z^{*})\sin 2RQ_z/2R \qquad (5.4.28)$$

where $u_z^* = \frac{1}{2}(\ell\alpha/\ell^*)^2 Q_z^2 \approx 0.454 Q_z^2$ in Ge. In an isotropic band the corresponding result is

$$J_{NN'}^{osc} \approx Q_z^{-3} F_{NN'}(0) \sin 2RQ_z/2R = -\delta_{NN'} Q_z^{-3} \sin 2RQ_z/2R \qquad (5.4.29)$$

though this is clearly only valid when N = N'.

For scattering across the inmost Landau band at the top of a sub-zone we have $Q_z = Q_o$, and hence $u_z^* = 16.0$. For this type of scattering (which is the most important, as it produces the basic magnetoresonance) we may compare the oscillatory and non-oscillatory parts of $W^{EHD}$ as

$$J_{NN}^{*osc}/J_{NN}^{*} \approx 18.3 F_{NN}(16.0)/R \qquad (5.4.30)$$

For B = 0.01T the ratio is $5.8 \times 10^{-7}$ for 0-0 scattering, but is increased to 0.25 for 4-4 scattering. The oscillatory part of the EHD scattering is markedly reduced by the anisotropy for the lowest Landau band, but is affected hardly at all for some higher bands. At very high fields where the higher Landau bands are not occupied the oscillatory part of the scattering rate is so small that it would not be observable in the final conductivity. This is not true, however, at the experimental values of B (0.01-0.05T), where up to 40 Landau bands may be populated. It is interesting that the only field-dependent term in (5.4.30) is $R^{-1}\alpha B^{-\frac{1}{2}}$, the other factors being purely geometrical.

Inversion of the Relaxation Matrix

We now have all the information needed to assemble the relaxation matrix $\{R\}$ and evaluate the vector $\{\tau\}$ of relaxation times for any desired energy. $\{R\}$ is a summation of terms due to phonon scattering and the steady and oscillatory parts of the EHD scattering. For reasons which will become apparent we shall henceforth discard the phonon contribution, so

that we shall calculate the conductivity in the presence of EHD's only. Certainly the phonons have little effect on the oscillations to be expected (at least in our elastic scattering approximation) and in any case the EHD scattering is dominant at low fields, as already noted. We shall also regard the oscillatory part of $\{R\}$ as a small perturbation to the steady EHD scattering. The equation for the relaxation times becomes

$$\{R^s + R^{osc}\}\{\tau\} = \{1\} \tag{5.4.31}$$

where $\{R^s\}$ is the steady and $\{R^{osc}\}$ the oscillating part of $\{R\}$. This has the approximate solution

$$\{\tau\} = \{R^s\}^{-1}\{1\} + \{R^s\}^{-1}\{R^{osc}\}\{R^s\}^{-1}\{1\} \equiv \{\tau^s\} + \{\tau^{osc}\} \tag{5.4.31a}$$

where $\{\tau^{osc}\}$ will be a linear combination of oscillatory terms containing factors $\sin 2R Q_z$, where $Q_z$ is the appropriate dimensionless $q$ vector for transition between particular pairs of Landau bands. The postulated origin of the magnetoresistance oscillations is the 'beating' of these oscillatory components of $\tau$ with the top of each Landau sub-zone, and in particular the component due to transition across the inmost band, for which $Q_z = Q_o$.

Defining the new constant $t^{EHD} = (\hbar^3/8\pi m_z V^2 n^{EHD} \ell^3 a^2)$ which is numerically approximately $1.03\times10^{-12} B^{3/2}$ and has the dimensions of a time, the steady part $\{R^s\}$ of the relaxation matrix may be written

$$\{R^s\} = (t^{EHD})^{-1}\{X\}\{D(K)\} \tag{5.4.32}$$

Here $\{D(K)\}$ is defined to be the diagonal matrix with elements $K_N$ along the diagonal, and hence the dimensionless matrix $\{X\}$ is <u>symmetric</u>, with its elements given by

$$X_{NN'} = \delta_{NN'} \sum_{M=0}^{P} \{J^*_{NM}(|K_N+K_M|) + J^*_{NM}(|K_N-K_M|)\}/K_N K_M$$

$$+ \{J^*_{NN'}(|K_N+K_{N'}|) - J^*_{NN'}(|K_N-K_{N'}|)\}/K_N K_{N'} \tag{5.4.33}$$

With this notation the steady part $\{\tau^S\}$ of the relaxation time vector is $t^{EHD}\{T^S\}$, where the dimensionless vector $\{T^S\}$ is the solution of

$$\{X\}\{D(K)\}\{T^S\} = \{1\} \text{ or } \{X\}\{KT^S\} = \{1\} \tag{5.4.34}$$

where $\{KT^S\}$ is a column vector with elements $K_N T_N^S$.

The solution of (5.4.34) for $\{KT^S\}$ turns out to be particularly simple. An important property of $\{X\}$, apart from its symmetry, is that its row sums, given by

$$\sum_{M=0}^{P} X_{NM} = \sum_{M=0}^{P} 2J^*_{NM}(|K_N+K_M|)/K_N K_M \tag{5.4.35}$$

are very small at energies near the top of a sub-zone. In this case the smallest K is $K_P = 2.97$ which, given the inverse fourth power in $J^*$, makes the row sum of order $10^{-4}$. Now it may be shown (see Appendix 6) that for such a matrix the approximate solution of (5.4.34) is that the $K_N T_N^S$ are all equal to each other, taking the value of the inverse of the average row sum of $\{X\}$ . We therefore have, to a very good approximation,

$$K_N T_N^S = (P+1)/\sum_{N,M} 2J^*_{NM}(|K_N+K_M|)/K_N K_M \equiv Y_P(K) \tag{5.4.36}$$

where $Y_P(K)$ is dimensionless, depending only on the order (P+1) of the relaxation matrix and on the position within the $(P+1)^{th}$ sub-zone, indicated by K.

It is important to note that $Y_P$ is completely independent of magnetic field; it is determined solely by the set of values $K_N$ occurring at a point in Landau sub-zone P determined by <u>one</u> parameter K. Whatever the magnetic field there will still be one point in sub-zone P with the same set of values $K_N$ and hence the same value $Y_P$. This implies that the

shape of the complete steady relaxation time spectrum is the same for all values of the magnetic field. Once the $Y_p(K)$ have been calculated, all that is needed to determine the spectrum exactly are the values of the scaling factors $t^{EHD}$ (time scale) and $\hbar\omega_c$ (energy scale).

This great simplification may be made because the $J^*_{NM}$ do not contain any terms directly dependent on magnetic field. This is not true of the $J^{*osc}_{NM}$, which contain the field dependent parameter R; hence the importance of splitting off the oscillatory part of $\{R\}$ to be considered separately. At first sight the parameter $C^{ph}$ in the phonon transition rates would appear to preclude simplification similar to the above, as it occurrs in the factor $\coth(0.79C^{ph}Q_z)$. Simplification may be achieved, however, if : (1) the argument of coth is large enough that it is approximately 1 independent of B (2) the argument is so small that the coth term is approximately the inverse of its argument, in which case $C^{ph}$ may be taken into the constant multiplying $\{R\}$. Unfortunately the experimental regime falls between these two extremes. In any case the dependence on B in the multiplying factors in front of the relaxation matrices is different for the EHDs and the phonons, so that the two can certainly not be combined in a simple way. Regime (1) for the phonons corresponds to high temperature and low fields, and has already been mentioned in §4.6 because of its simple solution. Regime (2) corresponds to high fields and very low temperatures, and will be treated briefly later.

It remains to choose a suitable parameter K to describe the position of a particular value of energy within a sub-zone. In Landau sub-zone P with $(P+\frac{1}{2})\hbar\omega_c \leq \varepsilon < (P+\frac{3}{2})\hbar\omega_c$ we shall define K by

$$K = \{(\varepsilon/\hbar\omega_c) - (P+\tfrac{1}{2})\}^{\frac{1}{2}} \qquad (5.4.37)$$

which ranges from 0 at the bottom of the sub-zone to 1 at the top. In terms of K, the $K_N$ are

$$K_N = (2m_z/m_c)^{\frac{1}{2}}(K^2+P-N)^{\frac{1}{2}} \approx 2.97(K^2+P-N)^{\frac{1}{2}} \qquad (5.4.38)$$

We note that $K_P \propto K$, which means that the important oscillation $\sin 4RK_P$ due to P-P intra-band transitions is particularly simple to investigate using this parameter.

The values of the $Y_P(K)$ are plotted in Fig. 5.11. It is found that they all vary to a good approximation as the sixth power of K, the coefficient $Y_P$ of $K^6$ increasing roughly linearly for small N>0. In particular $Y_o(K) \approx 3.13\times10^{4}K^6$, so that

$$\tau_o^s = t^{EHD}Y_o(K)/K_o \approx 1.09\times10^{-8}K^5B^{3/2} \approx 0.510\varepsilon^{5/2}B^{-1} \qquad (5.4.39)$$

where $\varepsilon$ is measured in eV from the bottom of the sub-zone, and B is in Tesla. We note that at the top of sub-zone 0, $\omega_c\tau_o \approx 1.42\times10^{4}B^{5/2}$, a fact we shall comment on later.

For the phonons we define $t^{ph} = 2\pi\hbar^2\ell^2\rho s/1.58m_zD^2 \approx 4.72\times10^{-10}B^{-1}$, and hence

$$\{R^{ph}\} = (t^{ph})^{-1}\{\chi^{ph}\}\{D(K)\} \qquad (5.4.40)$$

For suitable values of B and T (which will be discussed later) the coth factor in the phonon transition rate is approximately 1, and the elements of $\{\chi^{ph}\}$ are

$$\chi^{ph}_{NN'} = \delta_{NN'}\sum_{M=0}^{P}(|K_N+K_M|+|K_N-K_M|)/K_NK_M + (|K_N+K_{N'}|-|K_N-K_{N'}|)/K_NK_{N'} \qquad (5.4.41)$$

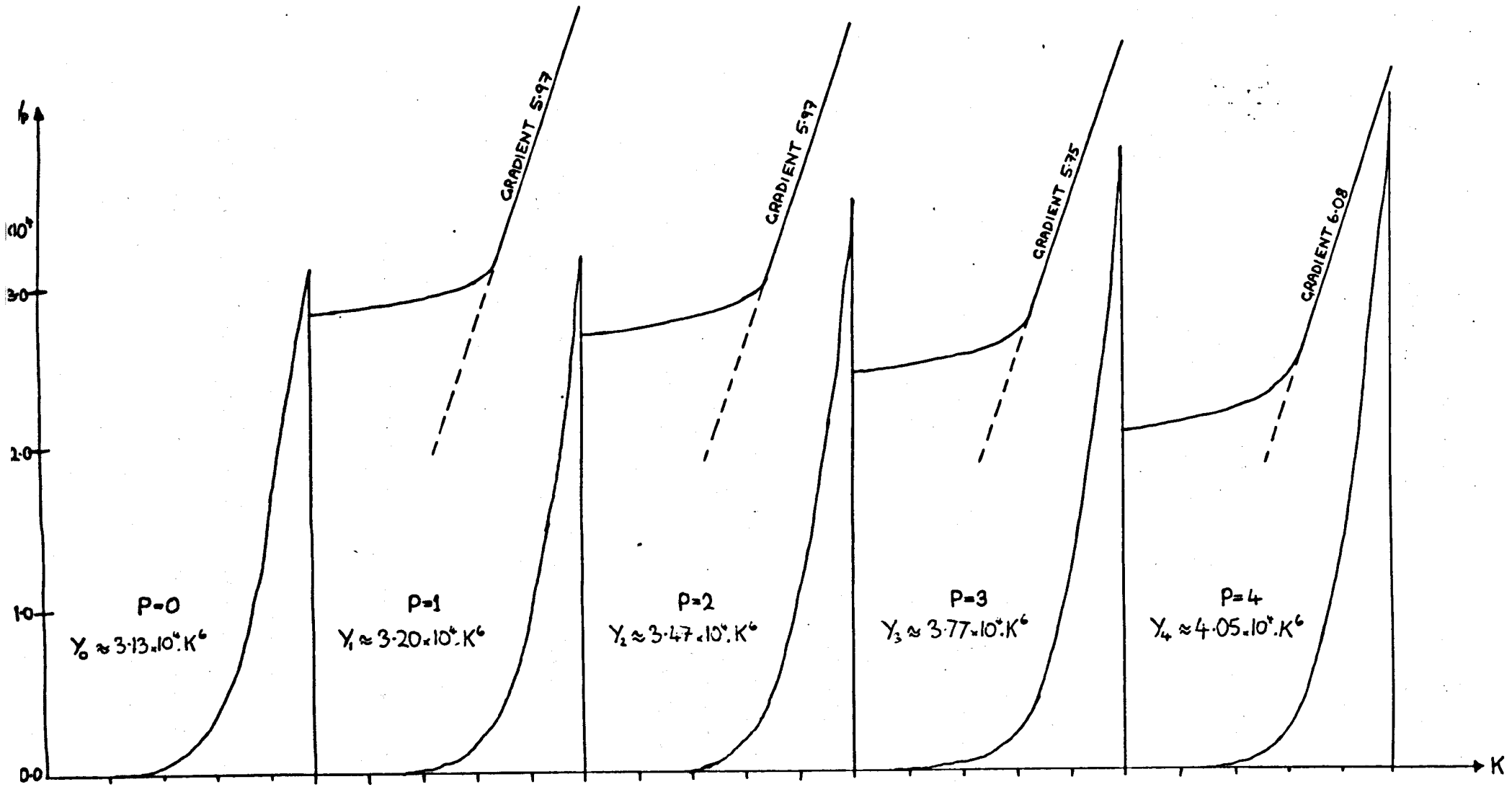


Fig. 5.11 The relaxation time functions $Y_p(K)$ for germanium. Inset are log-log plots showing approximate $K^6$ dependence

The elements of $\{KT^{ph}\}$ obtained by inverting this matrix are no longer equal, as the row sums of $\{\chi^{ph}\}$ are not small enough. The values of the $T^{ph}$ are plotted in Fig. 5.12.

Evaluation of the EHD Conductivity

In evaluating $\sigma_{zz}$ from (5.4.2) it is convenient to split it into a sum of contributions from each Landau sub-zone, rather than each Landau sub-band as implied in that expression. We therefore write

$\sigma_{zz} = \sum_{P=0}^{\infty} \sigma_P$ where $\sigma_P$ is the contribution from the energy range $(P+\frac{1}{2})\hbar\omega_c < \varepsilon < (P+3/2)\hbar\omega_c$. In each sub-zone the variable of integration is changed to K, in terms of which $\varepsilon = \hbar\omega_c(K^2+P+\frac{1}{2})$. We also introduce the new dimensionless ratio $\beta = \hbar\omega_c/kT \approx 9.90\ B/T$, and obtain

$$\sigma_P = (n_e e^2 t^{EHD}/m_z)(2\beta^3/\pi)^{\frac{1}{2}} \sinh(\beta/2)\, e^{-(P+\frac{1}{2})\beta} \int_0^1 dK K e^{-\beta K^2} \sum_{N=0}^{P} K_N T_N \qquad (5.4.42)$$

Using the results of the previous sub-section for the steady part of $\sigma_p$, we have $\sum_{N=0}^{P} K_N T_N \approx (P+1)Y_p(K)$ and $Y_P(K) \approx Y_p K^6$, whence the integral may be performed analytically. The resulting expression for $\sigma_{zz}^s$, the steady part of the total conductivity, is

$$\sigma_{zz}^s = (n_e e^2 t^{EHD}/m_z)(2\pi\beta^5)^{-\frac{1}{2}}(1-e^{-\beta})(3-e^{-\beta}(3+3\beta+3/2\beta^2+\tfrac{1}{2}\beta^3)) \times$$
$$\times \sum_{P=0}^{\infty} Y_p(P+1)e^{-P\beta} \qquad (5.4.43)$$

The values of this expression are plotted for a wide range of values of $\beta$ in Fig. 5.13.

The Quantum Limit (QL) occurrs when $\beta$ is so large that only the lowest sub-zone is occupied. The value of B required to make $\beta$ equal to 5 is about 1 Tesla at the $2^oK$ temperature used experimentally by Eaves et al. However, slightly higher values of $\beta$ are required before $\sigma_{zz}^s$ reaches

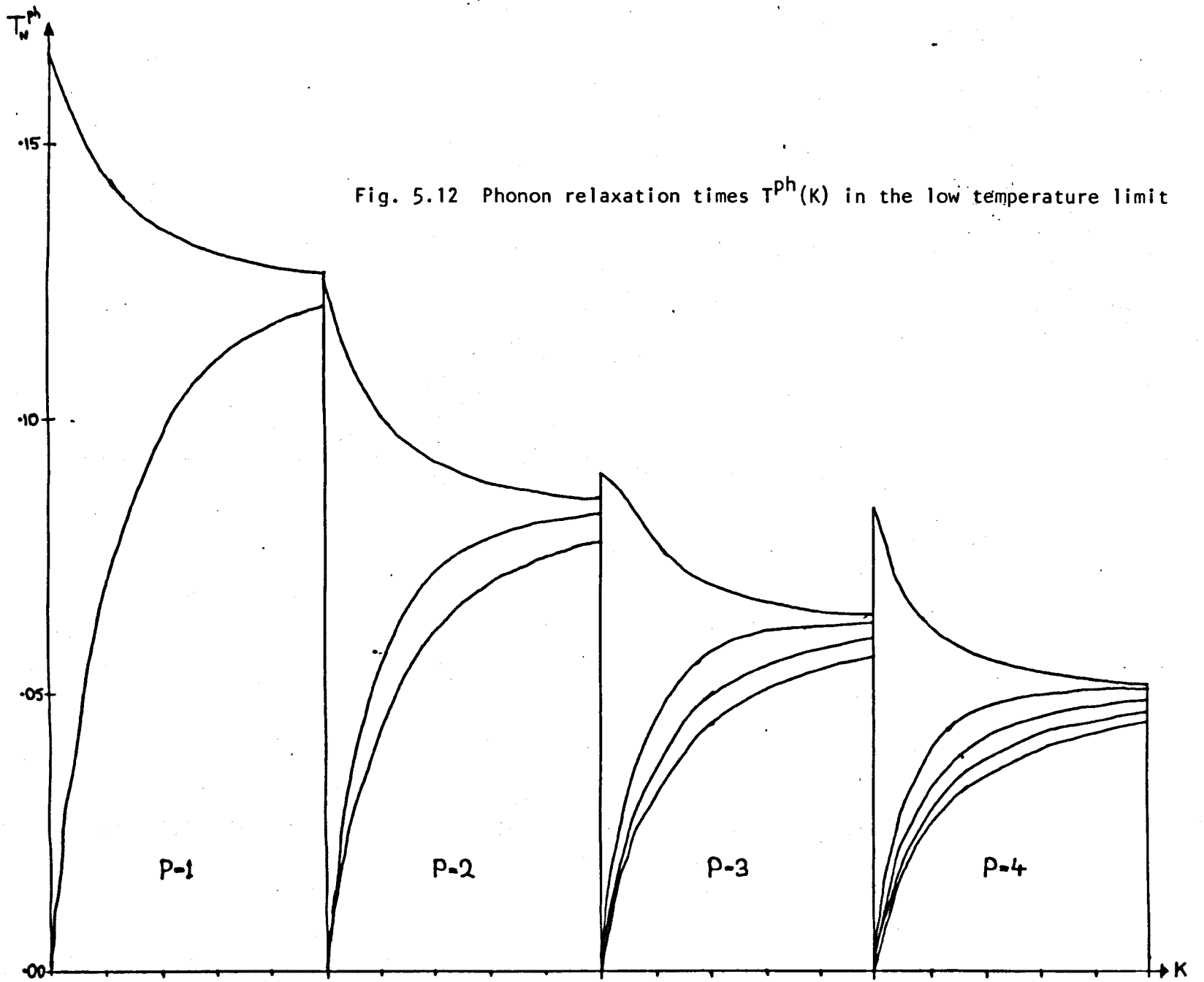


Fig. 5.12 Phonon relaxation times $T^{ph}(K)$ in the low temperature limit

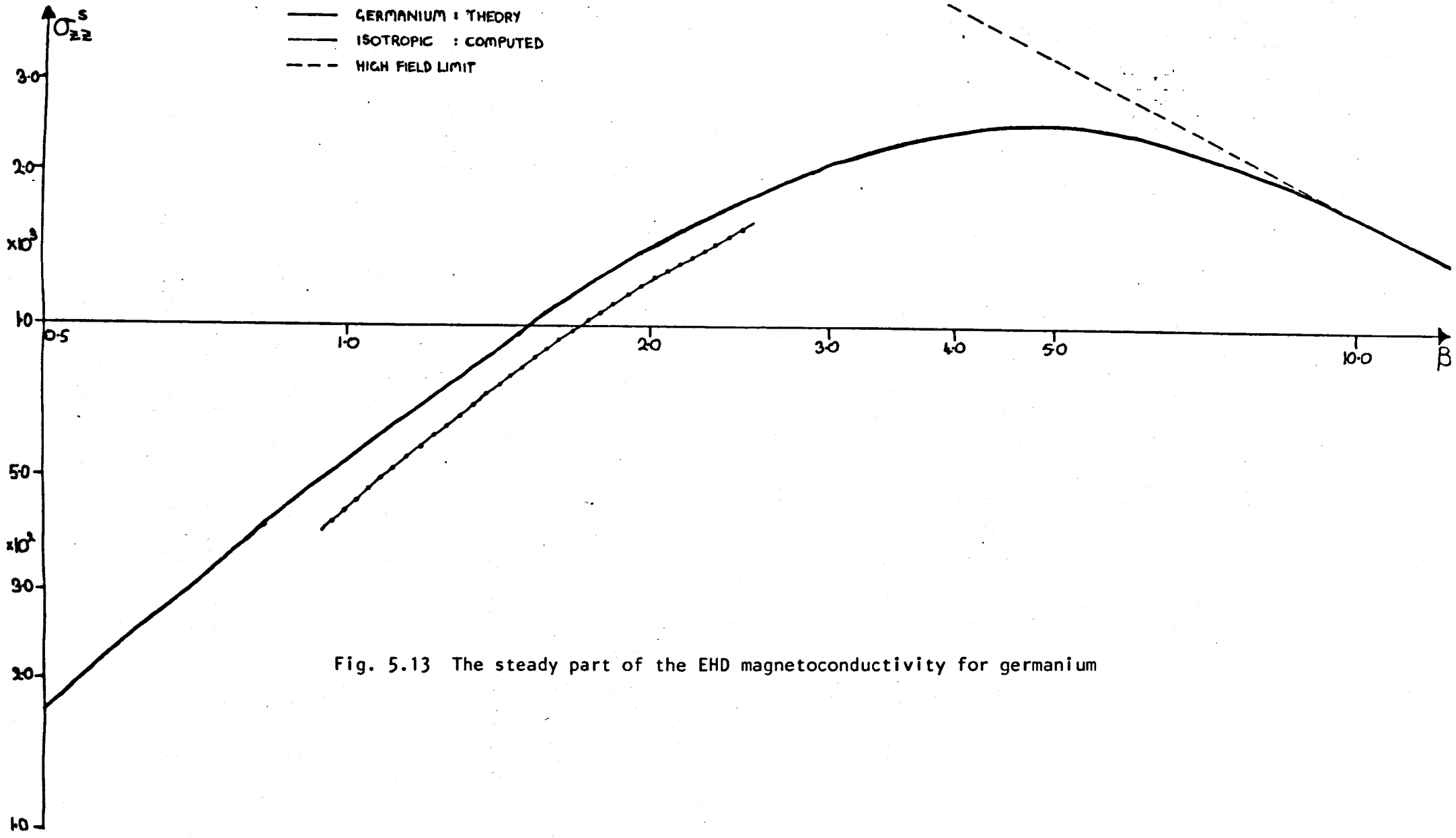


Fig. 5.13 The steady part of the EHD magnetoconductivity for germanium

its simplestlimiting form, which from (5.4.43) is

$$\sigma^{s}_{zz} \underset{B\to\infty}{\to} 3Y_o(n_e e^2 t^{EHD}/m_z)(2\pi\beta^5)^{-\frac{1}{2}} \qquad (5.4.44)$$

Given the dependence of $t^{EHD}$ and $\beta$ on B and T, we see that this varies as $B^{-1}$ and $T^{5/2}$.

The oscillatory part of the conductivity comes from the $\Sigma K_N T_N^{osc}$ term in (5.4.42). Defining the dimensionless symmetric matrix $\{\chi^{osc}\}$ in the obvious way, and noting that $\{R^s\}^{-1} = t^{EHD}\{D(K^{-1})\}\{\chi^s\}^{-1}$ where $\{D(K^{-1})\}$ is the diagonal matrix with diagonal elements $K_N^{-1}$, we have

$$\{\tau^{osc}\} = t^{EHD}\{T^{osc}\} = t^{EHD}\{D(K^{-1})\}\{\chi^s\}^{-1}\{\chi^{osc}\}\{D(K)\}\{D(K^{-1})\}\{\chi^s\}^{-1}\{1\} \qquad (5.4.45)$$

Now $\{D(K)\}\{D(K^{-1})\} = \{I\}$, the identity matrix, and $\{\chi^s\}^{-1}\{1\} = \{KT^s\} = \{1\}\{\chi^s\}^{-1}$ as an identity in row or column vectors. Therefore the summation involved in $\sigma_p$ may be simplified:

$$\sum_{N=0}^{P} K_N T_N^{osc} = \{D(K)\}\{T^{osc}\} = \{KT^s\}\{\chi^{osc}\}\{KT^s\} = \sum_{N,M=0}^{P} K_N T_N^s K_M T_M^s \chi_{NM}^{osc} \qquad (5.4.46)$$

Using the expression for the elements $\{\chi^{osc}\}$ corresponding to (5.4.33) and collecting like terms together, we have

$$\sum_{N=0}^{P} K_N T_N^{osc} = \tfrac{1}{2} \sum_{N,M=0}^{P} \{K_N T_N^s + K_M T_M^s)^2 J_{NM}^{*osc}(K_N + K_M) +$$

$$+ (K_N T_N^s - K_M T_M^s)^2 J_{NM}^{*osc}(|K_N - K_M|)\}/K_N K_M \qquad (5.4.47)$$

From our previous approximate solution for the steady part of the relaxation time, the second term in the above expression is zero, and it

reduces to

$$\sum_{N=0}^{P} K_N T_N^{osc} \approx 2Y_P(K)^2 \sum_{N,M=0}^{P} J_{NM}^{*osc}(K_N+K_M)/K_N K_M \qquad (5.4.48)$$

In our approximation the $J^{*osc}$ have factors which are sine functions of their arguments; however, as the relationship between K and the argument of $J^{*osc}$ is in general non-linear, the shape of each oscillatory component as a function of K is complex. To obtain the oscillatory part of $\sigma_p$, each oscillatory term is integrated from 0 to 1 with $Ke^{-\beta K^2}$. Since the period of the oscillations is short and the integral is sharply cut off at the upper limit, we again make the approximation that the surface term in an integration by parts is dominant. For each oscillatory component the variable of integration must be changed from K to $(K_N+K_M)$, after which the surface term is

$$\int_0^1 \sum K_N T_N^{osc} K e^{-\beta K^2} dK \approx \sum_{N,M=0}^{P} \left[ \frac{e^{-\beta K^2} 2KY_P(K)^2 F_{NM}(u_z^*) \cos 2R(K_N+K_M)\, dK/d(K_N+K_M)}{4R^2 K_N K_M (K_N+K_M)^3} \right]^{K=1} \qquad (5.4.49)$$

where $u_z^* = 0.454(K_N+K_M)^2$. In fact our approximation here is not so good as previously, as the derivative of $Y_P(K)^2$ is large, making the next term in the integration by parts of a similar magnitude to the first (unless R is very large). The above expression should give a qualitative description of the oscillation, however. Since $dK_N/dK = (2m_z/m_c)K/K_N$, the derivative may be evaluated, whence

$$\int_0^1 \sum K_N T_N^{osc} K e^{-\beta K^2} dK \approx (m_c/2m_z)(e^{-\beta Y_P^2/4R^2}) \sum_{N,M=0}^{P} \left[ \frac{F_{NM}(u_z^*) \cos 2R(K_N+K_M)}{(K_N+K_M)^4} \right]^{K=1} \qquad (5.4.50)$$

As a proportion of $\sigma_p$ this falls off rapidly with increasing magnetic field because of the additional $e^{-\beta/R^2}$ factor.

At the top of the zone the value of $K_N$ is $(P+1-N)^{\frac{1}{2}}(2m_z/m_c)^{\frac{1}{2}}$. Thus it can be seen that while the same N-M transition in different Landau sub-zones will give rise to different values of $K_N+K_M\big|_{K=1}$, the same value of $K_N+K_M$ may be obtained from a sub-zone L bands higher in the transition N+L→M+L. Thus the 0-0 transition in sub-zone 0 gives rise to the same 'frequency' in $\sigma_{zz}$ as the 1-1 transition in sub-zone 1, the 2-2 transition in sub-zone 2, etc. For this 'fundamental frequency' $K_N = K_M = (2m_z/m_c)^{\frac{1}{2}}$, giving rise to a $\cos\{4R(2m_z/m_c)^{\frac{1}{2}}\}$ term. Since $R = a/\ell = a(eB/\hbar)^{\frac{1}{2}}$ the argument of the cosine is $4a(2em_z/m_c\hbar)^{\frac{1}{2}}B^{\frac{1}{2}}$, which means that this term in the conductivity is periodic in $B^{\frac{1}{2}}$, with fundamental period

$$\Delta_{oo} = (\pi/2a)(\hbar m_c/2em_z)^{\frac{1}{2}} \qquad (5.4.51)$$

as first postulated by Eaves et al (1976), and verified numerically by Barker and Bridges (1978). Now, however, we may also give an expression for the magnitude of the component of this frequency, and of all the other frequency components present. Combining (5.4.50) with (5.4.42), the magnitude of the fundamental frequency component is

$$(n_e e^2 t^{EHD}/m_z)(\beta^3/2\pi)^{\frac{1}{2}}(1-e^{-\beta})(m_c/2m_z)^3/64R^2 \sum_{P=0}^{\infty} Y_P^2 F_{PP}(16.0)e^{-(P+1)\beta} \qquad (5.4.52)$$

The ratio of this component to the steady part of $\sigma$ is plotted in Fig. 5.14 for a range of values of B.

The other oscillation frequencies present in $\sigma_{zz}(B)$ are found by considering all the possible values of $(K_N+K_M)\big|_{K=1}$ for higher sub-zones. Clearly these values are $(\sqrt{S+1}+\sqrt{T+1})(2m_z/m_c)^{\frac{1}{2}}$ where S and T are non-negative integers. If $S \geq T$ only sub-zones $P \geq S$ contribute such terms, which give rise to a component in $\sigma_{zz}(B)$ periodic in $B^{\frac{1}{2}}$ with

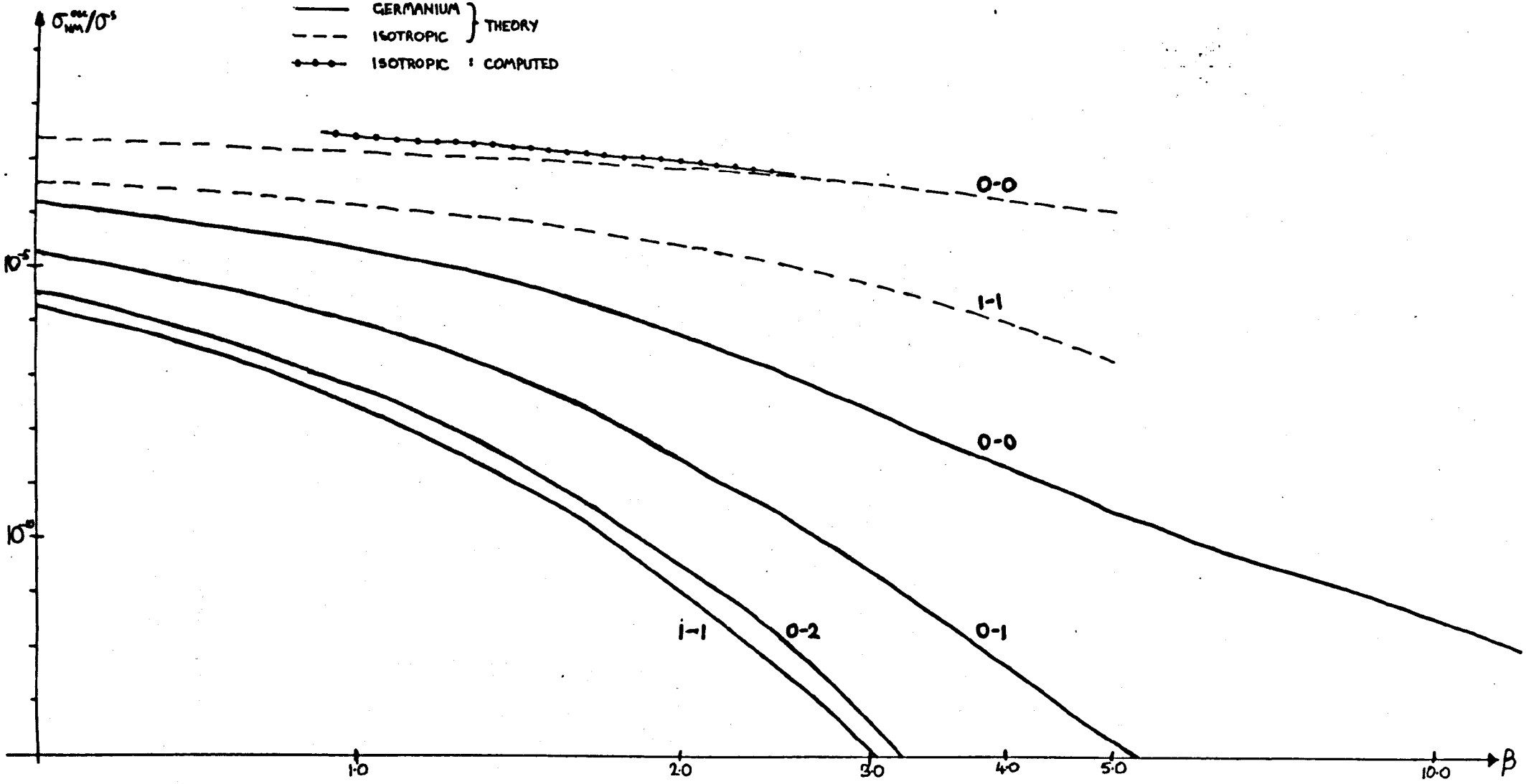


Fig. 5.14 Magnitudes of the oscillatory components of the magnetoconductivity, as a proportion of the steady part

period

$$\Delta_{ST} = 2\Delta_{oo}/(\sqrt{S+1}+\sqrt{T+1}) \tag{5.4.53}$$

the magnitude of the frequency component being

$$(n_e e^2 t^{EHD}/m_z)(\beta^3/2\pi)^{\frac{1}{2}}(1-e^{-\beta})(m_c/2m_z)^3/4R^2 \times$$

$$\times \sum_{P=S-1}^{\infty} Y_P^2 F_{P-S+1,P-T+1}(4.0(\sqrt{S+1}+\sqrt{T+1})^2) e^{-(P+1)\beta}(\sqrt{S+1}+\sqrt{T+1})^{-4} \tag{5.4.54}$$

The ratios of these components to the steady part are also plotted in Fig. 5.14

This completes our calculation of the EHD magnetoresonance in germanium, but before going on to discuss the phonons we shall briefly mention the corresponding results in a material of isotropic band structure, as these may be compared with data we have computed numerically. It will be seen from a comparison of (5.4.23) and (5.4.24) that $J^*_{NM}$ and $J_{NM}$ differ by a factor of approximately 6, and hence the $Y_p$ calculated for an isotropic material are approximately $\frac{1}{6}$ of their values in Ge. The values of $m_z$ and $m_c$ (involved also in $t^{EHD}$ and $\beta$) are also changed, the result being that the steady part of the conductivity in the isotropic material is approximately 0.058 of that for Ge at 0.135 times the magnetic field. The oscillatory part of $\sigma$ differs also in that the $F_{NM}$ factors in (5.4.52) and (5.4.54) are replaced by $\delta_{NM}$ (in our crude approximation), so that all oscillations due to inter-band transitions disappear. This replacement leads to a marked increase in the comparitive size of the oscillations over that for Ge, as is illustrated in Fig. 5.14.

The Acoustic Phonon Conductivity

There are essentially four regimes which we shall mention with regard to acoustic phonon scattering : high or very low temperatures in combination

with either a high magnetic field (QL) or a lower field for which several Landau bands are occupied. The high or low temperature approximation consists of replacing $\coth(0.79C^{ph}Q_z)$ in (5.4.25) either by $(0.79C^{ph}Q_z)^{-1}$ or by 1 respectively, while the QL occurrs when only one Landau band is populated. We may assume that the QL occurrs when $\beta > 5$; we remember that $\beta \approx 9.90B/T$.

In the QL the highest value of $Q_z$ we need to consider is twice that corresponding to an energy of about 5kT; we may show that this value is $2(2m_z/m_c)^{\frac{1}{2}}(5/\beta)^{\frac{1}{2}}$. Hence the maximum value of $(0.79C^{ph}Q_z)$, bearing in mind that $C^{ph} \approx 1.5B^{\frac{1}{2}}/T$, is approximately $5.0T^{-\frac{1}{2}}$. For the high temperature approximation to be valid this must be less than about 0.2, so that T is greater than $600^{o}K$. For the low temperature approximation it must be greater than about 3, so that T is less than about $3^{o}K$. In either case B must be greater than 0.5T to ensure that $\beta > 5$.

Outside the QL the highest value of $Q_z$ occurring is $Q_o \approx 5.94$, and hence the maximum value of $(0.79C^{ph}Q_z)$ is approximately $7.04B^{\frac{1}{2}}/T$. For the high temperature approximation this must be less than 0.2. If $T \geq 600^{o}K$ this will be true for any value of B which is nonQL, otherwise B must be less than $8\times10^{-4}T^2$. For the low temperature approximation the expression must be greater than 3. If T is $\leq 3^{o}K$ this can occur for $0.16T^2 \leq B \leq 0.5T$, while for $T \geq 3^{o}K$ no low temperature approximation is possible. The position of the four regimes in the B-T plane is shown in Fig. 5.15. We note that for $T = 2^{o}K$ the low temperature approximation applies for $B \geq 0.67$ Tesla, while the high temperature approximation applies for $B \leq 0.0064$ Tesla; thus neither applies to the experimental regime of Eaves et al.

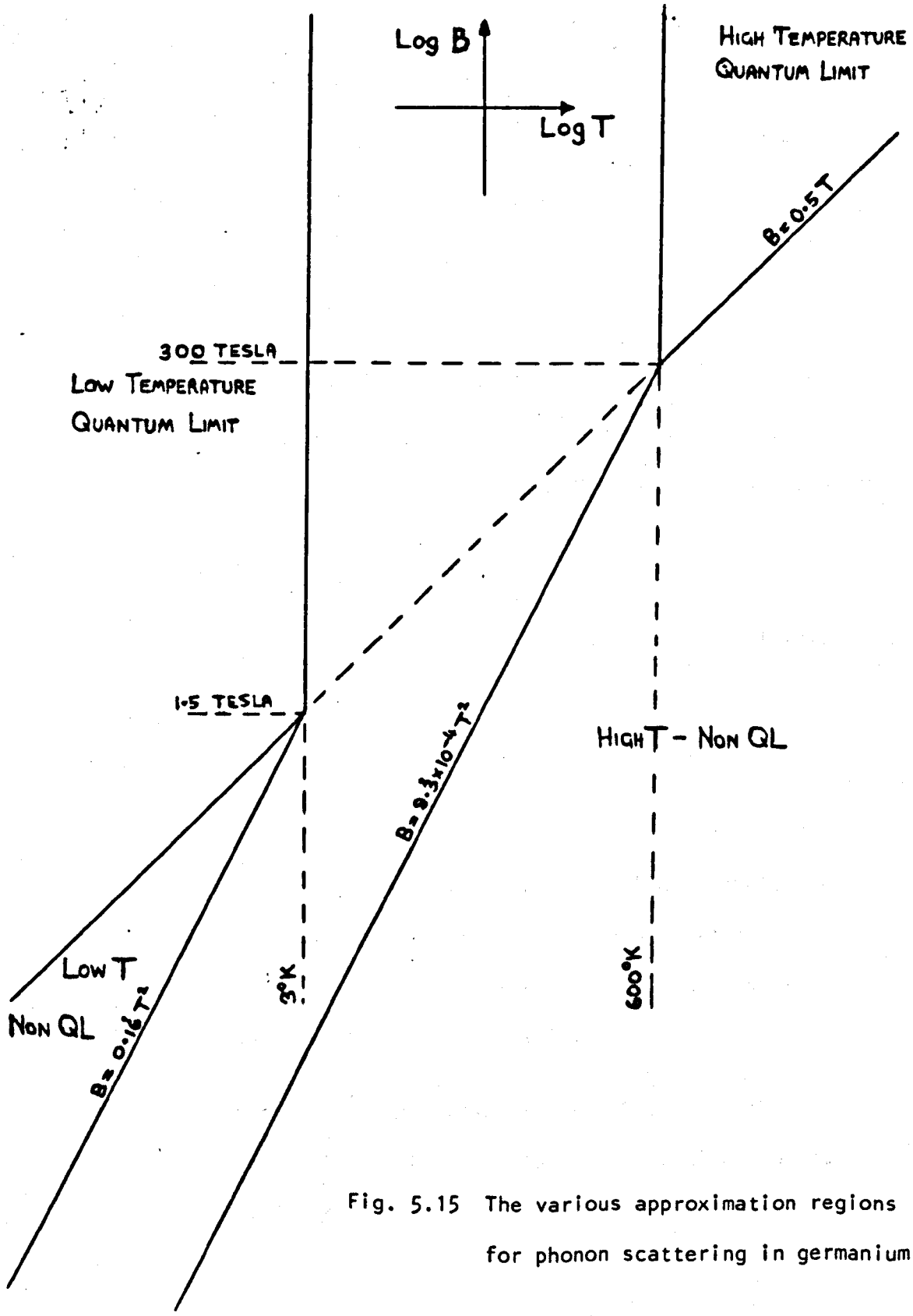


Fig. 5.15 The various approximation regions for phonon scattering in germanium

In the high temperature approximation $W_{NM}^{ph}$ is constant, independent of N,M and $Q_z$ and equal to $(0.79t^{ph}C^{ph})^{-1}$. From the work of §4.6 it follows that the relaxation times at any energy are all the same and equal to $0.40t^{ph}C^{ph}(\sum_{M=0}^{P} K_M^{-1})^{-1}$. We shall not pursue this further except in the QL where $\tau_o = 1.17t^{ph}C^{ph}K$. The integral corresponding to (5.4.42) for $\sigma_{zz}$ may then be performed, and we have

$$\sigma_{zz}^{ph} \underset{\substack{B\to\infty \\ T\geq 600^oK}}{\to} 3.48C^{ph}(n_e e^2 t^{ph}/m_z)(2\pi\beta)^{-\frac{1}{2}} \qquad (5.4.55)$$

varying as $B^{-1}$ and $T^{\frac{1}{2}}$.

The low temperature approximation has already been mentioned in (5.4.41). In the QL $T_o^{ph}$ is constant and equal to $\frac{1}{4}$, so that again the integral for $\sigma_{zz}$ may be performed:

$$\sigma_{zz}^{ph} \underset{\substack{B\to\infty \\ T\leq 3^oK}}{\to} 0.27(n_e e^2 t^{ph}/m_z) \qquad (5.4.56)$$

varying as $B^{-1}$ and independent of temperature.

The Validity of the Numerical Approximations

We will conclude this section with a brief discussion of the validity of the essentially mathematical approximations we have made in several places in order to arrive at an analytical expression for $\sigma_{zz}$, leaving discussion of the physical approximations until later.

We first approximated $W^{EHD}$ by neglecting the sinRQ term in the Fourier transform of the potential; this is a large R approximation and is valid down to B < 0.01 Tesla. Next, the exact integral for $J^*$ is

replaced by the approximation (5.4.23); this is a large $Q_z$ approximation valid for the important values of $Q_z$ for N,M at least up to 4, though it becomes poorer as N and M increase (see Fig. 5.10). The approximation (5.4.28) for $J^{*osc}$ is much poorer; it works well for low values of $Q_z$, but by the top of the Landau zone may underestimate the true value by as much as a factor of 10. Numerical integration found no simple dependence of $J^{*osc}$ on the two parameters R and $Q_z$, however, and so (5.4.28) was accepted for want of something better. The approximation involved in inverting the relaxation matrix for the EHDs is very good indeed in the upper part of each zone, where it differs from the exact inversion by less than 0.2%; it is inadequate in the lower half, but this does not matter. Finally, the functional dependence of the $Y_p$ on K is well represented by $K^6$ in the upper part of the zone, again deteriorating in the lower half (see Fig. 5.11). We may therefore conclude that (5.4.43) gives a true picture of the steady part of the conductivity so long as only the first few Landau zones are occupied, but that the expressions (5.4.52 and 54) for the magnitude of the oscillatory components may be underestimates by a factor of 10 or more.

The only approximation we have made in the phonon calculation (apart from those already discussed) is to replace the exact integral for $W^{ph}$ by (5.4.25). This has been found to be accurate for all values of $Q_z$ for N,M up to at least 4.

## 5.5 Comparison with Numerical Calculation and Experiment

This section consists of two parts; firstly, a comparison of the approximate analytic formulae of the previous section with a purely numerical evaluation of the conductivity, and, secondly, a comparison with the experimental results and theory of Eaves et al (1976).

In view of the many mathematical approximations made in the previous section in order that analytical formulae could be produced, it is desirable to check the final expressions (5.4.43) and (5.4.54) against a more direct numerical evaluation of the conductivity in which the only approximations are those of numerical analysis. Such a calculation has been performed by Barker and Bridges (1978) using electron wave-functions for an isotropic material, but retaining the correct Ge values of $m_z$ and $m_c$ at all other points. This calculation included phonon scattering, but for certain values of $\beta$ the conductivity due to EHD scattering only is available; these values should be approximately 0.162 times the value for the steady part of $\sigma$ given by (5.4.43), as discussed in the previous section. The magnitudes of the oscillatory components may be compared with the upper curves of Fig. 5.14.

In Fig. 5.16 the relaxation times computed in the first two sub-zones for two particular values of the magnetic field are compared with those calculated from (5.4.39). It will be seen that there is some discrepancy, probably due to the fact that the $Y_p$ for the isotropic case are not exactly 0.162 times those for Ge as we have assumed. The ratios of the relaxation times at the top of the sub-zone are exactly as predicted ($1/\sqrt{2}$ : 1 for zone 1, $1/\sqrt{3}$ : $1/\sqrt{2}$ : 1 for zone 2).

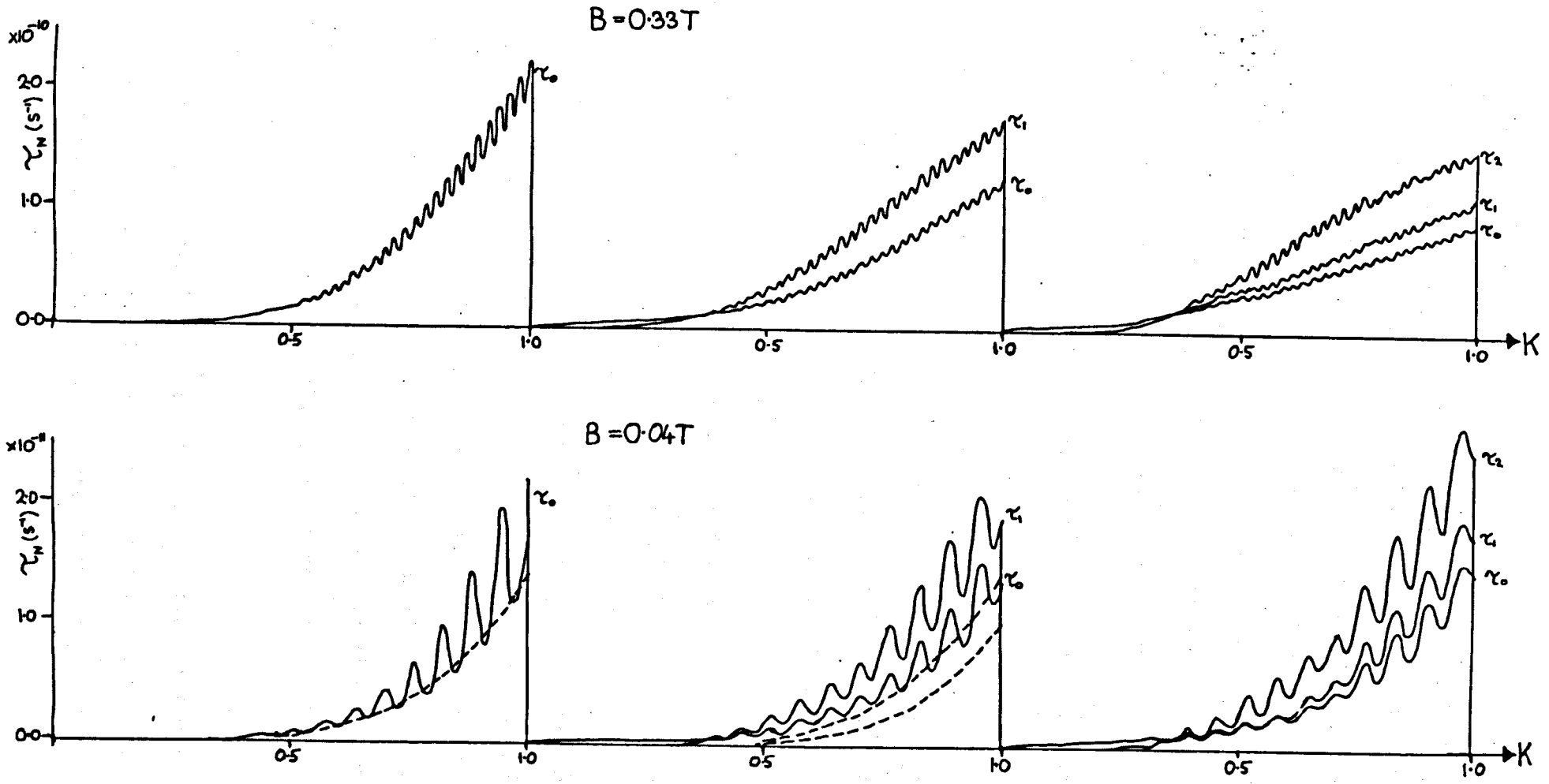


Fig. 5.16 Numerically computed relaxation times for EHD scattering in an isotropic band material

Since the splitting of the relaxation times is so marked, it is to be expected that any attempt to invert the relaxation matrix approximately by use of the 'Argyres formula' $\tau_N^{-1} = \sum_{N'} R_{NN'}$ will fail. In fact it does so spectacularly, as may be seen in Fig. 5.17 where such a procedure has been adopted. The singular behaviour and negative values obtained for $\tau$ are physically unacceptable, and show the danger of this approximate method for calculation when the scattering is not isotropic.

In Fig. 5.18 we plot relaxation times for pure phonon scattering for the same two values of magnetic field. Firstly we note the much smaller splitting; in fact the 'Argyres formula' is a good approximation here. Clearly we are much nearer in character to the high-temperature regime than to the low-temperature limit plotted in Fig. 5.12. Secondly, the actual values of the relaxation times show that, for the isotropic material, phonon scattering is negligible at the lower field value (which is typical of the experimental work). This factor is eroded from both sides on going over to a Ge calculation, however, as this increases the phonon scattering and reduces the EHD scattering. The effect of combining EHD and phonon scattering of approximately equal strength is shown in Fig. 5.19, which also shows what happens when the phonons become the dominant mechanism (by reducing the depth of the EHD potential well). Clearly the simplifying assumptions as to the general shape of the relaxation time/energy spectrum, made in the previous section, break down when both scattering mechanisms are equally important. Fortunately this does not seem to be the case at the lower magnetic fields.

The values of the overall conductivity from the first three sub-zones have been plotted on Fig. 5.13. It may be seen that the comparison with the analytical formula is good, the difference again being a factor of about

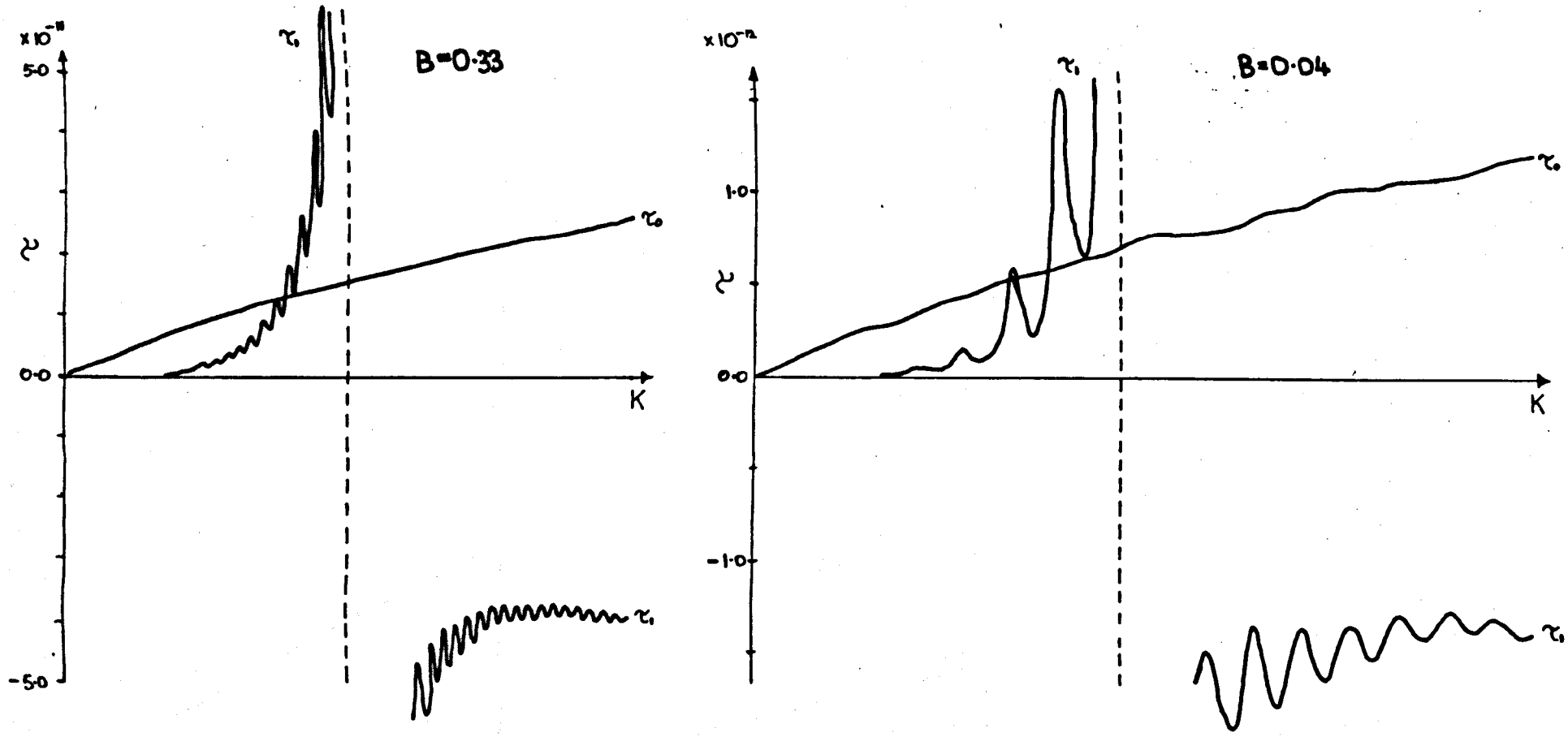


Fig. 5.17 Numerically computed Argyres 'relaxation times' in an isotropic band material

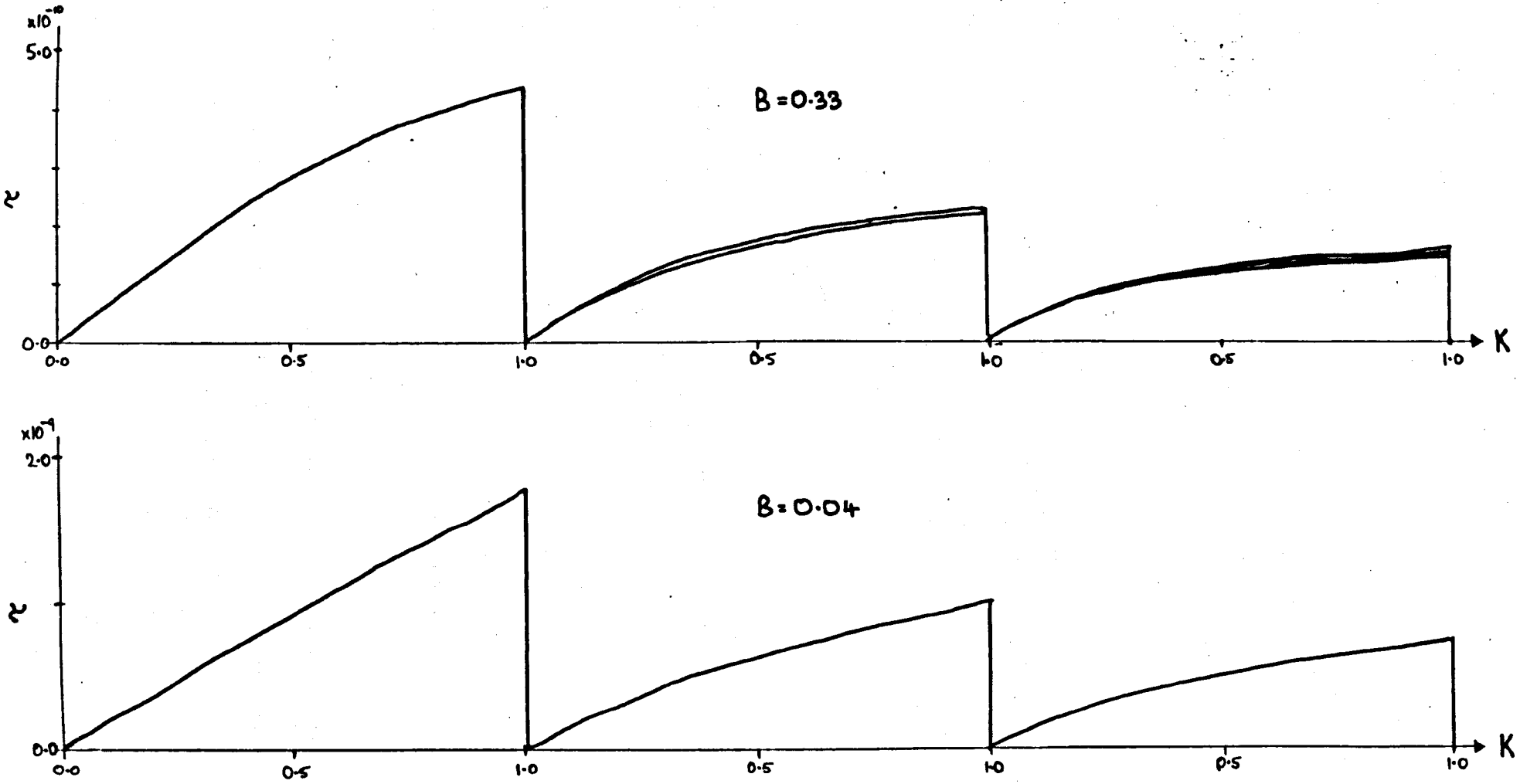


Fig. 5.18 Numerically computed relaxation times for phonon scattering in an isotropic band material

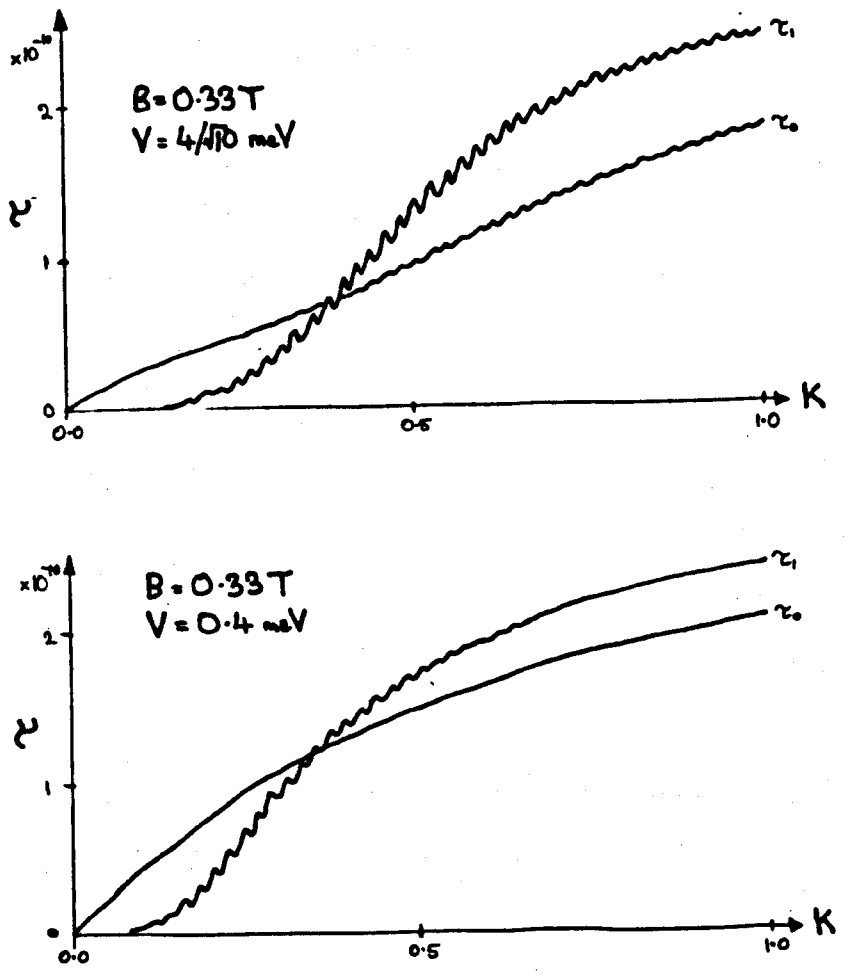


Fig. 5.19 Numerically computed relaxation times for mixed EHD and phonon scattering in an isotropic band material, for varying strength of EHD scattering

0.8 for the same reason as causes the difference in relaxation times. The calculated structure of the oscillatory component of $\partial\sigma/\partial\beta$ is shown in Fig. 5.20 and the magnitude of the fundamental frequency component as a fraction of overall calculated conductivity is plotted on Fig. 5.14 for comparison with the analytical value. It can be seen that the analytical formula underestimates the size of the oscillation for the lower values of magnetic field, as previously suggested.

The calculated oscillatory components of $\partial\sigma/\partial\beta$ for the first three sub-zones separately are Fourier analysed in Fig. 5.21, the transform being in the variable $2\pi\sqrt{B}/\Delta_{oo}$. The function plotted is the modulus of the Fourier transform, or Fourier power spectrum. The overall structure of the peaks is in very good agreement with that predicted by the analysis of §5.4. The main peak at the fundamental frequency is present in all sub-zones, and is sharp, indicating a nearly pure harmonic variation as predicted. The subsidiary peaks in the higher sub-zones also occur in exactly the right positions, and the low frequency components with multiplying factor $(K_N T_N - K_M T_M)^2$ are absent as expected. The ratio of the subsidiary peaks to the fundamental is not easy to estimate accurately (due to the noise from transforming over a finite interval) and is in any case only an average over the field range of the calculation, but it is not inconsistent with the predicted value. The only inconsistent feature is the presence of subsidiary peaks due to inter band transitions. (Those of period $2\Delta_o/(1+\sqrt{2})$, $2\Delta_o/(1+\sqrt{3})$, etc) which should not be present in an isotropic material if approximation (5.4.29) for $J^{osc}$ is accurate. Clearly it is not, and an accurate analytical formula for $\sigma$ in an isotropic material would have to take this into account.

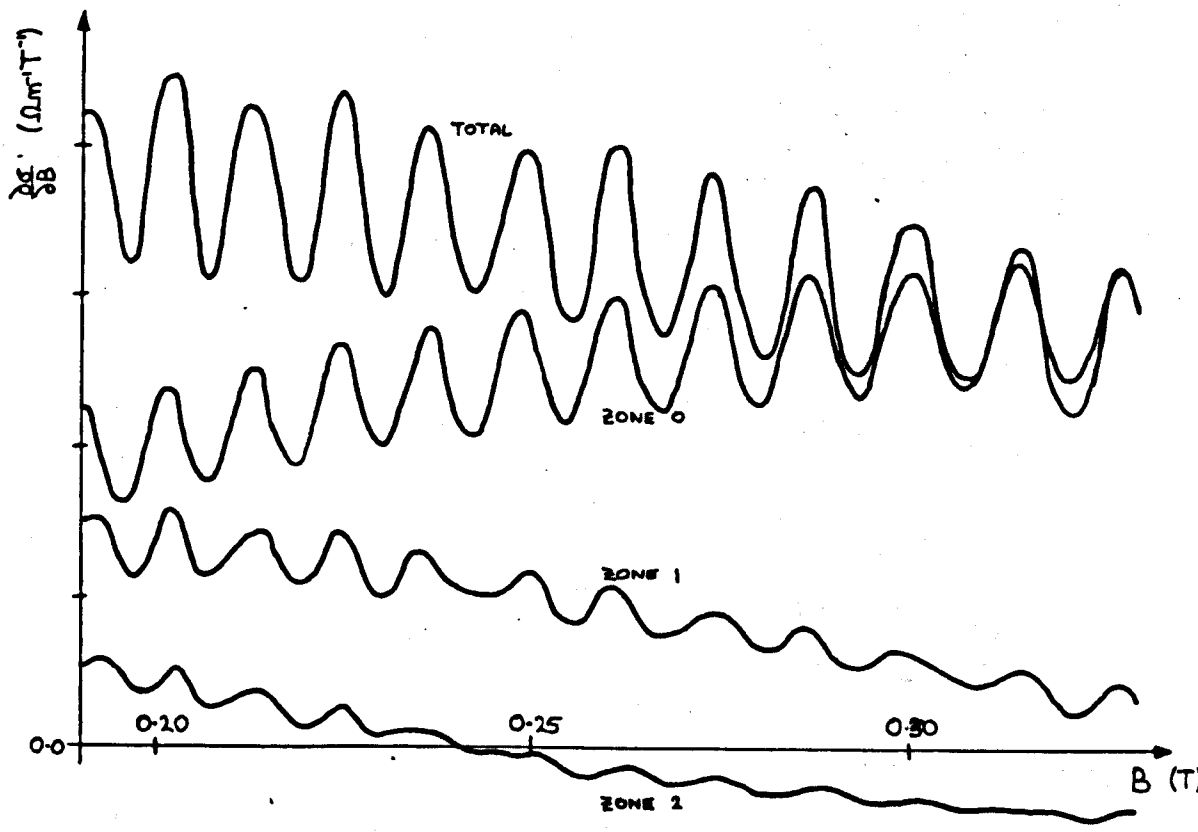


Fig. 5.20 Numerically computed zonal contributions to $\partial\sigma/\partial B$ for EHD scattering in an isotropic band material

Fig. 5.21 Fourier transforms in $B^{\frac{1}{2}}$ of the numerically computed zonal contributions to $\partial\sigma/\partial B$

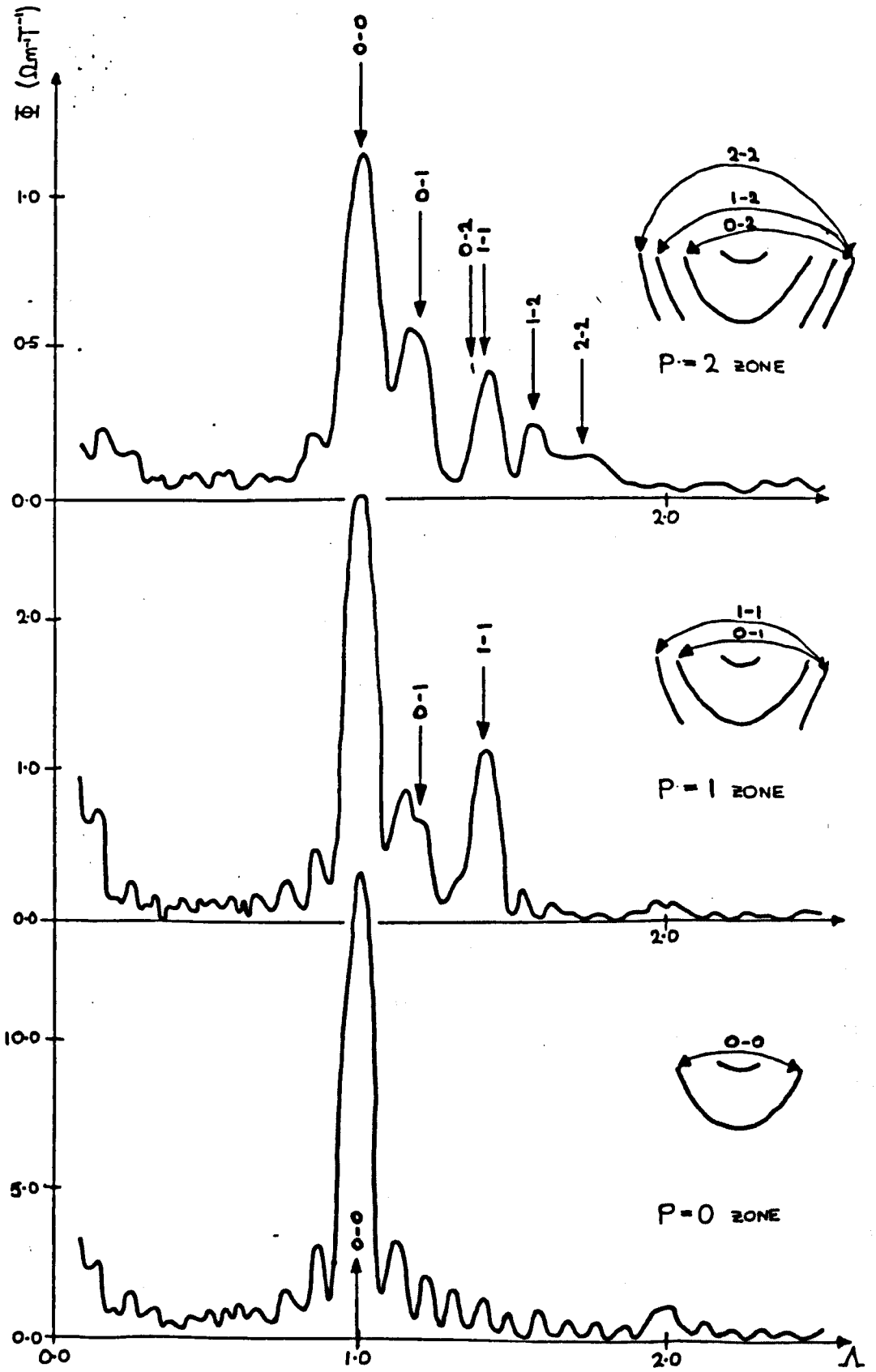

The comparison with experimental work must unfortunately be indirect and qualitative. We have been unable to extend either the analytical formulae of §5.4 or the numerical calculation to the lower ranges of magnetic field. In the case of the analytical formulae this is because several of the approximations used begin to break down; most notably (5.4.23) for $J^*$ which becomes increasingly poorer for the higher values of N which must be included at lower fields. The variation of $Y_p$ with K is thus no longer $K^6$. In the case of the numerical calculation, the increasing number of matrix elements and length of matrix inversion as higher sub-zones are brought in eventually make the computer time involved too long for it to be feasible.

In this situation the only comparison with the experimental work that can be in any way quantitative is to plot the Fourier transforms of the oscillatory components alongside each other. This has been done in Fig. 5.22. The main peak of the experimental data is seen to be fairly sharp, though broader than the theoretical one; we shall discuss possible reasons for this later. The value of the droplet radius in the numerical calculation was chosen so that the fundamental period would be that observed experimentally, and therefore it is not surprising that the peaks fall above each other. It is noticeable that the subsidiary peak structure due to higher order transitions is either not resolved or absent altogether in the experimental curve, although at lower field values it should in fact be more prominent. Even more unexpected is the prominent structure on the low frequency side of the main peak in the experimental transform. This is definitely not a feature of the non-oscillatory background (which has been subtracted from both sets of data before transorming), although it is not obvious in the untransformed data. We shall speculate as to possible origins for this structure in the following discussion.

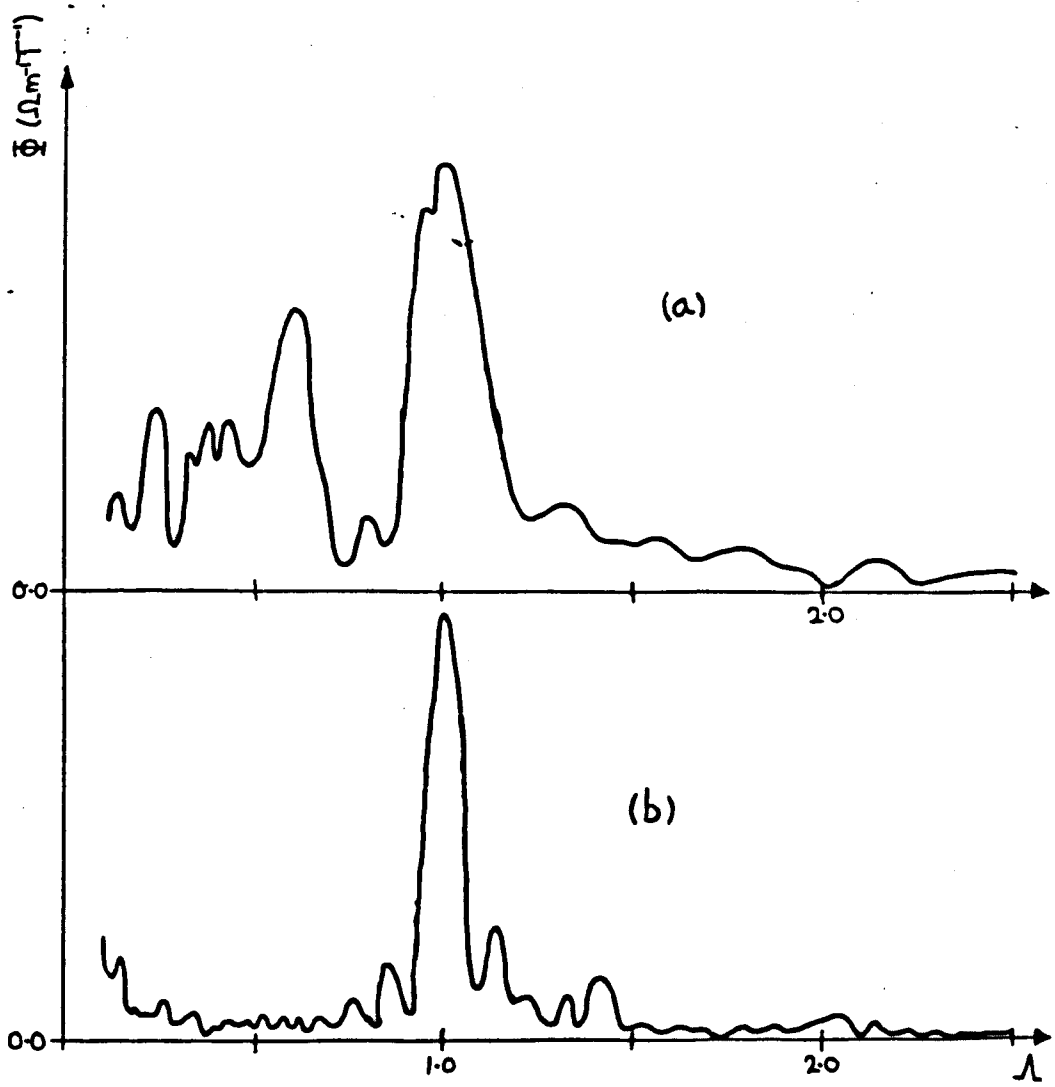


Fig. 5.22 Fourier transforms in $B^{\frac{1}{2}}$ of magnetoconductivity curves:

a) Experimental data of Eaves et al

b) Numerically computed data for isotropic band material

The only other information we have about the experimental data is that the oscillations disappeared above B = 0.06T and their amplitude was approximately 1% of the overall conductivity at the point where they were strongest. The fall off with increasing B has been explained in the the previous section; it is due to extra $e^{-\beta}$ factors in the magnitude of the oscillatory components. The amplitude of 1% of background is higher than would be obtained by extrapolating Fig. 5.14, but this was already believed to underestimate the size of the oscillation, and so is consistent with the experimental data. We may summarise, therefore, by saying that the agreement of our computed and theoretically derived results with experiment is reasonably good, though various points will be discussed in greater depth in the next section.

## 5.6 Discussion and Conclusions

In this section we shall discuss the previous theoretical study with regard to the various approximations we have made, the comparison of the calculated results with the experimental data, and possible improvements which might be made in future calculations. For convenience we shall split this into sub-sections : Comparison with experiment, Approximate treatment of the EHD's, Other approximations, Self-consistency of the transport theory, Conclusions.

### Comparison with experiment

Referring to Fig. 5.22 we see that areas of agreement with experiment may be summarised as: the oscillation of the magnetoconductivity, periodic in $B^{\frac{1}{2}}$, with a fairly sharp peak in the Fourier power spectrum. Areas of disagreement are: the broader fundamental peak, the lack of subsidiary peaks at higher frequencies, and the prominent structure on the low frequency side of the fundamental peak. We shall see below that a broader peak in the power spectrum may easily arise, due either to a variation in droplet radii or a slight softening of the sharp edge of the potential well; indeed, it is surprising that the experimental peak is as sharp as it is. The complete absence of the higher frequency subsidiary peaks is harder to account for, and detracts from the usefulness of our more detailed calculation. Contrary to our previous speculation (Barker and Bridges 1978), this cannot happen due to the overlap of many closely spaced peaks, as the frequencies obtained from (5.4.53) are well separated, apart from a small number of coincidences. It is more likely that the peaks are broadened beyond detection by either of the two methods mentioned above, or by collision broadening (which tends to affect higher Landau bands more than the lower ones; see Kubo et al 1965). We note

that in a similar size-magnetoresonance experiment in which scattering was by cylindrical potentials, the higher order resonances have been observed in the Fourier transform of the conductivity (Nicholas and Stradling, 1979).

The very prominent low frequency structure in Fig. 5.22 we can only postulate as being due to hole conduction, although Eaves et al (1976) disregard this as being small. It would be extremely difficult to perform an exact calculation of the hole conductivity, as the detailed shape of the hole bands is very complex, especially near the band edge (Dresselhaus et al 1955, Kittel 1971). However, the overall shape of the hole valleys is considerably more isotropic than those in the conduction band, and we might hope for an approximate picture in which an $m_z$ and an $m_c$ could be defined for holes and would be approximately equal. Then, since the ratio $(m_c/m_z)^{\frac{1}{2}}$ appears in the period of the magnetoconductivity oscillations, any peak in the Fourier power spectrum which is due to holes would be separated from that due to electrons because of the different anisotropy ratios, the positions of the peaks $\Lambda_e:\Lambda_h$ being in the ratio 1:0.48. Returning to Fig. 5.22, it may be seen that the low frequency structure is thus in the correct position for hole conduction to be a plausible explanation of its origin.

The experimentally observed disappearance of the oscillations with increasing magnetic field is easily explained, as three separate factors contribute to it. Firstly, the phonon scattering becomes increasingly dominant at higher fields, so that the EHD oscillations become proportionately smaller. Secondly, there are extra $e^{-\beta}$ terms in the oscillatory part of the EHD conductivity which make it proportionally smaller than the steady part as the field increases. Finally, as the

quantum limit is approached the coefficient of the oscillatory part in the lowest sub-zone becomes dominant, and this is very small as previously noted.

Approximate treatment of the EHDs

In our theoretical model we have assumed that the EHDs may be regarded as potential scatterers in the form of spherical square wells,whose radius and depth are the same for each drop. The validity of this model needs to be considered very carefully, as it is fundamental to the calculation we have performed. The most important simplification we have made is to regard the droplet of electron-hole liquid, a very complex system physically, as a single simple potential scatterer as far as electrons in the conduction band are concerned. The justification for this is the observed work function for electrons, against removal from the EHL, of a few meV (Pokrovsky and Svistunova 1969, 1970a, b). We assume that an electron enters the drop, gains kinetic energy due to the lower background potential of the EHL in which it travels, but does not interact with it in any other way before leaving the droplet again. We also assume that the magnetic field inside the drop is the same as that outside, so that the scattering potential is an addition to the magnetic field in the electron Hamiltonian, rather than a replacement of it.

The above picture ignores the possibility that the electron might be scattered while it is within the droplet, either by an individual particle or by exciting a bulk mode of oscillation of the EHL. Clearly neither of these two scattering processes need be elastic, and both might well lead to temporary or permanent capture of the incident electron. In the case of permanent capture later scattering would also be affected by the Coulo mb repulsion of the additional charge present. There is experimental evidence

that EHDs carry quite substantial electric charges of the order of a few hundred times e (Pokrovsky and Svistunova, 1974; Nakamura, 1977), so that this is clearly an important effect. Without a much more detailed knowledge of the nature of the EH liquid/plasma, however, we do not feel capable of evaluating the importance of either of these two mechanisms. Suffice it to say that, while they must contribute to the scattering, the experimentally observed oscillations are good evidence for the presence of an overall effective potential well.

The penetration of the magnetic field into the EHD would again be very difficult to treat precisely. It is our belief, however, that since the plasma is composed of neutral particles, and the magnetic field is in principle static, penetration of the field will occur , with only small local distortion around the edge of the drop. As we have previously mentioned thereis experimental evidence for flattening of EHDs parallel to the axis of a strong magnetic field, but scattering by a spheroidal potential would be qualitatively little different from scattering by the perfect spheres of our model.

The sharp edged square well potential of our model is obviously an idealisation, as we would expect it to attain its full depth over a distance at least as large as an exciton. Since this is approximately 0.018 μm, the radius of an EHD is indefinite to within about 1%. Further, we should allow for the possibility that not all the EHDs are the same size; indeed, there seems to be no obvious reason why they should be.

A distribution of droplet radii is easily allowed for by replacing the Fourier transform of the droplet potential in (5.4.9) by a function averaged over the radius distribution. Assuming a gaussian distribution of

droplet radii centred on $a_o$, width $\gamma$, we would have

$$<|U(q)|>^2 = \int da\ \exp(-(a-a_o)^2/2\gamma)\,(16\pi^2V^2/\sqrt{2\pi}q^6)\,(\sin qa - qa\cos qa)^2 \qquad (5.6.1)$$

On evaluating this integral we find that the dominant term is $|U(q,a_o)|^2\exp(-2q^2\gamma^2)$, so that the original Fourier transform is modulated by a gaussian damping of width $\gamma^{-1}$. At the top of the lowest sub-zone q is $2(2m_z/m_c)^{\frac{1}{2}}.\ell^{-1}$, and hence the damping factor is $\exp(-16m_z/m_c(\gamma/\ell)^2) \approx \exp(-1.3\times10^5 B(\gamma/a_o)^2)$. It is obvious that the radius distribution must be very sharp in comparison with $a_o$ for damping to be avoided. For $\gamma/a_o$ = 1% and B = 0.04T the damping factor is 0.59, and rapidly becomes smaller for higher fields. The effect of a soft potential edge could be treated almost identically, with a similar effect.

It therefore seems that the very existence of the magnetoconductivity oscillations is strong evidence in favour of a sharp distribution of droplet radii and a sharp edged potential. This is surprising, as there seems to be no reason for the droplets all to be the same size. Barker (private discussion) has suggested that the EHDs giving rise to the oscillation have only just nucleated, at constant size and near the surface of the sample, while older, partially evaporated EHDs are deeper in the sample and possibly beyond the penetration of the magnetic field. This is still an open question, however.

Other Approximations

We have made two other approximations in our treatment of the conduction band electrons of the Ge sample. The first of these is to use the effective mass approximation, combined with plane wave rather than Bloch states. Apart from the most precise work this is almost universally used in Ge calculations, and has been shown to work well; we shall discuss

it no further.

More importantly, we have ignored the inelasticity of the phonon contribution to the scattering, although our argument of §5.3 gives no justification for this. In an inelastic calculation electron states will be linked by phonon transitions to states of different energy, determined by drawing straight lines of gradient $\pm\hbar s$ on the Landau level scheme. The distribution function f may still be written in terms of a relaxation time and independent of $k_y$, but the $\tau$'s can no longer be determined by inverting a finite matrix. States of energy $\varepsilon$ are linked by phonon transitions to states of higher and higher energy, in an infinite hierarchy which is only cut off by the increasingly small product of phonon interaction matrix elements or the fall off in the equilibrium distribution function. In view of the small contribution of phonon scattering in comparison with the EHDs, the most likely result of a calculation taking this inelasticity into account would seem to be a slight broadening of the peak in the Fourier power spectrum; this awaits a more careful study.

Self consistency of the transport theory

For our calculation of the conductivity to be valid, the conditions necessary for the use of our scattering and transport approximations must be fulfilled. In particular, we must check that the conditions for use of the Born approximation are satisfied and secondly that collision broadening effects will be small.

A measure of the importance of collision broadening is the value of $\omega_c\tau$ at the top of a sub-zone (see Kubo et al, 1965); for the effect to be negligible this must be much larger than 1. The factor determining the validity of the Born approximation is the ratio of the electron

wavelengths inside and outside the potential ($k_N/K_{NN}$ in the notation of §3); this must approach 1. A condition which will be sufficient in our case is that $V/\hbar\omega_c$ should be small.

For the parameters of our problem, and measuring B in tesla and V in meV, the value of $\omega_c\tau$ at the top of zone 0 is $2.27\times10^5 B^{5/2}/V^2$, and of $V/\hbar\omega_c$ is V/B. Substituting in the values V = 4meV and B = 0.04T used experimentally, we obtain $\omega_c\tau = 4.54$ and $V/\hbar\omega_c = 100$. Both of the above conditions are therefore clearly violated!

Faced with this difficulty, there appear to be two courses of action open to us. Firstly, we may attempt to improve on the two deficient aspects of our calculation, by treating the scattering more exactly with the methods §3, and by performing a collision broadened transport calculation. This is unlikely to give results in agreement with the experimental work, however, as may be readily shown. The effect of using exact scattering matrix elements in place of the Born approximation may be seen by comparison with the analagous problem of one dimensional scattering by a square well potential. The scattering matrix elements for reflection have been plotted in Fig. 5.23; it is seen that for energies less than the depth of potential the oscillations of the reflection coefficient are very irregular. If this irregularity carries over into the 3D problem the relaxation times would no longer have the regular oscillatory structure necessary to produce the periodicity in the magnetoconductivity.

The effect of collision broadening, so long as it is not too large, is to smooth off the sharp peaks in the overall sawtooth structure of the relaxation time spectrum, as may be seen in the work of Kubo et al (1965). The appearance of oscillations in the magnetoconductivity, however, depends on a sharp cut off at the top of each Landau sub-zone; the effect of any

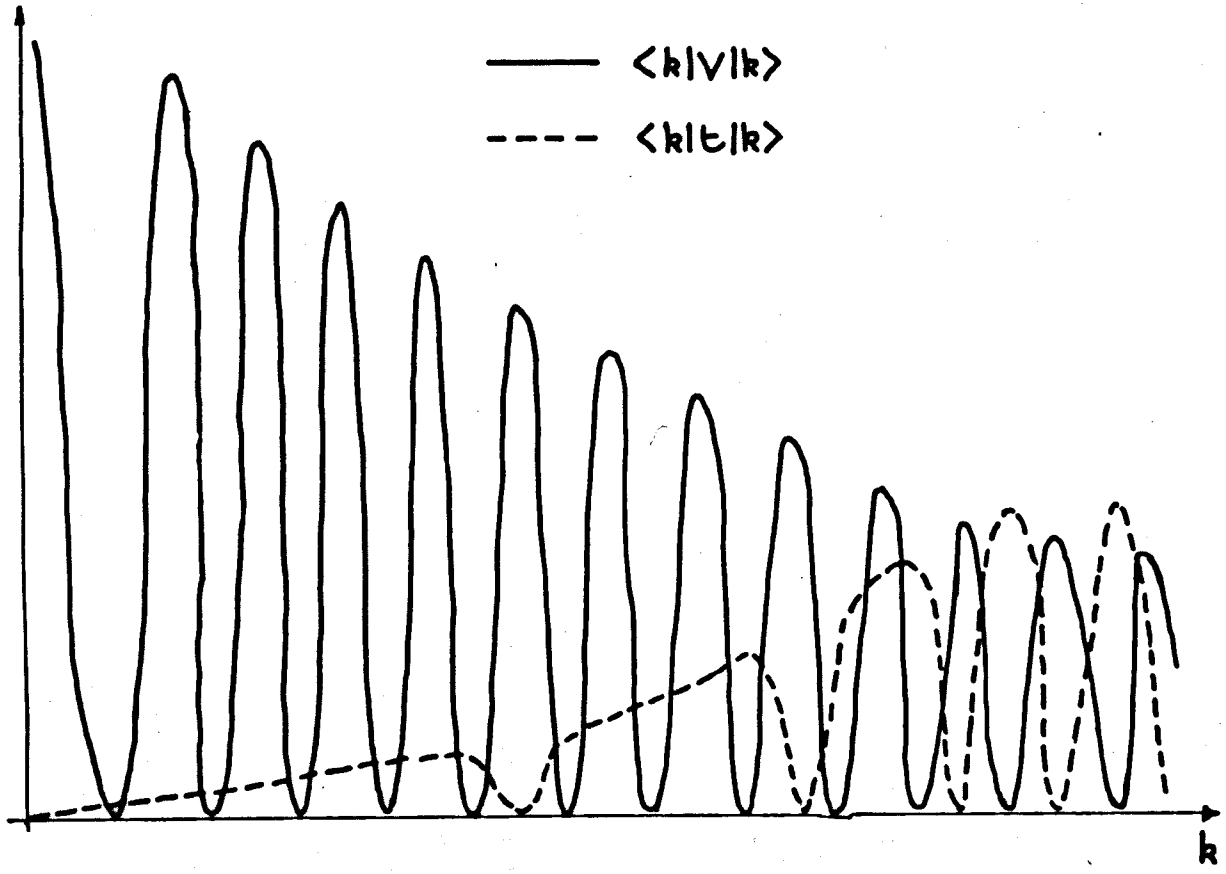


Fig. 5.23 Schematic comparison of the t matrix and Born approximation elements for reflection in one dimensional scattering from a square well. Curves not to same scale

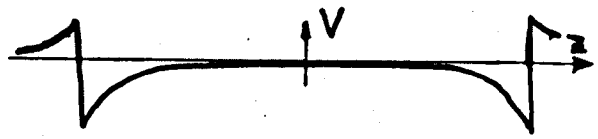


Fig. 5.24 Possible form of the effective scattering potential of an EHD seen by an incident electron

smoothing would be to drastically reduce the magnitude of the oscillation, again in disagreement with the experimental observations.

The second method of approach is to look for reasons for altering the parameter V to a much smaller value which would satisfy the conditions for approximation. We find one immediately in the remarks made previously about electron capture, and the observations of large electric charges on EHDs. These tally with the fact that a potential of size 1 μm and depth 4meV should have a very large number of bound states. In one dimension a square well has approximately $2/\pi(m_z Va^2/2\hbar^2)^{\frac{1}{2}}$ bound states (see, e.g., Schiff 1968), which gives about 150 for the above parameters. In 3D we would expect the number to be much larger. If a large number of these states are occupied by electrons the potential would no longer be a square well, but would be filled in to some degree in the middle, and have a Coulomb shape outside the radius of the EHD. The exact potential shape would have to be calculated by a self consistent, Hartree type, method. Starting from a sharp, deep square well, however, one would expect a sharp and quite deep step to remain at the original position of the potential edge, the result being a hollow shell potential of the sort shown in Fig. 5.24. This is a much weaker potential than the original, giving more favourable conditions for the Born approximation and small collision broadening, while retaining the oscillatory structure of the Fourier transform which is the source of the magnetoresonance. The infinite Coulomb tail could cause difficulties in calculation, and clearly screening effects would have to be considered; the phonon part of the scattering would also be much more important than before.

We would expect, however, that while the steady part of the magnetoconductivity would be greatly changed, the structure of the oscillatory

components would be qualitatively unaltered.

## Conclusions

In summary, our magnetoconductivity calculation has provided strong evidence in favour of the original explanation by Eaves et al (1976) of the magnetoresonance phenomenon observed by them. We have shown that a more detailed transport calculation than they performed does indeed give rise to an oscillation with the same striking $B^{\frac{1}{2}}$ periodicity as was observed. We have also proved the usefulness of the relaxation matrix formalism in this context, without which a relaxation time description of the transport is not feasible. It has been shown that the introduction of a matrix inversion need not necessarily complicate the analysis unduly; the simplifying features present here would apply also for certain other types of scattering.

From the experimental point of view the usefulness of this resonance phenomenon is that it can provide a potentially very accurate measurement of the EHD radius. More indirectly, it is also evidence of a very narrow distribution of droplet radii, and for the action of the EHDs as scatterers in the manner described. Some unexplained features remain, however, and it seems to us that further experimental investigation is required. The two most important points are the lack of higher frequency resonances of the type we have predicted theoretically, and the question of the hole contributions to the conductivity. Further experiments should, if possible, be conducted at lower temperatures in order to remove the unwanted phonon scattering, and should be designed with an ultimate Fourier transform in $B^{\frac{1}{2}}$ in mind. Higher field work is not required, however, as we have shown this would make the oscillations undetectable.

Our theoretical work on this system could be extended in several areas. There would be no fundamental difficulty in carrying the present calculation to lower magnetic fields, in which case a direct comparison with experimental work would be possible. We have also shown that the effect of a hollow shell potential for the EHDs should be investigated, though a more careful study of the EHDs themselves would first be needed. Unfortunately this system does not seem to readily lend itself to a more exact analysis of the scattering by the methods of §3. The basic difficulty is the very large size of the potential, which means that a very large number of different angular momentum values contribute to each t matrix element. This problem would be less severe with a hollow shell potential, however, and further investigation along these lines might also prove fruitful.

# CHAPTER 6

## Summary

Our aim in the work described in this thesis has been to develop a sound and general basis for the calculation of longitudinal magnetoconductivities in the high field quantum regime. We have extended earlier work in this field by a more careful treatment of potential scattering in a magnetic field, applicable in principle to potentials of arbitrary size and shape. We have also developed a more general solution of the Boltzmann equation which enables any elastic scattering mechanism to be treated exactly, even when more than one Landau level is occupied. Finally, we have applied the above theoretical methods to a detailed study of the electron-hole-drop size magnetoresonance in germanium, enabling a more detailed interpretation of experimental data than hitherto.

The theory of potential scattering in a magnetic field has been treated in detail in §3. A particular separation of the Schrödinger equation has been chosen which leads to a quasi one-dimensional picture of the scattering, in which one dimensional equations for scattering in a finite number of channels are coupled by potentials which are radial transforms of the original three-dimensional potential. The picture thus obtained is physically appealing and readily interpretable in terms of a semi-classical picture of the scattering process.

General properties of particle conservation and time reversal symmetry have been shown to apply to our scattering equations, an elegant proof being made possible by a simple extension of the Wronskian theorem for the true one dimensional problem. We have also shown that resonant bound states of the potential below the bottom of many Landau sub-bands are a general feature of the theory. These seem to us to be of particular interest, as

they should be present for almost all scattering potentials. It is not at present clear, however, whether these resonant states can manifest their presence in any directly observable manner.

We have developed Green's Function methods for the solution of the scattering equations for general potentials, which reproduce the Born series for weak scattering, and which can also be resummed in order to give convergence when dealing with a strong potential. These methods have been applied to scattering potentials in the form of cylindrical square wells; to our knowledge the first time that any extended potential has been treated beyond the Born approximation in a magnetic field. As well as obtaining scattering matrix elements for the potential, we have also found the explicit analytical form of a typical resonant 'bound' state wave function, and given a simple physical explanation of the nature of its decay. Scattering by $\delta$-function potentials has also been briefly treated, obtaining results in general agreement with previous work, although certain modifications are introduced.

We would like now to extend this work to cover scattering by more realistic extended potentials, in particular ionised impurities. These will clearly be difficult to deal with analytically, but it is to be hoped that a numerical evaluation of the resummed Green's Functions would not be prohibitively difficult. Unfortunately, however, the electron-hole-droplet scattering potentials used in our later transport calculation appear to be very difficult to treat beyond the Born approximation because of their extremely large size. On a lighter note, it is our ambition to animate a scattering wave packet on a computer VDU; the results should be visually very appealing!

The transport theory developed in §4 is directed specifically towards the calculation of longitudinal magnetoconductivities from a Boltzmann equation. Starting from the Kubo formula and using the resolvent super operator method of analysis for its conciseness and elegance, the Boltzmann equation with transition rates in the Born approximation has been derived. Existing resolvent theory has also been extended to higher order in the scattering, enabling a Boltzmann equation with t-matrix scattering rates to be derived, and therefore enabling the preceding scattering theory to be used in transport calculations.

Having obtained a Boltzmann transport equation, we have described a general method of solution, applicable to any elastic scattering mechanism even when several Landau bands are occupied. We have shown that in general it is impossible to define a single relaxation time for scattering at a particular energy (as is often assumed), but that a solution in terms of a finite small number of such times is always possible, their number being given by the number of occupied Landau sub-bands at the energy in question. The times are obtained from a finite number of simultaneous equations, solved by inverting a 'relaxation matrix'. By an analysis of the time dependent relaxive decay of perturbations to the electron distribution function we have shown that the new parameters are not in fact the true relaxation times of the system, but their relationship to these has been shown. We have also been able to give a general proof of the positive definiteness of the true decay constants of the system and also of the conductivity; it is interesting that the new 'relaxation times' appearing in the conductivity need not be positive definite, though they usually will be. In addition to the exact formalism we have discussed a number of situations in which a simple inversion of the relaxation matrix is possible; these are the only cases which were previously soluble. We have also shown how the new formalism goes over to the zero magnetic field solution in the limit of low magnetic field; an interesting and non-trivial

exercise.

There is now much scope for the application of the above relaxation matrix theory to other elastic scattering mechanisms, of which the most important would appear to be the ionised impurity. This problem is complicated, however, by the need to determine the form of the screening of the Coulomb potential in a magnetic field before scattering matrix elements can be worked out. This is an unsolved problem as yet, though an approach on the lines of the scattering theory of §3 may be feasible. The time dependent relaxive decay is also an area which would repay further investigation, especially in experimental work. It would be extremely interesting to see if a time resolution of the response to a pulsed electric field can reveal the multiple decay constant nature of the relaxation process.

Finally, we have devoted §5 to a detailed investigation of a problem of particular interest and importance, the electron-hole-drop magnetoresonance in germanium. This phenomenon is useful, both as a measure of the droplet radius, and also as a probe of the scattering interaction between the drops and free electrons. We have shown the necessity of using the relaxation matrix technique in this problem, and have been able to obtain good analytical approximations to the solution in spite of its apparent complexity. The results of our analysis have verified the original interpretation of the observed magnetoresistance oscillation, and we have also shown how a more detailed Fourier analysis of the conductivity/magnetic field curve should reveal further structure related to the droplet radius. Certain difficulties remain with the self-consistency of the theory as applied to this particular problem, and we believe these indicate that the true scattering potential is less strong and deep than that which we have used as a model. We have indicated that the potential is more likely to

be in the form of a hollow shell, still with a sharp spherical step, but also possibly with a Coulomb tail. The logical next step from our present work is to carry out a calculation based on such a potential; the details of this would be complex and probably require numerical techniques, but the principles should be exactly as before. Another possible extension of the present calculation would be to incorporate the exact scattering theory of §3, though we have given reasons for our belief that a different model for the potential would render this unnecessary. Neither of these modifications will produce any startling qualitative changes in the predicted conductivity/field curve, however, and the calculation already performed provides a sound basis for the understanding of this particular phenomenon.

## APPENDIX 1

### The Transformation Coefficient

From (2.1.28) we have

$$I = \langle N,k_y,k_z|N',m,k_{z'}\rangle_{\text{Landau}} =$$

$$= \iiint_{\text{Box}} L^{-1}\phi_N(x+\ell^2k_y)e^{-ik_yy}e^{-ik_zz}e^{i(-xy+xY-Xy)} \times$$

$$\times (2\pi L)^{-\frac{1}{2}}\phi^m_{N'}(\rho)e^{-im\phi}e^{ik_{z'}(z-Z)}dxdydz \qquad (A.1.1)$$

where $\rho = ((x-X)^2 + (y-Y)^2)^{\frac{1}{2}}$, $\rho\cos\phi = (x-X)$, $\rho\sin\phi = (y-Y)$. Assuming $m > 0$, and defining $q_y = (x-X)/\ell^2$, $q_x = (y-Y)/\ell^2$, $q_\perp^2 = q_x^2+q_y^2$, we have

$$\phi^m_{N'}(\rho) = (-1)^M G_{N'M}(q_x,q_y,0,0) \qquad (A.1.2)$$

where $M = N'+m$ and $G_{NM}$ is defined in (2.1.25). From (2.1.24) this is equivalent to

$$\phi^m_{N'}(\rho) = (-1)^m e^{i\ell^2q_x.q_y/2}\int_{-\infty}^{\infty}\phi_{N'}(x'+\ell^2q_y)e^{iq_xx'}\phi_M(x')dx'$$

$$= (-1)^m e^{i(x-X)(y-Y)/2\ell^2}\int_{-\infty}^{2\infty}\phi_{N'}(x'+x-X)e^{ix'(y-Y)/\ell^2}\phi_{N'+M}(x')dx' \qquad (A.1.3)$$

Substituting this into the integral of (A.1.1), the terms in y may be collected together and integrated

$$\int_{-L/2}^{L/2} dy\ e^{i(-\ell^2k_y-X+x')y/\ell^2} = 2\ell^2\sin(x'-X-\ell^2k_y)L/2\ell^2.(x'-X-\ell^2k_y)^{-1} \qquad (A.1.4)$$

When the limit $L\to\infty$ is taken we may replace this part of the integral (A.1.1) by the $\delta$ function $2\pi\ell^2\delta(x'-X-\ell^2k_y)$. We may now perform the x' and z integrals in (A.1.1), leaving

$$I = \delta_{k_z k_{z'}} e^{-ik'_z Z} \int_{-\frac{L}{2}}^{\frac{L}{2}} dx \phi_N(x+\ell^2 k_y)\phi_{N'}(x+\ell^2 k_y) \times$$

$$\times e^{-iXY/2\ell^2} e^{-ik_y Y}(-1)^m(2\pi\ell^2/L)^{\frac{1}{2}}\phi_{N'+M}(X+\ell^2 k_y) \qquad (A.1.5)$$

Then the orthonormality property (2.1.16) of the $\phi$'s gives our final result

$$I = \delta_{NN'}\delta_{k_z k_{z'}} e^{-i(k_y Y+k_z Z+XY/2\ell^2)}(-1)^m(2\pi\ell^2/L)^{\frac{1}{2}}\phi_{N+M}(X+\ell^2 k_y) \qquad (A.1.6)$$

A similar calculation for $m < o$ shows that (A.1.6) is valid in this case also.

## APPENDIX 2

### The Wronskian Theorem

We here develop the equivalent of the Wronskian theorem (see Messiah, 1964) for the infinite set of coupled equations (3.2.5). Let $\underline{f}_1$ and $\underline{f}_2$ be infinite dimensional vector functions of z. We define the Wronskian of $\underline{f}_1$ and $\underline{f}_2$ to be

$$W(\underline{f}_1,\underline{f}_2;z) = \underline{f}_1\cdot\underline{f}_2' - \underline{f}_1'\cdot\underline{f}_2 = \sum_{N=0}^{\infty}(f_{1N}f_{2N}' - f_{1N}'f_{2N}) \qquad (A2.1)$$

We shall assume throughout that $\underline{f}_1$ and $\underline{f}_2$ are well behaved functions of z and all infinite sums are convergent. Now let $\underline{f}_1$ and $\underline{f}_2$ obey the infinite set of coupled differential equations on $(-\infty,\infty)$

$$\begin{aligned} &\underline{f}_1'' + \underline{E}_1\cdot\underline{f}_1 = 0 \quad \text{or} \quad f_{1N}'' + \sum_{M=0}^{\infty}F_{1NM}f_{1M} = 0 \\ &\underline{f}_2'' + \underline{E}_2\cdot\underline{f}_2 = 0 \quad \text{or} \quad f_{2N}'' + \sum_{M=0}^{\infty}F_{2NM}f_{2M} = 0 \end{aligned} \qquad (A2.2)$$

where the matrices $\underline{E}_1(z)$ and $\underline{E}_2(z)$ are both real and symmetric. Then the rate of change of the Wronskian is

$$W'(\underline{f}_1,\underline{f}_2) = \underline{f}_1\cdot\underline{f}_2'' - \underline{f}_1''\cdot\underline{f}_2 = \underline{f}_1\cdot(\underline{E}_1-\underline{E}_2)\cdot\underline{f}_2 \qquad (A2.3)$$

In particular, if $\underline{E}_1 = \underline{E}_2$ then $W(\underline{f}_1,\underline{f}_2)$ is a constant. Note also that this result is independent of any boundary conditions imposed on $\underline{f}_1$ and $\underline{f}_2$.

We now note that the Schrödinger equation (3.2.5) is a member of the class (A2.2), and hence the Wronskian theorem (A2.3) applies to its solutions. Let $\underline{f}_1$ be the solution of (3.2.5) given asymptotically by

eqns. (3.2.8), and Let $\underline{f}_2 = \underline{f}_1^*$, which also satisfies (3.2.5) since $\underline{\underline{E}}$ is real.

$$W(\underline{f}_N, \underline{f}_N^*; -\infty) = 2iL^{-1}\{\sum_{OC} k_M |R_{MN}|^2 - k_N\} \tag{A2.4}$$

$$W(\underline{f}_N, \underline{f}_N^*; +\infty) = -2iL^{-1} \sum_{OC} k_M |T_{MN}|^2$$

By (A2.3) these are equal, so that we have the number conservation result

$$\sum_{OC} k_M (|R_{MN}|^2 + |T_{MN}|^2) = k_N \tag{A2.5}$$

To prove time reversal symmetry for the R's (i.e. for collisions in which the sign of $k_z$ is changed) $\underline{f}_1$ is as before and $\underline{f}_2$ is given asymptotically by eqns. (3.2.8) with N changed to N!

$$W(\underline{f}_N, \underline{f}_{N'}; -\infty) = -2iL^{-1}(k_N R_{NN'}, -k_{N'} R_{N'N})$$

$$W(\underline{f}_N, \underline{f}_{N'}; +\infty) = 0 \tag{A2.6}$$

We therefore have from (A2.3)

$$k_N R_{NN'} = k_{N'} R_{N'N} \tag{A2.7}$$

which is equivalent to time reversal symmetry of the t matrix elements, using (3.2.12).

To prove this symmetry for the T's $\underline{f}_2$ is taken to be the function $\underline{f}_{N'-}$ with asymptotic behaviour at $\infty$

$$f_{NN'-} \to \begin{matrix} z = -\infty: \; L^{-\frac{1}{2}} T_{NN'-} e^{-ik_N z} \\ z = +\infty: \; L^{-\frac{1}{2}} R_{NN'-} e^{+ik_N z} + \delta_{NN'} L^{-\frac{1}{2}} e^{-ik_N z} \end{matrix} \quad (OC's) \tag{A2.8}$$

with obvious behaviour for the CC's. The Wronskian is then

$$W(\underline{f}_N, \underline{f}_{N'-}; -\infty) = -2iL^{-1}k_N T_{NN'-}$$

$$W(\underline{f}_N, \underline{f}_{N'-}; +\infty) = -2iL^{-1}k_{N'} T_{N'N} \qquad \text{(A2.9)}$$

The Wronskian theorem then gives

$$k_N T_{NN'-} = k_{N'} T_{N'N} \qquad \text{(A2.10)}$$

which is the required time-reversal symmetry.

Finally, although the inversion symmetry (3.2.19) is obvious if $V(\rho,z) = V(\rho,-z)$, we may prove it formally by the above methods. Let $\underline{f}_1$ be $\underline{f}_N$ as before, and $\underline{f}_2$ be $\underline{f}_{N-}$ defined by (A2.8) above. Then it is easily shown that $\underline{f}_3$ defined by $\underline{f}_3(z) = \underline{f}_2(-z)$ satisfies the equation

$$\underline{f}_3'' + \underline{E}_3 \cdot \underline{f}_3 = 0 \qquad \text{(A2.11)}$$

where $\underline{E}_3(z) = \underline{E}_1(-z)$. But now if $V(\rho,z) = V(\rho,-z)$, then $\underline{E}_3 = \underline{E}_1$, and so the Wronskian of $\underline{f}_1$ and $\underline{f}_3$ must be constant on $(-\infty,\infty)$. At $+\infty$ the Wronskian is zero, and so it must be zero everywhere, in which case it is easy to show that $\underline{f}_1 = \underline{f}_3$. We therefore have

$$T_{MN-} = T_{MN}$$

$$R_{MN-} = R_{MN} \qquad \text{(A2.12)}$$

which is the inversion property required.

## APPENDIX 3

### The Low Field Limit of the Relaxation Time

The first requirement is to obtain the low field limit of the Landau states. Since, for given values of $\varepsilon$ and $k_z$, N diverges as the field drops to zero, the orbital part of the energy is better described by the new variable $\varepsilon_\perp$, given by

$$\varepsilon_\perp = (N+\tfrac{1}{2})\hbar\omega_c = \varepsilon - \hbar^2 k_z^2/2m_e \qquad (A3.1)$$

Only the x part of the Landau state is not of plane wave form, but in the limit of low field this may be obtained from the WKB approximation so that

$$|\lambda\rangle = |\varepsilon_\perp k_y k_z\rangle = (\sqrt{2}/L\ell\sqrt{\pi})e^{ik_z z}e^{ik_y y}\cos(k_x(x)x+\phi(x))/(k_x(x))^{\frac{1}{2}} \qquad (A3.2)$$

where

$$k_x(x) = (2m\varepsilon_\perp/\hbar^2-(x/\ell^2+k_y)^2)^{\frac{1}{2}} \qquad (A3.3)$$

This applies so long as $k_x(x)$ is real; outside this range of x the wave function vanishes. The x part of $|\lambda\rangle$ is thus a simple harmonic oscillator wave function with a very large value of N, as illustrated in Fig. A3.1. $\phi(x)$ is a phase correction factor which varies slowly with x, and which will henceforth be ignored.

The scattering out term of the Boltzmann equation involves evaluating

$$\sum_{\lambda'} |\langle\lambda|V_i|\lambda'\rangle|^2 \gtrsim \delta(\varepsilon_\lambda-\varepsilon_{\lambda'}) \qquad (A3.4)$$

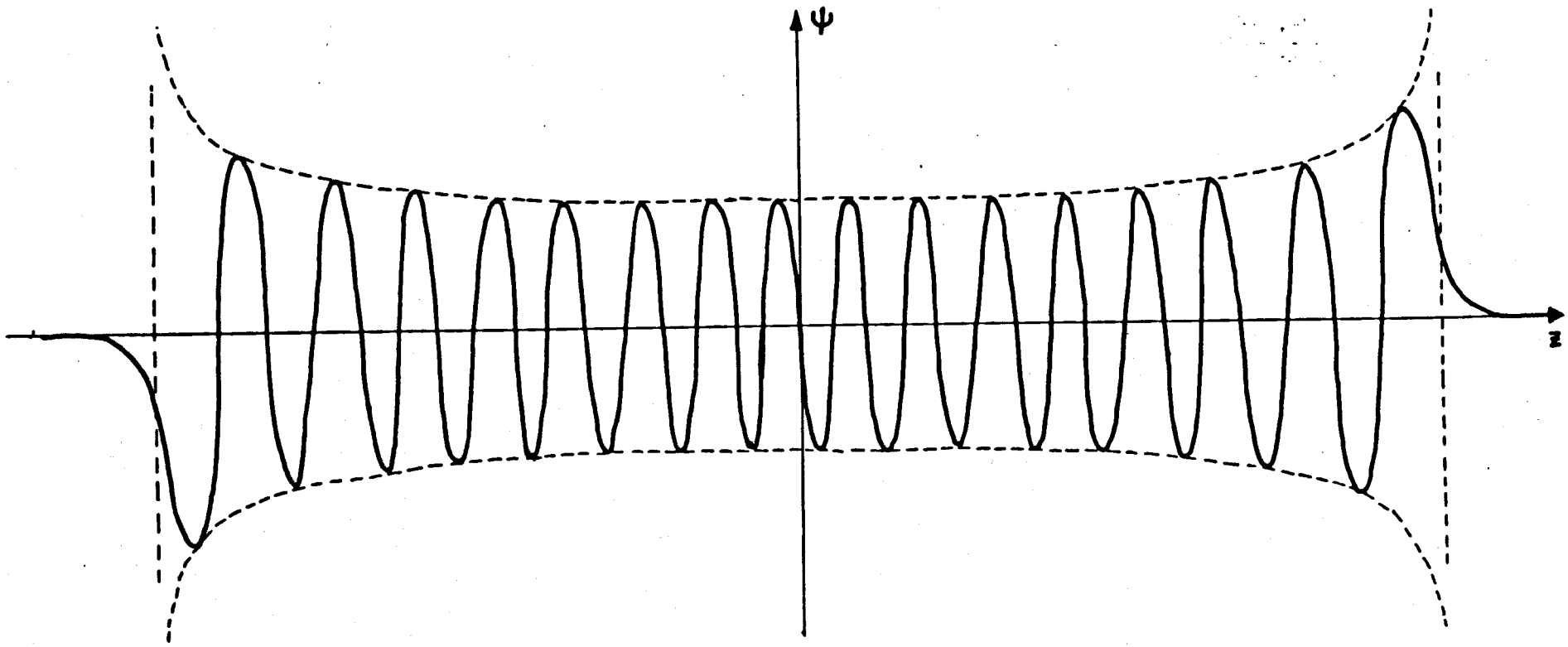


Fig. A 3.1 A simple harmonic oscillator wave function for large N (31)

where the $\langle\rangle_s$ bracket denotes summation and averaging over scatterer position $\underline{R} = (X,Y,Z)$. It is easily shown that

$$\langle\lambda|V_i|\lambda'\rangle = (2\pi L^2 \ell^2 \sqrt{k_x}\sqrt{k_{x'}})^{-1} e^{iz(k_{z'}-k_z)} e^{iY(k_{y'}-k_y)} \times$$

$$\times \{e^{iX(k_{x'}-k_x)}\tilde{V}(\underline{k}_1) + e^{iX(k_{x'}+k_x)}\tilde{V}(\underline{k}_2)\} \qquad \text{(A3.5)}$$

$$+ \text{complex conjugate}$$

where $\underline{k}_1 = (k_{x'}-k_x,\ k_{y'}-k_y,\ k_{z'}-k_z)$ and $\underline{k}_2 = (k_{x'}+k_x,\ k_{y'}-k_y, k_{z'}-k_z)$, and $\tilde{V}(\underline{q})$ is the spatial Fourier transform of the scattering potential, which we shall assume to be spherically symmetric. We have assumed that $k_x$ and $k_{x'}$ are effectively constant over the extent of the potential, so that $k_x$ equals its value at the centre of the potential:

$$k_x = (2m_e\varepsilon_\perp/\hbar^2 - (X/\ell^2+k_y)^2)^{\frac{1}{2}} \qquad \text{(A3.6)}$$

and similarly for $k_{x'}$.

On forming $|\langle\lambda|V|\lambda'\rangle|^2$ we obtain 16 terms, four of which are independent of X. It is not difficult to show that these are the only terms which contribute when the averaging over X is performed. The others all contain factors of the form $e^{ik(X)X}$ where, as may be seen in (A3.6), $k(X)$ varies very slowly with X as $\ell^2$ becomes large; hence the oscillatory nature of the factor means that its integral with any slowly varying function of $k(X)$ goes to zero in the limit $\ell^2 \to \infty$. The terms which are left therefore sum to

$$|\langle\lambda|V|\lambda'\rangle|^2 = (2\pi^2 L^4 \ell^4 k_x k_{x'})^{-1}\{|\tilde{V}(\underline{k}_1)|^2 + |\tilde{V}(\underline{k}_2)|^2\} \qquad \text{(A3.7)}$$

which is to be summed over $|\lambda'\rangle$ and averaged over R.

The Y and Z averages are trivial. The X average is restricted by $-k_y-k_\perp \leqslant X/\ell^2 \leqslant -k_y+k_\perp$ where $k_\perp$ is defined as $(2m\varepsilon_\perp/\hbar^2)^{\frac{1}{2}}$; this is so that $k_x$ as defined by (A3.6) is real, and hence the non-zero part of the wave function is being used. For similar reasons $k_{y'}$ is restricted by $-k_{y'}-k'_\perp \leqslant X/\ell^2 \leqslant -k_{y'}+k'_\perp$. It is therefore permissible to use the two changes of variable defined by:

$$k_{y'} = k'_\perp \sin\phi - X/\ell^2 \qquad\qquad X/\ell^2 = k_\perp \sin\theta - k_y$$

We then have

$$\langle |\langle\lambda|V|\lambda'\rangle|^2 \rangle_s = \int (\hbar\omega_c)^{-1} d\varepsilon \int (L/2\pi)\, dk_z\, n_s/L\ell^2 8\pi^3 \int_{-\pi/2}^{\pi/2} d\theta \int_{-\pi/2}^{\pi/2} d\phi \{ |\tilde{V}(\underline{k}_1)|^2 + |\tilde{V}(\underline{k}_2)|^2 \} \tag{A3.8}$$

where $\underline{k}_1 = (k'_\perp \cos\phi - k_\perp \cos\theta,\ k'_\perp \sin\phi - k_\perp \sin\theta,\ k_{z'} - k_z)$ and similarly for $\underline{k}_2$. The factors $1/k_x$, $1/k_{x'}$ appearing in the WKB approximation have therefore corrected for our integrating linearly in $k_y$, instead of around the circle $k_x^2 + k_y^2 = k_\perp^2$, as would have been natural in the absence of the field.

It is easily seen that the two $\tilde{V}$ terms may be combined by extending the $\phi$ integration to the range $(-\pi,\pi)$; then, however, the $\phi$ integration is clearly independent of $\theta$. The $\theta$ integral may therefore be performed, to give,

$$\langle |\langle\lambda|V|\lambda'\rangle|^2 \rangle_s = (n_s/8\pi^3) \int (\hbar^2/m_e)\, d\varepsilon_\perp \int dk_z \int_{-\pi}^{\pi} d\phi\, |\tilde{V}(\underline{k}_1)|^2 \tag{A3.9}$$

We note that, since $\underline{k}_1$ may be written $\underline{k}'-\underline{k}$, $\tilde{V}(\underline{k}_1) = \tilde{V}(\underline{k}'-\underline{k}) = \langle \underline{k}|V|\underline{k}'\rangle$

The expression (A3.9) therefore shows explicitly how the summation over Landau states in (A3.4) goes over to an integral over all space (in

cylindrical polars) of matrix elements between plane wave states $|\underline{k}>$. The scattering in terms may be treated similarly on assuming that $\tau(\varepsilon_\perp,\varepsilon)$ is independent of $\varepsilon_\perp$. The extra $k_{z'}/k_z$ factor in this case gives rise to the $\cos\theta$ part of the familiar formula (4.6.16), after the further substitution $\varepsilon'_\perp = \varepsilon\sin^2\theta$.

## APPENDIX 4

### Matrix Theory

We wish to find general properties of matrices $\{R\}$ which may be written in the form

$$\{R\} = \{\mathbb{D}(k^{-1})\}\{S\} \tag{A4.1}$$

where $\{\mathbb{D}(k^{-1})\}$ is the diagonal matrix with elements $\delta_{NN'}k_N^{-1}$ and $\{S\}$ is real, symmetric and positive definite. The properties of the eigenvalues and eigenvectors are particularly important; the eigenvalue equation for $\{R\}$ is

$$\sum_M R_{NM} f_M^i = \omega^i f_N^i \tag{A4.2}$$

which, by (A4.1) is equivalent to

$$\sum_M S_{NM} f_M^i = \omega^i k_N f_N^i \tag{A4.3}$$

and, by the symmetry of $\{S\}$, also to

$$\sum_N f_N^j S_{NM} = \omega^j k_M f_M^j \tag{A4.4}$$

We therefore have

$$\sum_{N,M} f_N^j S_{NM} f_M^i = \omega^i \sum_N k_N f_N^j f_N^i = \omega^j \sum_M k_M f_M^j f_M^i$$

from which we may deduce that either $\omega^i = \omega^j$ or that the eigenvectors $f^i$, $f^j$, are orthogonal in the sense that $\sum_N k_N f_N^j f_N^i = 0$. A similar argument shows that the $\omega^i$ are real. By taking appropriate linear combinations we may arrange that the eigenvectors form an orthonormal set, such that

$$\sum_N k_N f_N^j f_N^i = \delta_{ij} \qquad \text{(A4.5)}$$

Now, any vector may be expressed in terms of the eigenvectors $f^i$, using the transform pair:

$$a_N = \sum_i a^i f_N^i k_N \qquad a^j = \sum_N a_N f_N^j \qquad \text{(A4.6)}$$

In particular

$$R_{NM} = \sum_i R_N^i f_M^i k_M \qquad R_N^j = \sum_M R_{NM} f_M^j = \omega^j f_M^j \qquad \text{(A4.7)}$$

Thus

$$R_{NM} = \sum_i \omega^i f_N^i f_M^i k_M \qquad \text{(A4.8)}$$

This is known as the spectral representation of $\{R\}$ (see Bickley & Thompson, 1964), in which all the elements are expressed in terms of the eigenvalues and eigenvectors. Since $\{R\}$ is not symmetric, the additional factor k is introduced.

The spectral representation is extremely useful for calculating powers of $\{R\}$, for it follows from the orthonormality property of the eigenvectors that any integral power is given by

$$\{R^n\}_{NM} = \sum_i (\omega^i)^n f_N^i f_M^i k_M \qquad \text{(A4.9)}$$

immediately in its own spectral representation. Of particular interest is the inverse:

$$\{R^{-1}\}_{NM} = \sum_i (\omega^i)^{-1} f_N^i f_M^i k_M \qquad \text{(A4.10)}$$

We may also use this representation to show that all the $\omega^i$ are

positive definite. We note that the spectral representation of {S} is

$$S_{NM} = \sum_i \omega^i k_N f_N^i f_M^i k_M \qquad \text{(A4.11)}$$

Pre and post-multiplying by the arbitary vector a of (A4.6), we have

$$\sum_{N,M} a_N S_{NM} a_M = \sum_i \omega^i (a^i)^2 \qquad \text{(A4.12)}$$

Since {S} is positive definite, the RHS of (A4.12) must be positive definite for all non zero vectors a. This is only possible if all the $\omega^i$ are positive definite.

## APPENDIX 5

### The Approximation of $J^*_{NM}$

From (5.4.13) and (5.4.21) we have

$$J^*_{NM} = (2\pi)^{-1}\iint dQ_x dQ_y Q^{-4} F_{NM}\{(\ell^*/\ell)^2 Q_x^2/2 + (\ell/\ell^*)^2(Q_y-\alpha Q_z)^2/2\} \quad (A5.1)$$

Since $F_{NM}$ is the more complex function of its argument, we change variables to $P_x = (\ell^*/\ell)Q_x$, $P_y = (\ell/\ell^*)(Q_y-Q_z)$, so that the integral becomes

$$J^*_{NM} = (2\pi)^{-1}\iint dP_x dP_y Q^{-4} F_{NM}(\tfrac{1}{2}(P_x^2+P_y^2)) \quad (A5.2)$$

where $Q = \{(\ell/\ell^*)^2 P_x^2 + (\ell P_y/\ell^*+\alpha Q_z)^2+Q_z^2\}^{\frac{1}{2}}$. We now expand $Q^{-4}$ in a double Taylor series about $P_x = 0$, $P_y = 0$; at which point $Q = Q_z(1+\alpha^2)^{\frac{1}{2}} \equiv Q_i$:

$$Q^{-4} = Q_i^{-4}\{1+Q_i^{-2}\{\ell/\ell^*)^2 P_x^2+(\ell^*/\ell)^2 P_y^2+2(\ell^*/\ell)P_y\alpha Q_z\}\}^{-2}$$

$$= Q_i^{-4}\{1-2Q_i^{-2}\{\ \ \} + 3Q_i^{-4}\{\ \ \}^2 - \ldots .\}$$

We are here assuming that $Q_z$ is large enough that this expansion converges throughout the region for which $F_{NM}$ is largest; this assumption breaks down as $Q_z$ approaches zero. Taking only terms up to degree two in $P_x$ and $P_y$, we have

$$Q^{-4} \approx Q_i^{-4} - Q_i^{-6}.4(\ell^*/\ell)\alpha Q_z P_y - Q_i^{-6}\{2(\ell/\ell^*)^2 P_x^2 + 2(\ell^*/\ell)^2 P_y^2$$

$$- 12Q_i^{-2}(\ell^*/\ell)^2\alpha^2 Q_z^2 P_y^2\} \quad (A5.3)$$

Defining the integrals:

$$I^{o}_{NM} = \iint dP_x dP_y F_{NM}(\tfrac{1}{2}(P_x^2+P_y^2))$$

$$I^{y}_{NM} = \iint dP_x dP_y P_y F_{NM}(\tfrac{1}{2}(P_x^2+P_y^2)) = 0 \qquad \text{(A5.4)}$$

$$I^{xx}_{NM} = \iint dP_x dP_y P_x^2 F_{NM}(\tfrac{1}{2}(P_x^2+P_y^2)) = \iint dP_x dP_y P_y^2 F_{NM}(\tfrac{1}{2}(P_x^2+P_y^2))$$

we have

$$J^{*}_{NM} \approx (1+\alpha^2)^{-2} I^{o}_{NM} Q_z^{-4} + (1+\alpha^2)^{-3}\{12(\ell^*/\ell)^2\alpha^2/(1+\alpha^2) - 2(\ell/\ell^*)^2 - 2(\ell^*/\ell)^2\} I^{xx}_{NM} Q_z^{-6}$$

(A5.5)

Changing variables in the integrals to $P_r$ and $\theta$ given by $P_x = P_r\cos\theta$, $P_y = P_r\sin\theta$, and then defining $u = P_r^2/2$, we have

$$I^{o}_{NM} = 2\pi \int_0^\infty F_{NM}(u)\, du$$

(A5.6)

$$I^{xx}_{NM} = \int_0^{2\pi} 2\cos^2\theta d\theta \int_0^\infty u F_{NM}(u) d\theta = 2\pi \int_0^\infty u F_{NM}(u)\, du$$

Standard properties of associated Laguerre polynomials (see, e.g., Jackson, 1941) may be used to show that $I^{o}_{NM} = 2\pi$ and $I^{xx}_{NM} = 2\pi(N+M+1)$. We therefore have, after substituting in the Ge values of $\ell, \ell^*$ and $\alpha$ from §2.2,

$$J^{*}_{NM} \approx 0.162 Q_z^{-4} + 0.471(N+M+1) Q_z^{-6} \qquad \text{(A5.7)}$$

## APPENDIX 6

### The Inversion of Matrices of Small Row Sum

We shall give an approximate evaluation of the vector $\{X\}^{-1}\{1\}$ where $\{X\}$ is a PxP symmetric matrix whose row (and column) sums are small compared with the individual elements of $\{X\}$. We first note that the determinant of $\{X\}$ is unchanged if we replace the $N^{th}$ row with the sum of all the rows, and then the $M^{th}$ column with the sum of all the columns. This gives

$$||X|| = \begin{vmatrix} X_{11} & X_{12} \cdots \cdots \delta_1 \cdots \cdots X_{1P} \\ X_{21} & \cdots \quad \delta_2 \\ \vdots & \quad \vdots \\ \vdots & \quad \delta_{N-1} \\ \delta_1 & \delta_2 \cdots \quad \delta_{M-1} \; (\delta_1+\delta_2+\cdots\delta_p) \; \delta_{M+1} \cdots \delta_p \\ \vdots & \quad \delta_{N+1} \\ \vdots & \quad \vdots \\ X_{p1} & \quad \delta_p \quad\quad\quad X_{pp} \end{vmatrix} \qquad \text{(A6.1)}$$

To first order in $\delta$'s, therefore,

$$||X|| = (\delta_1+\delta_2+\cdots+\delta_p)Y_{NM} \;, \quad \text{any N, M} \qquad \text{(A6.2)}$$

where $Y_{NM}$ is the cofactor of $X_{NM}$. It is clear, therefore, that all the cofactors must be the same, to zeroth order in $\delta$'s. But we have

$$\{X\}^{-1}_{NM} = ||X||^{-1}.Y_{MN} = (\delta_1+\delta_2+\cdots+\delta_p)^{-1}Y^{-1}_{MN}Y_{MN} = (\delta_1+\cdots\delta_p)^{-1} \qquad \text{(A6.3)}$$

Therefore all the elements of $\{X\}^{-1}$ are the same, and

$$\{X\}^{-1}\{1\} = P(\delta_1 + \ldots\ldots + \delta_p)^{-1} \qquad \text{(A6.4)}$$

## APPENDIX 7

### Table of Constants and Parameter Values

1. Universal Constants

| | | |
|---|---|---|
| $\hbar$ | Planck's Constant | $1.05 \times 10^{-34}$ Js |
| $m_e$ | Electron Mass | $9.11 \times 10^{-31}$ Kg |
| e | Electron charge | $1.16 \times 10^{-19}$ C |
| k | Boltzmann's Constant | $1.38 \times 10^{-23}$ JK$^{-1}$ |

2. Physical Parameters of Germanium

| | | |
|---|---|---|
| $m_\ell$ | Longitudinal valley mass, conduction band | $1.59 \times m_e$ |
| $m_t$ | Transverse valley mass, conduction band | $0.082 \times m_e$ |
| $\rho$ | Density | 5,320 kg m$^{-3}$ |
| s | Velocity of sound | 5,490 ms$^{-1}$ |
| D | Deformation potential, conduction band | 11.4 eV |

3. Parameter values assumed in fitting experimental data

| | | |
|---|---|---|
| T | Temperature | $2^{o}$K |
| V | Depth of electron-hole-droplet potential | 4 meV |
| a | Electron-hole-droplet radius | 1.1 μm |
| $n^{EHD}$ | Number density of electron-hole-droplets | $10^{16}$ m$^{-3}$ |
| $n_e$ | Number density of free carriers | $10^{20}$ m$^{-3}$ |

## 4. Parameters used in computational analysis

| | | |
|---|---|---|
| $\ell$ | Landau length | $(\hbar/eB)^{\frac{1}{2}} = 0.0256.B^{-\frac{1}{2}}\mu m$ |
| $m_c$ | Cyclotron mass (B along {100}) | $0.135\ m_e$ |
| $m_z$ | Kinetic mass (B along {100}) | $0.581\ m_e$ |
| $\omega_c$ | Cyclotron frequency | $(eB/m_c) = 1.3 \times 10^{12}B\ s^{-1}$ |
| $\ell^*$ | Landau length in ellipsoidal valley (B along {100}) | $1.28\ \ell$ |
| $\alpha$ | Gradient of orbit-centre line (B along {100}) | 1.22 |
| Q,K | Dimensionless wave vectors | $Q,K = \ell q, \ell k$ |
| R | Droplet radius/Landau length | $a/\ell = 43B^{\frac{1}{2}}$ |
| $C^{ph}$ | Phonon constant | $\hbar s/\ell kT = 0.75B^{\frac{1}{2}}$ |
| $Q_o$ | Dimensionless momentum transfer for transition across the top of the first Landau sub-zone in Ge | $(8m_z/m_c)^{\frac{1}{2}} = 5.94$ |
| $t^{EHD}$ | Dimensionless EHD relaxation time | $\hbar^3/8\pi n^{EHD} a^2 \ell^3 m_z V^2 = 1.03 \times 10^{-12}B^{3/2}$ |
| $t^{ph}$ | Dimensionless phonon relaxation time | $2\pi\hbar^2\ell^2\rho s/1.58m_z D^2 = 4.72 \times 10^{-10}B^{-1}$ |
| $\beta$ | Dimensionless Landau band energy | $\hbar\omega_c/kT = 9.90B/T$ |
| $\Delta_{oo}$ | Period of fundamental oscillation, in $B^{\frac{1}{2}}$ | $(\pi/2a)(\hbar m_c/2em_z)^{\frac{1}{2}} = 0.01247\,T^{\frac{1}{2}}$ |

## APPENDIX 8

## Notation and Abbreviations

### Magnetic States and Quantum Numbers

| | |
|---|---|
| $\Omega, L$ | Quantization volume and side length |
| $N$ | Landau band number |
| $P(\varepsilon)$ | Highest Landau band number occupied at a given energy |
| $\underline{k}, k_y$ | Wave numbers of electron states |
| $k_N$ | Wave numbers in Landau band N at a given energy |
| $K_N, K_Z \equiv \ell k_N, \ell k_z$ | Dimensionless wave numbers. |
| $m$ | Angular momentum about z axis |
| $\phi_N$ | N'th harmonic oscillator wave function (2.1.14) |
| $H_N$ | N'th Hermite polynomial (2.1.15) |
| $\phi_N^m$ | Radial wave function in axisymmetric gauge (2.1.22) |
| $L_N^m$ | Associated Legendre polynomial (2.1.23) |
| $F_{NN'}$ | Matrix element of plane wave between Landau states (2.1.29) |

### Scattering Theory

| | |
|---|---|
| $\Psi^o$ | Free state full wave function |
| $\Psi^+$ | Scattering state full wave function |
| $f_N^m(z)$ | Longitudinal part of separated wave function |
| $V_{NM}^m(z)$ | Radial transform of scattering potential between free states (3.2.6) |
| $R_{NM}^m, T_{NM}^m$ | Reflection and transmission coefficients for scattering (3.2.8) |
| $G_N^{mo+}$ | Free propagator/causal Green's Function in Landau channel N |
| $G_N^{m+}$ | Full propagator/causal Green's Function in Landau channel N |

Transport Theory

| | |
|---|---|
| $\hat{\mathcal{H}}.\hat{A}$ | Liouville or commutator generating super operators for Hamiltonians (4.2.5) |
| $\hat{R} \equiv (\hat{H}-is)^{-1}$ | Resolvent super operator |
| is | Small positive imaginary part given to energy to ensure causality |
| $\hat{U}$ | Scattering part of Liouville operator |
| $\hat{\Sigma}(\hat{\Sigma}_{ss})$ | Self energy super operator (single-site) |
| $\rho(\rho^o)$ | Density matrix (equilibrium) |
| $f\ (f^o)$ | Electron distribution function (equilibrium) |
| $N_s(n_s)$ | Number of scatterers (density) |
| $P_{\lambda\lambda'}(\omega_{\lambda\lambda'})$ | Transition rates between states (without energy preserving δfunction) |
| $\{W_{NM}\}$ | Matrix of transition rates summed over $k_y$ (4.4.13) |
| $\{R(\varepsilon)\}$ | Relaxation matrix at a given energy (4.4.14 and 15) |
| $P(\varepsilon)$ | Highest Landau band number at a given energy |
| $\tau_N(\varepsilon)$ | 'Relaxation time' in Landau band N at a given energy (4.4.7 and 10) |

Germanium Magnetoconductivity Calculation

| | |
|---|---|
| $F^*_{NM}$ | Angular averaged value of $F_{NM}$ in germanium (5.4.13) |
| $J^*_{NM}(J^{*osc}_{NM})$ | Steady part of dimensionless integral for W (oscillating part) (5.4.21 and 22) |
| $T_N$ | Dimensionless relaxation time (5.4.34) |
| $Y_P$ | Dimensionless value of $K_N T_N$ (Approximately independent of N) (5.4.36) |

Abbreviations

| | |
|---|---|
| QL | Quantum Limit: significant occupation of only one Landau band |
| TL | Thermodynamic Limit: $\Omega \to \infty, N_s \to \infty, N_s/\Omega = n_s$, constant |
| OC | Open channel: Landau band in which free propagation is possible at given energy |
| CC | Closed channel: Landau band in which propagation is not possible at given energy |
| EHD | Electron-hole droplet: droplet of electron-hole 'liquid' |

Bibliography

ADAMS & HOLSTEIN 1959 J. Phys. Chem. Solids 10 254.

ADAMS & KEYES 1962 Progress in Semiconductors 6 85.

ALEKSEEV, BAGAEV, GALKINA, GOGOLIN, PENIN, SEMENOV & STOPACHINSKY 1970 Sov. Phys. JETP Lett. 12 140

ALTARELLI & LIPARI 1974 Phys. Rev. B 9 1733

ARGYRES & ADAMS 1956 Phys. Rev. 104 900

ARGYRES 1958 J. Phys. Chem. Solids 4 19

ARGYRES 1959 J. Phys. Chem. Solids 8 124

ARGYRES 1960 Phys. Rev. 132 1527

ASNIN, ROGACHEV & RYVKIN 1968 Sov. Phys. JETP Lett. 9 248

ASNIN, ROGACHEV &SABLINA 1970 Sov. Phys. JETP Lett. 11 99

BAGAEV, GALKINA, GOGOLIN & KELDYSH 1969 Sov. Phys. JETP Lett. 10 195

BAGAEV, GALKINA, PENIN, STOPACHINSKY & CHURAEVA 1972 Sov. Phys. JETP Lett. 16 83

BARDEEN & SHOCKLEY 1950 Phys. Rev. 80 72

BARKER 1973a J. Phys. C 6 880

BARKER 1973b J. Phys. C 6 2663

BARKER & HEARN 1973 J. Phys. C 6 3097

BARKER 1976 J. Phys. C 9 4397

BARKER & BRIDGES 1977 J. Phys. C 10 4523

BENOIT A LA GUILLAUME, VOOS, SALVAN, LAURANT & BONNOT 1971 Compt. Rend. Acad. Sci. Paris 272 B 236

BENOIT A LA GUILLAUME, VOOS, SALVAN 1971 Phys. Rev. Lett. 27 1214

BENOIT A LA GUILLAUME, VOOS & SALVAN 1972 Phys. Rev. B 5 3079

BICKLEY & THOMPSON 1964 'Matrices' Edinburgh University Press

BOCCHIERI & LOINGER 1957 Phys. Rev. 107 337

BOLTZMANN 1872 S. B. Akad. Wiss. Wien (II) 66 275

BRINKMAN, RICE, ANDERSON & CHUI 1972 Phys. Rev. B 7 1508

BUTCHER 1973 IAEA Summer School: Electrons in Crystalline Solids, IAEA, Vienna

BUTTNER 1974 Proc. 12th Int. Conf. Semiconductors, Stuttgart

BYCHKOV 1961 Sov. Phys. JETP 12 483

CHESTER & THELLUNG 1959 Proc. Phys. Soc. 73 745

CHESTER 1963 Rep. Prog. Phys. XXVI

COMBESCOT & NOZIERES 1972 J. Phys. C. 5 2369

CONWELL 1967 Solid St. Phys. Suppl. 9

DAVYDOV & POMERANCHUK 1940 J. Phys. USSR 2 147

DRESDEN 1961 Rev. Mod. Phys. 33 265

DRESSELHAUS, KIP & KITTEL 1955 Phys. Rev. 100 618

DUBINSKAYA 1969 Sov. Phys. JETP 29 436

EAVES, MARKIEWICZ & FURNEAUX 1976 Proc. 13th Int. Conf. Semiconductors, Rome 910

EAVES, MARKIEWICZ & FURNEAUX 1977 J. Phys. C 10 L531

EDWARDS 1958 Phil. Mag. 3 1020

EFROS 1965 Sov. Phys. Solid State 7 1206

ELLIOTT & LOUDON 1959 J. Phys. Chem. Solids 8 382

FANO 1957 Rev. Mod. Phys. 29 74

FENTON & HAERING 1967 Phys. Rev. 159 593

FERMI 1950 'Nuclear Physics' University of Chicago Press

FUKAI, KAWAMUTA, SEKIDO & IMAI 1964 J. Phys. Soc. Japan 19 30

GAVRILENKO, KONONENKO, MANDEL'SHTAM, MURZIN & SAUNIN 1977 Sov. Phys. JETP Lett. 26 95

GELL-MANN & GOLDBERGER 1953 Phys. Rev. 91 398

GERHARDTS & HAJDU 1971 Z. Physik. 245 126

GOLDSTEIN 1950 Classical Mechanics

GREENWOOD 1958 Proc. Phys. Soc. 71 585

GROSSMANN, SHAKLEE & VOOS 1977 Solid. St. Comm. 23 271

GUREVICH & FIRSOV 1961 Sov. Phys. JETP 13 137

GUREVICH & FIRSOV 1965 Sov. Phys. JETP 20 489

HARPER 1955 Proc. Phys. Soc. A68 874, 879

HAYNES 1966 Phys. Rev. Lett. 17 860

HENSEL, PHILLIPS & RICE 1973 Phys. Rev. Lett. 30 227

HENSEL, PHILLIPS & THOMAS 1977 Solid. St. Phys. 32 88

HERRING & VOGT 1956 Phys. Rev. 101 944

JEFFRIES, MARKIEWICZ & WOLFE 1974 Proc. 12th Int. Conf. Semiconductors, Stuttgart 101

JEFFRIES, WOLFE & MARKIEWICZ 1976 Proc. 13th Int. Conf. Semiconductors, Rome 879

JOG & WALLACE 1978 J. Phys. C 11 2763

JOHNSON & LIPPMANN 1949 Phys. Rev. 76 828

KAHN & FREDERIKSE 1959 Solid. St. Phys. 9

KAHN 1960 Phys. Rev. 119 1189

KELDYSH 1968 Proc. 9th Int. Conf. Semiconductors, Moscow 1303

KIRKPATRICK 1973 Proc. 5th Int. Conf. Amorphous and Liquid Semiconductors, Garmisch-Partenkirchen 183

KITTEL 1971 'Introduction to Solid State Physics' (4th Ed.) John Wiley

KNOX 1963 Solid St. Phys. Suppl. 5

KOHN 1948 Phys. Rev. 74 1763

KOHN & LUTTINGER 1957 Phys. Rev. 108 590

KUBO 1957 J. Phys. Soc. Japan 12 570

KUBO, HASHITSUME & HASEGAWA 1959 J. Phys. Soc. Japan 14 56

KUBO, MIYAKE & HASHITSUME 1965 Solid. St. Phys. 17

LANDAU 1930 Z. Physik 64 629

LANDWEHR 1967 Physics of Solids in Intense Magnetic Fields: Ed. Haidemanakis, Plenum Press

LANGER 1960 Phys. Rev. 120 714

LEVINGER & FRANKL 1961 J. Phys. Chem. Solids 20 281

LIPPMANN & SCHWINGER 1950 Phys. Rev. 79 469

LODDER & VAN ZUYLEN 1970 Physica 50 524

LUTTINGER 1951 Phys. Rev. 84 814

LUTTINGER & KOHN 1955 Phys. Rev. 97 869

LUTTINGER & KOHN 1958 Phys. Rev. 109 1892

MANSFIELD 1970 J. Phys. C 4 2084

McLEAN 1961 Prog. in Semiconductors 5 55

MESSIAH 1964 'Quantum Mechanics' Vol I

MILLER & OMAR 1961 Phys. Rev. 123 74

MIYAKE 1973 J. Phys. Soc. Japan 35 551

MOORE 1967 Phys. Rev. 160 607

MOTT & MASSEY 1949 'The Theory of Atomic Collisions' : Oxford University Press.

NAKAMURA 1977 Solid St. Comm. 21 1111

NICHOLAS, STRADLING & EAVES 1976 Proc. 13th Int. Conf. Semiconductors, Rome 1117

NICHOLAS & STRADLING 1979 J. Phys. C 12 2829

OHTAKA & KONDO 1977 Physica B 85 1

OTTAVIANI, CANALI, NAVA & MAYER 1973 J. Appl Phys. 44 2917

PAIGE1964 Prog. in Semiconductors 8

PAULI 1928 Festschriftzum 60 Geburtstage A. Sommerfelds : Leipzig-Hierzel

PEIERLS 1933 Z. Physik 81 186

POINCARÉ 1890 Acta Math. 13 67

POKROVSKY & SVISTUNOVA 1969 Sov. Phys. JETP Lett. 9 261

POKROVSKY, KAMINSKY & SVISTUNOVA 1970 Proc. 10th Int. Conf. Semiconductors, Cambridge, Mass.

POKROVSKY & SVISTUNOVA 1970 Sov. Phys. Semiconductors 4 409

POKROVSKY & SVISTUNOVA 1971 Sov. Phys. JETP Lett. 13 212

POKROVSKY 1972 Physica Status Solidi A11 385

POKROVSKY & SVISTUNOVA 1974 Proc. 12th Int. Conf. Semiconductors, Stuggart 71

PRIEUR, ETIENNE, SANDER, BENOIT A LA GUILLAUME & VOOS 1976 Proc. 13th Int. Conf. Semiconductors, Rome 906

RICE 1974a Proc. 12th Int. Conf. Semiconductors, Stuttgart 23

RICE 1974b Phys. Rev. B 9 1540

RICE 1977 Solid St. Phys. 32 1

RODBERG & THALER 1967 'Introduction to the Quantum Theory of Scattering' : Academic Press

ROHLFING& POKROVSKY 1975 Phys. Rev. B 12 3242

ROMAN 1965 'Advanced Quantum Theory' : Addison-Wesley

ROSE, SHORE & RICE 1978 Phys. Rev. B 17 752

ROTH & ARGYRES 1966 Semiconductors and Semimetals 1 159

SCHIFF & SNYDER 1939 Phys. Rev. 55 59

SCHIFF 1968 'Quantum Mechanics', 3rd ed. : McGraw-Hill

SCHWINGER 1947 Phys. Rev. 72 742

SCOTT & MOORE 1972 Physica 62 312

SERRE & LEROUX-HUGON 1974 Proc. 12th Int. Conf. Semiconductors, Stuttgart 244

SHOCKLEY 1953 Phys. Rev. 90 491

SHUBNIKOV & DeHAAS 1930 Nature 126 500

SIBEL'DIN, BAGAEV, TSVETKOV & PENIN1973 Sov. Phys. Solid State 15 121

SKOBOV 1960 Sov. Phys. JETP 10 1039

SLATER 1967 'Quantum Theory of Molecules & Solids', Vol 3

THOMAS, PHILLIPS, RICE & HENSEL 1973 Phys. Rev. Lett. 31 386

TITEICA 1935 Ann. Physik 22 129

VAN HOVE 1955 Physica 21 517

VAVILOV, ZAYATS & MURZIN 1969 Sov. Phys. JETP Lett. 10 192

VITINS, AGGARWAL & LAX 1978 Proc. High Field Conf., Cambridge, Mass

VITINS, AGGARWAL & LAX 1979 J. Magn Mater. 11 123

VOOS 1974 Proc. 12th Int. Conf. Phys. Semiconductors, Stuttgart 33

WOLFE, FURNEAUX & MARKIEWICZ 1976 Proc. 13th Int. Conf. Semiconductors, Rome 954

WORLOCK, DAMEN, SHAKLEE & GORDON 1974 Phys. Rev. Lett. 33 771

YAFET, KEYES & ADAMS 1956 J. Phys. Chem. Solids 1 137

ZIMAN 1963 'Electrons & Phonons' : Oxford University Press